CORA Cork Open Research Archive
Cartlann Taighde Oscailte Chorcaí

Title	Characterisation of the non-muscle α-actinins
Authors	Foley, Kate
Publication date	2013
Original Citation	Foley, K. 2013. Characterisation of the non-muscle α-actinins. PhD Thesis, University College Cork.
Type of publication	Doctoral thesis
Rights	© 2013, Kate Foley - http://creativecommons.org/licenses/by-nc-nd/3.0/
Download date	2024-04-20 13:53:48
Item downloaded from	https://hdl.handle.net/10468/1180

UCC
University College Cork, Ireland
Coláiste na hOllscoile Corcaigh

Characterisation of the non-muscle α-actinins

Thesis submitted for the degree of

Doctor of Philosophy

By

Kate Foley

Department of Biochemistry

National University of Ireland

Cork

Head of Department: Professor Tom Cotter

Supervisor: Dr. Paul Young

Submitted: January 2013

In memory of my Grandfathers

Edward Foley

&

Martin Langan

Table of Contents

Declaration 6

Acknowledgements 7

Abbreviations 8

Abstract 10

1 Introduction 12

1.1 Origin and evolution of the actinin family 13

1.1.1 Actinin structure 13

1.1.2 Actinin homologs 13

1.1.3 The spectrin superfamily 14

1.1.4 Theory #1: Ancestral actinin contained four spectrin-like repeats 16

1.1.5 Theory #2: Ancestral actinin contained one spectrin-like repeat 16

1.1.6 The "2R hypothesis" 18

1.1.7 Functional divergence within the actinin family 19

1.2 Dimerisation of actinin isoforms 22

1.2.1 The actinin rod domain facilitates dimerisation 22

1.2.2 Evolutionary basis for homodimer and heterodimer formation 23

1.2.3 Evidence of heterodimer formation between actinin isoforms 24

1.3 Actin-binding and cross-linking functions of actinin 26

1.3.1 The structure of the rod domain facilitates actin-crosslinking 26

1.3.2 Alternative splicing of actinin affects its actin-binding properties 28

1.4 The non-muscle actinin isoforms 33

1.4.1 Localisation of the non-muscle actinin isoforms 33

1.4.2 Functions of the non-muscle actinin isoforms 35

1.5 The muscle actinin isoforms 40

1.5.1 Localisation of the muscle actinin isoforms 40

1.5.2 Actinin-3 deficiency 40

1.5.3 Evidence of distinct functions of actinin-2 and -3 41

1.6 Regulation of actinin 42

1.6.1 Processing by proteases 42

1.6.2 Binding to phosphatidylinositol intermediaries 43
1.6.3 Phosphorylation by kinases 43
1.6.4 Binding of calcium 44
1.7 Actinin-interacting partners 46
1.7.1 The actinin rod domain: A structural platform for protein interactions 46
1.7.2 Actinin interacts with a diverse array of proteins 46
1.8 Summary 52
2 Materials and Methods 53
2.1 Cell Biology 54
2.1.1 Antibodies, cell lines and reagents 54
2.1.2 Cell culture and DNA transfections 54
2.1.3 Platelet isolation 55
2.1.4 siRNA knockdown 56
2.1.5 Migration assays 56
2.1.6 Immunofluorescence 56
2.2 SDS-PAGE and Immunoblotting 57
2.2.1 Cell lysate preparation 57
2.2.2 SDS-PAGE and Western blotting 57
2.2.3 Native polyacrylamide gel electrophoresis (Native-PAGE) 58
2.3 Molecular Biology 58
2.3.1 Plasmid construction 58
2.3.2 Reverse transcriptase PCR (rtPCR) 63
2.4 Protein purification 63
2.4.1 Protein expression and purification 63
2.4.2 Tandem affinity purification 64
2.5 Yeast two-hybrid analysis 65
2.5.1 Yeast two-hybrid assays 65
2.5.2 Yeast two-hybrid screens 65
2.6 *In vitro* binding assays 66
2.6.1 *In vitro* heterodimer binding assays 66
2.6.2 Actin-cosedimentation assays 66

2.7 Determination of the relative amount of actinin-1 and -4 within and between cell lines 67
2.8 Analysis of evolutionary conservation of the actinin rod dimerisation interface 67
2.9 Protein identification by mass spectrometry 68
3 Results 71
3.1 The non-muscle actinins: Antibody characterisation, migration and localisation 72
3.1.1 Antibody characterisation 73
3.1.1.1 Antibody-specificity tests 73
3.1.1.2 Antibody detection efficiency 74
3.1.2 Effect of actinin knockdown on cell migration 77
3.1.2.1 Optimisation of siRNA-mediated knockdown of actinin 77
3.1.2.2 Scratch wound assays to monitor the effect of individual and combined actinin-1 and -4 knockdown on cell migration 80
3.1.3 Determination of the specific protein domain responsible for the distinct localisation patterns observed for actinin-1 and -4 85
3.1.3.1 Cloning and expression of GFP-tagged actinin-1 and -4. 85
3.1.3.2 Development of chimeric actinin-1/-4 proteins: Cloning strategy 88
3.1.3.3 Expression and localisation of chimeric actinin-1 and -4 proteins 93
3.2 Analysis of alternative splicing patterns and actin-binding characteristics of the non-muscle actinins 96
3.2.1 Analysis of alternative splicing patterns of actinin-1 and -4 exon 19 and actinin-4 exon 8 97
3.2.2 Determination of the actin-binding affinities of the non-muscle actinins 102
3.2.2.1 Optimisation of actin-binding assays 102
3.2.2.2 Determination of the actin-binding affinity of actinin-1 (exon 19a), actinin -4 (exon 8a, 19a) and actinin-4 (exon 8b, 19a) 104
3.2.2.3 Comparison of the actin-bundling capacity of actinin-1 (exon 19a) and actinin -4 (exon 8a, 19a) 108

3.2.3 Determination of the calcium sensitivity of actin-binding for the non-muscle actinins 109
3.2.3.1 Determination of the calcium sensitivity of actin-binding and -bundling for actinin-1 (exon 19a) and actinin-4 (exon 8a, 19a). 109
3.2.3.2 Determination of the calcium sensitivity of actin-binding for brain-specific actinin-1 (exon 19a+19b) 110
3.2.3.3 Determination of the calcium sensitivity of actin-binding for the alternatively spliced actinin-4 exon 8b variant 111
3.3 Analysis of heterodimer formation between the non-muscle actinins 112
3.3.1 Evolutionary conservation of the actinin dimer interface 113
3.3.2 Non-muscle actinins have the potential to form heterodimers 114
3.3.2.1 Yeast two-hybrid analysis of actinin heterodimer formation. 114
3.3.2.2 *In vitro* binding assay analysis of actinin-1 and -4 homodimeric versus heterodimeric interactions. 115
3.3.3 Actinin-1 and -4 heterodimer formation in cultured cells. 117
3.3.3.1 Heterodimers are present in cells grown under a variety of conditions 117
3.3.3.2 Non-muscle actinin heterodimers are prevalent in many cancer cell lines. 118
3.3.3.3 Knockdown of actinin-4 results in a shift from heterodimer to homodimer formation 119
3.3.4 The relative abundance of actinin homodimers and heterodimers in cell lines. 120
3.3.5 Analysis of actinin isoforms present in platelets 121
3.4 Identification of non-muscle actinin-interacting partners 122
3.4.1 Yeast two-hybrid screening 123
3.4.1.1 Identification of suitable actinin-1 and -4 bait proteins 123
3.4.1.2 Preliminary yeast two-hybrid screens 124
3.4.1.3 Yeast two-hybrid screen of a brain cDNA library employing the actinin-1 rod as bait 126
3.4.2 Tandem Affinity Purification (TAP) of actinin-1 and -4. 131
3.4.2.1 Development and expression of TAP-tagged actinin-1 and -4 proteins 131

3.4.2.2 Analysis of actinin-interacting proteins identified by Tandem Affinity Purification 134

4 Discussion 139

4.1 The effect of the non-muscle actinins on cell migration and localisation 140

4.1.1 Antibody characterisation 140

4.1.2 The effect of actinin-1 and -4 knockdown on cell migration 140

4.1.3 Determination of the specific protein domain responsible for the distinct localisation patterns observed for actinin-1 and -4. 142

4.2 Alternative splicing and actin-binding properties of the non-muscle actinins 144

4.2.1 Actin-binding and calcium sensitivity properties of the non-muscle actinins ... 144

4.2.2 Alternative splicing of non-muscle actinin exon 8 and exon 19 145

4.2.3 Muscle alternative splice variants 148

4.2.4 Brain alternative splice variants 148

4.3 The non-muscle actinin heterodimer 149

4.4 Actinin-interacting partners 153

4.4.1 Yeast two-hybrid screens 154

4.4.2 Identification of putative actinin-4 interactions by TAPTAG Purification 156

4.5 Summary 158

5 Conclusion 161

6 Bibliography 164

7 Appendix 182

Declaration

This thesis is my own work and has not been submitted for another degree either at University College Cork or elsewhere.

Kate Foley

Kate Foley

02/05/13

Date

Acknowledgements

Firstly, I would like to thank my supervisor Dr. Paul Young for the opportunity to work in his laboratory and for his support, advice and encouragement over the past four years. I would also like to thank members of the Biochemistry Department, in particular the members of my thesis committee, Prof. Rosemary O' Connor, Prof. Tommie McCarthy and Dr. Justin McCarthy for their input and advice over the course of this programme. I would also like to thank Dr. Kellie Dean for her great efforts in coordinating the Ph.D. Scholars Programme in Cancer Biology and for her support throughout the years. I would like to thank the Health Research Board, Ireland for providing the funding that facilitated this work.

My thanks to members of the Young lab, Victoria Heimer-McGinn, Orthis Saha and to all those who have passed through the lab while I have been there, Ronan McCarthy, Anita Murphy, Anjali Pai and Gary Williamson. I would like to thank David for always being there for me over the past four years. Finally, I would like to thank my sister Jennifer and my parents Martin and Cora for their endless support.

Abbreviations

Protein Domains

ABD	Actin-binding domain
ABD-R2	Actin-binding domain and spectrin-like repeats 1 and 2
R	Rod domain
R1-R2	Spectrin-like repeats 1 and 2
R2-R3	Spectrin-like repeats 2 and 3
R1-R4	Spectrin-like repeats 1-4 (rod domain)
RC	Rod and calmodulin domain
R3-CaM	Spectrin-like repeats 3 and 4 and CaM domain
CaM	Calmodulin-like domain
C	Calmodulin-like domain
A1RC4	ABD of actinin-1/rod and CaM domain of actinin-4
A4RC1	ABD of actinin-4/rod and CaM domain of actinin-1
A1R4C1	ABD of actinin-1/rod domain of actinin-4/CaM domain of actinin-1
A4R1C4	ABD of actinin-4/rod domain of actinin 1/CaM domain of actinin-4

Miscellaneous

aa	Amino Acid
ATP	Adenosine Triphosphate
BLAST	Basic Local Alignment Search Tool
BSA	Bovine Serum Albumin
Ca^{++}	Calcium
$CaCl_2$	Calcium Chloride
cDNA	Complementary DNA
DAPI	4’6’-Diamino-2-Phenylindole Dihydrochloride
DMEM	Dulbecco’s Modified Eagles Medium
DMSO	Dimethyl Sulfoxide
DNA	Deoxyribonucleic Acid
DTT	Dithiothreitol
EDTA	Ethylenediamine Tetra-Acetic Acid
EGF	Epidermal Growth Factor
EGTA	Ethylene Glycol Tetraacetic Acid
FBS	Foetal Bovine Serum
GFP	Green Fluorescent Protein
GST	Glutathione-S-Transferase
HEK	Human Embryonic Kidney

H_2O	Water
IR	Infrared
IPTG	Isoppropylthio-β-Galactosidase
kb	Kilobase
KCl	Potassium Chloride
kDa	Kilodalton
KPO_4	Potassium Phosphate
LB	Luria-Bertani
MBP	Maltose-Binding Protein
$MgCl_2$	Magnesium Chloride
$MgSO_4$	Magnesium Sulfate
$NaCl_2$	Sodium Chloride
NaF	Sodium Floride
Na_2HPO_4	Sodium Phosphate Dibasic
NaH_2PO_4	Monosodium Phosphate
NaN_3	Sodium Azide
Na_3VO_4	Sodium Orthovanadate
NDMA	N-Methyl-D-Aspartate
NEB	New England Biolabs
Ni	Nickel
NP40	Nonyl Phenoxypolyethoxylethanol
PBS	Phosphate-Buffered Saline
PCR	Polymerase Chain Reaction
PFA	Paraformaldehyde
PMSF	Phenylmethanesulfonylfluoride
RNA	Ribonucleic Acid
rtPCR	Reverse Transcriptase Polymerase Chain Reaction
SDS-PAGE	Sodium Dodecyl Sulphate-Polyacrylamide Gel Electrophoresis
TAP	Tandem Affinity Purification
TBS	Tris-Buffered Saline
TBST	Tris-Buffered Saline (Plus Tween20)
TEV	Tobacco Etch Virus
YFP	Yellow Fluorescent Protein
X-Gal	5-Bromo-4-Chloro-Indolyl-β-D-Galactopyranoside

Abstract

Actinins are cytoskeleton proteins that cross-link actin filaments. Evolution of the actinin family resulted in the formation of Ca^{++}-insensitive muscle isoforms (actinin-2 and- 3) and Ca^{++}-sensitive non-muscle isoforms (actinin-1 and -4) with regard to their actin-binding function. Despite high sequence similarity, unique properties have been ascribed to actinin-4 compared with actinin-1. Actinin-4 is the predominant isoform reported to be associated with the cancer phenotype. Actinin-4, but not actinin-1, is essential for normal glomerular function in the kidney and is able to translocate to the nucleus to regulate transcription. To understand the molecular basis for such isoform-specific functions I have comprehensively compared these proteins in terms of localisation, migration, alternative splicing, actin-binding properties, heterodimer formation and molecular interactions for the first time. This work characterises a number of commercially available actinin antibodies and in doing so, identifies actinin-1, -2 and -4 isoform-specific antibodies that enabled studies of actinin expression and localisation. This work identifies the actinin rod domain as the predominant domain that influences actinin localisation however localisation is likely to be effected by the entire actinin protein. si-RNA-mediated knockdown of actinin-1 and -4 did not affect migration in a number of cell lines highlighting that migration may only require a fraction of total non-muscle actinin levels. This work finds that the Ca^{++}-insensitive variant of actinin-4 is expressed only in the nervous system and thus cannot be regarded as a smooth muscle isoform, as is the case for the Ca^{++}-insensitive variant of actinin-1. This work also identifies a previously unreported exon 19a+19b expressing variant of actinin-4 in human skeletal muscle. This work finds that alternative splice variants of actinin-1 and -4 are co-expressed in a number of tissues, in particular the brain. In contrast to healthy brain, glioblastoma cells express Ca^{++}-sensitive variants of both actinin-1 and -4. Actin-binding properties of actinin-1 and -4 are similar and are unlikely to explain isoform-specific functions. Surprisingly, this work reveals that actinin-1/-4 heterodimers, rather than homodimers, are the most abundant form of actinin in many cancer cell lines. Taken together this data suggests that actinin-1 and -4 cannot be viewed as distinct entities from each other but rather as proteins that can exist in both homodimeric and heterodimeric forms. Finally, this work employs yeast two-

hybrid and proteomic approaches to identify actinin-interacting proteins. In doing so, this work identifies a number of putative actinin-4 specific interacting partners that may help to explain some of the unique functions attributed the actinin-4. The observation of alternative splice variants of actinin-1 and -4 combined with the observed potential of these proteins to form homodimers and heterodimers suggests that homodimers and heterodimers with novel actin-binding properties and interaction networks may exist. The ability to behave in this manner may have functional implications. This may be of importance considering that these proteins are central to such processes as cell migration and adhesion. This significantly alters our view of the non-muscle actinins.

1 Introduction

1.1 Origin and evolution of the actinin family

1.1.1 Actinin structure

The α-actinins (actinins) are a family of actin-binding proteins. A general domain structure is conserved between actinin proteins. Actinin is a dimer composed of two antiparallel monomers (Figure 1.1). Each monomer consists of an N-terminal actin-binding domain (ABD), a rod domain composed of four spectrin-like repeats (R1-R4) and a C-terminal calmodulin-like domain (CaM) (Sjoblom et al., 2008). There are four isoforms of actinin (actinin-1 and -4). Vertebrates possess four actinin genes (ACTN1-4). These are the Ca^{++}-sensitive non-muscle isoforms (actinin-1 and -4) and the Ca^{++}-insensitive muscle isoforms (actinin-2 and -3).

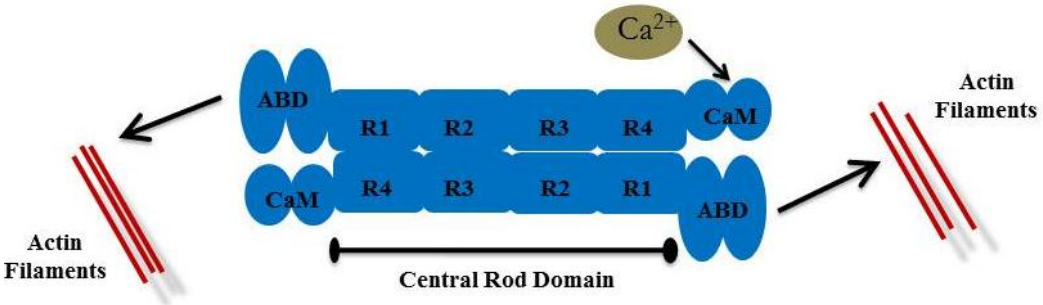

Figure 1.1 The structure of actinin. Actinin is a dimeric protein that consists of two anti-parallel monomers. Each monomer contains an N-terminal actin-binding domain (ABD), a rod domain composed of four spectrin-like repeats (R1-R4) and a C-terminal calmodulin-like domain (CaM). The presence and spatial arrangement of the two ABDs of actinin facilitate crosslinking of actin filaments. Binding of calcium (Ca^{++}) to the CaM domain results in a conformational change that inhibits the actin-binding function of the neighbouring ABD (Noegel et al. 1987) The rod domain faciliates dimerisation.

1.1.2 Actinin homologs

The actinins are an ancient family of actin-binding proteins. The actinins have homologs in slime mould, fungi and metazoans but are not present in plants (Lek et al., 2010a). While actinin is not an essential gene of *D. discoideum* (Wallraff et al., 1986), reports indicate there is continuous expression of actinin throughout the developmental stages of *D. discoideum* (Witke et al., 1986). This study observed high diversity of actinin among different strains of *D. discoideum* and concluded that

the functional sites of actinin are highly conserved. *C. elegans* expresses a single actinin gene. Deletion mutant studies of actinin in *C. elegans* also indicate that actinin is not an essential gene (Moulder et al., 2010). Animals were viable with mild effects on actin organisation (Moulder et al., 2010). These studies suggest that actinin is not an essential gene, at least in these invertebrates. In *Drosophila*, a single gene is variably spliced to generate one non-muscle and two muscle-actinin isoforms. Actinin mutations in *Drosophila* result in either lethal or flightless phenotypes (Fyrberg et al., 1998; Fyrberg et al., 1992). In flightless phenotypes disruption of muscle Z-discs is obvious however, no non-muscle phenotype is apparent (Roulier et al., 1992). This suggests that, in *Drosophila* at least, non-muscle actinins may not be essential for normal development. It is important to note that Roulier *et al*. mutation studies resulted in severely reduced, but not absent non-muscle actinin levels. It cannot be ruled out that residual non-muscle actinin levels may be capable of maintaining normal function in non-muscle cells. While these studies suggest that actinin may not be an essential gene, knockout and mutation studies of actinin result in disease phenotypes. This will be discussed in further detail in Section 1.4.2.4.

1.1.3 The spectrin superfamily

Actinin is a member of the spectrin superfamily that includes spectrin, utrophin and dystrophin. It is believed that an actinin–like precursor has given rise to members of the spectrin superfamily (i.e. actinin, spectrin and dystrophin) by means of gene duplication and gene rearrangements (Virel & Backman, 2004). Although these proteins differ in their number of spectrin-like repeats, amino acid analysis has suggested that all three protein families arose from a single common ancestral protein that was actinin-like (Dubreuil, 1991). Actinin has an N-terminus resembling that of β-spectrin and dystrophin, a short-repeated α-helical repeat common to the whole family and Ca^{++}-binding EF-hands at the C-terminus related to those of α-spectrin and dystrophin (Dubreuil, 1991). It is thought that evolution of the spectrin-like repeat occurred in two steps. In the first step the number of repeats increased creating proteins of different lengths. In the second step the number of repeats

became fixed and proteins began to diverge at the DNA level (Thomas et al., 1997). Figure 1.2 depicts these two phases in the evolution of the spectrin-like repeat.

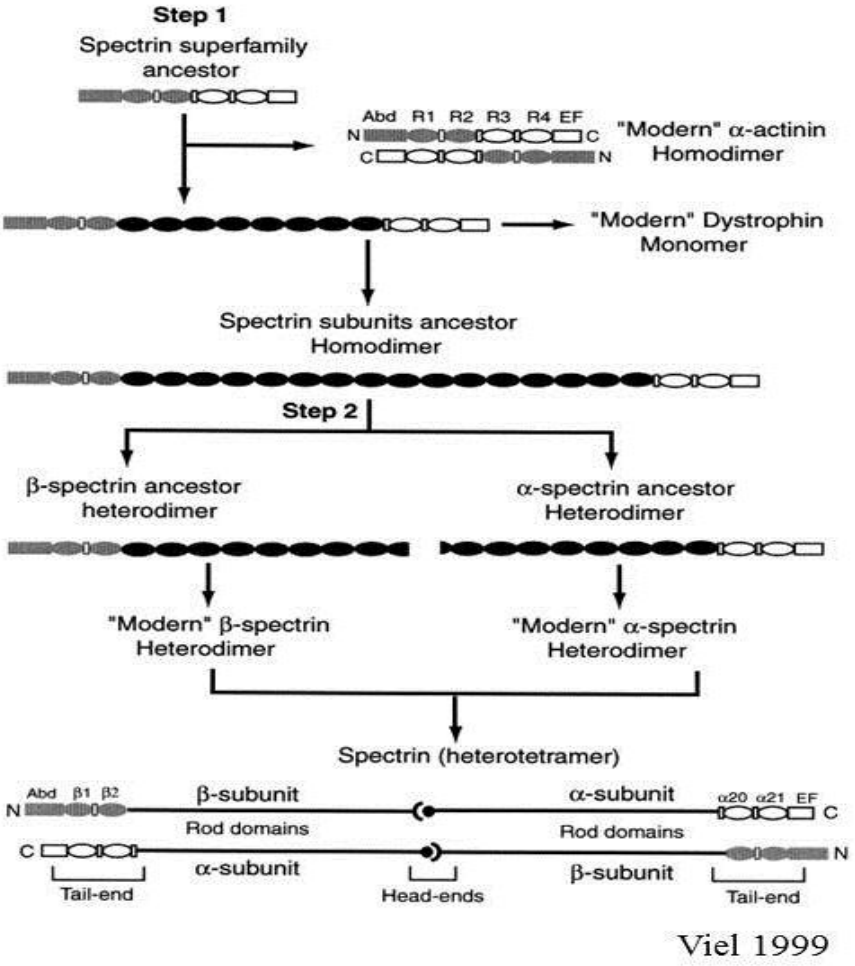

Figure 1.2 Model of the evolution of the spectrin superfamily. Step 1: Gene duplication and gene rearrangements gave rise to various members of the spectrin superfamily. The successive addition of repeats resulted in formation of the spectrin subunit ancestor, an elongated actinin-like protein. This step is proposed to have resulted in an early length determination of each spectrin superfamily member. Step 2: Genes encoding each specific spectrin subunit probably arose from the genes encoding the actinin-like ancestor. Consequently the repeats responsible for the spectrin subunit ancestor or actinin self- association were split between two distinct polypeptide chains still capable of forming heterodimers and now able to form a heterotetramer. Shaded ovals represent repeats.(Viel, 1999).

The actin-binding domain of actinin contains two calponin homology domains (CH1 and CH2). It is noteworthy that phylogenetic analysis based on these domains, groups CH1 and CH2 of actinin, spectrin, and dystrophin together, supporting the theory that these proteins are derived from a common ancestral protein (Gimona et al., 2002).

As previously discussed the evolution of the spectrin-like repeat describes the emergence of an ancestral actinin protein that contained four spectrin-like repeats. However, two theories exist regarding the number of repeats possessed by ancestral actinin.

1.1.4 Theory #1: Ancestral actinin contained four spectrin-like repeats

In 1999, Viel suggested that the ancestor of actinin possessed four spectrin-like repeats (Viel, 1999). It is thought that an ancestral gene expressing four spectrin-like repeats underwent duplication giving rise to one stable lineage leading to modern actinin genes while the second gene acquired additional repeats leading to the spectrin subunit ancestor (Figure 1.2). This theory implies that the cross-linking function of actinin dates back to its origin.

1.1.5 Theory #2: Ancestral actinin contained one spectrin-like repeat

In contrast, studies by Backman and Virel indicate that the evolution of actinin can be divided into two phases (Virel & Backman, 2004), (Virel & Backman, 2007). In short, the first phase occurred in invertebrates and was characterised by two rounds of intragenic duplication that increased the number of spectrin-like repeats from one to four. In the primordial actinin, the rod domain was short, spanning a single spectrin-like repeat. An intragenic duplication added a second repeat, followed by yet another intragenic duplication. As the single repeat in *E. histolytica* actinin appears most related to the first repeat (R1), it is likely that this repeat was the first to evolve. Likewise, as the two repeats of the fungi *S.pombe* actinin are closest to repeat R1 and R4, this suggests that R4 arose through intragenic duplication. The second intragenic duplication added repeats R2 and R3. The second phase in the evolution of actinin resulted in the appearance of four isoforms in vertebrates.

Viel's theory indicates that an ancestral actinin containing four spectrin-like repeats would have been capable of cross-linking actin (Viel, 1999). However, Backmans and Virel's initial report suggested that ancestral actinins containing less than four spectin-like repeats may not have been capable of forming dimers and

therefore cross-linking actin (Virel & Backman, 2004). This idea was based on the fact that spectrin-like repeats R2 and R3 that are required for dimerisation (Djinović-Carugo et al., 1999) were absent in ancestral actinins. However, further work by Virel *et al.* detected actinins in *E. histolytica* with one and two spectrin-like repeats respectively both of which were capable of forming dimers and thus cross-linking actin (Virel & Backman, 2006), (Virel & Backman, 2007).

Phylogenetic analysis further supports Viral and Backman's theory of actinin evolution (Virel & Backman, 2007). In phylogenetic trees, spectrin-like repeats 1 (R1) from all actinins are grouped together regardless of the total number of repeats they possess. In invertebrates, the sequence conservation has a similar trend to that observed in vertebrates with R1 being the most conserved repeat and R3 the least conserved. Spectrin-like repeats R1 and R4 of actinins with two and four repeats, respectively, are also grouped together. Therefore, R1 and R2 of fungi and *E. histolytica* 2 are closely related to R1 and R4 of actinins with four repeats. Similarly spectrin-like repeats R2 and R3 of actinins with four repeats are placed on separate but very close branches in the phylogenetic trees. Together this suggests a plausible evolutionary pattern of the rod domain of actinin (Figure 1.3). In any case, the actinin family have evolved as proteins that are primarily known for their ability to cross-link actin with both Ca^{++}-sensitive and -insensitive isoforms.

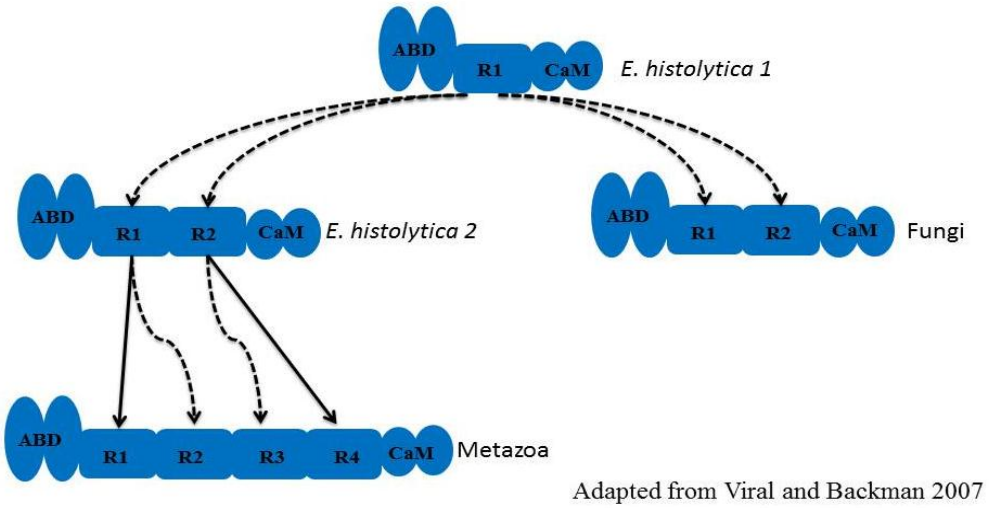

Figure 1.3 Evolution of the actinin rod domain. The ancestor of actinin contained a single repeat (R1). Due to an intragenic duplication, this single domain observed in *E.histolytica 1* was doubled and an actinin with two spectrin repeats evolved. This step gave probably rise to the fungi isoforms of actinin as well as a protozoan actinin such as *E. histolytica 2*. A second intragenic duplication caused an extension by two more repeats, thereby giving rise to a rod domain containing four spectrin repeats. As spectrin repeat 4 (R4) of invertebrates and vertebrates are closely related to spectrin repeat 2 (R2) of fungi, it seems reasonable to suggest that in the last duplication the repeats were inserted between repeats R1 and R2 of the ancestral actinin.

1.1.6 The "2R hypothesis"

Phylogenetic analysis based on the amino acid sequence of the actin-binding domain of actinin indicates that two rounds of genome duplication, known as the "2R hypothesis", occurred early in vertebrate evolution resulting in two vertebrate branches (Hughes, 1999; Durand, 2003). These two vertebrate branches denote the Ca^{++}-sensitive non-muscle isoforms (actinin-1 and -4) and the Ca^{++}-insensitive muscle isoforms (actinin-2 and -3). The "2R hypothesis" that proposes the genome of jawed vertebrates has been shaped by two rounds of whole genome duplication is increasingly supported by genome-wide analysis of key chordate species (Kasahara, 2007). In contrast phylogenetic analysis based on the nucleotide sequence of the actin-binding domain of actinin indicates that the Ca^{++}-insensitive actinin-2 evolved initially, followed first by the Ca^{++}-insensitive actinin-3 and then by the Ca^{++}-sensitive actinins (1 and 4). This theory does not support the "2R hypothesis". Figure 1.4 depicts the two contrasting actinin gene topologies suggested by phylogenetic analysis of amino acid versus nucleotide sequence. It has been suggested that phylogenetic analyses based on protein sequences are generally considered to be more reliable than those derived from the corresponding DNA sequences because it is believed that the use of encoded protein sequences circumvents the problems caused by nucleotide compositional biases in the DNA sequences (Foster & Hickey, 1999). It is noteworthy to mention that while the evolution of actinin can be explained by intragenic duplication followed by genome duplication as discussed, the phylogeny observed today could also be explained by independent duplication of individual genes or gene segments (Hughes, 1999).

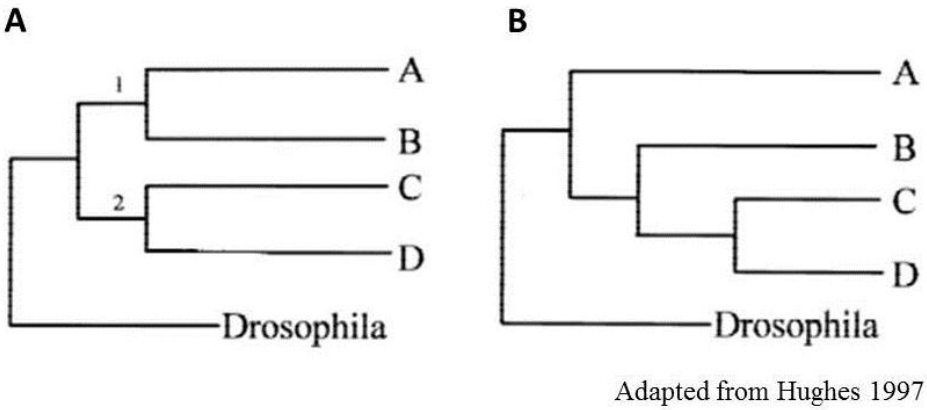

Figure 1.4 Two different reported phylogenies of the actinin gene family in vertebrates. (A) Topology of the form (AB) (CD), which supports the hypothesis of two rounds of gene duplication (2R hypothesis) early in vertebrate history as suggested by phylogenetic analysis of amino acid sequence. This suggests that A is a sister group to B, and C is a sister group to D. (Virel & Backman, 2007), (Virel & Backman, 2004) . (B) Topology of the form (A) (BCD) as suggested by phylogenetic analysis of nucleotide sequence (Dixson et al., 2003). This alternative topology is one in which one of the four paralogues diverged prior to the others. The topology of the relationships among B, C, and D does not support the "2R hypothesis".

1.1.7 Functional divergence within the actinin family

As discussed the "2R hypothesis" suggests that two rounds of gene duplication resulted in four actinin genes (Virel & Backman, 2004), (Virel & Backman, 2007). It is proposed that developmental genes such as actinin that follow this 1:4 rule, are forced, shortly after duplication to diverge in function so as to avoid the fate of most duplicated genes i.e. gene loss (Lek et al., 2010b). This paradigm of gene duplication and divergence resulting in alterations in protein function and expression patterns has emerged as an important concept in gene evolution (Louis, 2007). The paradigm allows for two general scenarios, neo-functionalisation and sub-functionalisation (Figure 1.5). There are two main characteristics that distinguish between these two scenarios (Force et al., 1999). In the sub-functionalisation scenario both duplicates are subjected to adaptive changes whereby they become "specialised", while in neo-functionalisation only one duplicate is subjected to adaptive changes whereby it becomes specialised, with the other maintaining ancestral function (Des Marais & Rausher, 2008). Hence, in the sub-functionalisation model, both duplicates develop an optimised ancestral function (Des Marais & Rausher, 2008). The "sub-functional" model is more likely if the pre-duplicated gene can perform functions of both duplicated genes. Conversely the "neo-functional" model is more likely if the pre-duplicated gene can perform the

functions of only one duplicated gene (Lek et al., 2010b). Functional divergence after duplication comes in two forms: (i) divergence of the protein coding sequence, resulting in changes in protein structure, function and interactions and (ii) divergence in regulatory sequence resulting in altered expression patterns (Louis, 2007). It is noteworthy that "specialisation" is not limited to optimisation of a protein interaction, it can also be associated with weakening or loss of an interaction (Lek et al., 2010b).

Phylogenetic analysis shows that actinins of each isoform are grouped together (Virel & Backman, 2004). This implies a higher degree of similarity between a particular isoform of all organisms than between the isoforms of a single organism (Virel & Backman, 2004). Conservation of actinin structure suggests that any functional divergence between the actinin isoforms is likely to be due to changes in surface or mechanical properties introduced through slightly altered physiochemical properties of the substituting residues (Lek et al., 2010b). The actinins interact with a diverse range of proteins in muscle and non-muscle cells, with the spectrin-like repeats mediating the majority of these interactions (Lek et al., 2010b; Djinovic-Carugo et al., 2002). Any minor changes to these protein interactions, due to sequence divergence or changes in overall actinin levels, may affect the overall properties of actinin-containing complexes both in the muscle and non-muscle environments. For example, in the case of the muscle isoforms, actinin-3 deficiency affects muscle function which will be discussed in more detail in Section 1.5.2. While actinin-2 protein levels are increased in actinin-3 deficiency they cannot rescue the observed effects on muscle function (Seto et al., 2011). Z disk proteins such as ZASP, titin and vinculin exhibit a higher binding affinity for actinin-2 compared with actinin-3 (Seto et al., 2011). The protein–protein interactions at the Z-disk determine the stability and rigidity of the Z-disk. The distinct affinities of the muscle actinins for sarcomeric proteins combined with the absence of actinin-3 could result in altered Z-disk protein composition. Altogether this highlights protein binding affinity as a potential mechanism of evolutionary divergence (Seto et al., 2011).

In addition to divergence in protein sequence and binding affinity, the altered tissue-specific expression patterns observed in the sarcomeric actinins suggest a divergence in regulatory regions (Lek et al., 2010b). In humans, actinin-2 is expressed in the heart, in all skeletal muscle fibres, and in the brain, whereas actinin-

3 is expressed only in fast twitch glycolytic skeletal muscle fibres, is not present in cardiac muscle, and has low levels of expression in the brain (Mills et al., 2001). The variation in tissue expression patterns suggests that after gene duplication, degenerative changes in actinin-3 regulatory regions have restricted its expression compared to actinin-2, rather than novel changes in actinin-2 regulatory regions allowing for a greater range of tissue expression (Lek et al., 2010b). Actinin-3 appears to perform a specialised function in fast twitch muscle fibres which will be discussed in Section 1.5.2, however it cannot compensate for mutations in actinin-2 known to result in cardiomyopathy (Chiu et al., 2010). An actinin-2 mutation located in the actin-binding domain that prevents actinin binding to the muscle LIM protein results in cardiomyopathy (Mohapatra et al., 2003). These studies support the notion that disruption of Z-disc proteins can lead to cardiomyopathy. While the restricted expression profile of actinin-3 prevents it from rescuing defects resulting from actinin-2 mutations, it may relieve evolutionary constraints placed on functions that are not required in fast twitch muscle fibres and allow specialised functions develop in fast twitch fibres that may be disadvantageous in other tissues (Lek et al., 2010b).

At this point it is unclear whether the muscle actinin isoforms underwent neo- or sub-functionalisation. Actinin-3 has only a subset of the actinin-2 expression profile. Actinin-2 is able to compensate for the absence of actinin-3 with no overt disease phenotype (although human and mouse studies demonstrate that the presence or absence of actinin-3 influences 'normal' variation in skeletal muscle performance- see Section 1.5.2). This suggests that actinin-2 has conserved many if not all the functions of the pre-duplicated gene and that actinin-3 has lost many of these functions but at the same time has evolved a new function in fast muscle fibres. Altogether this evidence tends to support neo-functionalisation evolution of the muscle actinins. Further studies are required to define the specialised functions of actinin-3 and to determine total actinin levels in muscle fibres of individuals with different actinin-3 genotypes (Lek et al. 2010b). This will determine whether loss of specialised actinin-3 function or merely gene dosage can explain the variations in skeletal muscle performance associated with actinin-3 deficiency (Lek et al., 2010b). It is noteworthy that studies to date carried out on actinin-3 deficiency have not shown any link to a gene dosage effect (Delmonico et al., 2008; Norman et al., 2009; Walsh et al., 2008). With regard to the non-muscle actinins (actinin-1 and -4) it is apparent from the literature that actinin-4 has developed unique functions supporting

its role is cancer development and kidney disease. The mechanism through which actinin-4 exerts these unique functions remains to be elucidated. Overall studies of the muscle actinins highlight protein interaction networks and binding-affinities as potential areas where homologs can diverge to become paralogs (Lek et al., 2010b). Alternative splicing of actinin is another mechanism through which this family of proteins have increased their functional diversity. This is discussed in more detail in Section 1.3.2

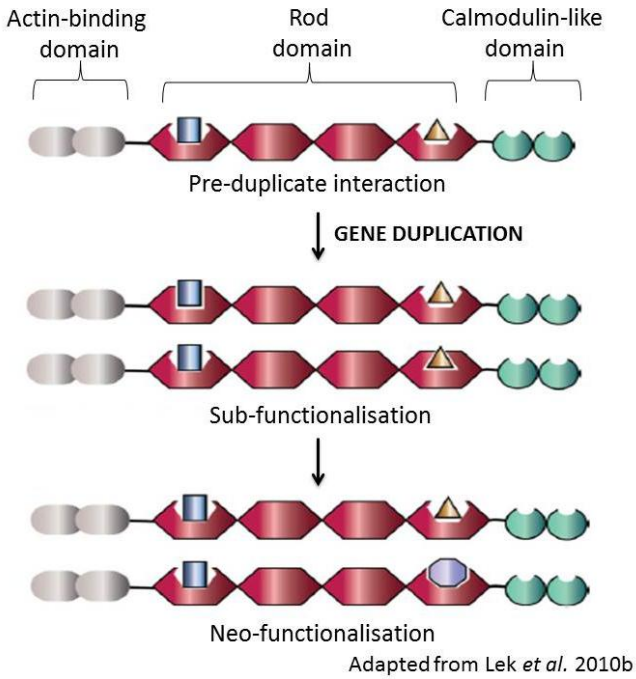

Figure 1.5 Duplication of a gene capable of multiple interactions/functions, there are two possible distinct scenarios besides gene loss. 1) Sub-functionalisation, where one interaction site is optimised in each of the copies. 2) Neo-functionalisation, where one copy retains the ancestral interaction sites while the other is free to evolve new interaction sites.

1.2 Dimerisation of actinin isoforms

1.2.1 The actinin rod domain facilitates dimerisation

The rod domain is composed of four spectrin-like repeats. Figure 1.1 shows the four spectrin-like repeats (R1-R4) of each monomer engaging in pair wise interactions with R4-R1 of the opposing subunit (Djinović-Carugo et al., 1999; Ylänne et al., 2001; Young & Gautel, 2000). The rod domain is responsible for dimerisation and forms a spacer of fixed length between the ABDs in the resulting antiparallel dimer (Djinović-Carugo et al., 1999). Crystal structure studies of actinin-

2 (muscle isoform) reveal that in order to generate a maximally stable antiparallel dimer, all four repeats are required, although it appears that R2-R3 forms the structural principle that governs the entire rod (Djinović-Carugo et al., 1999). The rod domain is extremely stable suggesting that the ABD and CaM domains of actinin do not make a dominant contribution to dimerisation (Djinović-Carugo et al., 1999). The rod domain is twisted from one end to the other which may play an important role in stabilising the protein (Ylänne et al., 2001). The spectrin-like repeats and the linkers between them confer an important mechanical property on actinin (Otey & Carpen, 2004). This structure provides support against the mechanical stresses endured by actinin in locations such as the muscle sarcomere and stress fibres. Since high sequence conservation exists between the muscle and non-muscle isoforms it is likely that this model holds true for the non-muscle actinins.

1.2.2 Evolutionary basis for homodimer and heterodimer formation

Protein–protein interaction networks in several eukaryotic organisms contain significantly more self-interacting proteins than expected if such homodimers randomly appeared in the course of evolution (Ispolatov et al., 2005). Homodimers have twice as many interaction partners as non-self-interacting proteins (Ispolatov et al., 2005). More specifically, the likelihood of a protein to physically interact with itself was found to be proportional to the total number of its binding partners. Duplication of self-interacting proteins can create a pair of paralogous proteins that can potentially interact with each other. Studies show that this phenomenon occurs more frequently than can be explained by chance alone (Ispolatov et al., 2005). Similar to homodimers, proteins involved in heterodimers with their paralogs on average have twice as many interacting partners as the rest of the protein interaction network. Altogether this points to the conclusion that most interactions between paralogs are inherited from ancestral homodimeric proteins, rather than established *de novo* after duplication. It is noteworthy that the actinin-related protein spectrin has evolved to form both α /β heterodimers and heterotetramers (Figure 1.2).

1.2.3 Evidence of heterodimer formation between actinin isoforms

Gache *et al.* identified two actinin subunits in human platelets *a* and *c*, which give rise to three isoforms, two homodimers *aa* and *cc*, and one heterodimer *ac* (Gache at al., 1984). Their studies indicated that these isoforms were Ca^{++}-sensitive. Further work determined that the actin-binding function of the *aa* homodimer was more sensitive to calcium than that of the *cc* homodimer. However, calcium had similar effects on the actin cross-linking function of both homodimers (Landon et al., 1985). Altogether this suggests that heterodimer formation occurs between Ca^{++}-sensitive platelet actinin isoforms. Chan *et al.* found that the muscle isoforms, actinin-2 and -3 form heterodimers *in vitro* and *in vivo*. They identified heterodimer formation between transfected actinin-2 and -3 in COS cells (Chan et al., 1998). Interestingly, heterodimer formation was only evident when actinin-2 and -3 were co-expressed simultaneously. It was hypothesised that this was due to rapid homodimerisation occurring when each isoform was expressed separately. They also identified heterodimer formation between endogenous muscle actinin isoforms in skeletal muscle. While heterodimer formation has been reported to occur between the muscle isoforms (actinin-2 and -3), it has not been systematically examined for the non-muscle isoforms (actinin-1 and -4). However, the aforementioned studies of Ca^{++}-sensitive actinins, isolated from platelets, suggest that non-muscle actinin heterodimer formation may occur (Landon et al., 1985). Figure 1.6 shows a schematic representation of non-muscle homo- and heterodimer formation.

Figure 1.6 Schematic representation of homo- and heterodimer formation between the non-muscle actinins. Actinin-1 (red) and -4 (green) are currently viewed as homodimers that are distinct from each other. However, conserved amino acids between the dimeric interface of actinin-1 and -4 suggest that heterodimer formation may occur between these non-muscle actinin isoforms.

Actinin-1 and -4 are generally regarded as distinct homodimeric entities, despite the fact that they are co-expressed in many tissues and cell types. The ability of muscle actinins to homodimerise and heterodimerise adds a degree of evolutionary freedom for the asymmetric divergence of each proteins interaction network, which may result in a new or specialised function of the complexes formed (Figure 1.7). With this in mind, it will be interesting to determine if the non-muscle actinins are in fact capable of forming heterodimers.

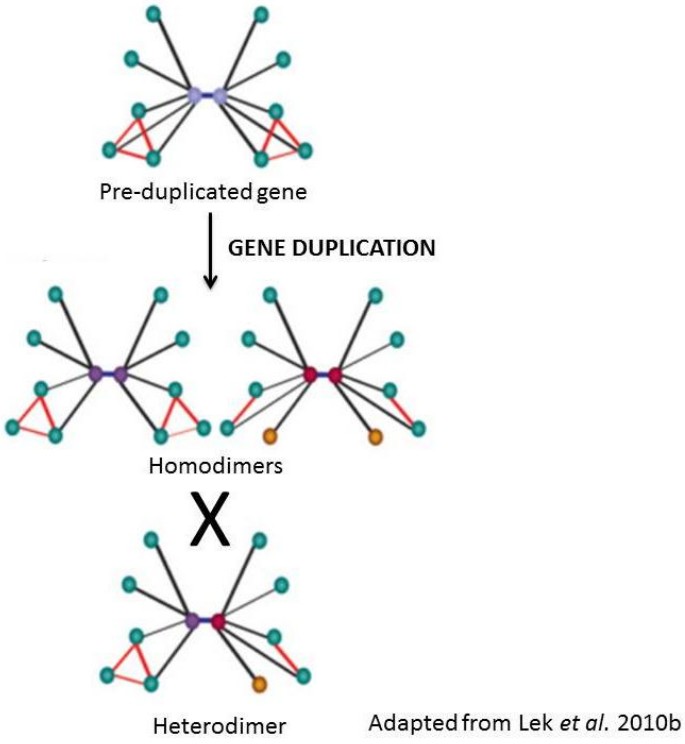

Figure 1.7 Heterodimer formation increases the divergence of protein networks and functions. The asymmetric divergence of protein interaction networks after duplication allows for an increase in complexity and possible novel functions. Before duplication, dimerisation allowed for larger complexes. After duplication and divergence of protein interaction networks, homodimerisation allows for larger complexes with slightly altered functions, while heterodimerisation increases complexity and has the potentially to result in novel functions (Lek et al. 2010b).

1.3 Actin-binding and cross-linking functions of actinin

1.3.1 The structure of the rod domain facilitates actin-crosslinking

Actinin is primarily known for its ability to bind and cross-link actin filaments. The spectrin-like repeats of the rod domain define the elongated shape of the molecule as well as the anti-parallel association of the subunits that places the functional domains (actin-binding domain and calmodulin-like domain) at the ends of each molecule (Djinović-Carugo et al., 1999). The symmetry of the dimer rod domains allows the alignment of anti-parallel actin-binding domains that facilitate actin cross-linking. In skeletal and cardiac muscle, actinin links actin filaments originating from adjacent sarcomeres. In this case the orientation of actin-binding domains is complementary to the anti-parallel orientation of actin filaments in the Z disk (Figure 1.8A). However, this ordered lattice formed by the actinin-actin interactions in skeletal and cardiac muscle is not maintained in smooth muscle and non-muscle cells. Here actin filaments can assume both parallel and anti-parallel orientations (Figure 1.8B). This difference in cross-linking topology requires a 180^{0} difference in the orientation of actin-binding sites. While the 90^{0} twist of the rod domain stabilises the dimer, it restrains the orientation of the actin-binding sites of actinin (Ylänne et al., 2001). Electron microscopic studies combined with the fact that the actin-binding domain is susceptible to proteolytic cleavage suggest that this domain has an in-built flexibility that facilitates this shift in orientation (Ylänne et al., 2001; Taylor & Taylor, 1993; Winkler et al., 1997; Mimura & Asano, 1986). Therefore while the molecular structure of the rod domain facilitates dimer formation and therefore actin cross-linking, the flexibility provided by the neck of the actin-binding domain allows for variable actin filament orientations.

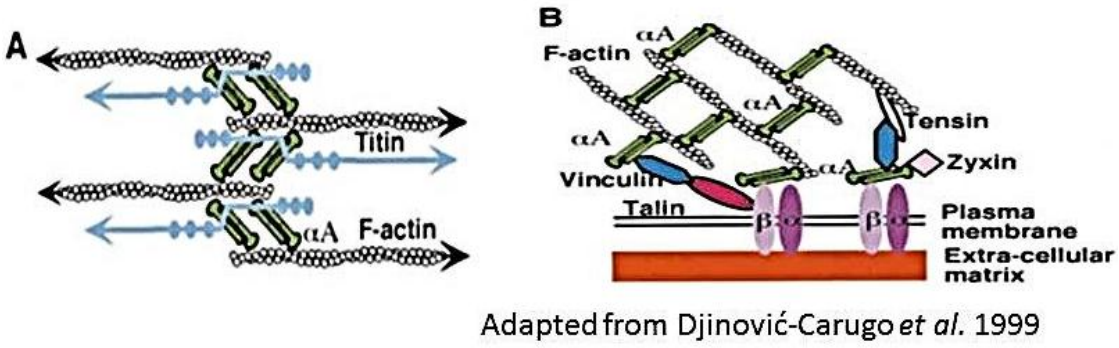

Figure 1.8 The different orientations of actin filaments coordinated by actinin. (A) Muscle actinin (green) cross-links actin filaments (white) from adjacent sarcomeres. Titin (blue) interacts with actinin at two sites (actin-binding domain and the rod domain). Titin provides binding sites for numerous proteins and is thought to play an important role as sarcomeric ruler and as blueprint for the assembly of the sarcomere (Young et al., 1998). (B) Non-muscle actinin (green) located at a focal adhesion site where it links the cytoskeleton to membrane associated structures.

Studies of slime mould *Dictyostelium discoideum* actinin indicate that the molecular architecture of the actinin dimer allows the binding of calcium to the CaM domain of one monomer to sterically prevent the actin-binding function of the ABD of the neighbouring monomer (Noegel et al., 1987). The ABD and CaM domains of actinin are highly conserved and are the two known sites of alternative splicing of human actinin. Functional diversity between isoforms has arisen through exon duplication and the formation of alternative splice variants (Lek et al. 2010a). Tandem duplication has occurred in the case of a number of actinin exons (Figure 1.9). However, tandem exon duplication is restricted to exons 8 and 19 in humans.

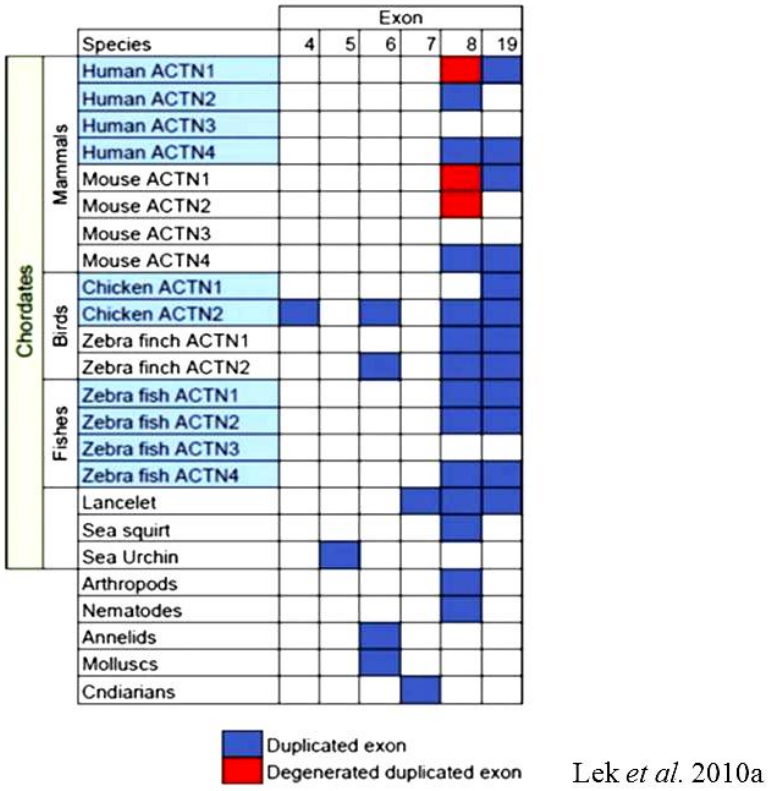

Figure 1.9 Tandem exon duplication across animal actinin genes. Duplication across the actin-binding domain (exon 1-8) is present in all animals. Duplication of exon 19 within the EF-hand domain is restricted to chordates. Duplicated exons were considered degenerate if splicing acceptor and donor sites were lost and/or contained a stop codon (Lek et al. 2010a)

1.3.2 Alternative splicing of actinin affects its actin-binding properties

1.3.2.1 Actin-binding domain: Exon 8 splicing

Alternative splicing of exon 8 in the actin-binding domain occurs broadly in metazoans and has been maintained in mammalian actinin-4 but not actinin-1 (Lek et al. 2010a). Splicing results in expression of either exon 8a or 8b. There are three amino acid differences between actinin-4 8a and 8b variants. These are asparagine (aa 248) to glycine, alanine (aa 250) to leucine and serine (aa 262) to cysteine (Honda et al., 2004). Figure 1.10 shows amino acid sequence alignments of human exon 8a and 8b variants. The actin-binding domain of actinin contains two calponin homology domains (CH). Splicing of exon 8 modifies the C-terminal of the CH2 domain and may function as a way of altering actin-binding affinity and regulation (Lek et al. 2010a). Evidence to support this includes the fact that the CH1 domain is

essential for actin-binding whereas the CH2 domain is thought to acts as a modifier for actin-binding (Gimona et al., 2002). Reports suggest that CH1 and CH2 domains may have evolved to perform different functions (Bañuelos et al., 1998). Point mutations within exon 8 cause a kidney disease called focal segmental glomerulosclerosis (FSGS) and are reported to result in an actinin-4 variant with an increased affinity for actin (Kaplan et al., 2000). Interestingly, these point mutations occur in conserved sites adjacent to the three altered amino acid sites in the actinin-4 8b variant (Figure 1.10). The functional significance of alternative splicing of exon 8 is not clear, though specific expression of actinin-4 exon 8b occurs in small cell lung cancer, high grade neuroendocrine tumours and is also reported to have enhanced actin-binding and altered subcellular localisation compared to the 8a variant (Honda et al., 2004; Miyanaga et al., 2012). Altogether this information supports the theory that exon 8 may be a key sequence that influences actin-binding affinity. It is also noteworthy that exon 8 encodes a protein segment thought to play a key role in regulating actin binding based on structural studies (Franzot et al., 2005). Thus alternative splicing of exon 8 may alter actin-binding properties but this has not been thoroughly investigated.

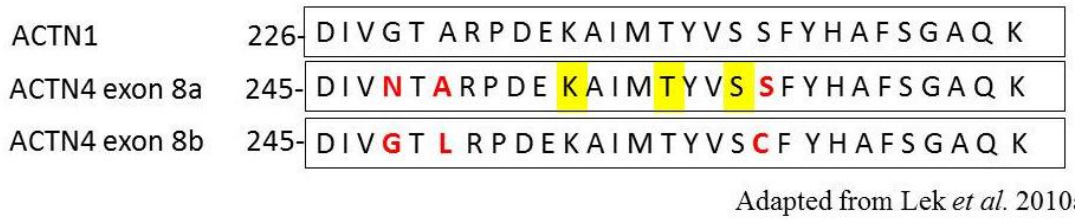

Figure 1.10 Alignment of amino acid sequences of human actinin exon 8a and 8b variants. Alternative splicing of actinin-1 exon 8 does not occur. The three amino acids that differ between actinin-4 variants 8a and 8b are highlighted in red. The amino acids whose point mutations result in FSGS are highlighted in yellow.

It is noteworthy that alternative splicing of exon 8 occurs in the muscle isoform actinin-2 (Lek et al. 2010a). Alternative splicing of actinin-2 exon 8 occurs in *C. elegans*, it also results in a non-muscle actinin-2 isoform in *D. melanogaster* and a brain-specific actinin-2 isoform in humans (Lek et al. 2010a). Despite the conservation of this isoform in both vertebrates and non-vertebrates, little is known about its function. Human but not mouse brain expresses alternate actinin-2 exon 8

(Lek et al. 2010a). Based on these observations, alternative splicing of actinin-2 may have functional significance for brain development and function in humans.

Alternative splicing of exon 6 in molluscs and annelids and exon 7 in *B. floridae* also acts to modify the sequence of the CH2 domain of actinin (Lek et al. 2010a). Therefore, alternative splicing within the CH2 domain may allow actinin to vary its actin-binding properties. No alternative splice variants of actinin-3 have been identified.

1.3.2.2 Calmodulin-like domain: Exon 19 splicing

The EF-Hand Motif

The calmodulin-like domain is the second site of alternative splicing of actinin. It contains two EF-hand motifs. The EF-hand motif is the most common Ca^{++}-binding motif. It consists of a helix-loop-helix structure composed of ~12 residues. Six of these residues are ligands that coordinate Ca^{++} ions with the pattern X·Y·Z·Y·X··Z where X,Y,Z,-X,-Y and –Z refer to the vertices of the calcium coordination octahedron and the dots represent intervening residues (Lewit-Bentley & Réty, 2000; Imamuras et al., 1994). The key characteristic of the EF-hand is its ability to change confirmation upon binding calcium which results in transition from a closed to an open state. This change in confirmation translates regulatory signals into functional responses. In the case of the antiparallel actinin dimer the proximity of each ABD to the CaM domain of the opposing monomer may facilitate calcium regulation of actin-binding and cross-linking.

Exon 19 splicing of actinin

Alternative splicing of exon 19 affects the EF-hand motifs of actinin-1 and -4 resulting in either Ca^{++}-sensitive or -insensitive isoforms with regard to their actin-binding function. Alternative splicing of exon 19 was first described for actinin-1 (Waites et al., 1992). The splicing of exon 19a or 19b is usually mutually exclusive and these isoforms are commonly refered to as the "non-muscle" and "smooth muscle" isoforms respectively, although the latter is also expressed in cardiac and skeletal muscle as well as in the adult brain (Kremerskothen et al., 2002). The non-

muscle exon (19a) forms the C-terminus of the first EF hand and its inclusion results in a functionally Ca^{++}-sensitive EF-hand. Inclusion of the downstream smooth muscle exon (19b) results in a Ca^{++}-insensitive EF-hand (Figure 1.11). In 2002, a novel brain-specific actinin-1 isoform was discovered in the rat. In this brain-specific isoform both exons 19a and 19b were combined in the same transcript (19a+19a). Figure 1.11 shows the corresponding protein sequences of human actinin-1 and -4. Actinin-2 and -3 have lost this alternative splicing mechanism and therefore only express Ca^{++}-insensitive isoforms. Studies indicate the EF-hand II may not be essential for Ca^{++}-sensitivity (Witke et al., 1993).

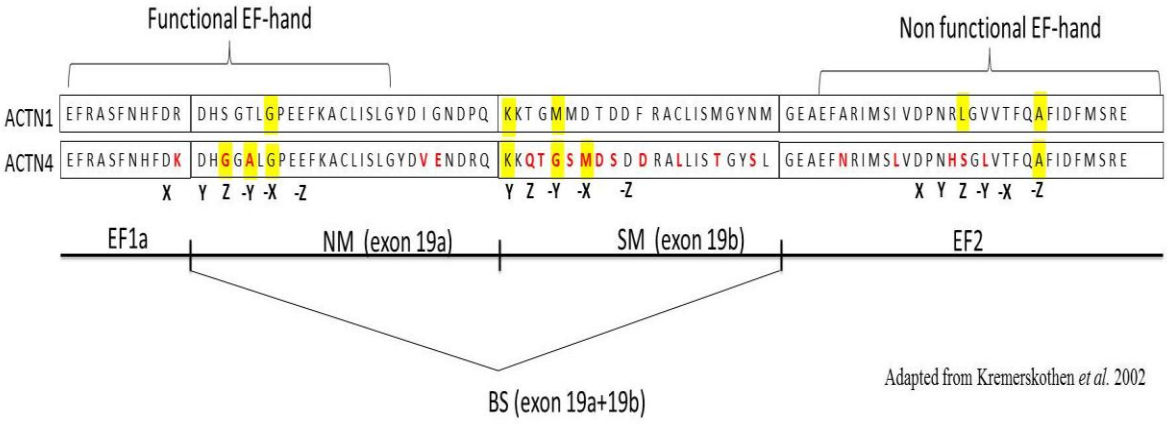

Figure 1.11 Amino acid sequences of human actinin-1 and -4 EF-hand motifs. Amino acids are shown in one letter code. Boxes and line segments represent the exon 19 variants deduced from the actinin genes. An actinin-1 brain-specific isoform (19a+19b) has only been detected in the rat brain. No brain-specific isoform (19a+19b) of actinin-4 has been detected. X,Y,Z,-Y,-X and –Z indicate the vertices of calcium coordination. Of the Ca^{++}-coordinating amino acids, those that do not possess oxygen-containing side-chains are highlighted (yellow). Note: more actinin-1 Ca^{++}-coordinating amino acids of exon 19a possess oxygen-containing side-chains than the corresponding region of actinin-4. Differences in amino acid sequence between actinin-1 and -4 are highlighted in red on the actinin-4 sequence. (NM=non-muscle, SM-smooth-muscle and BS=brain-specific).

Effect of exon 19 splicing on the calcium sensitivity of actinin

In the 1970s actinin was originally isolated from skeletal muscle. Since then actinin has been isolated from a number of cells and tissues including HeLa cells (Burridge & Feramisco, 1981), platelets (Rosenberg et al., 1981), macrophages (Bennett et al., 1984), brain (Duhaiman & Bamburg, 1984), skeletal muscle (Duhaiman & Bamburg, 1984), smooth muscle (Duhaiman & Bamburg, 1984), kidney (Kobayashi &

Tashima, 1983) and lung (Imamura & Masaki, 1992). Actinin isolated from different sources has been classed into two groups: Ca^{++}-sensitive and Ca^{++}-insensitive with regard to their actin-binding function. As discussed previously, the alternative splicing of exon 19 results in Ca^{++}-sensitive (19a) and Ca^{++}-insensitive (19b) actinin isoforms. In 1992, the first distinction was made within the Ca^{++}-sensitive group of non-muscle actinins. Imamura *et al.* identified a non-muscle actinin from chicken lung tissue, the Ca^{++} sensitivity of which was much lower than that of other reported non-muscle actinin (Imamuras et al., 1994). Sequence analysis of this "low-Ca^{++}-sensitive type non-muscle actinin" revealed that differences existed when compared to the sequence of previously identified non-muscle actinin. These differences occurred in the amino-terminal region, spectrin-like repeats and in the EF-hand motifs of the CaM domain. More specifically, a defect in one of the five oxygen-containing amino acid side chains involved in liganding calcium was observed, suggesting the lower Ca^{++}-sensitivity observed may be attributed to this defect. The isoform observed by Imamura *et al.* represents chicken actinin-4. Figure 1.11 shows corresponding amino acid sequences from human actinin-1 and -4. Here we observe an alteration in two of the five oxygen-containing amino acid side chains of actinin-4 when compared to actinin-1. Based on this sequence analysis it would be interesting to determine if the sequence differences in the EF-hand 1 motif of human actinin-1 and -4 could result in varying degrees of Ca^{++} sensitivity between these two non-muscle isoforms. It is noteworthy that substitutions of certain Ca^{++} liganding residues of the Ca^{++}-binding loop can be accommodated without affecting Ca^{++} ligand geometry (Grabarek, 2006). Disruption of possible Ca^{++}-coordination sites, by replacement of charged amino acids with alanine in the EF-hand motif, has little effect on Ca^{++}-dependent inactivation of L type calcium channels (Zhou et al., 1997). In fact the inhibitory effect of calcium was attributed to a sequence downstream of the EF-hand motif. However, other studies report the role of the EF-hand motif in the Ca^{++} sensitivity of L-type calcium channels (Zühlke & Reuter, 1998). It may be that certain Ca^{++} liganding residues are more important than others in mediating the effects of calcium. Similar to the calmodulin-like domain (CaM) of actinin, calmodulin contains as C-terminal Glu ligand at position –Z. The refinement of the crystal structure of calmodulin has delineated the critical role of this glutamic acid residue in calcium-binding (Babu et al., 1988). Mutations of this ligand are reported to impair the calcium-binding properties of calmodulin (Sites et al., 1992). Figure

1.11 shows that this glutamic acid residue positioned at -Z is conserved between actinin-1 and -4.

Different actin-binding affinities and/or Ca^{++} sensitivites may help to explain functional differences between the non-muscle actinins. The actin-binding affinities and Ca^{++} sensitivies of actinin-1 and -4 and their splice variants have not been directly compared in a comprehensive manner.

1.4 The non-muscle actinin isoforms

1.4.1 Localisation of the non-muscle actinin isoforms

The non-muscle isoforms are present in multiple subcellular regions, including cell-cell and cell-matrix contact sites, cellular protrusions, lamellipodia and stress fibre dense regions (Otey & Carpen, 2004). Figure 1.8B shows a focal adhesion site where actinin links the cytoskeleton to membrane associated structures. In 1989, actinin-1 was first sequenced from a human placental cDNA library (Millake et al., 1989). Actinin-4 was identified by immunoscreening of a human foreskin keratinocyte (HFK) cDNA library (Honda et al., 1998). Honda *et al.* observed distinct localisation patterns of the non-muscle actinins in a number of cancer cell lines. Actinin-1 localises specifically at the ends of actin stress fibres, at focal adhesions and adheren junctions (Honda et al., 1998). In contrast, actinin-4 co-localises with actin stress fibres and is dispersed in the cytoplasm and the nucleus (Honda et al., 1998). Actinin-4 is highly concentrated in the cytoplasm where cells are sharply extended and stains intensely at the edges of cell clusters (Honda et al., 1998). Actinin-4 is observed at the leading edge of migrating epithelial cancer cells (Honda et al. 1998). Araki *et al.* confirmed the localisation of actinin-1 at focal adhesion sites and suggested that this isoform may be a structural component involved in cell adhesion rather than force generation (Araki et al., 2000). Araki *et al.* proposed that actinin-4 was unlikely to contribute to cell adhesion as it is predominantly associated with moving structures such as dorsal ruffles (Araki et al., 2000). They demonstrated that actinin-4 concentrations relative to F-actin were higher in peripheral inward curved ruffles and dorsal circular ruffles, presumed precursor forms of

macropinosomes, than in straight linear ruffles, while actinin-1 concentrations were uniform among the different types of ruffles.

1.4.1.1 Nuclear localisation of actinin-4

As mentioned, Honda *et al.* observed the nuclear localisation of actinin-4 but not actinin-1 in a number of cancer cells (Honda et al., 1998). Inhibition of the PI-3 kinase–mediated signalling pathway induces nuclear translocation of actinin-4 (Honda et al., 1998). Inhibition of actin polymerisation has a similar effect indicating that translocation of actinin-4 is also caused by loss of its association with the cytoplasmic actin cytoskeleton (Honda et al., 1998). Nuclear localisation appears to be a unique characteristic of actinin-4. Actinin-4 is too large to simply diffuse through the nuclear pore complex into the nucleus. In 2010, the molecular mechanism underlying the nucleoplasmic shuttling of actinin-4 was determined (Kumeta et al., 2010). Actinin-4 was found to be imported into the nucleus through the nuclear pore complex in an importin-independent manner and exported by the chromosome region maintenance-1 (CRM1)-dependent pathway (Kumeta et al., 2010). Nuclear accumulation of actinin-4 is also observed in A431 cells treated with tumour necrosis factor (TNF) or epidermal growth factor (EGF) in association with the p65 subunit of nuclear factor NF-κB (Babakov et al., 2008). It has been reported that the interaction of actinin-4 with NF-κB may be mediated by adhesion to extracellular matrix proteins (Bolshakova et al., 2007). Extracellular matrix proteins such as laminin and fibronectin have been shown to modulate changes in the intracellular distribution of actinin-1 and -4 (Bolshakova et al., 2007). Nuclear localisation of actinin-4 is supported by its detection in nuclear complexes by mass spectrometry (Khotin et al., 2009).

1.4.2 Functions of the non-muscle actinin isoforms

1.4.2.1 Role in migration

Actinin and its interactions play a role in cell migration. Cell migration can be divided into four processes: extension of the leading edge of the cell, adhesion to the substratum, disassembly of focal adhesion complexes and subsequent retraction of the trailing end of the cell. Actinin is essential for the binding of microfilaments to integrins in focal adhesion complexes. Changes in actinin result in the breakage of links between microfilaments and integrins and result in the subsequent retraction of the stress fibre (Rajfur et al., 2002). Studies of adhesion assembly and disassembly identified a hierarchical mechanism for the formation of adhesions in which paxillin accumulation is followed by organised actinin, which in turn is followed by visibly organised α5 integrin (Laukaitis et al., 2001). Adhesion disassembly involved severing of the integrin–cytoskeletal linkage and the translocation and dispersal of paxillin and actinin–containing cytoskeletal complexes at the cell rear (Laukaitis et al., 2001). Actin and actinin orchestrate the assembly and maturation of nascent adhesions in a myosin II motor-independent manner (Choi et al., 2008). To date, most migration studies have been carried out in planer dishes that constitute a 2-dimensional (2D) environment. Studies of cells within a more physiological 3-dimentional (3D) matrix show that focal adhesion proteins, including actinin and paxillin do not form aggregates but are diffusively distributed throughout the cytoplasm (Fraley et al., 2010). However, despite the absence of detectable focal adhesions, focal adhesion proteins still modulate cell motility by affecting protrusion activity and matrix deformation (Fraley et al., 2010). Therefore both in 2D and 3D matrixes actinin is a critical component involved in cell migration.

1.4.2.2 Role in endocytosis

Actinin-4 is closely associated with newly formed micopinosomes and gradually dissociates from these structures as they mature (Araki et al., 2000). Similar redistribution of actinin-4 is observed during phagocytosis. This suggests that actinin-4 may play the same role in the two mechanistically analogous types of endocytosis, i.e. macropinocytosis and phagocytosis (Araki et al., 2000). Actinin-4 is

part of a complex containing BERP, myosin V and the endosome-associated protein hrs, which is necessary for efficient transferrin receptor recycling (Yan et al., 2005).

1.4.2.3 Role in cytokinesis

Cytokinesis in mammalian cells involves remodelling of equatorial actin filaments mediated by actinin. F-actin-binding and cross-linking activities of actinin are required for its equatorial localisation (Low et al., 2010). Cytokinesis requires tightly regulated remodelling of the cortical actin network mediated by actinin (Mukhina et al., 2007; Reichl & Robinson, 2007). Studies suggest that the Ca^{++} sensitivity of actinin is required for its equatorial accumulation that is crucial for the initial equatorial actin assembly (Jayadev et al., 2012). It remains to be seen if actinin-1 and -4 are differentially involved in this process.

1.4.2.4 Unique role of actinin-4 in the kidney

The different localisation patterns observed for the non-muscle actinins indicates that they may have different functions. In keeping with this theory are reports that actinin-4 has a unique function in the kidney. Mutations in actinin-4 cause a form of kidney disease called focal segmental glomerulosclerosis (FSGS) (Kaplan et al., 2000). Podocytes play a key role in the maintenance of glomerular permselectivity (Pavenstädt et al., 2003). In the healthy kidney, podocytes are in contact with the extracellular matrix. Podocytes form a tight network of interdigitating foot processes, that are bridged by filtration-slit diaphragms, and permselectivity of the glomerular capillary wall is dependent on the maintenance of podocyte structure and of their foot processes (Cybulsky & Kennedy, 2011) . Podocyte architecture is maintained by an organisation of actin filaments in the cytoplasm. FSGS is characterised by podocyte injury, leading to apoptosis, detachment, and podocytopenia (Cybulsky & Kennedy, 2011; Henderson et al., 2009; Michaud, 2003). It has been reported that disruption of focal adhesions using a truncated version of actinin renders osteoclasts more susceptible to apoptosis (Triplett & Pavalko, 2006). This highlights a role for actinin and focal adhesion signalling in cell survival. FSGS leads to increased urinary protein excretion and decreased kidney function. Renal insufficiency in

affected patients can often progress to end-stage renal failure, requiring either dialysis therapy or kidney transplantation. Interestingly *Actn4 -/- mice* develop FGSG even though they express normal levels of actinin-1 suggesting that actinin-1 and -4 are not functionally redundant (Kos et al., 2003). Despite the widespread distribution of actinin-4, histologic examination of mice shows abnormalities only in the kidneys (Kos et al., 2003). It was noted that leukocytes from *Actn4 -/-* mice demonstrated increased chemokinesis and chemotaxis (Kos et al., 2003). Hypotheses for the specific effect of actinin-4 deficiency on kidney function include the possibility that a podocyte-specific protein-protein interaction is altered by human disease–associated mutations, or that the unique structure of podocytes makes this cell type more susceptible to a subtle change in cytoskeletal architecture (Kos et al., 2003).

Alternative splice variant of actinin-4

The mutations that result in FSGS occur within exon 8 of the actin-binding domain and are reported to result in an actinin-4 variant with an increased affinity for actin (Kaplan et al., 2000; Weins et al., 2007). Interestingly, the point mutations responsible for FSGS occur in conserved sites adjacent to the three amino acids that were found to be altered in a splice variant of actinin-4 denoted "variant 8b" (see Figure 1.10). This actinin-4 8b variant is associated with small cell lung cancer and more recently high grade neuroendocrine pulmonary tumours (Honda et al., 2004; Miyanaga et al., 2012). Phosphorylation of an actinin-4 tyrosine residue, that lies in close proximity to a point mutation (Lys255Glu) seen in FSGS, occurs in human carcinomas (Shao et al., 2010; Lee et al., 2008; Rikova et al., 2007; Rush et al., 2005). Altogether this highlights this region of the actin-binding domain of actinin-4 as a hotspot for variations and disease-related mutations that may alter its actin-binding function.

1.4.2.5 Role in cancer

Actinin-1 and -4 are differentially regulated during the development and progression of astrocytomas (Quick & Skalli, 2010). Each of these isoforms uniquely contributes to distinct malignant properties of astrocytoma cells. Both actinin-1 and

actinin-4 make critical and distinct contributions to cytoskeletal organisation, rigidity-sensing, and to the motility of glioma cells (Sen et al., 2009). Silencing of actinin-1, but not actinin-4, blocks pressure-stimulated cell adhesion in a number of human colon cancer cell lines (Craig et al., 2007). Knockdown of actinin-4 but not actinin-1 significantly reduces neutrophil diapedesis (Celli et al., 2006). Simian virus 40-transformed 3T3 cells transfected with actinin-1 cDNA display a marked reduction in their ability to form tumours in mice (Glück et al., 1993). While actinin-4 has been reported to suppress tumourigenicity in the case of neuroblastoma cells (Nikolopoulos et al., 2000), it is the predominant non-muscle actinin isoform associated with the cancer phenotype (Table 1.1).

Actinin-4 is the predominant non-muscle isoform associated with cancer

There are many reports in the literature linking actinin-4 to the cancer phenotype (Table 1.1). Membrane ruffling is a parameter of tumour cell invasion and metastases (Jiang, 1995). Therefore, association of actinin-4 with membrane ruffling supports the idea that actinin-4 is a marker of cancer progression (Honda et al., 1998; Yamamoto et al., 2007; Miyanaga et al., 2012). Actinin-4 protein levels are elevated in a number of cancers including breast, ovarian, colorectal, bladder, pancreatic, ovarian and glioblastomas (Table 1.1). Actinin-4 enhances the motility and metastatic potential of various carcinoma cell lines (Table 1.1). This suggests that actinin-4 may have some unique characteristic that facilitates its role in cancer.

Although the non-muscle actinin isoforms show 87% amino acid identity, they are currently viewed as distinct entities (Honda et al., 1998). Each isoform is reported to exert distinct effects on cell migration, adhesion and proliferation depending on the cell type studied (Quick & Skalli, 2010; Sen et al., 2009; Craig et al., 2007; Glück & Ben-Ze'ev, 1994; Honda et al., 2005; Nikolopoulos et al., 2000). Overall it is clear that actinin-1 and -4 exert distinct functions and localisation patterns from each other. The mechanisms underlying these distinct functions have yet to be elucidated.

Actinin-4 and Cancer	Reference
Actinin-4 is associated with advanced and metastatic **ovarian** carcinoma	(Barbolina et al., 2010)
Actinin-4 expression in **ovarian** cancer is a novel prognostic indicator independent of clinical stage and histological type.	(Yamamoto et al., 2007)
Gene amplification and actinin-4 protein overexpression drive tumour development and histological progression in a high-grade subset of **ovarian** clear-cell adenocarcinomas	(Yamamoto et al., 2012)
Actinin-4 increases cell motility and promotes lymph node metastasis of **colorectal** cancer	(Honda et al., 2005)
Actinin-4 expression and gene amplification of actinin-4 in invasive ductal carcinoma of the **pancreas**	(Kikuchi et al., 2008)
Actinin-4 expression levels significantly correlate with worse survival after **pancreatic ductal adenocarcinoma** resection	(Welsch et al., 2009)
Actinin-4 is closely associated with an infiltrative histological phenotype and correlated significantly with a poorer prognosis in **breast** cancer	(Honda et al., 1998)
Actinin-4 is a nuclear receptor co-activator that promotes proliferation of MCF-7 **breast** cancer cells.	(Khurana et al., 2011)
An alternative splice variant of actinin-4 is present in small cell **lung** cancer	(Honda et al., 2004)
The expression of variant actinin-4 identified in small cell lung cancer is an independent prognostic factor for patients with high grade **neuroendocrine tumours**	(Miyanaga et al., 2012)
Actinin-4 mRNA and protein levels are elevated in **bladder** cancer cell lines that exhibit increased growth and invasion activity. Knockdown of actinin-4 inhibited invasion of bladder cancer cells.	(Koizumi et al., 2010)
Actinin 4 is elevated in high-grade **astrocytomas** compared to normal brains and low grade astrocytomas. Downregulation of actinin-4 reduces cell motility, adhesion, cortical actin, and RhoA levels in astrocytoma cells	(Quick & Skalli, 2010)
RNAi-mediated down-regulation of α-actinin-4 decreases invasion potential in **oral squamous cell carcinoma**	(Yamada et al., 2010)

Table 1.1 Actinin-4 is associated with cancer development and progression. Numerous reports exist in the literature linking actinin-4 to cancer. For clarity the various types of cancer that have been associated with actinin-4 are highlighted in bold.

1.5 The muscle actinin isoforms

1.5.1 Localisation of the muscle actinin isoforms

The muscle actinins are major structural components of the Z-disk of muscle sarcomeres, where they function to anchor the actin-containing thin filaments (Mills et al., 2001). Figure 1.8A shows the muscle Z disk where actinin cross-links antiparallel actin filaments from adjacent sarcomeres. Actinin-2 is expressed in all muscle fibres, whereas actinin-3 has a more specialised expression pattern and is expressed only in fast twitch glycolytic skeletal muscle fibres, with low levels of expression in the brain (Mills et al., 2001). At the amino acid level, human actinin-2 and actinin-3 are 80% identical and 90% similar (Mills et al., 2001).

1.5.2 Actinin-3 deficiency

Actinin-3 is absent from around one billion individuals worldwide due to homozygosity for a premature stop codon (R577X) (MacArthur et al., 2007). This nonsense mutation accounts for most cases of true actinin-3 deficiency (Mills et al., 2001). The fact that actinin-3 is not associated with an obvious disease phenotype, raises the possibility that the muscle actinin isoforms are functionally redundant in humans, and that actinin-2 is able to compensate for actinin-3 deficiency. However, given that actinin-3 has been highly conserved during vertebrate evolution, it is unlikely to be completely functionally redundant. This has been confirmed by demonstrating that the loss of actinin-3 influences the function of human skeletal muscle (Virel & Backman, 2004; Dixson et al., 2003). Two independent studies have reported associations between actinin-3 deficiency (R577X) and elite athlete status (Niemi & Majamaa, 2005; Yang et al., 2003). Loss of ACTN3 gene function alters mouse muscle metabolism and shows evidence of positive selection in humans (MacArthur et al., 2007). The frequency of the null genotype is lower in sprinting and power athletes and higher in endurance athletes. In fast twitch (glycolytic 2B) muscle fibres suffering from actinin-3 deficiency there is a shift towards a slow fibre phenotype with increased fatigue resistance, and an increase in oxidative enzyme activity. Actinin-3 deficiency reduces the activity of glycogen phosphorylase which

results in this fundamental shift towards more oxidative pathways of energy utilisation (Berman & North, 2010). The shift towards more efficient oxidative metabolism may underlie the selective advantage of the ACTN3 R577X allele during evolution (MacArthur et al., 2007). Interestingly this suggests that it may be beneficial for athletes to express actinin-3 for sprint events whereas it may be beneficial to lack actinin-3 for endurance events. Actinin-3 is one of only two genes (the other is CASP12) for which strong evidence exists for recent positive selection of a null allele in human populations (Yngvadottir et al., 2009). The CASP12 null allele, which has been positively selected for in non-African populations, results in the expression of a truncated protein that decreases the risk of developing sepsis (Saleh et al., 2004).

1.5.3 Evidence of distinct functions of actinin-2 and -3

Murine actinin-2 and -3 are differentially expressed, spatially and temporally, during embryonic development (Mills et al., 2001). In contrast to humans, murine actinin-2 does not completely overlap actinin-3 in postnatal skeletal muscle, suggesting that actinin-3 has an independent function (Mills et al., 2001). Supporting the idea that the muscle actinins may have independent functions is the report that actinin-2 deficiency results in sarcomeric defects in zebrafish that cannot be rescued by actinin-3 (Gupta et al., 2012). Actinin-3 appears to perform a specialised function in fast twitch muscle fibres as discussed, however due to its restricted expression pattern it cannot compensate for mutations in actinin-2 known to result in cardiomyopathy (Chiu et al., 2010). An actinin-2 mutation located in the actin-binding domain that prevents actinin binding to the muscle LIM protein results in cardiomyopathy (Mohapatra et al., 2003). Together, this information suggests that actinin-2 and -3 perform overlapping but distinct functional roles and that the phenotypic effects of actinin-3 deficiency are due primarily to functional differences between actinin-2 and -3 (MacArthur et al., 2007).

1.6 Regulation of actinin

As discussed, the literature reports actinins involvement in a number of cellular functions including proliferation, adhesion, migration and regulation of transcription. Many studies of actinin regulation have focused on its role in cell motility. Cell migration can be divided into four processes: extension of the leading edge of the cell, adhesion to the substratum, disassembly of adhesion complexes and subsequent retraction of the trailing end of the cell. Cell adhesion to the extracellular matrix is mediated by integrins which are linked to the cytoskeleton by proteins in focal adhesion complexes (FACs) (Webb et al., 2002). These FACs must be disassembled in order for cell movement to occur. The localisation of actinin in FACs suggests that it might serve to anchor the network of actin filaments to the plasma membrane thereby stabilising these adhesion sites.

The four main regulatory mechanisms of actinin are:

1) Processing by proteases
2) Binding to phosphatidylinositol intermediaries
3) Phosphorylation by kinases
4) Binding to calcium

1.6.1 Processing by proteases

Numerous mechanisms have been identified that regulate FAC disassembly through actinin. Structural proteins spectrin and talin are linked to actinin through vinculin. Together this complex links FACs to the cytoskeleton (Cuevas et al., 2003; Dourdin et al., 2001). Changes in cell shape activate a MAPK kinase kinase which activates a cysteine **protease** called calpain (Cuevas et al., 2003). It is proposed that calpain cleaves the structural proteins spectrin and talin and in this manner destabilises FACs (Cuevas et al., 2003). It is also proposed that actinin-zyxin association may promote disassembly and translocation of FACs facilitating cell retraction (Bhatt et al., 2002). This is supported by the fact that a spatial and temporal relationship exists between actinin and zyxin co-localisation and that their translocation is observed in areas of cell retraction. Conversely, in areas of cell protrusion actinin and zyxin are less associated and their translocation and disassembly are not observed. Calpain

inhibition disrupts actinin localisation to zyxin-containing focal contacts and FAC disassembly (Bhatt et al., 2002). In short, calpain regulates the composition of FACs and the specific localisation of actinin in FACs.

1.6.2 Binding to phosphatidylinositol intermediaries

Activation of **phosphatidyl-inositol-3 kinase** (PI-3 kinase) is another mechanism that is known to regulate FAC disassembly. PI-3 kinase binds actinin through the p85 subunit (Shibasaki et al., 1994). The PI-3 kinase lipid product **phosphatidy-inositol 3,4,5 triphosphate** (PtdIns (3, 4, 5)-P3) (PIP3) binds to actinin and decreases it's affinity for β-integrin and its ability to cross-link actin. This decrease in the affinity of actinin for integrin promotes cell de-adhesion with the underlying substratum (Greenwood et al., 2000). Migration is induced in breast cancer MCF-7 cells that overexpress the insulin-like growth factor 1 receptor (IGF-IR). Signalling between the IGF-IR kinase and actin required PI-3 kinase-generated phospholipids and was found to be mediated by actinin (Guvakova et al., 2002). Studies of actinin-2 determined that the interaction of titin and actinin is controlled by a phospholipid-regulated intramolecular pseudoligand mechanism (Young & Gautel, 2000). For more details on this mechanism see Section 1.6.4. The interaction of actinin and actin is stimulated by **phosphatidylinositol 4,5-bisphosphate** (PIP_2) (Fukami et al., 1992). Hydrolysis of PIP_2 on actinin by tyrosine kinase activation may be important in cytoskeletal reorganisation (Fukami et al., 1994). A model had been proposed in which actinin interacts with PIP2 in the plasma membrane and promotes full opening of NMDA receptors (Michailidis et al., 2007). The report suggests that actinin supports activation of NMDA receptors via tethering their intracellular tails to membrane PIP2. Mutations in the PIP2 binding site of actinin dramatically reduce NMDA currents.

1.6.3 Phosphorylation by kinases

In platelets, actinin is a target of **focal adhesion kinase** (FAK). Actinin-1 has been shown to be phosphorylated on tyrosine 12 by FAK (Izaguirre et al., 2001). This reduces the affinity of actinin-1 for actin and results in the spreading of platelets

(Izaguirre et al., 2001). Tyrosine residues of actinin-1 and -4 are phosphorylated following stimulation with epidermal growth factor (Shao et al., 2010). However, it was observed that actinin-4 is phosphorylated to a greater extent than actinin-1. Phosphorylation of actinin-4 decreases its actin-binding activity (Shao et al., 2010). Phosphorylation of actinin-1 induces pressure-induced adhesion in colon cancer cells through regulation of the focal adhesion-Src interaction (Craig et al., 2007). Silencing of actinin-1 but not actinin-4 blocked pressure-stimulated cell adhesion (Craig et al., 2007). Altogether this suggests that phosphorylation may differentially regulate actinin-1 and -4. **PKN** is a serine/threonine protein kinase. PKN binds to and phosphorylates the head-rod domain of intermediate filament proteins such as neurofilament and vimentin *in vitro* (Mukai et al., 1996). Polymerisation of neurofilament L protein *in vitro* was inhibited by phosphorylation by PKN. PKN is linked to the cytoskeletal network via a direct association between PKN and actinin. This suggests that actinin may also be subject to phosphorylation by PKN (Mukai et al., 1997). Upon TNF-α induced phosphorylation actinin binds directly to the cytoplasmic tail of ICAM-1 (Zhou et al., 2006). As mentioned actinin-4 is phosphorylated to a greater extent than actinin-1 post TNF-α stimulation. ICAM mobility and clustering is dependent on its association with actinin (Zhou et al., 2006). Altogether this evidence may support differential roles of actinin-1 and -4 in the regulation of ICAM-1. It is noteworthy that ICAM-1 expression determines the malignant potential of cancer (Roland et al., 2007).

1.6.4 Binding of calcium

Actinin-1 and -4 are known to be Ca^{++}-sensitive. Binding of Ca^{++} to the EF-hands within the CaM domain of actinin reduces its affinity for actin which provides an important mechanism for linking stress fibres to FACs. Calcium spikes are temporally correlated with movement and disassembly of focal adhesions (Giannone et al., 2004). Studies of slime mould *Dictyostelium discoideum* actinin indicate that the molecular architecture of the actinin dimer allows the binding of calcium to the CaM domain of one monomer to sterically prevent the actin-binding function of the neighbouring monomer via conformational change (Noegel et al., 1987), see Figure 1.1. It is proposed that at low calcium concentrations the CaM domain of actinin

wraps around the central (rod) domain permitting the actin-binding function of the neighbouring monomer. Following increases in calcium concentration, binding of calcium to the EF-hand structure causes the structure to fold back from the central part of the subunit, thus disturbing the interaction site of the neighbouring actin-binding domain with actin. The exact mechanism though which calcium regulates the actinin-actin interaction is unclear. However, mechanistic studies of phospholipid regulation of the actinin-titin interaction may provide an insight (Franzot et al., 2005; Young & Gautel, 2000).

The C-terminal CaM domain of actinin interacts with titin Z repeat motifs in the Z disk of the muscle sarcomere. Homologous sequences to Z disk motifs were detected in the actinin sequence, located between the actin-binding and the rod domain. These sequences act as a pseudoligand by interacting with the CaM domain of the neighbouring actinin monomer, thus preventing binding of actinin to the Z disk. It was found that this auto-inhibition of titin binding was released upon binding of a Z disk phospholipid to the actin-binding domain of actinin. Binding of the phospholipid also increased the actin-binding properties of actinin (Fukami et al., 1992). This regulatory mechanism is capable of controlling site-specific interactions of actinin. The intra-molecular contacts defined here provide a structural model for intrasterical regulation of all actinin isoforms whereby the actin-binding and CaM domains can act as flexible entities that can exist in either closed or open conformations. Indeed electron microscopic studies have revealed that the ABD can adopt several different conformations through a flexible neck region between the rod and the head (Winkler et al., 1997; Ylänne et al., 2001). Studies were carried out on a tail end of the α/β heterodimer constructed from the N-terminal fragment of the spectrin β-subunit consisting of the actin-binding domain plus repeats β1 and β2, and the C-terminal fragments of the spectrin α-subunit containing repeats α19 and α20 plus the calmodulin domain. Analysis of this "minispectrin" supports the idea that the rod connects to the actin-binding domain via a neck. This study showed that the actin-binding region of the spectrin α/β heterodimer retains it functional properties even in a truncated form (Raae et al., 2003).

It is likely that this form of regulation is common for many actinin interacting-proteins. Interestingly, it has been suggested that the release of these inter-subunit interactions at either end of the anti-parallel dimer may result in conformational changes in the rod domain as this region is believed to be

considerably twisted in the free state (Young & Gautel, 2000; Djinović-Carugo et al., 1999). Such conformational changes could affect the binding of proteins to the rod (Young & Gautel 2000). Altogether this suggests that although actinin appears to be composed of three distinct domains, conformational changes permit interactions with one domain to influence those of another.

1.7 Actinin-interacting partners

1.7.1 The actinin rod domain: A structural platform for protein interactions

This domain is reported to act as a structural platform for cytoskeleton protein assemblies (Djinovic-Carugo et al., 2002). One of the main functions of the rod domain is to act as a binding site for other proteins and its curved surface makes it an ideal platform for such interactions (Sjoblom et al., 2008; Djinovic-Carugo et al., 2002). The spectrin-like repeats of the rod domain have the ability to act as a docking platform for cytoskeletal and signal transduction proteins. This means the rod domain can function both as a structural platform for cytoskeletal proteins and as a switchboard for signal transduction (Sjoblom et al., 2008). The conserved acidic surface of the rod is a possible interaction site for the cytoplasmic tails of transmembrane proteins involved in recruiting actinin to the plasma membrane (Djinovic-Carugo et al., 2002) . Rod domain interactions have been described for both muscle and non-muscle actinins and include cytoskeletal proteins (Klaavuniemi et al., 2004; Young et al., 1998), cell adhesion molecules (Heiska et al., 1996; Nieset et al., 1997), signalling proteins (Mukai et al., 1997) and ion channels (Wyszynski et al., 1997).

1.7.2 Actinin interacts with a diverse array of proteins

As discussed the actinins are present at multiple subcellular locations (Otey & Carpen, 2004). This allows them to come into contact with a diverse array of proteins. The following is an inconclusive list of known actinin-interacting partners.

1.7.2.1 Integrin/cell adhesion/transmembrane proteins

The actinin dimer is uniquely well suited to provide a strong elastic platform for the docking of proteins (Otey & Carpen, 2004). In particular the rod domain of actinin is believed to act as an interface for numerous protein interactions (Djinovic-Carugo et al., 2002). The non-muscle isoforms are present in cell-cell and cell-matrix contact sites, cellular protrusions, lamellipodia and stress fibre dense regions. Actinin is known to interact with numerous transmembrane proteins, including many adhesion molecules including **ICAM1** and **β-integrin** (Otey & Carpen, 2004; Carpén et al., 1992; Otey et al., 1990). It is believed that the interaction between actinin and adhesion receptors may serve numerous functions. Linking transmembrane receptors to the cytoskeleton provides structural stability for adhesion sites. Actinin is essential for the binding of microfilaments to integrins in focal adhesion sites. Inactivation of actinin through chromophore-assisted laser inactivation (CALI) results in breakage of actinin-integrin interactions and the subsequent retraction of stress fibres (Rajfur et al., 2002). Actinin can promote the clustering of adhesion molecules such as **ICAM2** which may serve to enhance their function at adhesion sites. (Otey & Carpen, 2004; Heiska et al., 1996). The cytoplasmic domains of many adhesion molecules including **L-selectin** can regulate their affinity and adhesive activity through interactions with cytoskeleton proteins such as actinin (Otey & Carpen, 2004) (Dwir et al., 2001).

Neuronal synapses are a highly specialised type of cell-to-cell junction. Neurotransmitter receptors are clustered on the post-synaptic membrane. Calcium regulation of **NMDA receptors** has been postulated to involve a linkage between the receptor and the cytoskeleton (Rosenmund & Westbrook, 1993). Actinin has been identified in the post-synaptic density fraction by mass spectrometric analysis (Walikonis et al., 2000). Actinin and calmodulin bind competitively to the NR1 subunit of the NMDA receptor (Wyszynski et al., 1997). Overexpression of Ca^{++}-sensitive but not Ca^{++}-insensitive isoforms of actinin resulted in reduced inactivation (Krupp et al., 1999). Inactivation is thought to occur after the NR1 dissociates from actinin due to competitive displacement by calmodulin and due to a reduction in the affinity of actinin for NR1 after binding of calcium to actinin. The Ca^{++} -insensitive muscle isoform, actinin-2 is reported to bind to NR1 and NR2 subunits of the NMDA receptor (Wyszynski et al., 1997). Actinin-2 physically anchors NMDA

receptors in the post-synaptic membrane and organises the numerous signalling molecules that accumulate at this site (Wyszynski et al., 1998). Actinin-1 interacts with the **metabotropic glutamate receptor type 5b** and modulates the cell surface expression and function of this receptor (Cabello et al., 2007). Altogether this highlights that actinin functions to maintain the structural integrity of neuronal synapses, to regulate neurotransmitter receptors and that modulation of actinins affinity for proteins can alter cellular functions.

1.7.2.2 Kinases

Calcium/calmodulin dependent protein kinase II (CaMKII) is capable of integrating information conveyed by the amplitude, frequency, and duration of local calcium transients to which it is exposed (Robison et al., 2005). Actinin can bind to a number of regulatory molecules including CaMKII (Otey & Carpen, 2004; Walikonis et al., 2001). As a result it can serve as a scaffold to coordinate signalling molecules at adhesion sites. CaMKII is dynamically targeted to neuronal synapses where it associates with the NR2B subunit of the NMDA receptor, densin and actinin in the postsynaptic density (Robison et al., 2005; Walikonis et al., 2001).

1.7.2.3 Focal Adhesion/cell:cell junction components

Actinin has been shown to interact with focal adhesion components such as **vinculin** and **talin** (Wachsstock et al., 1987; Crawford et al., 1992). **Cadherins** are Ca^{++}-dependent cell surface glycoproteins involved in cell-to-cell adhesion. Cadherins are linked to cytoskeleton proteins via catenins. Three catenins, α-, β-, and γ-catenin have been identified (Nieset et al., 1997). It is proposed that cadherin/catenin complexes are linked to the actin cytoskeleton via a direct association between actinin and α-catenin (Knudsen et al., 1995; Nieset et al., 1997). Actinin-1 immunoprecipitates with cadherin-catenin complexes (Knudsen et al., 1995; Nieset et al., 1997).

Hemidesmosomes are multimeric protein complexes that attach epithelial cells to the underlying matrix and serve as cell surface anchorage sites for the keratin cytoskeleton. Two hemidesmosome components, the α6β4 integrin heterodimer and

a human autoantigen termed BP180, are transmembrane proteins that link the extracellular matrix to the keratin network in cells. BP180 interacts with the C-terminal domain of both actinin-1 and -4 (Gonzalez et al., 2001).

Actinin also associates with components of dense regions. These are periodic structures found along stress fibres and are believed to be analogs of sarcomeric Z-disks. Several **LIM and PDZ domain proteins** associated with dense regions are known to interact with actinin (Otey & Carpen, 2004). LIM proteins such as zyxin function as a scaffold for the assembly of protein complexes involved in regulating cell motility and differentiation, and zyxin cycles between the nucleus and the cytoplasm (Crawford et al., 1992; Drees et al., 1999; Reinhard et al., 1999). Zyxin binds to the smaller LIM domain protein CRP, and actinin binds directly to both **zyxin** and **CRP** (Pomiès et al., 1997).

The PDLIM Family

The PDLIM family of proteins possess an N-terminal PDZ domain and C-terminal LIM domain(s) (Velthuis & Bagowski, 2007). Functionally, all PDZ and LIM domain proteins share an important trait, i.e., they can associate with and/or influence the actin cytoskeleton (Velthuis & Bagowski, 2007). An example of such a protein is **PDLIM1 (CLP-36)** that binds to actinin via its PDZ domain and to a kinase Clik1 through its LIM domain (Vallenius et al., 2000; Bauer et al., 2000). ClikI is largely a nuclear enzyme but is reported to transit between the cytoplasm and the nucleus (Vallenius & Mäkelä, 2002). This highlights actinin as a platform for protein interactions, in particular those that can shuttle between the cytoplasm and the nucleus.

PDLIM2 (Mystique) interacts with actinin-4 and stabilises stress fibres (Torrado et al., 2004; Sistani et al., 2011). Reduced expression of PDLIM2 is found in podocytes of patients with minimal change nephrotic syndrome and membranous nephropathy (Sistani et al., 2011). Mutations in actinin-4 also result in a kidney disease called focal segmental glomerulosclerosis (FSGS), however normal PDLIM2 levels are observed in FSGS (Michaud, 2003; Sistani et al., 2011). While this indicates that these two proteins are essential for kidney function, it shows that the effects of PDLIM2 on the actin skeleton are not dependent on actinin-4 (Sistani et al., 2011). This suggests that different mechanisms underlie these kidney diseases.

PDLIM3 (ALP) is a skeletal muscle protein that associates with actinin-2 in muscle Z disks. Several PDZ-LIM proteins localise to the muscle Z-disk. Biochemical and yeast two-hybrid analyses demonstrate that the PDZ domain of ALP binds to the spectrin-like motifs of actinin-2 (Xia et al., 1997). ALP, the afore-mentioned CLP36 protein, and the Z band alternatively spliced PDZ-containing protein **PDLIM6 (ZASP/Cypher)** have a conserved region named the ZASP-like motif (ZM) between PDZ and LIM domains (Klaavuniemi et al., 2004). ALP and actinin-2 have two interaction sites. The ZM motif is required for the interaction of ALP with the actinin rod and for targeting of ALP to the Z-line, while the PDZ domain of ALP binds the C-terminus of actinin (Klaavuniemi et al., 2004). The ZM-motif of CLP36 also interacts with the rod domain of actinin-2 and ZASP/Cypher was found to co-localise with actinin in a similar manner as ALP (Klaavuniemi et al. 2004; Klaavuniemi & Ylänne, 2006). These results highlight the ZM-motif as an important actinin-interacting motif that could act to stabilise certain conformations of actinin-2 that may strengthen Z-disk integrity. Whether the ZM-motif represents a conserved interaction site or whether it is mainly a structural motif remains to be seen.

PDLIM4 (RIL) modulates actin stress fibre turnover and enhances the association of actinin with F-actin (Vallenius et al., 2004). **PDLIM5** (Enigma Homolog/ENH) is reported to co-localise with actinin at the Z disk of rat cardiomyocytes (Nakagawa et al., 2000). This study identified both actinin and actin in a GST-PDZ domain pull-down assay. Together this suggests that ENH and actinin may interact with each other. **PDLIM8** (LMO7) contains a LIM domain only and can also interact with actinin (Ooshio et al., 2004)

Taken together, these reports highlight that two highly conserved protein interaction domains (LIM and PDZ) bind to actinin. These two domains are shared by many proteins, suggesting that there are many potential actinin-interacting partners that have yet to be identified.

1.7.2.4 Palladin/Myotilin Family

Another family of proteins known to interact with actinin include **myotilin**, **myopalladin** and **palladin**. These proteins all contain at least one copy of the IgC2

domain (Salmikangas et al., 1999; Parast & Otey, 2000; Bang et al., 2001; Mykkänen et al., 2001) . Myotilin and myopalladin are both abundant in striated muscle where they interact with muscle actinin (Salmikangas et al., 1999; Bang et al., 2001). Palladin on the other hand binds and co-localises with actinin in stress fibre dense regions and focal adhesions (Parast & Otey, 2000). The minimal residues in human palladin required for binding actinin are located in the CaM domain and the motif is conserved among the other palladin family members, myotilin and myopalladin (Beck et al., 2011). All three palladin family members bind to the EF-hand repeats 3–4 of the C-terminal domain of actinin (Rönty et al., 2004). Truncated actinin lacking the CaM domain and down regulation of palladin result in stress fibre collapse suggesting that both these proteins are important in maintaining the structure of the cytoskeleton (Schultheiss et al., 1992; Parast & Otey, 2000). Studies suggest that dysregulation of palladin expression may play a key role in the invasive cell motility that characterises metastatic cancer cells as well as in the development of cardiovascular diseases (Goicoechea et al., 2009; Jin, 2011). Additionally, palladin is directly implicated in a rare inherited form of pancreatic cancer (Pogue-Geile et al., 2006). In that study, a point mutation (P239S) in palladin that falls within the actinin binding site was identified in an inherited form of highly penetrant pancreatic cancer, suggesting that alteration of palladin/actinin interactions may have direct effects on cell motility.

1.7.2.5 Transcription factors/nuclear proteins

Nuclear localisation of actinin correlates with its association with nuclear proteins such as the transcription factor **NF-κB** (Babakov et al., 2008) . Actinin has been identified in nuclear protein complexes by mass spectrometric analysis (Khotin et al., 2009). The hypothesis that actinin-4 acts as a possible signalling factor is supported by its nuclear enrichment upon myogenic differentiation (Goffart et al., 2006). Actinin-4 interacts with **histone deacetylase-7** (HDAC7) and potentiates the transcription activity of myocyte-enhancer factor-2, in part by antagonising HDAC7 (Chakraborty et al., 2006). Actinin-4 harbours a functional receptor interaction motif, interacts with nuclear receptors *in vitro* and in mammalian cells, and potently activates transcription mediated by nuclear receptors (Khurana et al., 2011).

1.8 Summary

To summarise, this information highlights actinin as a multi-functional protein family that exhibit diverse effects and localisation patterns by interacting with proteins involved in numerous functions including cell signalling, transcription, adhesion, proliferation and migration. Actinin is located at critical sites where its modulation can influence cell behaviour. The evolution of actinin resulted in the appearance of the Ca^{++}-sensitive non-muscle isoforms (actinin-1 and -4), and the Ca^{++}-insensitive muscle isoforms (actinin-2 and -3). Evolutionary studies have theorised that the four isoforms of actinin resulted from two rounds of genomic duplication known as the "2R hypothesis". This paradigm allows for two general scenarios, sub-functionalisation and neo-functionalisation. Sub-functionalisation suggests that both genes (i.e. ACTN1 and ACTN4) became specialised whereas neo-functionalisation suggests that only one gene became specialised while other retained the function of the ancestral gene. It is not yet clear which paradigm applies to either the non-muscle or muscle actinin isoforms. While the non-muscle isoforms actinin-1 and -4 exhibit a high degree of sequence similarity, discrepancies exist in the literature with regard to their localisation patterns and functions. In particular, actinin-4 is essential for normal glomerular function in the kidney, is overexpressed in several cancers and is able to translocate to the nucleus to regulate transcription. This suggests that actinin-4 may have become specialised to perform functions that cannot be compensated by actinin-1. Indeed evidence exists suggesting that these non-muscle isoforms are not functionally redundant. However the molecular basis for the isoform-specific functions of actinin-4 is unclear. Adding to this complexity is the fact that most studies of the non-muscle actinins to date have focused on each isoform in isolation. For this reason identifying and understanding the differential functions of the non-muscle actinins remains a challenge. In an effort to understand the molecular mechanisms underlying the unique functions of actinin-4 this work compares the non-muscle actinins in terms of localisation, migration, alternative splicing patterns, actin-binding properties, dimerisation properties and interacting partners.

2 Materials and Methods

2.1 Cell Biology

2.1.1 Antibodies, cell lines and reagents

The following antibodies were used: α-actinin-1 [Santa Cruz, California, USA, Cat# (H-2):17829], α-actinin-1 [Abnova, Taipei City, Taiwan, Cat# 3F1], α-actinin [Santa Cruz, California, USA, Cat# (H300):sc15335], α-actinin-2 [Santa Cruz, California, USA, Cat# (A-25): 130928], α-actinin-4 [Immunoglobe, Himmelstadt, Germany, Cat# IG701], α-actinin-4 was kindly provided by Dr. Kazufumi Honda (National Cancer Centre Research Institute, Tokyo, Japan). α-actinin [Sigma, Arklow, Ireland, Cat# BM75.2], α-sarcomeric actinin [Sigma, Arklow, Ireland, Clone# EA-53], α-GFP [Millipore, Cork, Ireland, Cat# MAB3580], α-GFP [Abcam, Cambridge, UK, Cat# ab290] and α-FLAG [Sigma, Arklow, Ireland, Cat# F3165]. IRDYE^{TM} 700DX conjugated α-mouse IgG, α-mouse IgM and α-rabbit IgG secondary antibodies were purchased from Rockland (Gilbertsville, USA). IRDYE®800CW conjugated α-mouse and α-rabbit secondary antibodies were purchased from LI-COR Biosciences (Cambridge, UK). AlexaFluor®488 α-mouse and α-rabbit secondary antibodies were purchased from Jackson Immuno Research Laboratories Inc. (Suffolk, UK). Chemicals were obtained from Sigma (Arklow, Ireland) unless otherwise stated and restriction enzymes were purchased from New England Biolabs (Hitchin, UK). Cell lines used included A172 and U373-MG that were purchased from Cell Line Services (Eppelheim, Germany). Human Embryonic Kidney 293 (HEK), MDA-MB-231, DU145, HeLa and MCF-7 cells were a kind gift from Prof. Rosemary O' Connor (University College Cork, Ireland). U87-MG and U118-MG cells were a kind gift from Dr. Justin McCarthy (University College Cork, Ireland).

2.1.2 Cell culture and DNA transfections

A172, HeLa, Human Embryonic Kidney cells 293 (HEK), MCF-7, MDA-MB-231 and U87-MG cells were cultured in Dulbecco's Modified Eagle Media (Sigma D6429), 10% foetal bovine serum (FBS), 1% penicillin/streptomycin and 1% L-glutamine. DU145 cells were cultured in RPMI (Sigma R8758), 10% FBS, 1% L-glutamine and 1% penicillin/streptomycin. U373-MG cells were cultured in Minimum Essential

Medium Eagle (Sigma M5650), 10% FBS, 1% L-glutamine, 1% penicillin/streptomycin, 0.1 mM non-essential amino acids and 1 mM sodium pyruvate. HEK cell DNA transfections were carried out using a calcium-phosphate based protocol. Media was changed 14 hr post transfection. For MCF-7 cell DNA transfections, cells were seeded so as to be 90% confluent for transfection. For each well of a 6-well dish, 2 µl of lipofectamine was added to 73 µl of serum-free medium (DMEM only) and incubated for 5 min at room temperature (Solution A). 1 µg of DNA was made up to a volume of 75 µl with DMEM only (Solution B). Solution A and B were mixed and incubated for 20 min at room temperature. Cells were washed in 1 ml of DMEM. 600 µl of DMEM was added to the solution A and B mix. The resulting 750 µl was added to the cells to be transfected and incubated for 5 hr at 37 °C. Transfection medium was replaced with serum-containing medium. Serum starvation of HeLa cells was carried out by growing a confluent cell monolayer in media containing 10% FBS. Cells were washed twice in PBS and grown for a further 48 hr in the absence of FBS. HeLa cell migration was induced by applying multiple scratches to a confluent cell monolayer using a sterile tip ~16 hr pre harvest. Confluent HeLa cell layers were obtained by seeding 800,000 cells in a 10 cm diameter plate 48 hr pre-harvest. Proliferating HeLa cells were obtained by seeding 200,000 cells ~16 hr pre-harvest.

2.1.3 Platelet isolation

Platelet isolation was facilitated by Ms. Martha Phelan and Dr. Paul Young (University College Cork, Ireland). 10 ml of whole blood was added to 10 ml wash buffer (36 mM citric acid, 5 mM glucose, 5 mM KCl, 2 mM $CaCl_2.2H_2O$, 1 mM $MgCl_2.6H_2O$, 103 mM NaCl) and centrifuged at 180 g at 21 ^{0}C for 12 min to obtain platelet rich plasma. Supernatant (platelet rich plasma) was recovered. 30 ml wash buffer was added to platelet rich plasma and centrifuged for 180 g at 21 ^{0}C for 12 min. Supernatant (platelet rich plasma) was recovered and centrifuged at 1500 g at 21 ^{0}C for 12 min to pellet platelets. The platelet pellet was resuspended in 50 ml wash buffer and centrifuged at 1500 g at 21 ^{0}C for 12 min. The platelet pellet was lysed in TAPtag lysis buffer, see Section 2.2.1 for details.

2.1.4 siRNA knockdown

Cells were seeded in 6-well dishes so as to be 50% confluent for transfection. Two Silencer Select® Pre-designed siRNAs targeting actinin-4 (ID: s959 and s960 Cat# 4427037) and two siRNAs targeting actinin-1 (ID: s966 and s967 Cat# 4427037) along with a non-targeting negative control (Cat# 4390843) were purchased from Ambion (Life technologies, Carlsbad, California, USA). Cells were transfected in serum-free media with 10 nM siRNA using 3 µl lipofectamine purchased from Invitrogen (Lifetechnologies, Carlsbad, California, USA). Transfection was conducted in 1 ml DMEM. 5 hr post transfection media was adjusted to 10% FBS. Cells were harvested 72 hr post transfection unless otherwise indicated.

2.1.5 Migration assays

Migration assays were performed on MCF-7, DU145, A172 and U373-MG cell lines. 72 hr post siRNA-mediated knockdown of actinin-1 and -4 uniform scratch wounds were induced on confluent cell monolayers using a sterile tip. The initial open area of each wound was measured (T0) and at specific time-points following wound induction using Image J software (Abramoff et al., 2004). Measurements that were taken just prior to wound closure were compared to initial wound areas and the percentage wound closure was calculated for each assay from MCF-7, A172, and U373-MG cell experiments. DU145 cells exhibited a higher migratory rate and wounds were fully closed at T12. Therefore, the percentage closure for DU145 cell assays was analysed at T8. The percentage closure was compared to that of control cells treated with a non-targeting siRNA.

2.1.6 Immunofluorescence

Glass coverslips were coated in poly-D-lysine and incubated for 2 hr. Coverslips were washed 3 times with water and allowed to dry. Cells grown on coverslips were washed twice in PBS and fixed in 4% PFA for 10 min on ice. Cells were washed 3 times in PBS and incubated for 1 hr in blocking buffer (0.1% triton-100, 5% goat serum,

2% bovine serum in PBS) at room temperature. Primary antibodies were incubated for 3 hr at room temperature. Secondary antibodies were incubated for 1 hr at room temperature. Antibodies were diluted and incubated in 5% goat serum, 2% bovine serum in PBS. Following the secondary antibody incubations cells were washed 3 times in PBS and mounted on glass slides using fluoromount (Sigma, Arklow, Ireland).

2.2 SDS-PAGE and Immunoblotting

2.2.1 Cell lysate preparation

Cells were harvested and washed twice in PBS. For heterodimer analysis cells were lysed in TAPtag lysis buffer [150 mM NaCl, 50 mM Tris-Cl pH 7.5, 1% NP40, 10% glycerol, 2 mM NaF, 1 mM Na_3VO_4 and 1 protease inhibitor cocktail tablet/10 ml (Roche, Clare, Ireland)] for 30 min. For migration assay analysis cells were lysed in RIPA lysis buffer [150 mM NaCl, 1% NP40, 0.5% deoxycholate, 0.1% SDS, 50 mM Tris-Cl pH 8.0 and 1 protease inhibitor cocktail tablet/10 ml (Roche, Clare, Ireland)] for 30 min on ice. Post incubation lysates were centrifuged at 16,100 g for 15 min at 4 ^{0}C. The Pierce BCA protein assay (Thermo Scientific, Waltham, USA) was used to quantify the protein concentration of lysates.

2.2.2 SDS-PAGE and Western blotting

Standard SDS-PAGE and Western blotting procedures were followed. Proteins were resolved by either 10% or 12% sodium dodecyl sulphate-polyacrylamide gel electrophoresis (SDS-PAGE), transferred to nitrocellulose membranes and blocked for 1 hr in TBST (10 mM Tris-HCl, pH 8.0, 150 mM NaCl, 0.1% (v/v) Tween 20, 4% (w/v) non-fat dried milk). SDS-PAGE gels were stained in Gel Code^{TM} Blue Safe Protein Stain (Thermo Scientific, Waltham, USA) for 1 hr and destained in deionized water for 2 hr. Primary and secondary antibodies were incubated in 4% milk TBST with the exception of α-GFP (Abcam, Cambridge, UK Cat# ab290) that was incubated in 3% BSA in PBS. Western blot detection was performed on an Odyssey Classic infrared scanner (LI-COR Biosciences, Cambridge, UK).

2.2.3 Native polyacrylamide gel electrophoresis (Native-PAGE)

For native polyacrylamide gel electrophoresis (Native-PAGE) the standard polyacrylamide gel electrophoresis protocol was followed with the exception that SDS, β-mercaptoethanol and boiling steps were omitted. The PROTEAN II xi cell electrophoresis instrument was employed (Bio-Rad, Hercules, California). Cells were washed twice in PBS and lysed in TAPtag lysis buffer [150 mM NaCl, 50 mM Tris-Cl pH 7.5, 1% NP40, 10% glycerol, 2 mM NaF, 1 mM Na_3VO_4 and 1 protease inhibitor cocktail tablet/10 ml (Roche, Clare, Ireland] for 30 min on ice and centrifuged at 16,100 g for 15 min at 4 ^{0}C. PAGE loading buffer (without SDS and β-mercaptoethanol) was added to lysates on ice. Samples were then loaded on 6% native polyacrylamide gels (without SDS). Lysates were run for 5 hr in PAGE running buffer (without SDS) at 24 mAMP. Running buffer was refreshed after 2.5 hr. Western blot detection was performed on an Odyssey Classic infrared scanner (LI-COR Biosciences, Cambridge, UK).

2.3 Molecular Biology

2.3.1 Plasmid construction

The following constructs were generated by PCR amplification and standard cloning procedures using human actinin-1 (exon 19a), actinin-2 and actinin-4 (exon 8a, 19a) sequences as templates unless otherwise stated. The sequence of all constructs was verified by sequencing. Unless otherwise stated primer annealing temperatures were set at 60 °C and 30 PCR cycles were performed. Primers are outlined Table 2.1.

2.3.1.1 Generation of human actinin-1 and -4 chimeric constructs

Swapping of calmodulin-like domains: Actinin-1 was digested from actinin-1 pGAD10 (Clontech, Saint-Germain-en-Laye, France) using Xho1 and EcoR1 and sub-cloned into the pEGFP-C2 vector (Clontech, Quintin, France). Actinin-4 was amplified from the actinin 4-pOTB7 clone using A4-ABD-F and A4-CaM-R primers

(35 cycles and annealing temperature 60 °C) and cloned into the pEGFP-C2 vector. Xma1 restriction sites were taken advantage of in order to digest CaM domains from each isoform (see restriction map of actinin isoforms Figure 3.14A). Actinin-4 had a second Xma1 site introduced by site-directed mutagenesis to facilitate this digest. Primers (A4-iXma-F and A4-iXma-R) were used to incorporate an XmaI site into a region 5' of the CaM domain of actinin-4. The protocol was followed as per Quikchange II XL Site-Directed Mutagenesis Kit (Stratagene, California, USA, Cat# 20052). In short, a PCR reaction was set up using 125 ng of primers and 10 ng of DNA template. 20 PCR cycles were performed with an annealing temperature of 60 ^{0}C. The PCR product was incubated with Dnp1 for 1 hr at 37 °C. DNA was transformed into XL10-GOLD cells which were grown at 37 °C. CaM domains and actinin pEGFP-C2 constructs lacking the CaM domains were obtained for each actinin isoform using XmaI digestion. In this manner CaM domains were swapped between each isoform. This resulted in AR1C4 pEGFP-C2 and AR4C1 pEGFP-C2 plasmids.

Swapping of actin-binding domains: Xho1 and BamHI restriction sites were used to digest the ABD from actinin-1 pEGFP-C2 and actinin-4 pEGFP-C2. Performing a separate digestion with EcoRI followed by partial digestion with BamHI resulted in a fragment of ~1800 bp which represented the RC domain of each isoform. The ABD and RC domain of each actinin isoform were subsequently swapped and ligated. The resulting chimeric sequences were cloned into pEGFP-C2 using XhoI and EcoRI. This resulted in A1RC4 pEGFP-C2 and A4RC1 pEGFP-C2 plasmids.

Swapping of rod domains: The AR1C4 and AR4C1 constructs (constructs with swapped CaM domains described previously), were digested with EcoRI, followed by partial digestion with BamHI which resulted in fragment ~1800 bp that represented the R1C4 and R4C1 domains, respectively. ABD1 and ABD4 were obtained by XhoI and BamHI digest of actinin-1 pEGFP-C2 and -4 pEGFP-C2. R1C4 and R4C1 domains were ligated with ABD4 and ABD1 domains respectively. This resulted in A4R1C4 pEGFP-C2 and A1R4C1 pEGFP-C2 plasmids.

2.3.1.2 Yeast two-hybrid constructs

Sequences encoding the rod domains of human actinin-1 (amino acids 267-739), actinin-2 (amino acids 274-746) and actinin-4 (amino acids 286-758) were amplified

by PCR, cloned into the pGAD10 prey vector (Clontech, Saint-Germain-en-Laye, France) and sub-cloned into the pLEX-K bait vector (Stenmark et al., 1995). Sequences encoding the CaM domain of actinin-1 (amino acid 746-893) and -4 (amino acid 759-912) were amplified by PCR, cloned into the pGAD10 prey vector and sub-cloned into a pLEX-K bait vector. Sequences encoding the ABD of actinin-1 (amino acids 1-259) and -4 (amino acids 1-278), R2-R3 of actinin-1 (amino acids 364-630) and -4 (amino acids 383-649), R1-CaM of actinin-1 (amino acid 267-893) and -4 (amino acids 286-912), and XR1-CaM of actinin-1 (amino acids 252-893) and -4 (amino acids 271-912) were amplified by PCR, cloned into the pGAD10 vector and sub-cloned into the bait vector PGBKT7 (Clontech, Saint-Germain-en-Laye, France). Primers used to amplify these domains are outlined in Table 2.1.

2.3.1.4 Bacterial expression constructs

The following actinin constructs were expressed as maltose-binding fusion proteins in the pET24 vector (Novagen, Quintin, France): actinin-1 R1-R2 (amino acids 267-494) and actinin-4 R1-R2 (amino acids 286-513). The following actinin constructs were cloned into the modified pET24 vector, pET24-His_6GST-TEV that encodes an N-terminal 6xHistidine tag followed by the glutathione-S-transferase (GST) sequence and a recognition site for TEV protease: full length actinin-1 (exon 19a), full length actinin-1 (exon 19a+19b), actinin-1 ABD-R2 (amino acids 1-494), actinin-1 R3-R4 (amino acids 495-739), full length actinin-4 (exon 8a, exon 19a), full length actinin-4 (exon 8b, exon 19a), actinin-4 ABD-R2 (exon 8a; amino acids 1-513), actinin-4 R3-R4 (amino acid 514-758). Actinin-1 R3-R4 (amino acid 495-739), actinin-1 R3-CaM (amino acids 495-893), actinin-4 R3-CaM (amino acids 514-912) and actinin-4 R3-R4 (amino acids 514-758) were cloned into another modified pET24 vector, pET nHis_6 that encodes an N-terminal 6xHistidine tag fused to the protein of interest. The alternatively spliced exon 8b and exon 19a+19b were amplified from human brain cDNA derived from a cDNA synthesis reaction using MVP^{TM} Total RNA, Human Frontal Cortex purchased from Agilent Technologies (Cork, Ireland). Primers used to amplify these regions are outlined (Table 2.1).

Actin-cosedimentation assay constructs: Sequences encoding full length actinin-1 (exon 19a) and full length actinin-4 (exon 8a, 19a) were sub-cloned from pGAD10 into pET24-His_6GST-TEV using XhoI and EcoRI. For brain specific actinin-1 (exon

19a+19b) the sequence encoding exon 19a+19b was PCR amplified from MVP™ Total RNA, Human Frontal Cortex purchased from Agilent Technologies (Cork, Ireland) using primers (A1-Brain-F and A1-CaM-R) and digested with XmaI and EcoRI. Removal of the sequence region encoding exon 19a from full length actinin-1 (exon 19a) pGAD10 using Xma1 and EcoR1 allowed it to be replaced with the exon 19a+19b amplified sequence thereby resulting in full length actinin-1 (exon 19a+19b) pGAD10. Full length actinin 1 (exon 19a+19b) was subsequently sub-cloned into the pET24-His$_6$GST-TEV vector using XhoI and EcoRI. For full length actinin- 4 (exon 8a, 19a), the ABD sequence including the exon 8b region was amplified from MVP™ Total RNA, Human Frontal Cortex purchased from Agilent Technologies (Cork, Ireland) using A4-ABD-F and A4-R2-R primers and sub-cloned using XhoI and BamHI into a pBluescript vector. Next an overlapping sequence encoding the R1-CaM domain was obtained from full length actinin-4 (exon 8a, 19a) pEGFP-C2 using an EcoRI digest followed by a partial BamHI digest. Finally, XhoI and BamHI digested ABD (exon 8b), BamHI and EcoRI digested R1-CaM domain and XhoI and EcoRI digested pET24-His$_6$GST-TEV vector were ligated together resulting in full length actinin-4 (exon 8b, 19a) pET24-His$_6$GST-TEV.

Homodimer versus heterodimer affinity assay constructs: ABD-R2 (exon 8a) and R3-CaM (exon 19a) domains of actinin-1 and -4 were amplified from actinin-1 and -4 pGAD10 templates. The amplified sequences were cloned into pET24-His$_6$GST-TEV and pET nHis$_6$ vectors respectively using XhoI and EcoRI. R1-R2 domains of actinin-1 (amino acids 267-494) and -4 (amino acids 286-513) were amplified and cloned as maltose-binding protein fusion proteins into pET24 and pET24-His$_6$GST-TEV vectors. R3-R4 domains of actinin-1 (amino acids 495-739) and -4 (amino acids 514-758) were cloned in pET24-His$_6$GST-TEV and pET nHis$_6$ vectors. Primers used to amplify these regions are outlined (Table 2.1).

2.3.1.5 Tandem affinity purification constructs

Full length actinin-1 (exon 19a) and -4 (exon 8a, exon 19a) with a carboxyl terminal Tandem Affinity Purification (TAP) tag and FLAG epitope tag were cloned into the pIRES2 vector (Clontech, Saint-Germain-en-Laye, France). The TAP tag consisted of the Protein A sequence, a TEV cleavage site and a calmodulin-binding peptide

(Xu et al., 2010). The internal ribosome entry site of the pIRES2 vector directed co-expression of green fluorescent protein (GFP) which was used to monitor transfection and expression efficiency. The control construct encoded a yellow fluorescent protein (YFP) with an amino terminal FLAG and TAP tag. Specifically, full length actinin-1 (exon 19a) and full length actinin-4 (exon 8a, exon 19a) were sub-cloned from pGAD10 (Clontech, Saint-Germain-en-Laye, France) to pEGFP-C2 vectors using XhoI and EcoRI. To facilitate fusion to a C-terminal FlagTAPtag it was necessary to remove the stop codon present at the C-terminus of each actinin prior to sub-cloning into a pCMV CFLAG TAPTAG vector. The pCMV CFLAG TAPTAG vector is based on pEGFP-N1 (Clontech, Saint-Germain-en-Laye, France) but with the GFP replaced with a TAPTAG-CFLAG (Xu et al., 2010). The C-terminal end of actinin-1 and -4 was amplified using reverse primers (A1-CaM-R-nostop and A4-CaM-R-nostop, respectively) that excluded a stop codon sequence from actinin-1 and -4. For actinin-1 full length actinin-1 pEGFP-C2 was transfected into DAM- SCS110 cells prior to PCR amplification so as to prevent methylation of an XbaI site that was required as part of the cloning strategy. This actinin-1 stop codon free sequence was subsequently digested with Xma1 and XbaI. Removal of the C-terminal sequence that included the stop codon sequence from actinin-1 pEGFP-C2 using Xma1 and XbaI allowed it to be replaced with the sequence lacking the stop codon. Full length actinin-1 was then sub-cloned into pCMV CFLAG TAPTAG using XhoI and KpnI. For actinin-4 stop codon free sequence was digested with SalI and KpnI. Removal of the C-terminal sequence that included the stop codon from actinin-4 pEGFP-C2 using SalI and KpnI allowed it to be replaced with the sequence lacking the stop codon. Full length actinin-4 was then sub-cloned into pCMV CFLAG TAPTAG using XhoI and KpnI. Full length actinin-1 with a C-terminal Flag and TAP tag was obtained using an XhoI digest followed by a partial XmaI digest and sub-cloned into a pIRES vector. Full length actinin-4 with a C-terminal Flag and TAP tag was sub-cloned into pIRES using an XhoI and XmaI digest.

2.3.2 Reverse transcriptase PCR (rtPCR)

Tissues were dissected from C57 BL6J mice and embryos. Animal experiments at University College Cork were approved by the University Ethics Committee and conducted under a license from the Irish Department of Health and Children. RNA was extracted using TriPure Isolation Reagent (Roche Applied Science, Burgess Hill, UK) according to the manufacturer's instructions. 1 ug of RNA was used per cDNA reaction using the Protoscript AMV First Stand cDNA synthesis kit (New England Biolabs, Hitchin, UK). 1 ul of cDNA was used per rtPCR reaction. For rtPCR analysis of actinin-4 exon 8, forward primers that flank exon 8 were used in conjunction with reverse primers specific for exon 8b and reverse primers that flank exon 8 were used in conjunction with forward primers specific for exon 8a. For analysis of actinin-1 and -4 exon 19, primers that flank this exon were used and bands corresponding to exon 19a (128 bp) and 19b (113 bp) were separated on 4% agarose gels. Primers are outlined Table 2.1.

2.4 Protein purification

2.4.1 Protein expression and purification

Actinin expression constructs described above were transformed into *E. coli* BL21 [DE3] CodonPlus RP cells (Agilent Technologies, Cork, Ireland). Protein expression was induced at 37 ^{o}C by addition of 0.1 mM isopropyl-β-D-thiogalactopyranoside (IPTG) and cells were harvested 4 hr post induction. Cell pellets were resuspended in PBS, 0.2% triton, 20 mM β-mercaptoethanol and 1 mM PMSF. Cells were lysed by sonication and addition of 0.1 mg/ml lysozyme for 30 min at 4 ^{0}C. Lysates were cleared by centrifugation at 39,000 g for 30 min at 4 ^{0}C. Purifications were carried out using either 3 ml glutathione-sepharose from GE Healthcare (Cork, Ireland) or nickel-agarose (Ni) beads (Novagen, Quintin, France) or amylose beads (New England Biolabs, Hitchin, UK). For GST purifications proteins were loaded on a glutathione-sepharose column pre-equilibrated with wash buffer (PBS, 0.1% triton, 5 mM β-mercaptoethanol). Columns were washed twice with 10 ml wash buffer and bound proteins were eluted in 10 mM glutathione, 50 mM Tris-HCl, pH 8.0. His_6-tagged

proteins were purified on a Ni-column pre-equilibrated with wash buffer (0.5 M NaCl, 50 mM KPO4 pH 8.0, 20 mM β-mercaptoethanol, 5 mM imidazole, 0.1% triton). Columns were washed twice with 10 ml wash buffer and bound proteins were eluted in either 20 mM or 200 mM imidazole pH 7.0, 20 mM β-mercaptoethanol. For full length actinins the His_6-GST tag was removed by incubation overnight with recombinant His_6-TEV protease (1 mg TEV protease/100 mg protein) at 4 ^{0}C. Ni-column purification was subsequently used to remove the cleaved His_6-GST tags and His_6-TEV protease. Finally purified proteins were concentrated using Amicon Ultra centrifugal filters (Millipore, Cork, Ireland). For amylose purifications of maltose-binding protein (MBP) tagged proteins, samples were loaded on amylose columns pre-equilibrated with wash buffer (20 mM Tris pH 7.4, 0.2 M NaCl, 1 mM EDTA). Columns were washed twice with 10 ml wash buffer and bound proteins were eluted in elution buffer (10 mM maltose, 20 mM Tris pH 7.4, 0.2 M NaCl, 1 mM EDTA).

2.4.2 Tandem affinity purification

Constructs encoding TAP-tagged actinin-1, -4 and YFP were transfected in HEK 293 cells and grown for 4 cell passages. Using a fluorescent microscope, YFP/GFP-expressing cells were selected over the course of ~10 passages. In this manner, stable cell pools in which >70% of cells were YFP/GFP positive were obtained. Five 15 cm^2 cell culture dishes were grown to confluence per purification. Cells were washed twice in PBS and lysed in 5 ml lysis buffer (150 mM NaCl, 50 mM Tris-Cl pH 7.5, 1% NP40, 10% glycerol, 2 mM NaF, 1 mM Na_3VO_4 and 1 protease inhibitor cocktail tablet/10 ml (Roche, Clare, Ireland) for 30 min and centrifuged at 16,100 g for 15 min at 4 ^{0}C. Lysates were run 5 times through columns containing 1 ml IgG beads (Stratagene, California, USA). Beads were washed 3 times in 10 ml of lysis buffer. 2 ml of TEV cleavage buffer (lysis buffer plus 0.5 mM EDTA, 1 mM DTT) and TEV protease (0.1 mg/ml) was added to the columns. Columns were incubated for 1.5 hr at room temperature, mixing occasionally. The eluate was adjusted to 2 mM $CaCl_2$ and added to 300 µl calmodulin sepharose beads. Beads were incubated for 1 hr at 4 ^{0}C. Beads were washed 3 times in 1 ml of wash buffer (lysis buffer plus 2 mM $CaCl_2$). Bound proteins were eluted in 300 µl 2X SDS-loading dye that was subsequently concentrated down to 50 µl. Elutions were loaded on 12% SDS-PAGE gels and run for

2 hr at 100 V. Each sample lane was divided into 6 gel segments that were sent for mass spectrometric analysis.

2.5 Yeast two-hybrid analysis

2.5.1 Yeast two-hybrid assays

Rod domains from actinin-1, -2 and -4 were cloned into both bait and prey vectors as described in Section 2.3.1.2. The *Saccharomyces cerevisiae* L40 reporter strain harbouring the *lacZ* and *His3* genes under control of the GAL4 upstream activating sequence was used for all analyses. To examine actinin heterodimerisation bait and prey constructs were transformed into the L40 strain using a standard lithium acetate transformation protocol and plated on agar plates lacking leucine and tryptophan to select for transformed plasmids. Colonies appeared within 5 days and were restreaked on selection agar plates lacking leucine, tryptophan and histidine to monitor HIS3 reporter gene activation. β-galactosidase reporter gene activation was also monitored by β-galactosidase assays. For these assays, colonies were grown on plates lacking leucine and tryptophan and transferred onto nylon membranes. Membranes were frozen and thawed twice in liquid nitrogen. The membranes were then placed on filter paper soaked in Z-buffer (130 mM Na_2HPO_4/NaH_2PO_4 pH 7.0, 10 mM $MgSO_4.7H_2O$, 0.001% β-mercaptoethanol, 0.85 mg/ml X-gal) and incubated for 18 hr at 37 ^{0}C.

2.5.2 Yeast two-hybrid screens

For yeast two-hybrid screens, L40 cells harbouring either actinin-1 or -4 R1-R4 (rod) domain pLEX bait constructs were transformed with a P3 mouse brain cDNA library in the pAD-GAL4 vector. The transformation efficiency for the actinin-1 screen was $2.4x10^6$ colony forming units and for actinin-4 was $6x10^5$ colony forming units. Selection for HIS3 reporter gene activation was performed on selection agar plates lacking histidine, leucine and tryptophan (SD-LWH) at 30 ^{o}C. Colonies appearing after 4-5 days were assayed for β-galactosidase reporter gene expression. Library plasmids were recovered from HIS3/β-gal reporter gene positive clones and their

inserts sequenced. Bait clones identified from the actinin-1 screen were tested for interaction with the actinin-4 bait by co-transforming plasmids directly into L40 cells.

2.6 *In vitro* binding assays

2.6.1 *In vitro* heterodimer binding assays

GST-tagged ABD-R2 and His_6-tagged R3-CaM regions from both actinin-1 and -4 were expressed, purified and dialysed into binding assay buffer (20 mM Tris pH 7.5, 50 mM NaCl, 5 mM β-mercaptoethanol). Experiments were designed to assay for homodimer and heterodimer formation. Briefly, 0.1 mg of GST-tagged ABD-R2 domain of actinin-1 or -4 was incubated with 50 µl GST beads which were subsequently mixed with 0.1 mg of R3-CaM domains of actinin-1 or -4. Beads were incubated for 30 min at 4 ^{0}C and washed 3 times in binding assay buffer for 5 min at 4 ^{0}C. Proteins were eluted in 50 µl 2X SDS-PAGE loading dye. Elutions were run on 12% SDS-PAGE gels and stained with Gel Code^{TM} Blue Safe Protein Stain (Thermo Scientific, Waltham, USA). Densitometric analysis was used to compare the levels of R3-CaM proteins bound to ABD-R2 proteins for heterodimer and homodimer formation. Note: initial experiments that used GST/MBP-tagged R1-R2 in combination with His-tagged or untagged R3-R4 domains of actinin-1 and -4 were set up in a similar manner, however neither heterodimer nor homodimer formation was observed.

2.6.2 Actin-cosedimentation assays

Human platelet actin (Cytoskeleton Inc., Denver, USA) was mixed in G-actin buffer (5 mM Tris pH 8.0, 0.2 mM $MgCl_2$, 0.2 mM ATP, 0.5 mM DTT). Actin and actinin proteins were cleared by ultra-centrifugation at 112,000 g for 30 min at 4 ^{0}C. Actin was polymerised by addition of 1/100 volume of 100X polymerisation buffer (2 M NaCl, 0.1 M $MgCl_2$) and incubated for 30 min at 4 ^{0}C. Actin and actinin proteins were mixed in 10 mM Tris-HCl pH 7.5, 100 mM NaCl, 1 mM NaN_3, 1 mM $MgCl_2$, 0.1 mM ATP, 0.1 mM DTT, 0.1 mM EGTA and incubated for 30 min at 30 ^{0}C. To determine the Kd for actin binding 2 µM actin was used per assay along with a range of actinin

concentrations (0.25-30 µM). For calcium (Ca^{++}) sensitivity analysis 2 µM actin and 2.5 µM actinin were mixed in a variety of free Ca^{++} concentrations (10 nM-1 mM) that were obtained using a Ca^{++}:EGTA buffer system. Polymerised actin was separated by ultracentrifugation at 112,000 g for 30 min at 30 ^{0}C. Pellets and supernatants were brought to the same total volume of SDS sample buffer, boiled, and equal volumes loaded on 12% SDS-polyacrylamide gels. Assays that omitted actin were used as controls for non-specific trapping of actinin. For actin-bundling assays 1 µM actin and 0.5 µM actinin were used and centrifugation was performed at 10,000 g.

2.7 Determination of the relative amount of actinin-1 and -4 within and between cell lines

Full length actinin-1 and -4 constructs in the pEGFP-C2 vector (Clontech, Quintin, France) were transfected into HEK 293 cells as described in Section 2.1.2. In order to determine their expression levels relative to each other Western blots of lysates were probed with α-GFP antibody. Subsequently lysates from cells transfected with these GFP-tagged actinin constructs were used to produce a standard curve to which specific actinin-1 and -4 antibody staining could be normalised. Using this standard curve in combination with lysates from various cell lines allowed comparison of the relative amount of actinin-1 and -4 within and between cells lines. Probing native gels with antibodies specific for actinin-1 and -4 followed by densitometic analysis allowed us to quantify the proportion of actinin-1 and -4 involved in heterodimer formation.

2.8 Analysis of evolutionary conservation of the actinin rod dimerisation interface

This analysis was based on the human actinin-2 rod domain for which the crystallographic structure is known (Ylänne et al., 2001). A multiple sequence alignment of this sequence with actinin-1 and -4 sequences from divergent species (human, mouse, frog, zebrafish and chicken) was generated using ClustalX (Larkin et al., 2007). With this alignment as input, the ConSurf server was used to calculate and plot conservation scores onto the actinin-2 rod domain 3D structure (Landau et al.,

2005; Ashkenazy et al., 2010). Conservation scores that are considered unreliable by ConSurf are coloured yellow and shown in stick rather than space filling representation (see Figure 3.36).

2.9 Protein identification by mass spectrometry

Mass spectrometric analysis was performed at the FingerPrints Proteomics facility at University of Dundee, Scotland. Peptides were obtained using an in-gel digestion protocol and extracted prior to analysis by 1D nLC-MS/MS using an LTQ Orbitrap Velos Pro mass spectrometer (Thermo Scientific, Hemel Hempstead, United Kingdom). MS/MS data was searched against the IPI-human database (91464 sequences; 36355611 residues; European Bioinformatics Institute www.ebi.ac.uk) using in-house Mascot software (Matrix Science, London, UK). Identified proteins were ranked according to Mascot protein scores and listed using protein symbols as identifiers in Excel software (Microsoft Corporation, Redmond, USA). The COUNTIF function of Excel was used to identify proteins present in one or both purified actinin complexes but not in the control sample. A Mascot protein score of 100 was then applied as a cut off value to limit results to proteins that have been very reliably identified. This roughly corresponds to proteins with two distinct peptide matches. In the case of proteins present in both actinin complexes, at least one of the protein scores had to be greater than 100. Probable environmental contaminants such as keratins were then removed. Information about the subcellular localisation and functions of the remaining proteins was obtained from the Uniprot database (www.uniprot.org). Proteins that were likely to be false positives based on clear subcellular localisations that differ from the cytoplasmic and nuclear localisations that have been reported for actinins were then eliminated (secreted, mitochondrial matrix and ER/Golgi lumenal proteins) to obtain the final filtered list of identified proteins.

Actinin-1	
A1-ABD-F (hm)	5’-TTTCTCGAGCACCATGGACCATTATGATTCTCAGCA-3’
A1-ABD-R (hm)	5’-TTTGAATTCTTAGGCTGCTGTCTCCGCCTTCTG-3’
A1-XR1 F (hm)	5’-TTTCTCGAGCGCCCAGAAGGCGGAGACAGC-3’
A1-R1-F (hm)	5’-TTTCTCGAGCGCCGTCAACCAGGAGAACGAG-3’
A1-R2-F (hm)	5’TTTCTCGAGCATCAACAATGCCTGGGGCTGCC-3’
A1-R2-R (hm)	5’-TTTGAATTCTGCAGTCGACTTACCTTCGCTTCTGAGTTAGGGCC-3’
A1-R3-F (hm)	5’-TTTCTCGAGCGAAGCTCTGGAGCGGACCGAG-3’
A1-R3-R (hm)	5’-TTTGAATTCTTACCTCTCATTGTGCTGCTGTCGG-3’
A1-R4-R (hm)	5’-TTTGAATTCTTAATCCCGGGTCAGGATCTGGTTC-3’
A1-CaM (hm)	5’-TTTCTCGAGCGCCAAGGGCATCAGCCAGGAG-3’
A1-CaM (hm)	5’-TTTGAATTCTTAGAGGTCACTCTCGCCGTAC-3’
A1-CaM-R-nostop (hm)	5’-TTTTCTAGAGGTACCCAAGCTTGAGGTCACTCTCGCCGTACAG-3’
A1-Brain-F (hm)	5’-GACAGCAGCACAATGAACGTCTACGCAAGCAGTTTGG-3’
A1-exon19-Flank-F (ms)	5’-GCCTCTTTCAACCACTTTGACCGG-3
A1--exon19-Flank-F (hm)	5’-GCCTCCTTCAACCACTTTGACCGG-3’
A1-exon19-Flank-R (ms)	5’-GATTCGGGCAAACTCTGCCTCTCC-3’
A1-exon19-Flank-R (hm)	5’-GATGCGGGCAAATTCTGCTTCTCC-3’
Actinin-4	
A4-ABD-F (ms)	5’-TTTCTCGAGCACCATGGTGGACTACCACGCAGCG-3’
A4-ABD-F (hm)	5’-TTTCTCGAGCACCATGGTGGACTACCACGCG-3’
A4-ABD-R (hm)	5’-TTTGAATTCTTAGGCGGCAGTTTCAGCCTTCTG-3’
A4-XR1-F (hm)	5’-TTTCTCGAGCGCGCAGAAGGCTGAAACTGCC-3’
A4-RI-F (hm)	5’-TTTCTCGAGCGCTGTCAACCAAGAGAACGAGCACC-3’
A4-R2-F (hm)	5’-TTTCTCGAGCATCAACAATGGCTGGCAGCACTTG-3’
A4-R2-R (hm)	5’-TTTGAATTCGTCGACTTACCTGCGACTATGTGTCAGAGAG-3’
A4-R3-F (hm)	5’-TTTCTCGAGCGAAGCCCTGGAGAAAACAGAG-3’
A4-R3-R (hm)	5’-TTTGAATTCTTAGTGCTCGTTGGACTGCTGCTTG-3’
A4-R4-R (hm)	5’-TTTGAATTCTTAGTCGCGGGTGAGGATCTGGTTC-3’
A4-CaM-F (hm)	5’-TTTCTCGAGCGCCAAGGGCATCAGCCAGGAG-3’
A4-CaM-R (hm)	5’-TTTGAATTCTCACAGGTCGCTCTCGCCATAC-3’
A4-CaM-R-nostop (hm)	5’-TTTGGTACCCAAGCTTCAGGTCGCTCTCGCCATACAAG-3’
A- iXmaI-F (hm)	5’-GATCCTCACCCGGGACGCCAAGGGC-3’
A4-iXmaI-R (hm)	5’-GCCCTTGGCGTCCCGGGTGAGGATC-3’
A4-exon8-Flank-F (hm/ms)	5’-GAGCTGATTGAGTATGACAAG-3’
A4-exon8a-specific-F (ms)	5’-GACATCGTGAACACAGCCC-3’
A4-exon 8a-specific-F (hm)	5’-GACATCGTGAACACGGCCC-3’
A4-exon8b-specific-R (hm/ms)	5’-CCTTCTCATCTGGCCTCAGA-3’
A4-exon8-Flank-R (ms)	5’-CGAATCCACTCTAGAAGATC-3’
A4-exon8-Flank-R (hm)	5’-GGATCCACTCCAGGAGGTC-3’
A4-exon19-Flank-F (ms)	5’-GCATCCTTCAACCATTTTGACAAGGA-3’
A4-exon19-Flank-F (hm)	5’-GCGTCCTTCAACCACTTCGAC-3’
A4-exon19-Flank-R (ms)	5’-TGATCCGGTTGAACTCAGCATCACC-3’

A4-exon19-Flank-R (hm)	5'-TGATGCGGTTGAACTCGGCCTCACC-3'
Actinin-2	
A2-R1-F (hm)	5'-TTTCTCGAGTGCTGTGAATCAAGAGAATGAGAGG-3'
A2-R4-R (hm)	5'-TTTGAATTCGGATCCTAATCTCTCGTCAGGATCTGAGTC-3'
Miscellaneous	
A1/2/4-mid-F (ms)	5'-GCCTTCATGCCCTCCGAGGG-3'
A1/2/4-mid-R (ms)	5'-CCCTCGGAGGGCATGAAGGC-3'
Myozenin-bp696-F (ms)	5'-GGGTTGATCCTCAGCAAAAAGTG-3'
Myozenin-R (ms)	5'-TTTGAATTCACAGCTCCTCTGTCTCTCC-3'
Controls	
GAPDH-F (hm)	5'-TGAAGGTCGGAGTCAACGGATTTGG-3'
GAPDH-R (hm)	5'-CATGTGGGCCATGAGGTCCACCAC-3'
Elongation-factor-1-F (ms)	5'-TGTGAAAACCACCGCTAATTCAAAGC-3'
Elongation-factor-1-R (ms)	5'-CCACAACATTCTTTCCTTCTGAAGG-3'

Table 2.1 Primers employed to amplify DNA sequences corresponding to specific actinin protein domains and splice variants. The specific domains/exons are indicated by the name of each primer. ABD=actin-binding domain. R1=spectrin-like repeat 1. R2= spectrin-like repeat 2. R3= spectrin-like repeat 3. R4= spectrin-like repeat 4. XR1=extended spectrin-like repeat 1 i.e. primer anneals upstream of repeat 1. CaM=calmodulin-like domain. Primer sequences are also outlined that are designed to amplify regions of myozenin, GAPDH and elongation factor 1. F=forward primer. R=reverse primer. Hm=human. Ms=mouse.

3 Results

3.1 The non-muscle actinins: Antibody characterisation, migration and localisation

Although actinin-1 and -4 exhibit a high degree of similarity they are reported to exhibit different localisation patterns and functions. In particular actinin-4 is reported to be associated with cancer metastasis. Nuclear localisation of actinin-4 but not actinin-1 has also been observed. I aimed to determine the mechanisms underlying the differential effects and localisation patterns of the non-muscle actinins.

In this part of the work my goals were to:

1) Characterise commercially available actinin antibodies to facilitate studies of actinin expression and localisation.
2) Examine the effects of individual and combined actinin-1 and -4 knockdown on cell migration.
3) Determine the specific actinin protein domain that is responsible for the observed distinct localisation patterns of the non-muscle actinins.

Ideally this work could i) identify particular cell line(s) in which differential functions of actinin-1 and -4 could be readily observed and thus provide a system in which to carry out mechanistic investigations and ii) map the differential functions of actinin-1 and -4 to a particular protein domain.

3.1.1 Antibody characterisation

3.1.1.1 Antibody-specificity tests

The aim of this work was to determine the specific actinin isoforms detected by a number of commercially available antibodies. This will aid efforts to determine the actinin isoforms present in various cell lines and tissues. Human and mouse GFP-tagged actinin-1, -2 and -4 constructs were generated. These constructs were transfected into Human Embryonic Kidney (HEK) cells. Lysates from cells were analysed by Western blot and probed using the various actinin antibodies indicated (Figure 3.1). Results are summarised in Table 3.1.

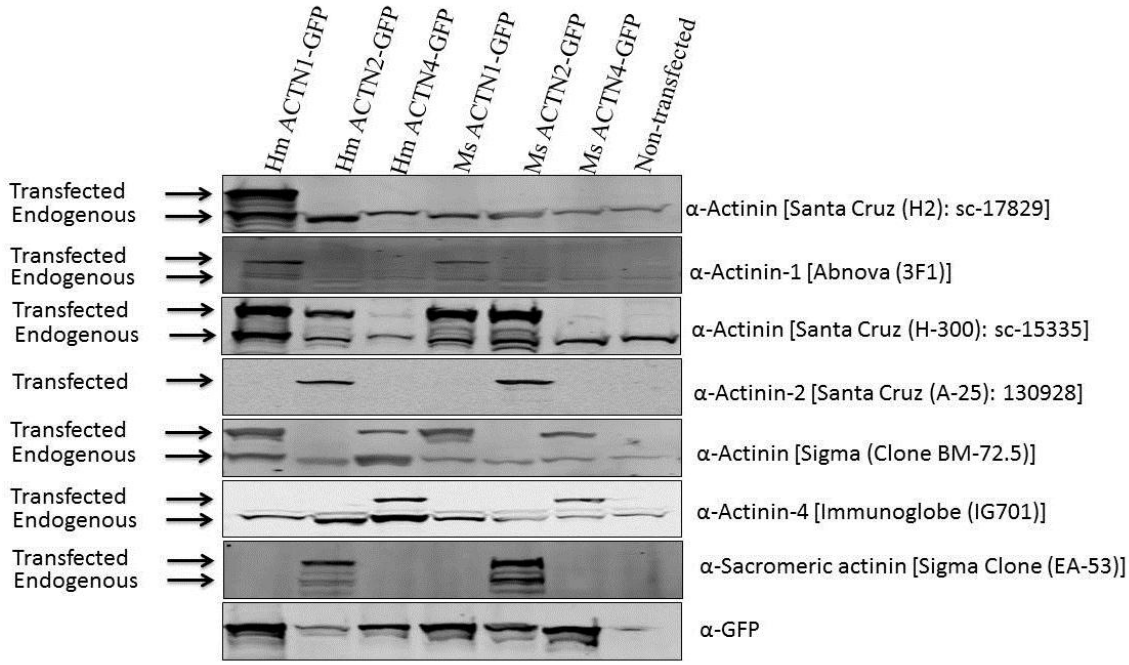

Figure 3.1 Isoform-specificity of actinin antibodies as determined by Western blot analysis. GFP-tagged human (hm) and mouse (ms) actinin-1, -2 and -4 (ACTN1/2/4) constructs were transfected into HEK cells. Lysates were probed with actinin antibodies as indicated. Arrows show position of transfected GFP-tagged and endogenous actinin proteins where detected. GFP was used as a loading control for transfected actinin levels. Molecular weight markers were used but are not shown. Bands are at expected sizes: endogenous actinin (~100 kDa) and transfected GFP-tagged actinin (~130 kDa).

	Species	Human			Mouse		
Antibody		1	2	4	1	2	4
α-Actinin [Santa Cruz (H-2): sc-17829)	Ms (M)	X					
α-Actinin-1 [Abnova (3F1])	Ms (M)	X			X		
α-Actinin [Santa Cruz (H300): sc15335)	Rb (P)	X	X	w	X	X	
α-Actinin-2 [Santa Cruz (A-25): 130928]	Rb (P)		X			X	
α-Actinin [Sigma (BM75.2)]	Ms (M)	X		X	X		X
α-Actinin-4 [Immunoglobe (IG701)]	Rb (P)			X			X
α-Sarcomeric Actinin [Sigma Clone (EA-53)]	Ms (M)		X			X	

Table 3.1 Isoform-specificity of actinin antibodies as determined by Western blot analysis. "X" denotes strong detection and "w" denotes weak detection. Rb=rabbit, Ms=mouse, M=monoclonal and P=polyclonal

3.1.1.2 Antibody detection efficiency

Through Western blot analysis of various cell lines and tissues I tested the detection efficiency of a number of commercially available actinin antibodies. Previously I determined that Abnova (3F1) was specific for human and mouse actinin-1 and that Santa Cruz (A-25) was specific for human and mouse actinin-2 (Figure 3.1 and Table 3.1). However, Western blot analysis of various cell lines and tissues showed that while these antibodies can detect high levels of transfected GFP-tagged actinin, they are less efficient at detecting endogenous levels of actinin (Figure 3.2A and 3.3A). The possibility that the cell lysis buffer may not have solubilised actinin is ruled out by the fact that actinin was detected in these samples by other antibodies (Figure 3.2B and 3.3A). Efforts using different antibody dilution buffers did not improve efficiency (data not shown). Therefore these antibodies were deemed unsuitable for detection of endogenous actinin-1 and -2. Sigma (BM72.5) was shown to be specific for human and mouse actinin-1 and -4 (Figure 3.1). This antibody successfully detected actinin in cell lines and tissues (Figure 3.2B and 3.3A). Immunoglobe (IG701) was shown to be specific for human and mouse actinin-4 (Figure 3.1). This antibody successfully detected actinin in cell lines and tissues lysed in a range of lysis buffers indicating that this antibody is efficient and that each of these lysis buffers is successful at solubilising actinin (Figure 3.2B and 3.3A+B). Santa Cruz (H300) was shown to detect human and mouse actinin-1 and -

2, and it also weakly detected human actinin-4 (Figure 3.1). This antibody detected actinin in cell lines and tissues (Figure 3.3A). Sigma (Clone EA-53) is reported to detect sarcomeric actinin. I found this antibody to be specific for human and mouse actinin-2 (Figure 3.1). This antibody detected actinin in cell lines and tissues (Figure 3.3A+C).

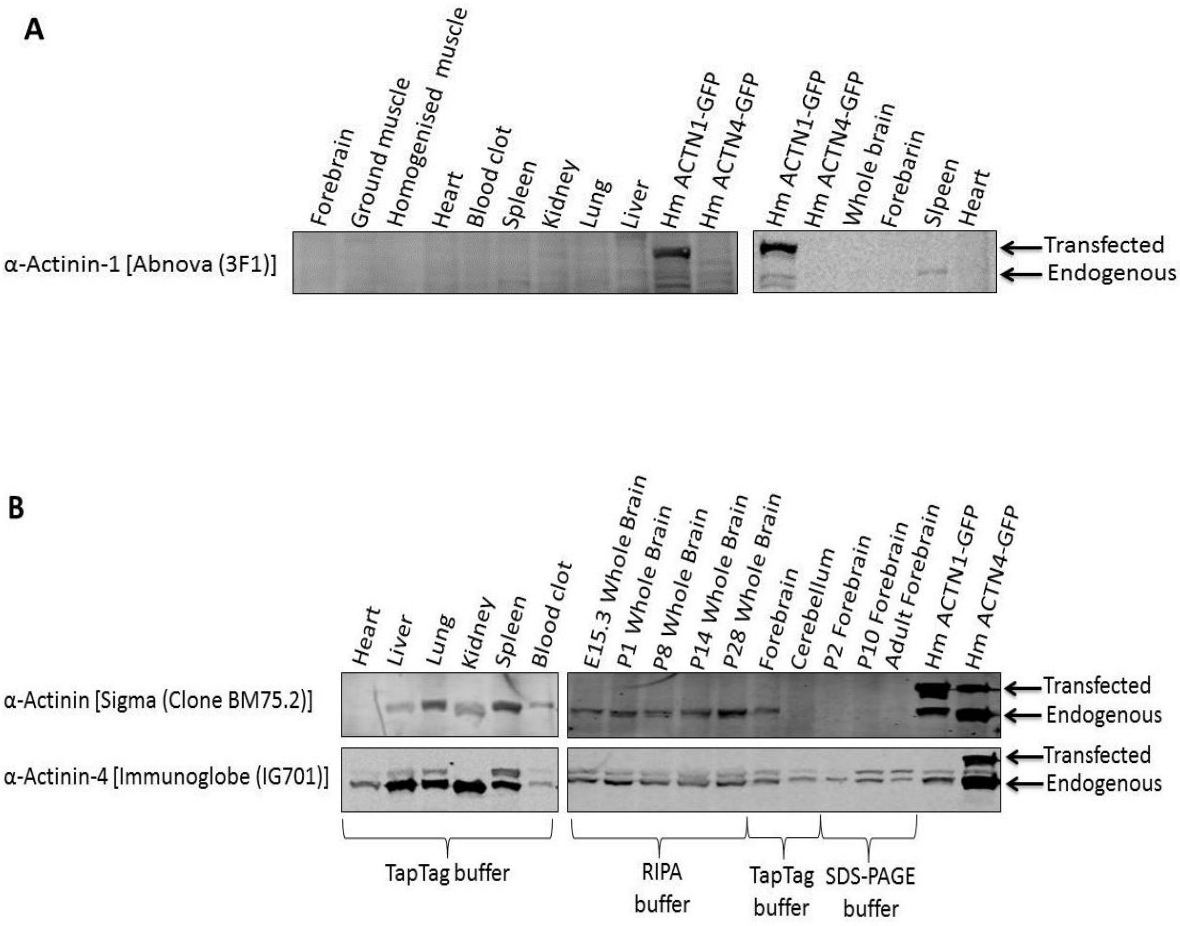

Figure 3.2 Optimisation of actinin antibodies from Abnova, Sigma and Immunoglobe. The detection efficiency of commercially available antibodies was determined by Western blot using lysates from various cell lines and tissues. Molecular weight markers were used but are not shown. Bands are at expected sizes.

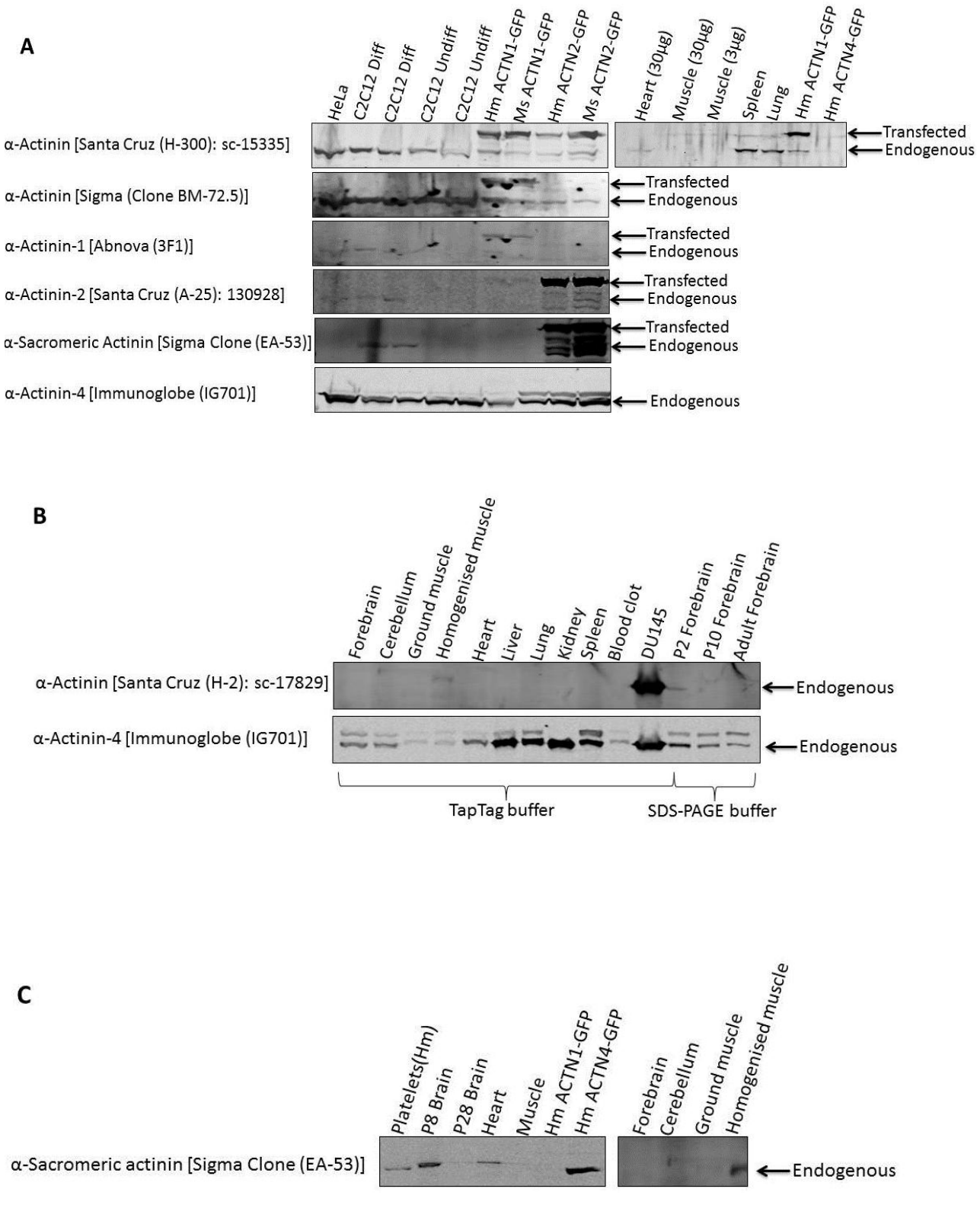

Figure 3.3 Optimisation of actinin antibodies from Santa Cruz, Abnova, Sigma and Immunoglobe. The detection efficiency of commercially available antibodies was determined by Western blot using lysates from various cell lines and tissues. Diff=differentiated, Undiff= undifferentiated. Molecular weight markers were used but are not shown. Bands are at expected sizes.

3.1.2 Effect of actinin knockdown on cell migration

3.1.2.1 Optimisation of siRNA-mediated knockdown of actinin

I first selected cell lines to utilise for the optimisation of siRNA-mediated knockdown of actinin-1 and -4. I probed a panel of cell lines with antibodies specific for actinin-1/-4 and actinin-4 (Figure 3.4). I selected COS-7 cells for actinin-1 siRNA optimisation. This decision was based on the fact that these cells do not contain detectable levels of actinin-4 relative to other cell lines in the panel. If successful actinin-1 knockdown could be achieved in this cell line then it could provide a good model for studying the effect of combined non-muscle actinin deficiency on cells. I selected MCF-7 cells for actinin-4 siRNA optimisation as these cells contained an intermediate level of actinin-4 relative to other cell lines in the panel and therefore may represent a cell type that meets two important characteristics: 1) expresses actinin-4, 2) actinin-4 expression levels are within a range that can be successfully knocked down by siRNA (Figure 3.4).

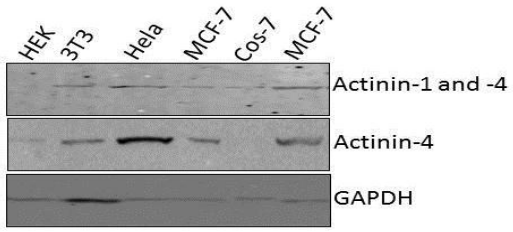

Figure 3.4 Western blot analysis of the levels of total non-muscle actinin (actinin-1/-4) and actinin-4 present in a panel of cell lines. GAPDH was used as a loading control. Molecular weight markers were used but are not shown. Bands are at expected sizes. Antibodies: Actinin-1 and -4 [Sigma BM 75.2] and Actinin-4 [Immunoglobe (IG701)].

I employed two siRNAs targeted against actinin-1 and -4 in COS-7 and MCF-7 cells, respectively (Figure 3.5A and B). I tested the efficiency of 10 nM of each siRNA over the course of 72 hr to knockdown actinin. I also included a 72 hr time-point using 50 nM siRNA in an attempt to achieve optimal actinin knockdown. I found that a maximum knockdown of 77% actinin-1 was achieved using 10 nM

siRNAa at 72 hr in COS-7 cells (Figure 3.5A). I found that a maximum knockdown of 90% actinin-4 was achieved using 10 nM siRNAa at 72 hr in MCF-7 cells (Figure 3.5B). The ultimate aim of this study was to monitor the effect of actinin knockdown on cell migration through a scratch wound assay. Preliminary work indicated that wild-type MCF-7 cells require ~24 hr to migrate and close a scratch wound (data not shown). For this reason I set up an actinin-4 knockdown experiment to mimic this time-frame in MCF-7 cells (Figure 3.5C). I found that actinin-4 knockdown levels were maintained throughout the time-frame required to perform a scratch wound assay. For this reason I selected MCF-7 cells to begin migration studies.

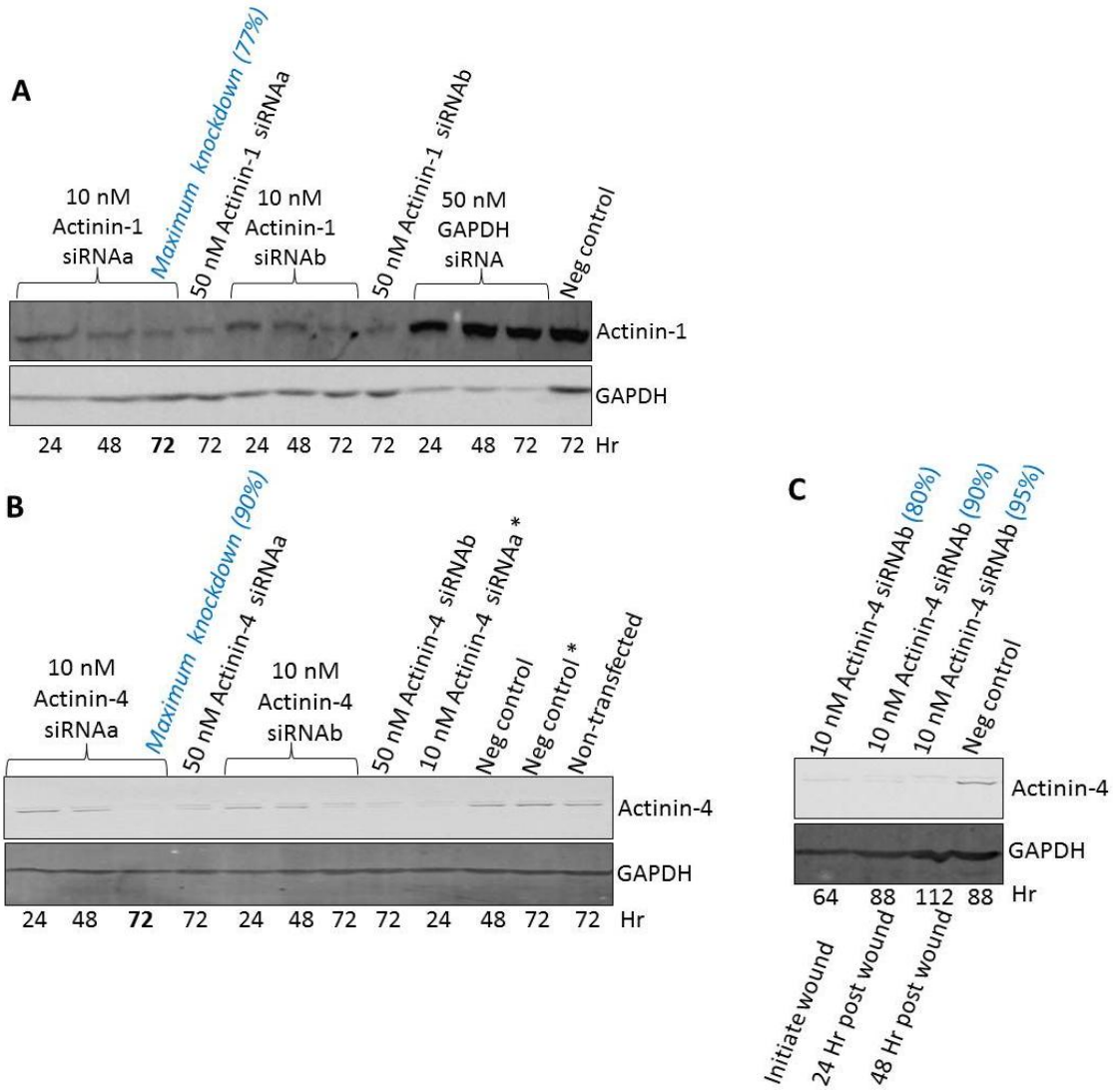

Figure 3.5 Optimisation of siRNA mediated-knockdown of actinin-1 and -4. siRNA-mediated knockdown of (A) actinin-1 in COS-7 cells and (B and C) actinin-4 in MCF-7 cells. Knockdown levels are highlighted in blue. *5 µl lipofectamine compared to standard 3µl. Molecular weight markers were used but are not shown. Bands are at expected sizes. Antibodies: Actinin-1 [Santa Cruz (H2):sc-17829] and Actinin-4 [Immunoglobe (IG701)].

I also tested the efficiency of these siRNAs to knockdown actinin in the breast carcinoma cell line MDA-MB-231 as this is an aggresssive migratory cancer cell line that may prove to be a good model for migration studies However, while I was able obtain >90% knockdown of actinin-1 (Figure 3.6A), I achieved <60% knockdown of actinin-4, even with increased siRNA concentrations (Figure 3.6B+C).

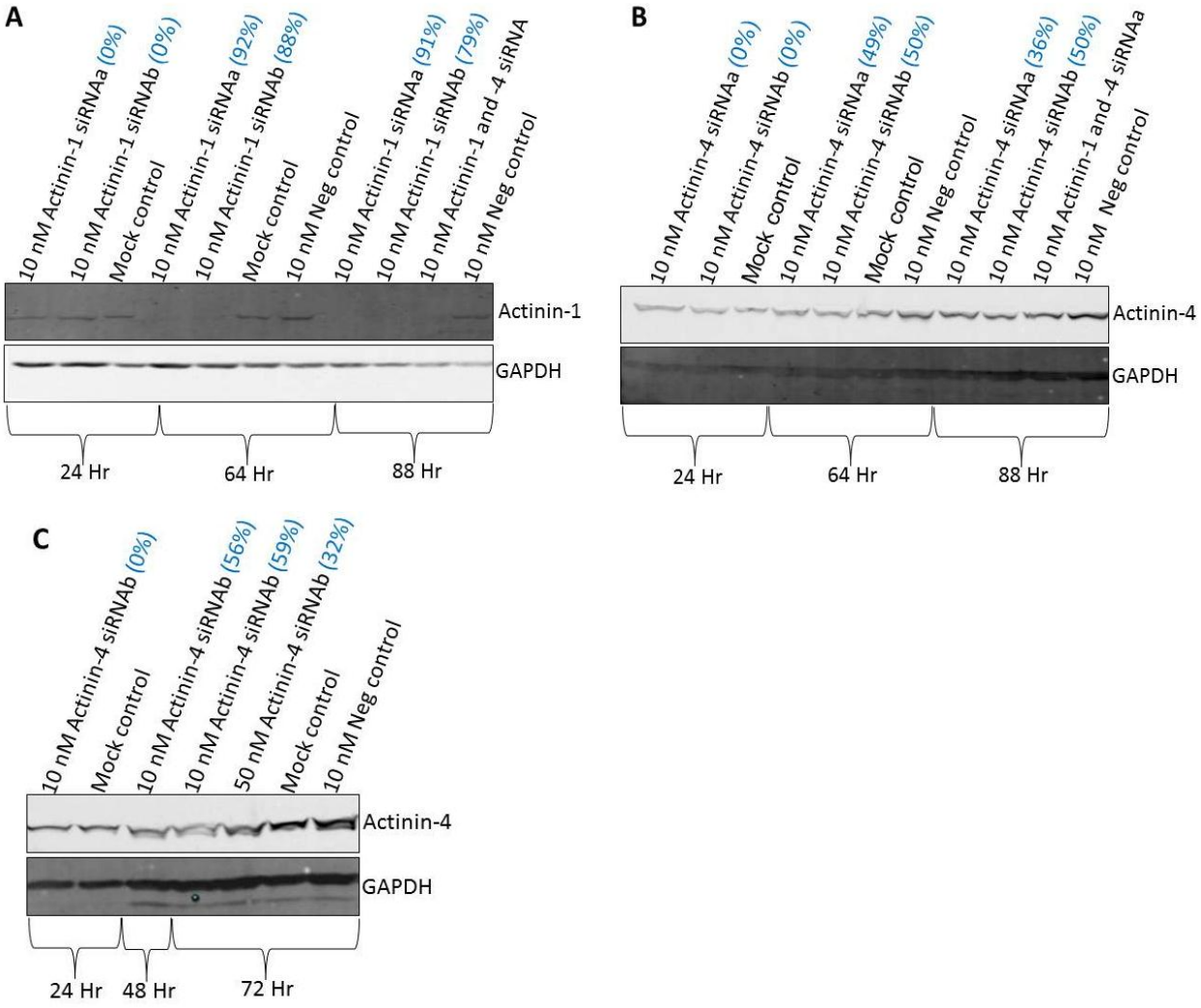

Figure 3.6 Optimisation of siRNA-mediated knockdown of actinin-1 and -4 in MDA-MB-231. Western blots of lysates post siRNA-mediated knockdown of (A) actinin-1 and (B and C) actinin-4 in MDA-MB-231 cells. The timeframe of the experiment was selected so as to facilitate a scratch wound migration assay. Knockdown levels achieved are highlighted in blue. Molecular weight markers were used but are not shown. Bands are at expected sizes. Antibodies: Actinin-1 [Santa Cruz (H2):sc-17829] and Actinin-4 [Immunoglobe (IG701)].

3.1.2.2 Scratch wound assays to monitor the effect of individual and combined actinin-1 and -4 knockdown on cell migration

3.1.2.2.1 MCF-7 cell scratch wound assays

siRNA mediated-knockdown of individual and combined actinin-1 and -4 was performed in MCF-7 cells as described in Materials and Methods Section 2.1.4. 72 hr post siRNA transfection scratch wounds were inflicted upon confluent cell layers (Figure 3.7 left image). 12 hr post scratch wound induction the area that remained open (Figure 3.7 right image) and the percentage of actinin knockdown achieved (Figure 3.8A) were quantified. The percentage wound closure for each assay was calculated (Figure 3.8B+C). Using a Student's T-Test no statistically significant effect was observed on MCF-7 cell migration as a result of individual or combined actinin-1 and-4 knockdown (n=3). The calculated p-values for actinin-1, actinin-4 and combined actinin-1 and -4 knockdown were 0.12, 0.14 and 0.48 respectively.

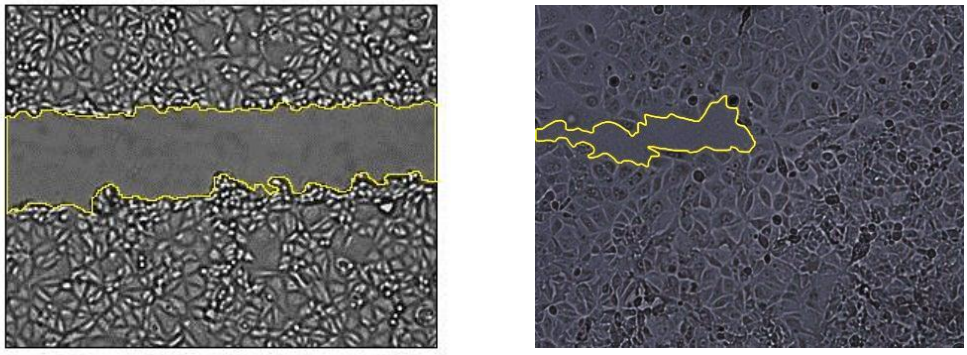

Figure 3.7 Scratch wound migration assay to monitor the effect of actinin-1 and -4 knockdown on MCF-7 cell migration. (A) Left: Sratch wound induced at T=O showing open area highlighted in yellow. Right: Scratch wound at T12 showing remaining open area highlighted in yellow. (T0-T12=closed area) (closed area/T0 X 100 = % closure).

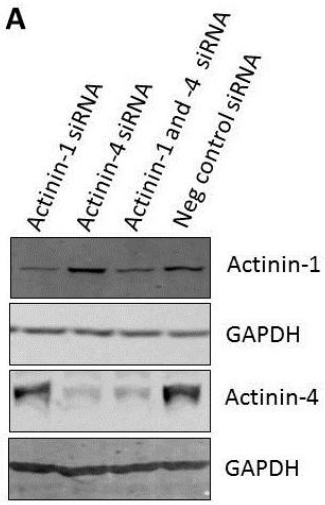

	% Knockdown	
siRNA	**Actinin-1**	**Actinin-4**
Actinin-1	67	-
Actinin-4	-	82
Actinin-1 and -4	60	74

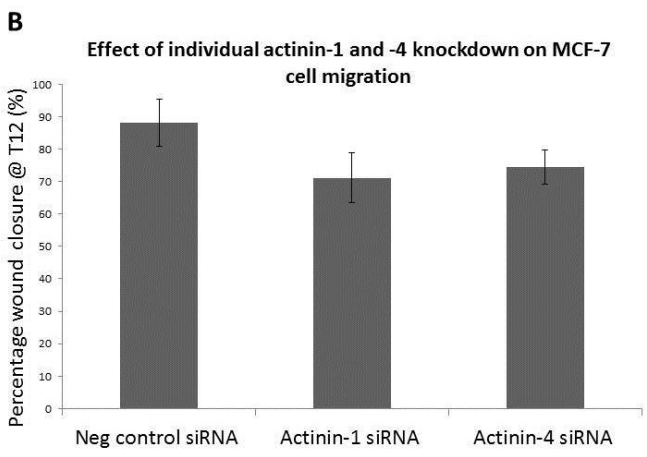

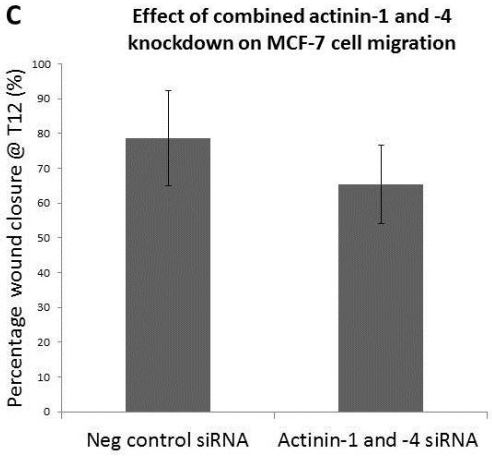

Figure 3.8 Scratch wound migration assay to monitor the effect of actinin-1 and -4 knockdown on MCF-7 cell migration. Left: Western blot showing MCF-7 cell lysates probed for actinin-1 and -4 post scratch wound assay. Molecular weight markers were used but are not shown. Bands are at expected sizes. Antibodies: Actinin-1 [Santa Cruz (H2):sc-17829] and Actinin-4 [Immunoglobe (IG701)]. Right: Summary of actinin knockdown levels obtained as determined by densitometric quantification of Western blot. Effect of (B) individual and (C) combined actinin-1 and -4 knockdown on MCF-7 cell migration. (n=3) (10 nM of each siRNA was used).

3.1.2.2.2 DU145 cell scratch wound assays

siRNA mediated-knockdown of individual and combined actinin-1 and -4 was performed in DU145 cells as described in Materials and Methods Section 2.1.4. 72 hr post siRNA transfection scratch wounds were inflicted upon confluent cell layers. 8 hr post scratch wound induction the percentage of actinin knockdown achieved (Figure 3.9A) and the percentage wound closure (Figure 3.9B) was quantified for each assay. No obvious effects were observed on DU147 cell migration as a result of individual or combined actinin-1 and -4 knockdown (n=2).

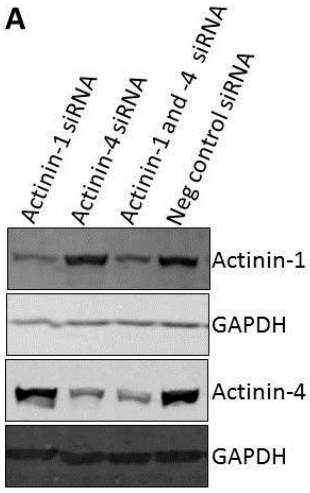

	% Knockdown	
siRNA	**Actinin-1**	**Actinin-4**
Actinin-1	63	-
Actinin-4	-	79
Actinin-1 and -4	70	73

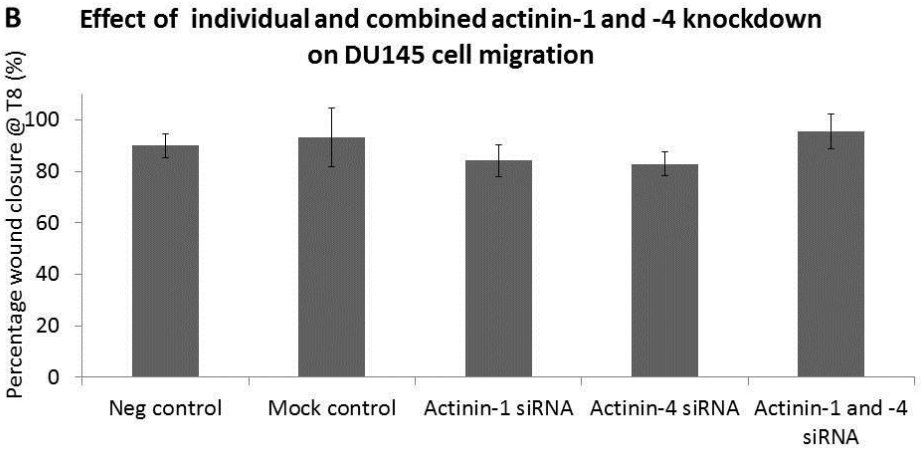

Figure 3.9 Scratch wound migration assays to monitor the effect of actinin-1 and -4 knockdown on DU145 cell migration. (A) Left: Western blot showing DU145 cell lysates probed for actinin-1 and -4 post scratch wound assay. Molecular weight markers were used but are not shown. Bands are at expected sizes. Antibodies: Actinin-1 [Santa Cruz (H2):sc-17829] and Actinin-4 [Immunoglobe (IG701)]. Right: Summary of actinin knockdown levels obtained as determined by densitometric quantification of Western blot. (B) Effect of individual and combined actinin-1 and -4 knockdown on DU145 cell migration. (n=2) (10 nM of each siRNA was used).

3.1.2.2.3 A172 cell scratch wound assays

siRNA mediated-knockdown of individual and combined actinin-1 and -4 was performed in A172 cells as described in Materials and Methods Section 2.1.4. 72 hr post siRNA transfection scratch wounds were inflicted upon confluent cell layers. 12 hr post scratch wound induction the percentage of actinin knockdown achieved (Figure 3.10A) and the percentage wound closure (Figure 3.10B+C) was quantified for each assay. No obvious effects were observed on A172 cell migration as a result of individual or combined actinin-1 and-4 knockdown (n=1).

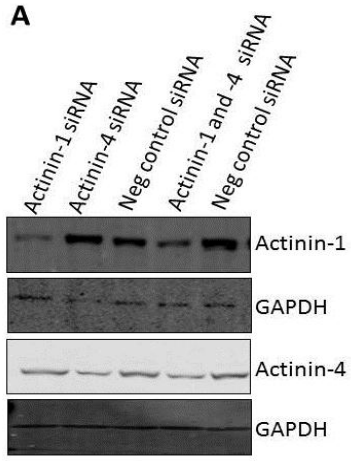

	% Knockdown	
siRNA	**Actinin-1**	**Actinin-4**
Actinin-1	67	-
Actinin-4	-	48
Actinin-1 and-4	55	45

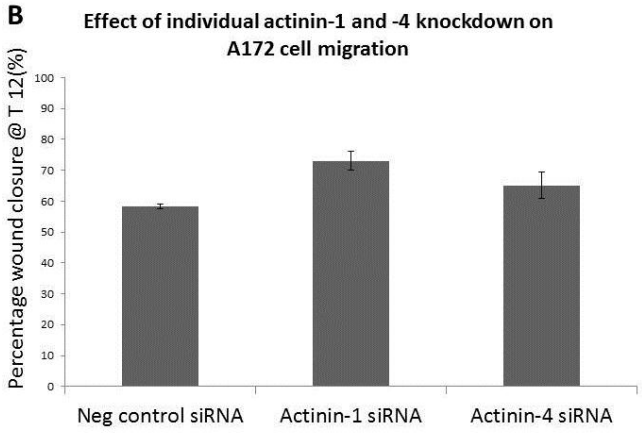

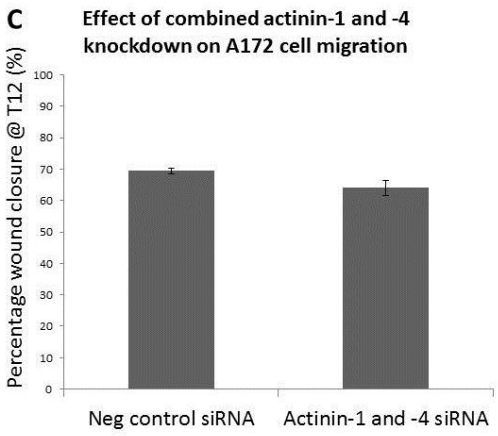

Figure 3.10 Scratch wound migration assays to monitor the effect of actinin-1 and -4 knockdown on A172 cell migration. (A) Left: Western blot showing A172 cell lysates probed for actinin-1 and -4 post scratch wound assay. Molecular weight markers were used but are not shown. Bands are at expected sizes. Antibodies: Actinin-1 [Santa Cruz (H2):sc-17829] and Actinin-4 [Immunoglobe (IG701)]. Right: Summary of actinin knockdown levels obtained as determined by densitometric quantification of Western blot. Effect of (B) individual and (C) combined actinin-1 and -4 knockdown on A172 cell migration. (n=1). (10 nM of each siRNA was used).

3.1.2.2.4 U373-MG cell scratch wound assays

siRNA mediated-knockdown of individual and combined actinin-1 and -4 was performed in U373-MG cells as described in Materials and Methods Section 2.1.4. 72 hr post siRNA transfection scratch wounds were inflicted upon confluent cell layers. 12 hr post scratch wound induction the percentage of actinin knockdown achieved (Figure 3.11A) and the percentage wound closure (Figure 3.11B+C) was quantified for each assay. No obvious effects were observed on U373-MG cell migration as a result of individual or combined actinin-1 and-4 knockdown (n=1).

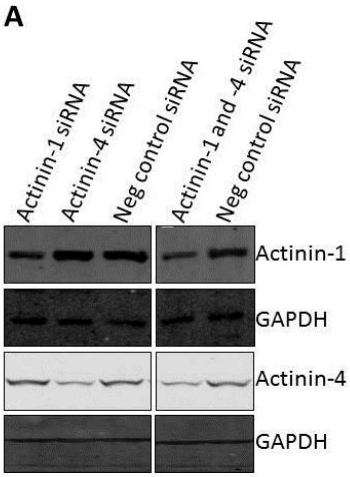

	% Knockdown	
siRNA	**Actinin-1**	**Actinin-4**
Actinin-1	54	-
Actinin-4	-	47
Actinin-1 and -4	40	58

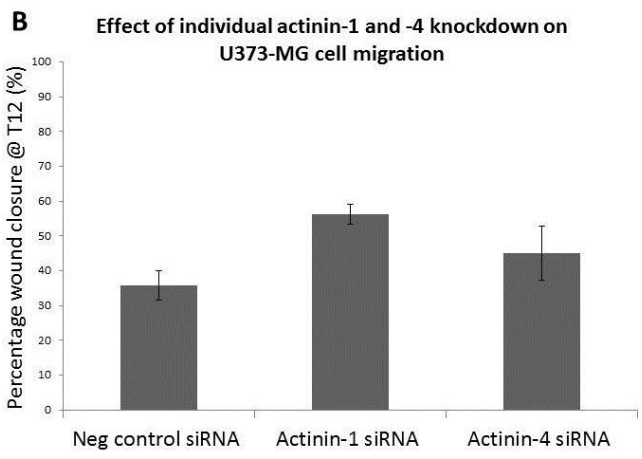

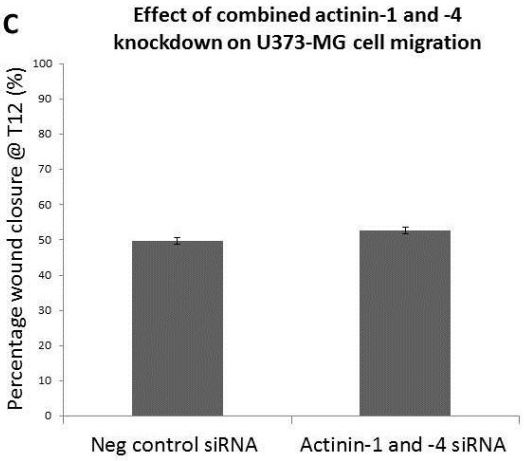

Figure 3.11 Scratch wound migration assays to monitor the effect of actinin-1 and -4 knockdown on U373-MG cell migration. (A) Left: Western blot showing U373-MG cell lysates probed for actinin-1 and -4 post scratch wound assay. Molecular weight markers were used but are not shown. Bands are at expected sizes. Antibodies: Actinin-1 [Santa Cruz (H2):sc-17829] and Actinin-4 [Immunoglobe (IG701)]. Right: Summary of actinin knockdown levels obtained as determined by densitometric quantification of Western blot. Effect of (B) individual and (C) combined actinin-1 and -4 knockdown on U373-MG cell migration. (n=1). (10 nM of each siRNA was used).

3.1.3 Determination of the specific protein domains responsible for the distinct localisation patterns observed for actinin-1 and -4.

3.1.3.1 Cloning and expression of GFP-tagged actinin-1 and -4.

Full length actinin-1 and -4 were cloned into GFP-expressing vectors (Figure 3.12A). These constructs were transfected and expressed in MCF-7 cells (Figure 3.12B). Localisation was monitored by fluorescent microscopy (Figure 3.12C). Although there is an overlap is the localisation of both isoforms, actinin-1-GFP tends to localise at stress fibre regions near focal adhesions sites while actinin-4-GFP tends to localise to cell membrane regions (Figure 3.12C). This corresponds to reports suggesting that actinin-1 localises specifically at the ends of actin stress fibres, at focal adhesions and adheren junctions (Honda et al., 1998). The observed localisation of actinin-4 is consistent with reports suggesting that actinin-4 localises to cell ruffles and at the edge of migrating cells (Araki et al., 2000; Honda et al., 1998). However, in contrast to reports in the literature this work does not observe nuclear localisation of actinin-4 (Honda et al., 1998). It has been suggested that nuclear localisation and interactions of actinin-4 may be effected by actin depolymerisation and by certain extracellular matrixes (Honda et al., 1998; Bolshakova et al., 2007). The discrepancies that exist between my observations of actinin-4 and those of reported nuclear localisation of actinin-4 may be due to differences in cell culture methods.

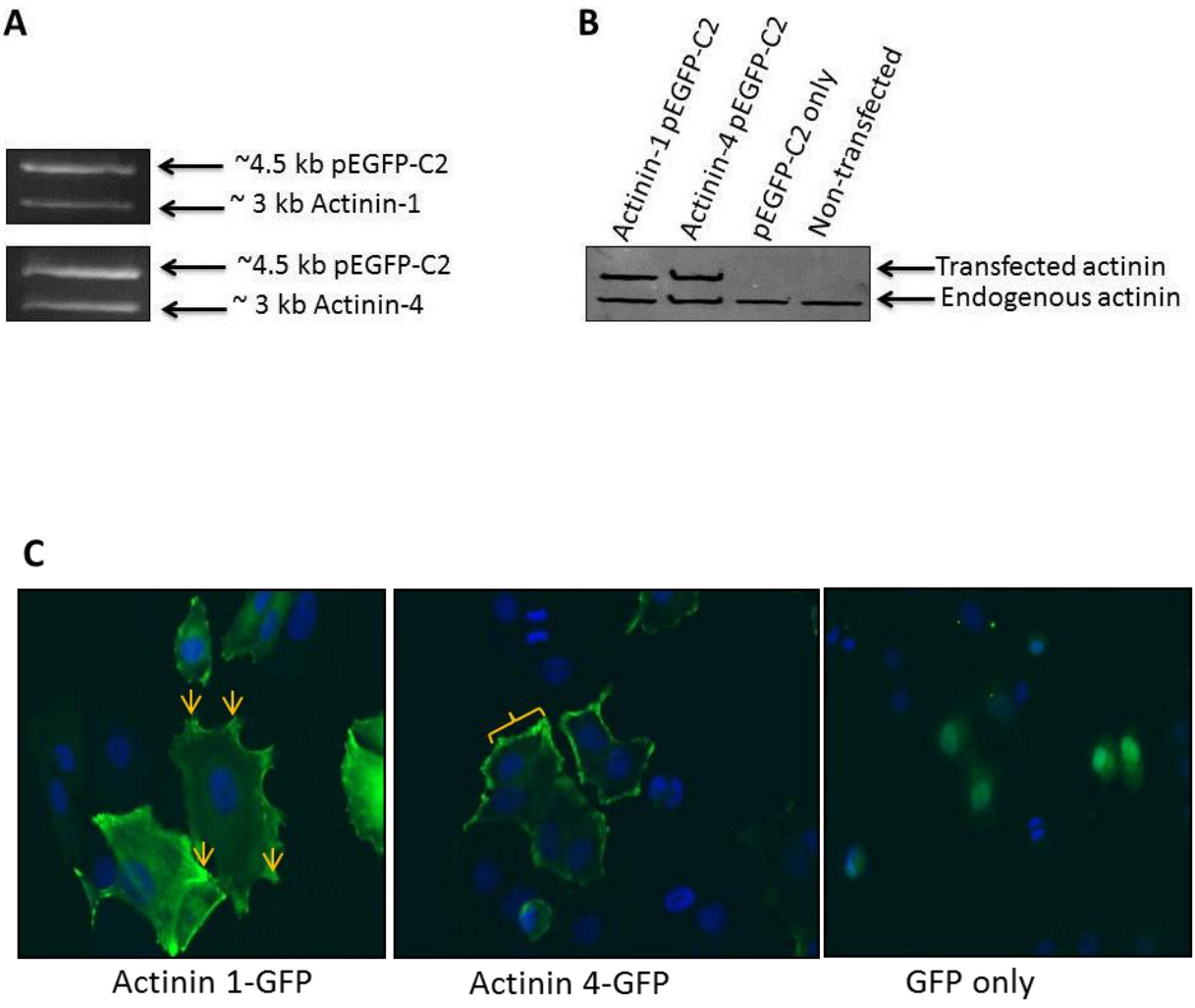

Figure 3.12 Cloning, expression and localisation of GFP-tagged actinin-1 and -4 in MCF-7 cells. (A) Agarose gels showing XhoI and EcoRI digested actinin-1 and -4 pEGFP-C2. ~3 kb bands represent full length actinin-1 and -4. MCF-7 cells were transfected with GFP-tagged actinin-1 and -4 constructs. (B) Western blot of transfected MCF-7 cell lysates probed with an antibody that detects actinin-1 and -4. Molecular weight marker was used but is not shown. Antibody: Actinin-1 and -4 [Sigma (BM 75.2] (C) Fluorescent microscopy of MCF-7 cells transfected with GFP-tagged actinin-1, -4 or GFP only. Actinin-1-GFP tends to localise to stress fibres and focal adhesions (yellow arrows) while actinin-4-GFP tends to localise to cell membranous regions (yellow bracket). Dapi stained nuclei (blue).

In order to ensure that transfected actinin isoforms were functioning correctly and binding to actin filaments I performed phalloidin staining of MCF-7 cells transfected with GFP-tagged actinin-1 and -4. I found that transfected actinin -1 and -4 both co-localised with actin (Figure 3.13).

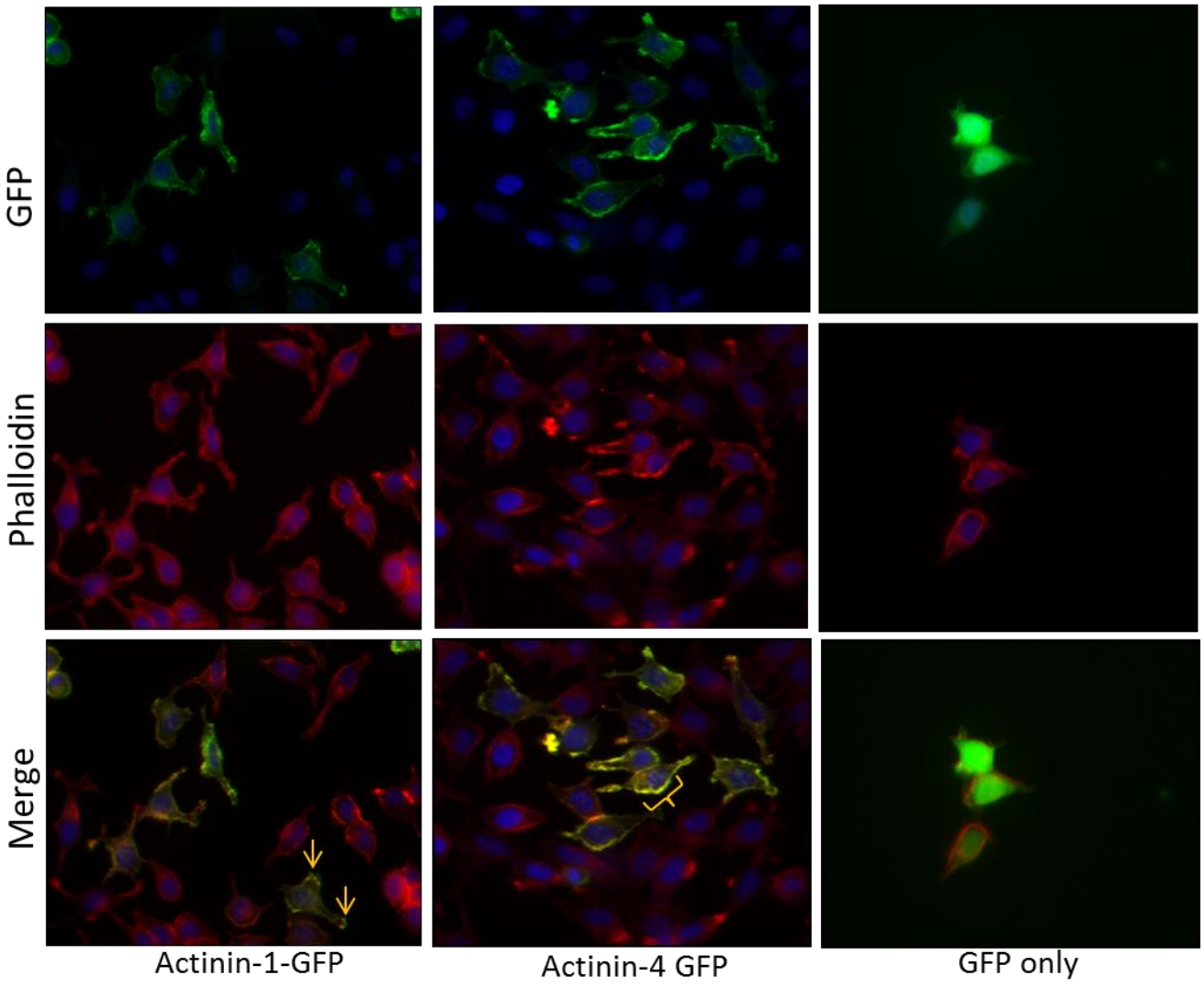

Figure 3.13 Co-localisation of GFP-tagged actinin-1 and -4 with actin filaments. GFP-tagged actinin (green). Actin filaments stained with phalloidin (red). Actinin-1-GFP present in stress fibres sites (yellow arrows). Actinin-4 GFP present in membranous regions (yellow bracket). Dapi stained nuclei (blue).

3.1.3.2 Development of chimeric actinin-1/-4 proteins: Cloning strategy

3.1.3.2.1 Switching calmodulin-like (CaM) domains between actinin-1 and -4

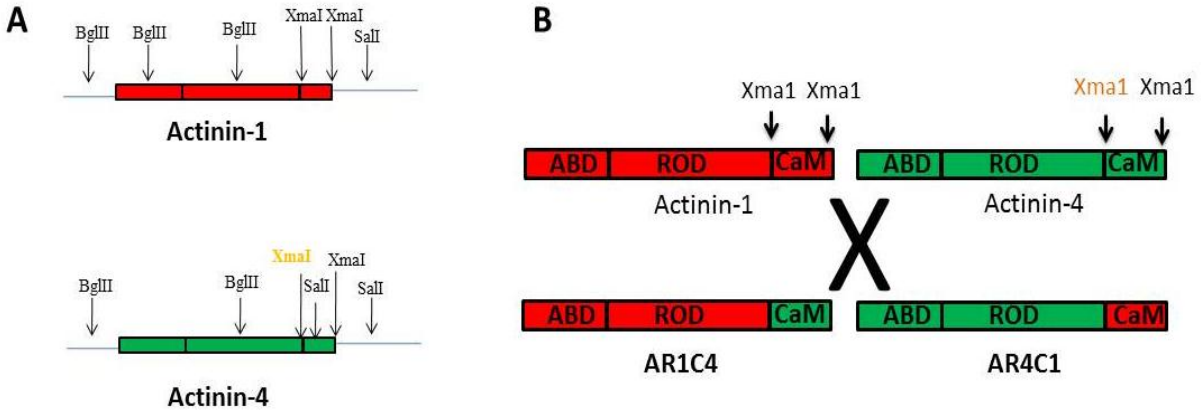

Figure 3.14 Cloning strategy for switching CaM domains between actinin-1 and -4. (A) Restriction sites employed for the cloning and confirmation of switched CaM domains between actinin-1 and -4. (B) Cloning strategy for switching CaM domains. Site-directed mutagenesis was used to introduce an XmaI site into the coding sequence of actinin-4 (highlighted in yellow). This site along with naturally occurring Xma1 sites was used to switch CaM domains. AR1C4 = (Actinin-1 actin-binding and rod domains, actinin-4 CaM domain). AR4C1 = (Actinin-4 actin-binding and rod domains, actinin-1 CaM domain).

Figure 3.14A highlights the restriction sites utilised to switch CaM domains between actinin-1 and -4 and to confirm that correct isoform domains were present in resulting constructs. Figure 3.14B denotes the cloning strategy followed in order to switch CaM domains between actinin-1 and -4. In short, site-directed mutagenesis was employed in order to insert an XmaI restriction site into the coding sequence of actinin-4. This new site along with the other natural occurring XmaI sites in actinin-1 and -4 were used to digest and subsequently switch CaM domains between actinin-1 and -4. XmaI, SalI and BglII confirmatory digests were performed on the resulting constructs in order to ensure they contained the correct actinin isoform domains. Figure 3.15 shows confirmatory XmaI, SalI and BgLII digests of (A) AR1C4 and (B) AR4C1 pEGFP-C2 constucts. Constructs resulting from AR1C4 colonies #2 and #3 show correct digest patterns (highlighted in blue) while the construct resulting from AR4C1 colony #1 also shows a correct digest pattern (highlighted in blue).

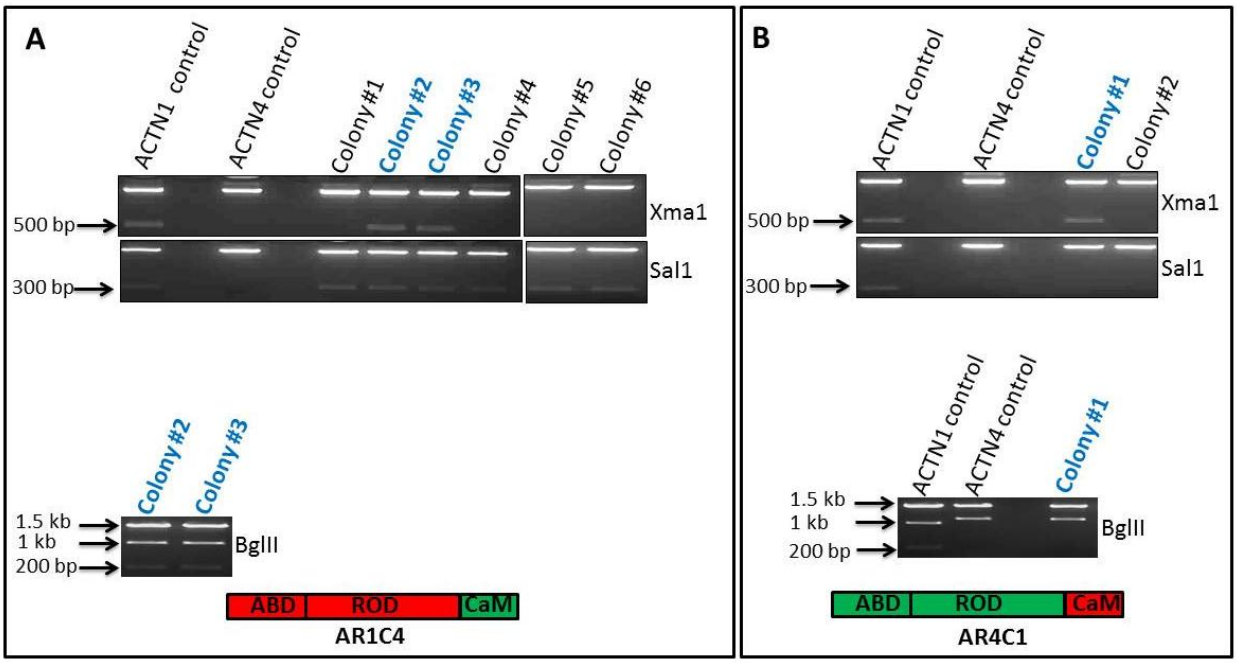

Figure 3.15 Confirmatory digests of switched CaM domains between actinin-1 and -4. XmaI, SalI and BglII restriction digests were performed on (A) AR1C4-pEGFP-C2 and (B) AR4C1-pEGFP-C2 constructs. DNA ladders were used but are not shown. Constructs showing correct digest patterns are highlighted in blue.

3.1.3.2.2 Switching actin-binding domains (ABD) between actinin-1 and -4

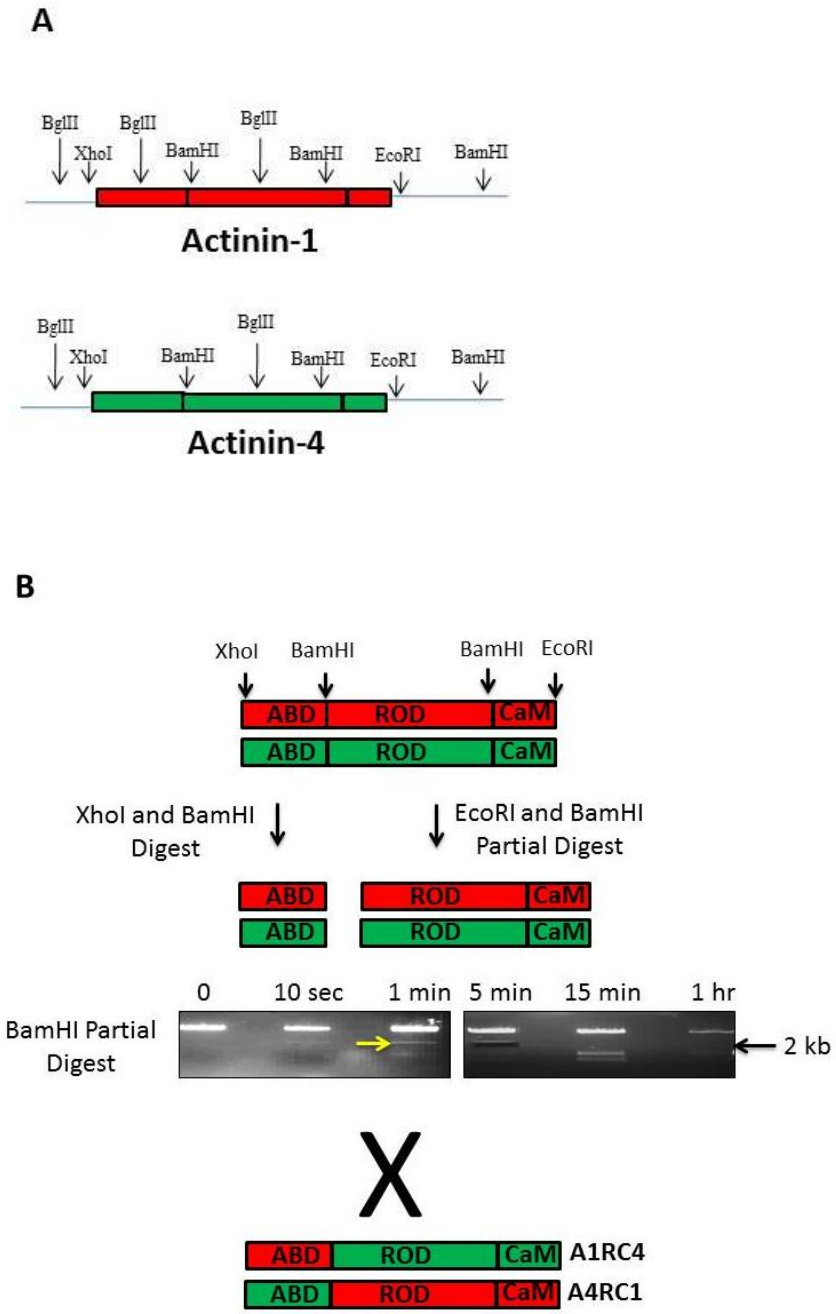

Figure 3.16 Cloning strategy for switching actin-binding domains between actinin-1 and -4. (A) Restriction sites employed for the cloning and confirmation of switched actin-binding domains between actinin-1 and -4. (B) Cloning strategy for switching actin-binding domains. XhoI and BamHI digest was used to obtain actin-binding domains of actinin-1 and -4. EcoRI digest followed by partial BamHI digest was used to obtain rod domains of actinin-1 and -4 from agarose gel (yellow arrow). DNA ladder was used but is not shown. A1RC4 = (Actinin-1 actin-binding domain, actinin-4 rod and CaM domains). A4RC1 = (Actinin-4 actin-binding domain, actinin-1 rod and CaM domains).

Figure 3.16A highlights the restriction sites utilised to switch actin-binding domains between actinin-1 and -4 and to confirm that correct isoform domains were present in resulting constructs. Figure 3.16B denotes the cloning strategy followed in order to switch actin-binding domains between actinin-1 and -4. In short, XhoI and BamHI digests were used to obtain actin-binding domains from actinin-1 and -4. EcoRI digest following by a partial BamHI digest was used to obtain the rod and CaM domains of actinin-1 and -4. BglII confirmatory digests were performed on the resulting constructs in order to ensure they contained the correct actinin isoform domains. Figure 3.17 shows confirmatory BglII digests of A1RC4 and A4RC1 pEGFP-C2 constucts. The construct resulting from A1RC4 colony #1 shows the correct digest pattern while both constructs resulting from A4RC1 colonies #1 and #2 show correct digest patterns. Figure 3.19 shows further confirmatory (A) SalI and BglII and (B) XhoI and EcoRI digests of these constructs.

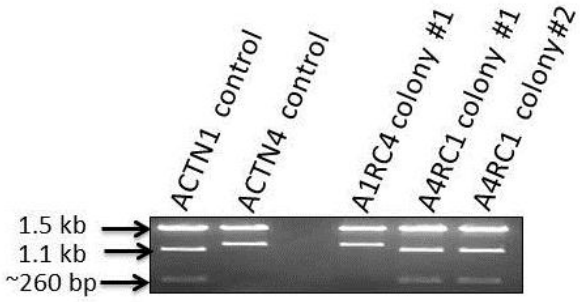

Figure 3.17 Confirmatory digests of switched actin-binding domains between actinin-1 and -4. BglII restriction digests were performed on A1RC4-pEGFP-C2 and A4RC1-pEGFP-C2 constructs. DNA ladder was used but is not shown. All constructs show correct digest patterns.

3.1.3.2.3 Switching rod domains between actinin-1 and -4

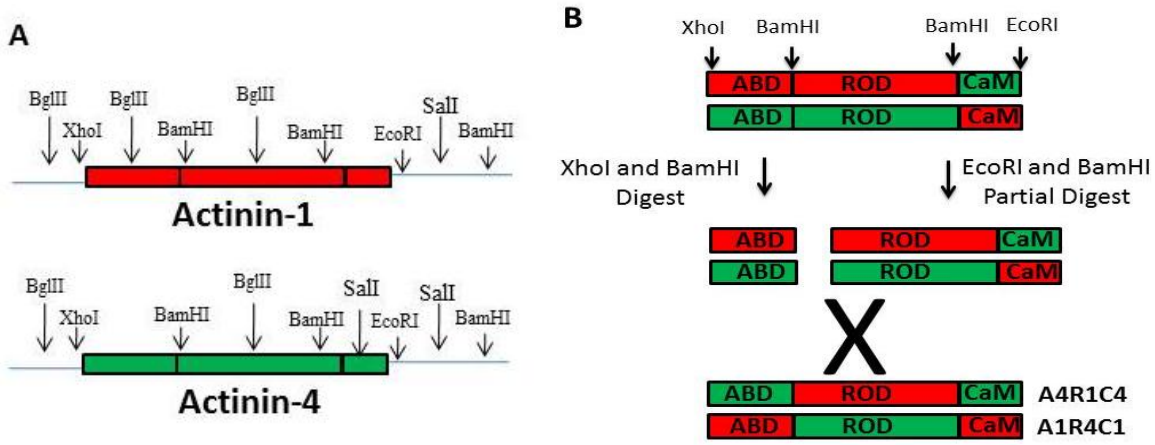

Figure 3.18 Cloning strategy for switching rod domains between actinin-1 and -4. (A) Restriction sites employed for the cloning and confirmation of switched rod domains between actinin-1 and -4. (B) Cloning strategy for switching rod domains. XhoI and BamHI1 digests were used to obtain actin-binding domains (ABD) of actinin-1 and -4. EcoRI digest followed by a BamHI partial digest was used to obtain R1C4 and R4C1 actinin domains. A4R1C4 = (Actinin-4 actin-binding domain, actinin-1 rod domain and actinin-4 CaM domain). A1R4C1=(actinin-1 actin-binding domain, actinin-4 rod domain and actinin-1 CaM domain).

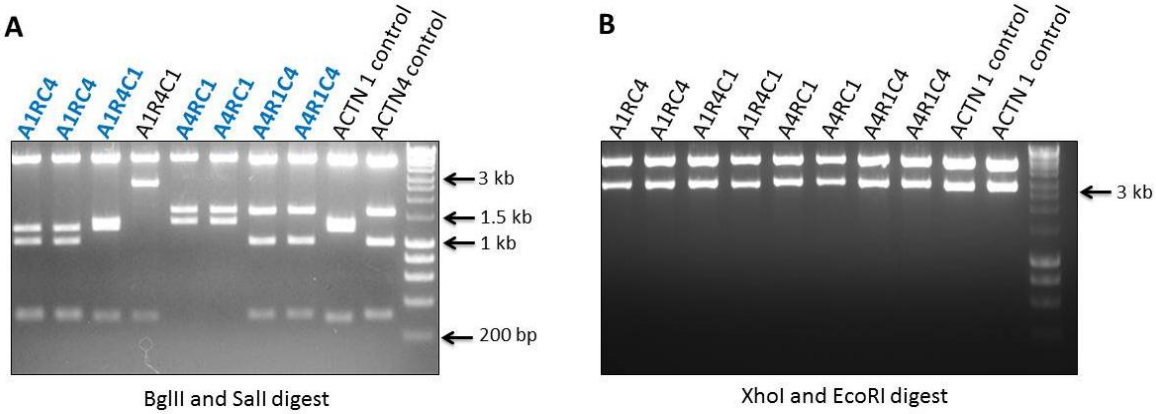

Figure 3.19 Confirmatory digests of switched rod domains and switched actin-binding domains between actinin-1 and -4. Confirmatory digests of A1R4C1, A4R1C4, A1RC4 and A4RC1-pEGFP-C2 constructs. (A) BglII and SalI digests. Constructs that showed correct digest patterns are highlighted in blue. (B) XhoI and EcoRI digest. All constructs showed correct digest pattern.

Figure 3.18A highlights the restriction sites utilised to switch rod domains between actinin-1 and -4 and to confirm that correct isoform domains were present in the

resulting constructs. Figure 3.18B denotes the cloning strategy followed in order to switch rod domains between actinin-1 and -4. In short, AR1C4 and AR4C1 constructs were digested with XhoI and BamHI in order to obtain actin-binding domains from actinin-1 and -4 respectively. EcoRI digest following by a partial BamHI digest was used to obtain the R1C4 and R4C1 domains of actinin. These actin-binding domains (A) and rod/calmodulin-like domains (RC) were then switched and ligated to obtain A1R4C1- and A4R1C4-pEGFP-C2 constructs. Figure 3.19 shows confirmatory (A) BglII and SalI digests and (B) XhoI an EcoRI digests of these constructs.

3.1.3.3 Expression and localisation of chimeric actinin-1 and -4 proteins

GFP-tagged chimeric actinin-1/-4 DNA constructs developed in Section 2.3.1.1 were transfected into MCF-7 cells. Protein expression of each construct was confirmed by Western blot (Figure 3.20).

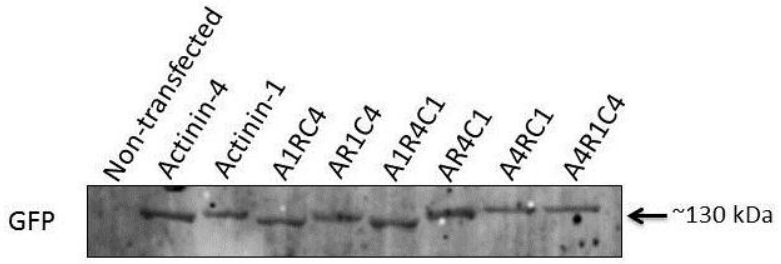

Figure 3.20 Expression of chimeric actinin-1/-4 proteins. Western blot of lysates of MCF-7 transfected with GFP-tagged chimeric actinin constructs. Antibody: GFP [Abcam (Cat# ab290)]. Molecular weight marker was used but is not shown.

MCF-7 cells were transfected with chimeric actinin-1/-4 pEGFP-C2 constructs. Localisation of chimeric actinin proteins was determined by fluorescent microscopy (Figure 3.21 Part1: A+B). While actinin-1 pEGFP-C2 localised at focal adhesion regions showing punctate staining, actinin-4 pEGFP tended to localise to membranous regions. Switching actin-binding domains between actinin-1 and -4 did not alter these localisation patterns (Figure 3.21 Part1: C+D), neither did switching CaM domains (Figure 3.21 Part 2: G+H). However, switching the rod domains of

actinin-1 and -4 appeared to cause a shift in this pattern of localisation (Figure 3.21 Part 2: E and F). This may not be surprising given that fact the rod domain of actinin has been described as a structural platform for protein assembles (Djinovic-Carugo et al., 2002). Many reported interactions of the rod domain form a direct link between actinin and membrane associated proteins including intergins and ICAMs (Otey et al., 1990; Carpén et al., 1992). The rod domain has also been reported to interact with proteins that may play a regulatory role in cytoskeleton rearrangement (Djinovic-Carugo et al., 2002; Mukai et al., 1997) . Altogether this implies that rod domain interactions may stongly influence the localisation of actinin within a cell.

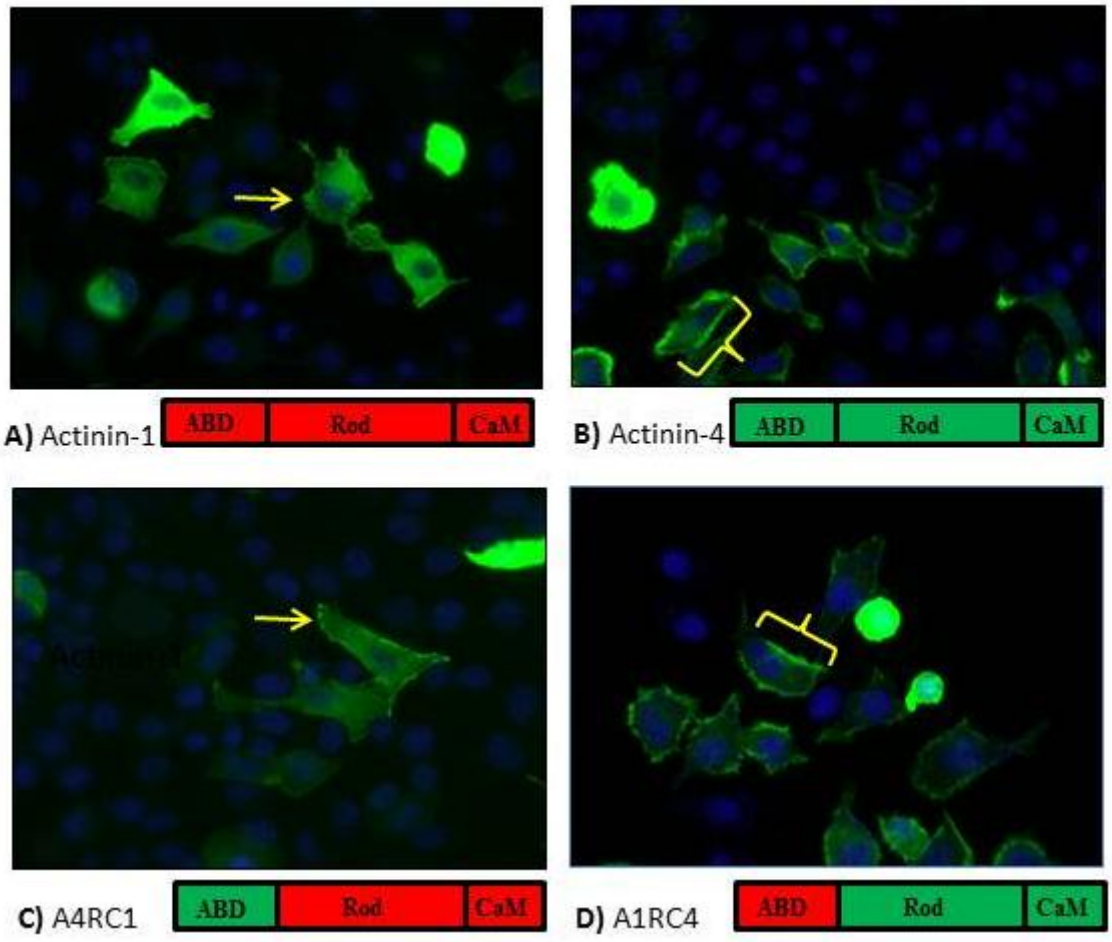

Figure 3.21 Part 1: Localisation of chimeric actinin-1/-4 proteins in MCF-7 cells. Fluorescent images of GFP-tagged A) Actinin-1, B) Actinin-4, C) A4RC1 and D) A1RC4 in MCF-7 cells (green). Dapi stained nuclei (blue). Yellow arrows highlight punctate localisation at stress fiber sites. Yellow brackets highlight membranous localisation.

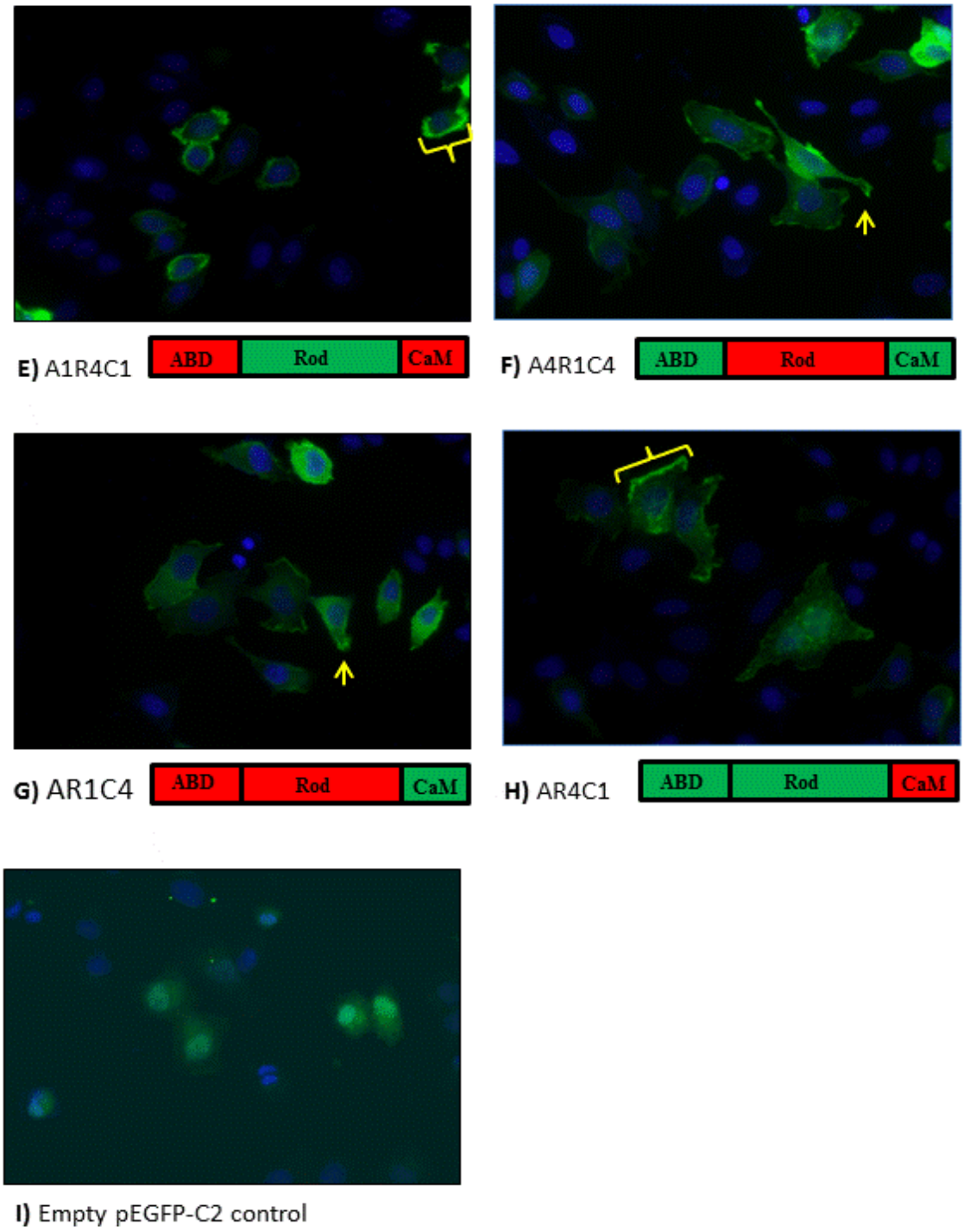

Figure 3.21 Part 2: Localisation of chimeric actinin-1/-4 proteins in MCF-7 cells. Fluorescent images of GFP-tagged E) A1R4C1, F) A4R1C4, G) AR1C4, H) AR4C1 and I) GFP control in MCF-7 cells (green). Dapi stained nuclei (blue). Yellow arrows highlight punctate localisation at stress fibre sites. Yellow brackets highlight membranous localisation.

3.2 Analysis of alternative splicing patterns and actin-binding characteristics of the non-muscle actinins

The development of alternative splicing patterns, distinct binding affinities and tissue-specific expression profiles have all been described as mechanisms of divergence employed by the actinin family. Differences in these protein characteristics may explain the observed differential effects of the non-muscle actinins. Splicing of exon 19 results in Ca^{++}-sensitive (exon 19a) or Ca^{++}-insensitive (exon 19b) expressing variants of actinin-1 and -4. Previously a brain-specific variant of actinin-1 that expresses both exon 19a+19b was detected in the rat brain. The Ca^{++} sensitivity of this brain-specific variant has not previously been determined. Alternative splicing of actinin-4 exon 8 results in either exon 8a or exon 8b expressing variants. The actinin-4 exon 8b-expressing variant is associated with small cell lung cancer and neuroendocrine tumours. Mutations that lie within this exon are associated with a form of kidney disease called focal segmental glomerulosclerosis (FSGS) and are reported to increase the affinity of actinin-4 for actin.

In this part of the work my goals were to:

1) Compare the tissue expression profiles of exon 8 and exon 19 alternative splice variants of actinin-1 and -4.
2) Compare the actin-binding affinities and calcium-sensitivities of the most widely expressed non-muscle actinin isoforms, namely actinin-1 (exon 19a) and actinin-4 (exon 8a, 19a).
3) Determine the calcium-sensitivity of the brain-specific actinin-1 exon 19a+19b expressing variant.
4) Compare the actin-binding affinities of actinin-4 exon 8a and exon 8b expressing variants.

3.2.1 Analysis of alternative splicing patterns of actinin-1 and -4 exon 19 and actinin-4 exon 8

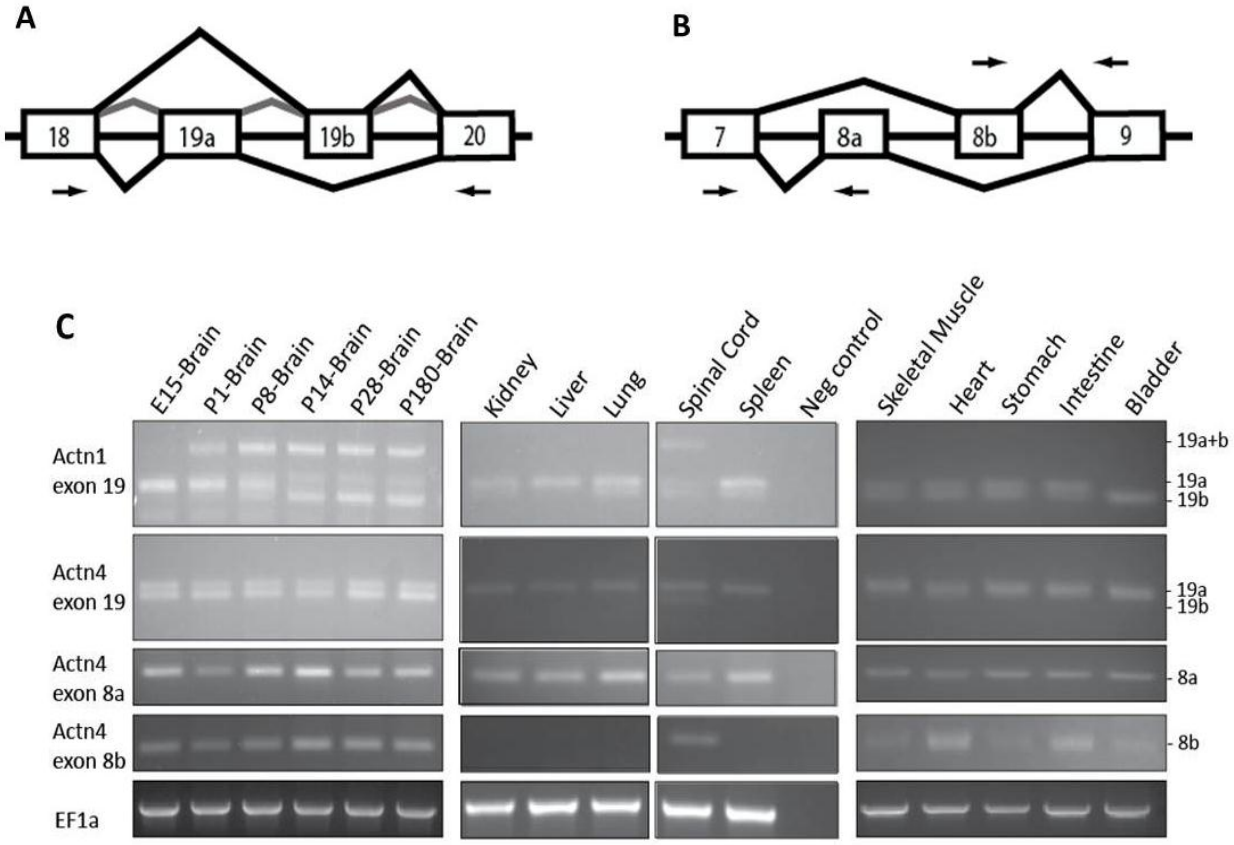

Figure 3.22 Analysis of the alternative splicing patterns of actinin-1 and -4 exons 8 and 19. (A) Schematic depiction of the alternative splicing of exon 19 that encodes part of the first EF-hand of the non-muscle actinins. Mutually exclusive splicing results in the inclusion of either exon 19a or 19b to generate Ca^{++}-sensitive and -insensitive isoforms respectively (black lines). Inclusion of both exons in the mature mRNA transcript can also occur for actinin-1 (Kremerskothen et al., 2002) (grey lines). Primers flanking exon 19 were used for rtPCR and are indicated by arrows. (B) Schematic depiction of mutually exclusive alternative splicing of exon 8 in actinin-4. Primer pairs in which one primer was specific for either exon 8a or 8b were used for rtPCR and are indicated by arrows. (C) rtPCR analysis of the alternative splicing patterns of actinin-1 and -4 exon 19 and actinin-4 exon 8 that occur in various murine tissues as indicated. The 15 bp size difference between exon 19a and 19b allows these two splice variants to be distinguished. Elongation factor-1 (EF1) PCRs were included as controls for cDNA levels. DNA ladders were used but are not shown. Bands are at expected sizes.

While the splicing of exon 19 in actinin-1 has been well characterised, the expression patterns of alternatively spliced actinin-4 isoforms has not been described in detail. Since splicing could confer unique properties to actinin-4 I employed reverse transcriptase PCR (rtPCR) to address this deficit in our knowledge. I first compared the tissue specificity of exon 19 splicing between actinin-1 and- 4 by examining a

panel of murine tissues. As previously reported for rat (Kremerskothen et al., 2002), the Ca^{++} -insensitive, exon 19b variant of actinin-1 was expressed in the maturing brain, cardiac and skeletal muscle, and in smooth muscle containing tissues such as stomach, intestine and bladder, while the brain-specific exon 19a+19b variant was expressed postnatally in the brain and in adult spinal cord (Figure 3.22). Actinin-1 exon 19a predominated in other tissues and in the immature brain (Figure 3.22). For actinin-4 expression of the exon 19a variant was even more widespread and this was the only isoform detected in non-neuronal tissues (Figure 3.22). In the brain the exon 19a and 19b variants of actinin-4 were equally abundant at all developmental stages examined and no 19a+19b isoform was detected (Figure 3.22). Thus in contrast to actinin-1, it is the Ca^{++}-sensitive, exon 19a version of actinin-4 that is expressed in skeletal muscle and smooth muscle, while the Ca^{++} insensitive, exon 19b variant is restricted to neural tissues. I would like to acknowledge Mr. Gary Williamson for his efforts in assisting me with mouse brain rtPCR analysis.

Actinin-4, unlike actinin-1, also exhibits alternative splicing of exon 8. The expression of actinin-4 exon 8 variants was examined by rtPCR using primers specific for exon 8a and 8b. The 8a variant was detected in all tissues examined (Figure 3.22). By contrast the 8b variant was restricted to the brain, spinal cord, skeletal and cardiac muscle, and smooth muscle rich tissues. I next wanted to assess the relative expression of the 8a and 8b exons in some of these tissues. Since the PCR products obtained with different exon specific primers cannot be directly compared, I instead used common flanking primers to amplify the exon 8 region of actinin-4 from mouse kidney, lung, intestine, heart, skeletal muscle and brain. Since exon 8a and 8b are exactly the same size the PCR products could not be distinguished by gel exlectrophporesis. Therefore I directly sequenced several independent PCR products for each murine tissue. Nucleotide variations between exon 8a and 8b allowed determination of the specific variants expressed by different tissues (Figure 3.23). Examination of sequencing chromatographs revealed that while exon 8b was by far the predominant variant expressed in the brain it was a very minor or undetectable component compared to exon 8a in the other tissues (Figure 3.23).

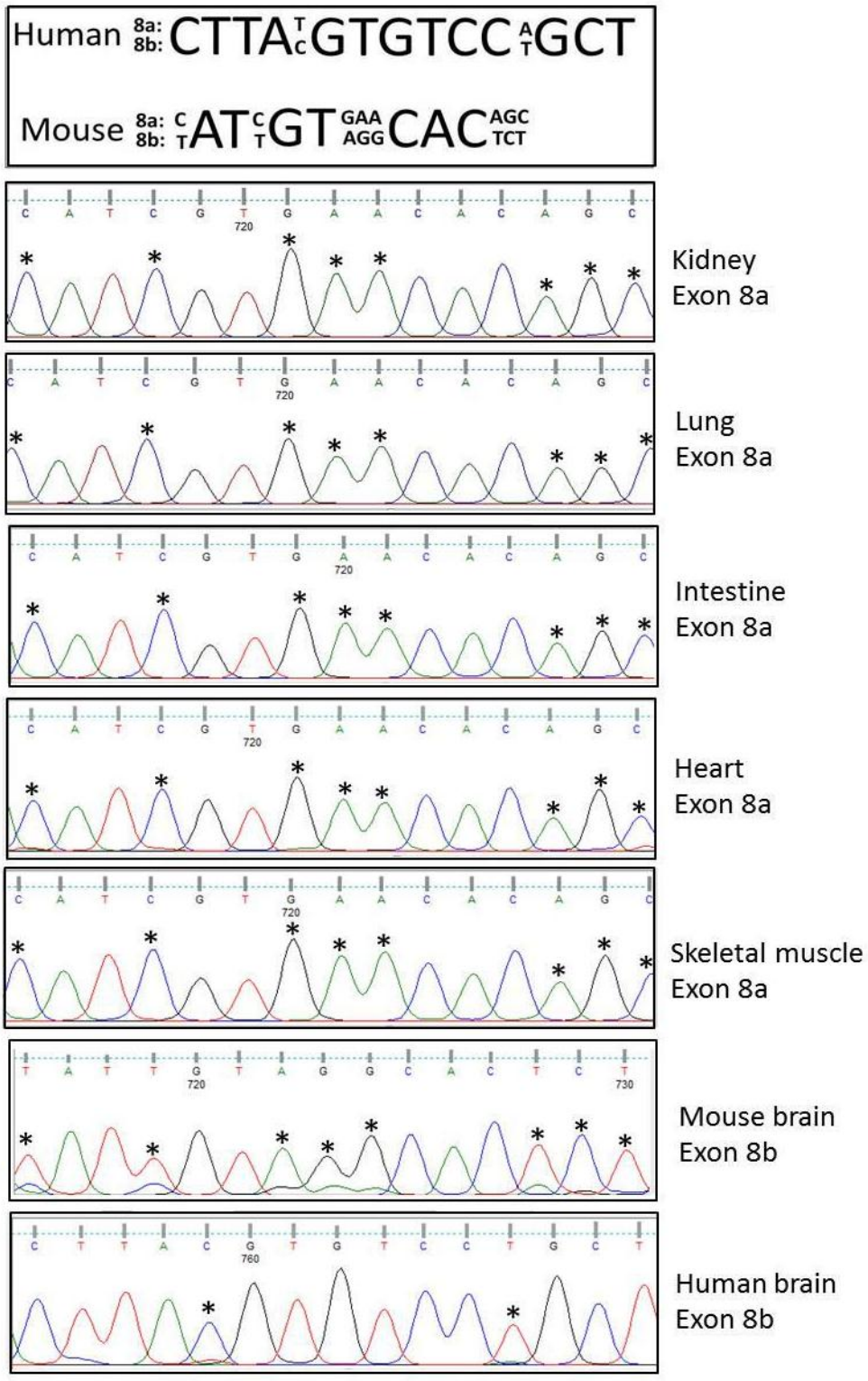

Figure 3.23 Sequence analysis of actinin-4 exon 8 splice variants present in various tissues. Nucleotide variations between actinin-4 exon 8a and 8b present in human and mouse sequences (top). These variations allow determination of the specific exon 8 splice variants present in tissues. cDNA prepared from various tissues was subject to PCR analysis using primers that flank exon 8. Chromatographs of resulting sequences show a nucleotide region that differs between exon 8a and exon 8b. Two murine kidney, lung, intestine, heart and skeletal muscle PCRs showed sequences representative of exon 8a. Five murine brain PCRs showed sequences representative of exon 8b while two human brain PCRs also showed sequences representative of exon 8b. * indicates nucleotides that differ between the sequences of exon 8a and 8b.

Since the analysis in mice revealed that both non-muscle actinins are expressed as multiple splice variants in neural tissues I wanted to establish if these splicing patterns were conserved in humans and whether alterations in splicing might occur in glioblastoma cells, given that actinin-4 is upregulated in glioblastomas and other cancers. rtPCR from normal adult human brain tissue showed that alternative splicing patterns for actinin-1 and -4 exon 19 and actinin-4 exon 8 are conserved between murine and human brain (Figure 3.24). Thus actinin-1 exon 19a+19b and 19b variants and actinin-4 exon 19a, 19b, 8a and 8b variants were detected, with exon 8b being the predominant actinin-4 exon 8 variant present as assessed by direct sequencing of PCR products generated with flanking primers (Figure 3.23). In four glioblastoma cell lines examined I found that there is a switch from exon 19b (Ca^{++}-insensitive) containing splice variants seen in normal brain to exclusively 19a (Ca^{++}-sensitive) variants of both actinin-1 and -4 (Figure 3.24). These cell lines appeared to express exclusively the actinin-4 exon 8a variant compared to the exon 8b that predominates in normal brain tissue (Figure 3.24).

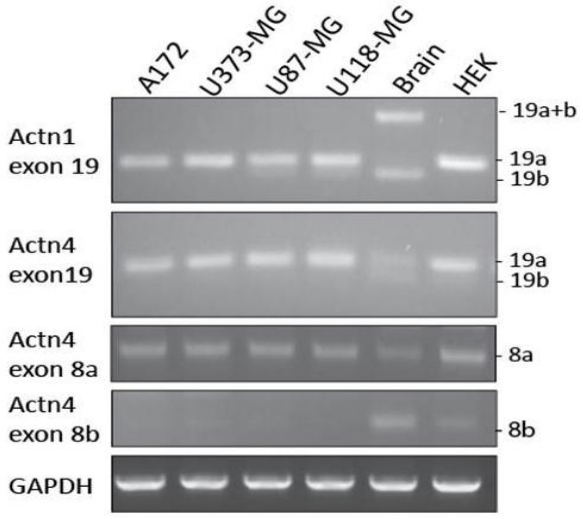

Figure 3.24 rtPCR analysis of the alternative splicing patterns of actinin-1 and -4 exon 19 and actinin-4 exon 8 that occur in normal human brain versus a panel of human glioblastoma cell lines. Primers flanking exon 19 were used for rtPCR analysis of exon 19. Primer pairs in which one primer was specific for either exon 8a or 8b were used for rtPCR analysis of exon 8. The 15 bp size difference between exon 19a and 19b allows these two splice variants to be distinguished. DNA ladders were used but are not shown. Bands are at expected sizes.

In contrast to its reported role in glioblastoma cells as a tumour promoter, actinin-4 has been reported to suppress the tumourigenicity of neuroblastoma cells

(Nikolopoulos et al., 2000). I aimed to investigate if the different effects observed in these cell types could be explained by the expression of alternative splice variants of actinin-4 exon 19. However, on analysis I found that in contrast to normal human brain, neuroblastoma cells similarly to glioblastoma cells only express the 19a (Ca^{++}-sensitive) variant of actinin-4 (Figure 3.25). Human Embryonic Kidney (HEK) cells also only express this Ca^{++} -sensitive variant of actinin-4.

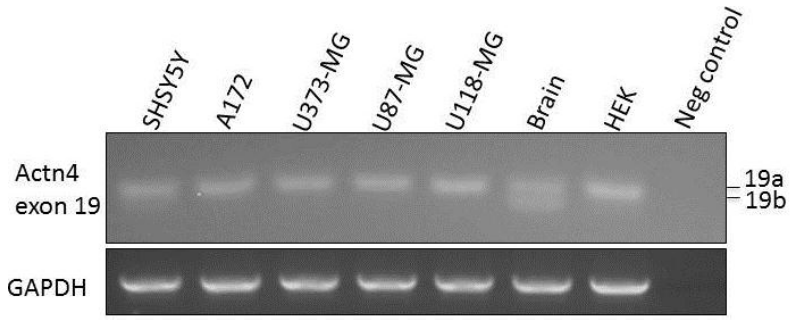

Figure 3.25 rtPCR analysis of the alternative splicing patterns of actinin-4 exon 19 that occur in normal human brain, glioblastoma and neuroblastoma cells. Neuroblastoma SH-SY5Y cells were compared to a panel of glioblastoma cells, normal brain and human embryonic kidney (HEK) cells. Primers flanking exon 19 were used for rtPCR. The 15 bp size difference between exon 19a and 19b allows these two splice variants to be distinguished. DNA ladders were used but are not shown. Bands are at expected sizes.

Having confirmed that actinin-1 and -4 exon 19 and actinin-4 exon 8 splicing was conserved between the human and mouse brain, I further investigated if splicing patterns were conserved in heart and skeletal muscle tissues. I found that while mouse heart and skeletal muscle tissues express both exon 19a (Ca^{++}-sensitive) and 19b (Ca^{++}-insensitive) variants of actinin-1 (Figure 3.22), human tissues only express the exon 19b (Ca^{++}-insensitive) variant (Figure 3.26). Furthermore I found that while both mouse and human tissues express the exon 19a (Ca^{++}-sensitive) variant of actinin-4 (Figure 3.22), human skeletal muscle also expresses the exon 19a+19b variant of actinin-4 (Figure 3.26). I also observed that the cervical carcinoma HeLa cell line, like glioblastoma and neuroblastoma cells only express the exon 19a (Ca^{++}-sensitive) variant of actinin-4.

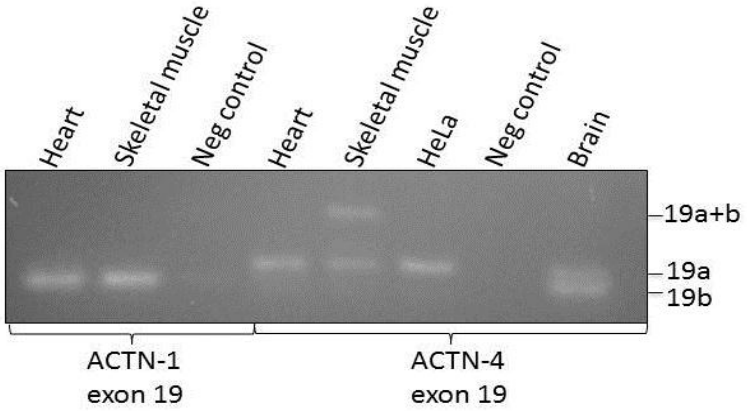

Figure 3.26 rtPCR analysis of the alternative splicing patterns of actinin-1 and 4 exon 19 that occur in human heart and skeletal muscle . Primers flanking exon 19 were used for rtPCR. The 15bp size difference between exon 19a and 19b allows these two splice variants to be distinguished. Alternative splicing of actinin-4 exon 19 in HeLa cells was also examined. DNA ladders were used but are not shown. Bands are at expected sizes.

3.2.2 Determination of the actin-binding affinities of the non-muscle actinins

3.2.2.1 Optimisation of actin-binding assays

In order to carry out actin-binding affinity assays I first needed to determine the concentration of actinin required to saturate the fixed concentration of actin (2 µM) that would be used in each actin binding assay. Figure 3.27 represents an actin saturation curve. 2 µM actin was incubated with increasing concentrations of actinin-1 (1-30 µM). Samples were centrifuged at 112,000 g to pellet bound actin. Pellet samples were subsequently analysed by Commassie-stained SDS-PAGE gels. The amount of actin in pellets was quantified by densitometry. From Figure 3.27 it is clear that initially the amount of actin in pellet samples is directly proportional to the concentration of actinin used. However, at a certain concentration of actinin-1 (~10-15 µM), the amount of actin present in pellet samples plateaus indicating that actin-binding has been saturated. Similar results were obtained for actinin-4 (data not shown).

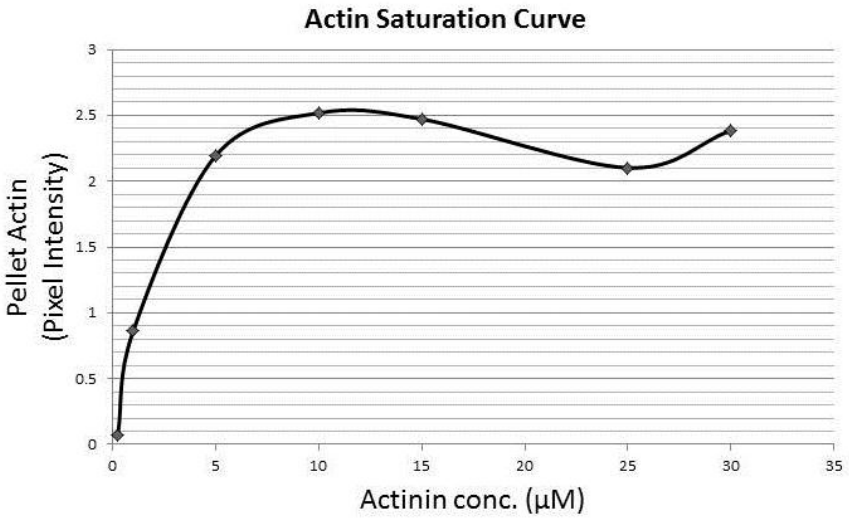

Figure 3.27 Actin saturation curve Increasing concentrations of actinin-1 were incubated with a fixed concentration of actin. Ultracentrifugation at 112,000 g was used to pellet bound actin. Pellet samples were analysed by Commassie stained SDS-PAGE gels. The amount of actin in pellet samples was quantified by densitometry. Graph of actinin concentration versus pellet actin was plotted.

Determining the actin-binding affinity (Kd) of actinin involves quantifying the concentration of free actinin present in actin-binding assays post incubation with actin. Prior to carrying out actin-binding assays I needed to ensure that I would be able to quantify this level of actinin by densitometry. I set up an actin-binding assay using 20 µM actinin. Post ultracentrifugation I loaded increasing volumes of supernatant containing free (unbound) actinin. There is a 30-fold increase in volume between the first and the last points on the graph. I then quantified the amount of actinin present in each lane using the Odyssey Imaging System (Licor). I found that the amount of actinin quantified by densitometry in each lane was directly proportional to the amount of actinin loaded (Figure 3.28). This confirmed that the densitometric quantification method employed was suitable for analysing actin-binding assays provided the amount of actinin used is within this range.

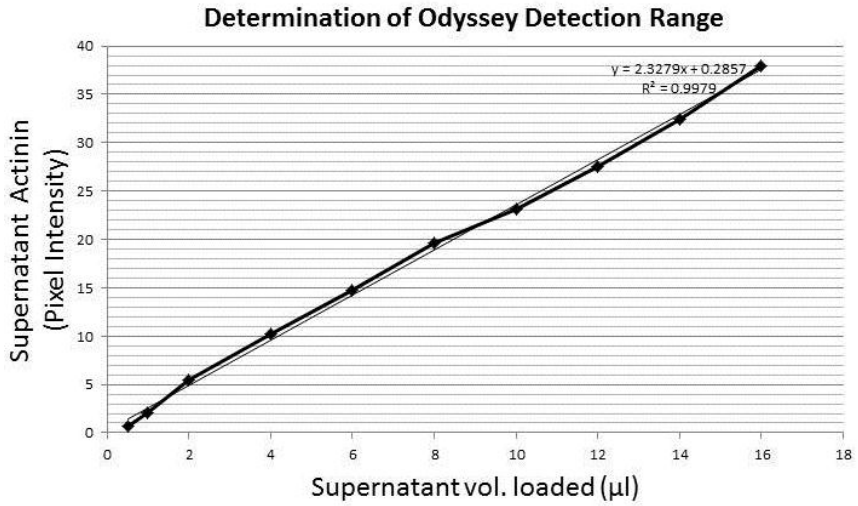

Figure 3.28 Determination of the Odyssey (Licor) detection range. Increasing volumes of free-actinin present in actin-binding assay supernatant samples (post-ultracentrifugation) were analysed by densitometry of SDS-PAGE gels using the Odyssey (Licor). The above graph shows that actinin concentration loaded is directly proportional to the resulting measurements proving that the Odyssey (Licor) is a suitable instrument for quantification for such actin-binding assays.

3.2.2.2 Determination of the actin-binding affinity of actinin-1 (exon 19a), actinin -4 (exon 8a, 19a) and actinin-4 (exon 8b, 19a)

The actin-binding properties of actinin-1 and -4 have not been directly compared. Since differences between the proteins in this regard might underlie distinct functions I employed actin cosedimentation assays to examine these properties. Full length actinins were recombinantly-expressed in *E. Coli* to ensure pure homodimeric proteins were obtained and an affinity tag was used for sequential purifications. This involved GST-column purification followed by TEV protease incubation to cleave the affinity tag. The protein elution was then subjected to HIS-column purification to remove the affinity tag and TEV protease, and the purified actinin protein was collected in the flow through (Figure 3.29).

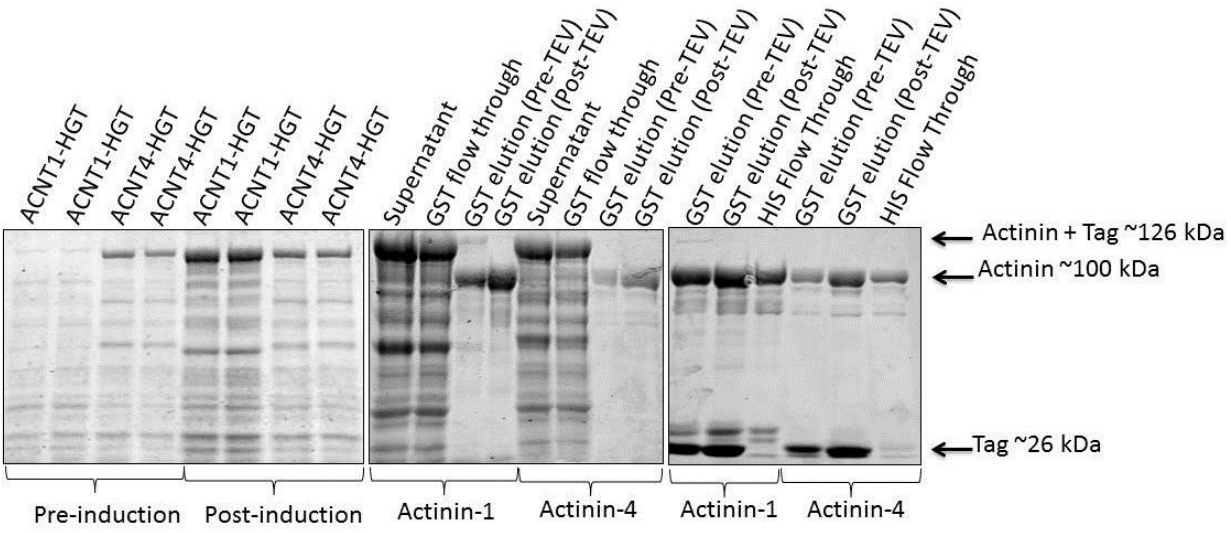

Figure 3.29 Expression and purification of full length actinin-1 and -4. Full length double tagged (GST and HIS) actinin-1 and -4 were recombinantly expressed in *E.coli*. Protein expression was induced by IPTG. Initial GST-column purification was followed by TEV protease incubation in order to cleave the affinity tag. The tag was subsequently removed by HIS-column purification. Purified actinin was obtained from the HIS-column flow through and dialysed into binding assay buffer. HGT=HIS_6/GST/TEV. Molecular weight marker was used but is not shown. Bands are at expected sizes.

Supernatants and pellets from actin-binding assays were analysed on Coomassie-stained SDS-PAGE gels and the proportion of actinin in each fraction was quantified (Figure 3.30). I first compared the affinity of actin-binding for the most widely expressed Ca^{++}-sensitive, actinin-1 (exon 19a) (n=3) and actinin-4 (exon 8a, 19a) (n=6) splice variants (Figure 3.31A+B) . In addition, actinin-4 (exon 8b, 19a) (n=3) was also examined to determine whether inclusion of exon 8b modulated actin binding properties (Figure 3.31C). A single ligand binding site was assumed and rectanglular hyperbolic curves were fit to plots of bound versus free actinin in order to calculate dissociation constants (Kd). Kd values calculated for actinin-1 (exon 19a), actinin-4 (exon 8a, 19a) and actinin-4 (exon 8b, 19a) were 1.93±0.56 µM, 2.96±0.38 µM and 3.96±1.19 µM respectively (Figure 3.31). However the differences in calculated Kd values between these isoforms did not reach statistical significance (Student's T-test). It appears therefore that the non-muscle actinins differ only very slightly in their binding affinity for actin filaments.

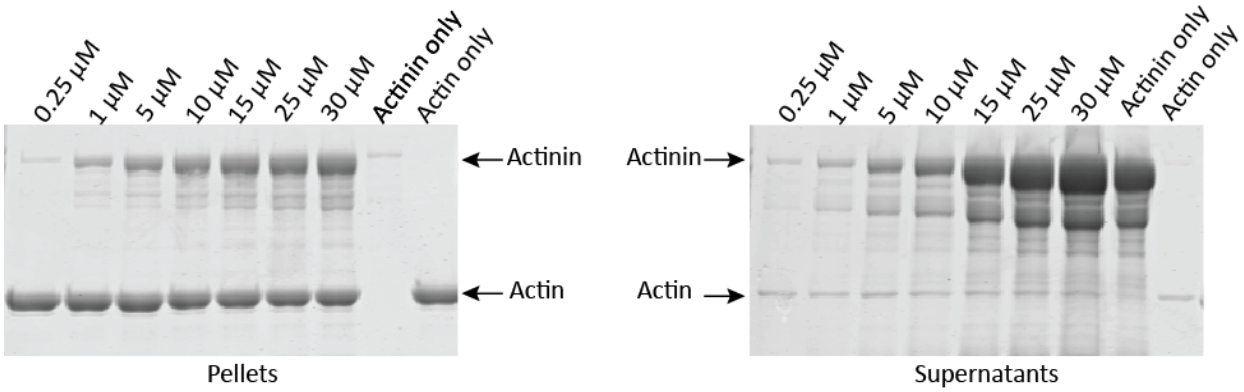

Figure 3.30 Actin binding affinity (Kd) assays of actinin-1 (exon 19a), actinin-4 (exon 8a, 19a) and actinin-4 (exon 8b, 19a). Actin binding assays were set up incubating increasing concentrations of actinin and fixed concentrations of actin. Ultracentrifugation was used to pellet bound actin. Pellet and supernatant samples were run on SDS-PAGE gels and analysed by densitrometry. Representative actin-binding assay for actinin-1 (exon 19a) is shown. Molecular weight markers were used but are not shown. Bands are at expected sizes.

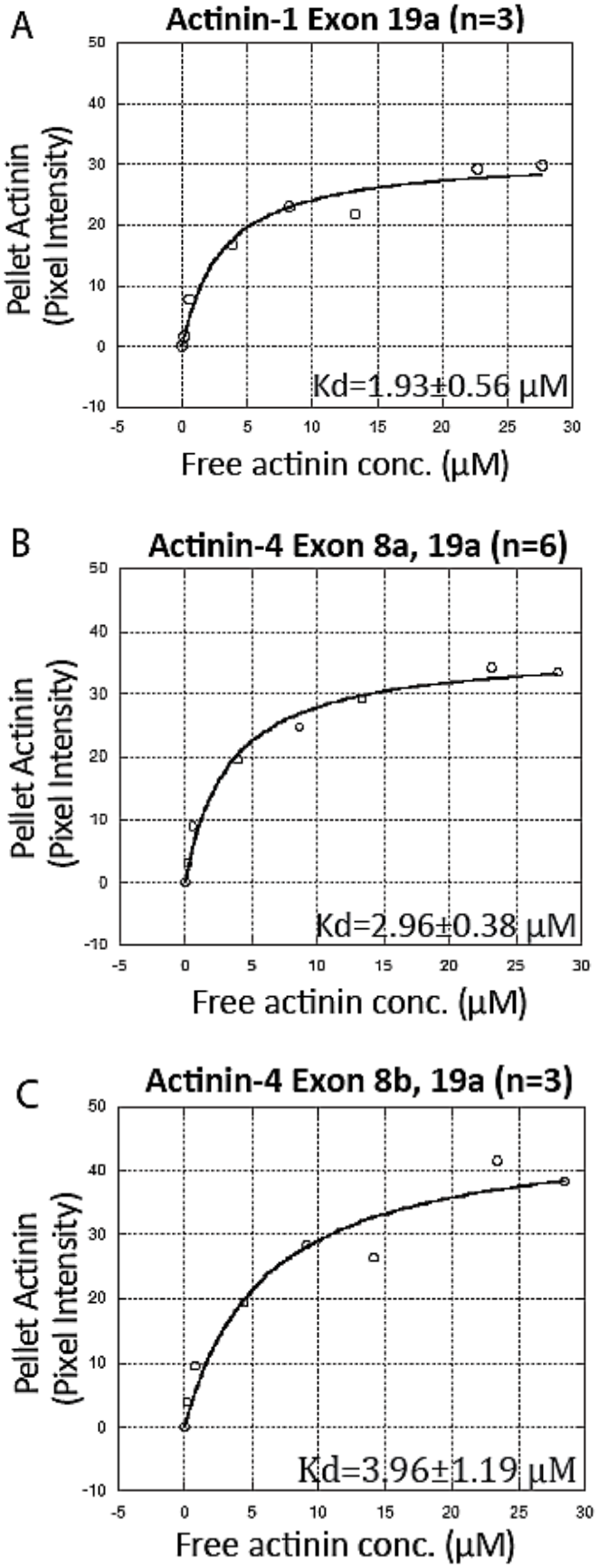

Figure 3.31 Actin binding affinity (Kd) assays of actinin-1 (exon 19a), actinin-4 (exon 8a, 19a) and actinin-4 (exon 8b, 19a). Actin-binding assays were set up by incubating increasing concentrations of actinin with fixed concentrations of actin. Ultracentrifugation was used to pellet bound actin. Graphs of free versus bound actinin were used to determine the Kd values of (A) actinin-1 (exon 19a) , (B) actinin-4 (exon 8a, 19a) and (C) actinin-4 (exon 8b, 19a).

3.2.2.3 Comparison of the actin-bundling capacity of actinin-1 (exon 19a) and actinin -4 (exon 8a, 19a)

I compared the capacity of actinin-1 (exon 19a) and actinin-4 (exon 8a, 19a) to bundle (cross-link) actin. Actin-bundling assays performed at 10,000 g showed that these actinin isoforms have similar actin-bundling capacities (Figure 3.32). Initially as actinin concentrations were increased I noticed an increase in the amount of actin detected in pellet samples. At a certain point (~1 µM) the amount of actin bundling plateaued for both of these non-muscle actinin isoforms.

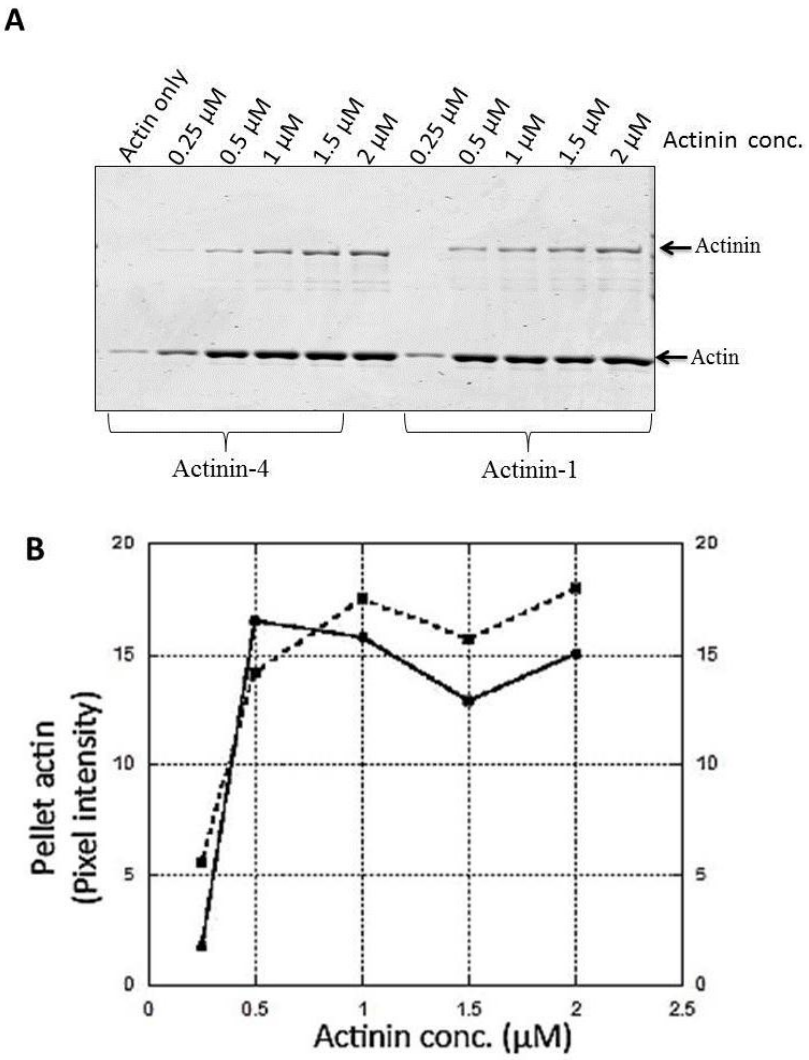

Figure 3.32 Comparison of the actin-bundling capacity of actinin-1 (exon 19a) and actinin-4 (exon 8a, 19a). Actin-bundling assays were set up by incubating increasing concentrations of actinin (0.5-2 µM) with fixed concentrations of actin. Centrifugation at 10,000 g was used to pellet bound actin. (A) Pellet and supernatant samples were analysed by Coomassie stained SDS-PAGE gels and analysed by densitometry. (B) Graph of actinin concentration versus pellet actin (n=1). Molecular weight marker was used but is not shown. Bands are at expected sizes.

3.2.3 Determination of the calcium sensitivity of actin-binding for the non-muscle actinins

3.2.3.1 Determination of the calcium sensitivity of actin-binding and bundling for actinin-1 (exon 19a) and actinin-4 (exon 8a, 19a).

The calcium sensitivity of actin-binding was evaluated for actinin-1 (exon 19a) and actinin-4 (exon 8a, 19a) splice variants. This comparison revealed very similar calcium sensitivities with actin-binding decreasing by 50-60% at free calcium concentrations above 10 µM (Figure 3.33A+B). There was also a dramatic decrease in actin-bundling at these free calcium concentrations, that again was similar for both actinins (Figure 3.33C).

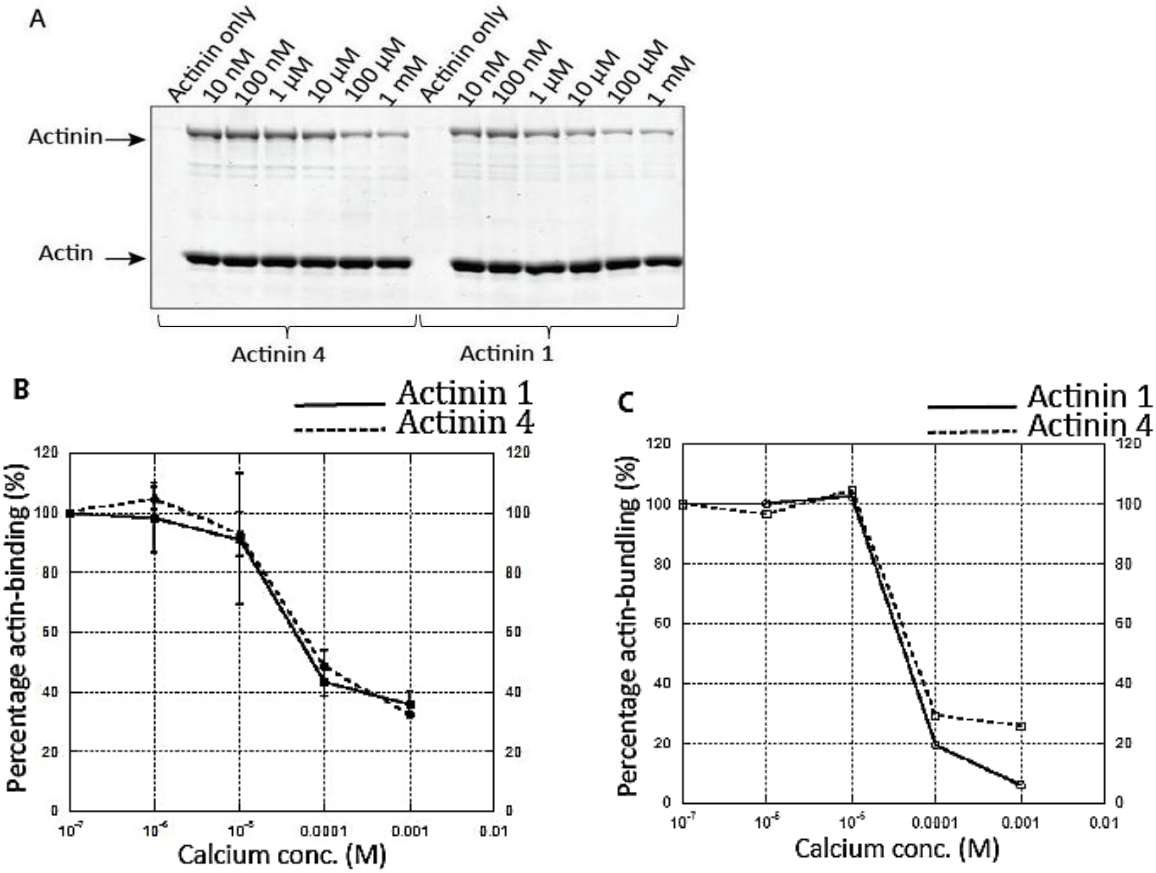

Figure 3.33 Calcium sensitivity assays comparing actinin-1 (exon 19a) and -4 (exon 8a, 19a). Actin-binding assays were set up using fixed concentrations of actinin and actin under increasing calcium concentrations (10 nM-1 mM). (A) The amount of bound actinin present in pellets post centrifugation was determined by densitometric analysis of Commassie stained SDS-PAGE gels. Molecular weight marker was used but is not shown. Bands are at expected sizes. Centrifugation was performed at 112,000 g for 30 min to monitor actin-binding and 10,000 g for 15 min to monitor actin-bundling. Graphs plotting calcium concentration versus percentage of total pellet actinin are shown for (B) actin-binding (n=3) and (C) actin-bundling experiments (n=1).

3.2.3.2 Determination of the calcium sensitivity of actin-binding for brain-specific actinin-1 (exon 19a+19b)

The calcium sensitivity of actin-binding was also compared for non-muscle actinin-1 (exon 19a) and brain-specific actinin-1 (exon 19a+19b) expressing splice variants (n=3). Figure 3.34A shows the expression and purification of actinin-1 non-muscle (exon 19a) and brain-specific (exon 19a+19b). Note: purified brain-specific actinin-1 runs at a higher molecular weight due to the inclusion of exon 19b. Brain-specific actinin-1 proved to be Ca^{++}-sensitive and displayed decreases in actin-binding of approximately 40% at free calcium concentrations of 1 mM (Figure 3.34B).

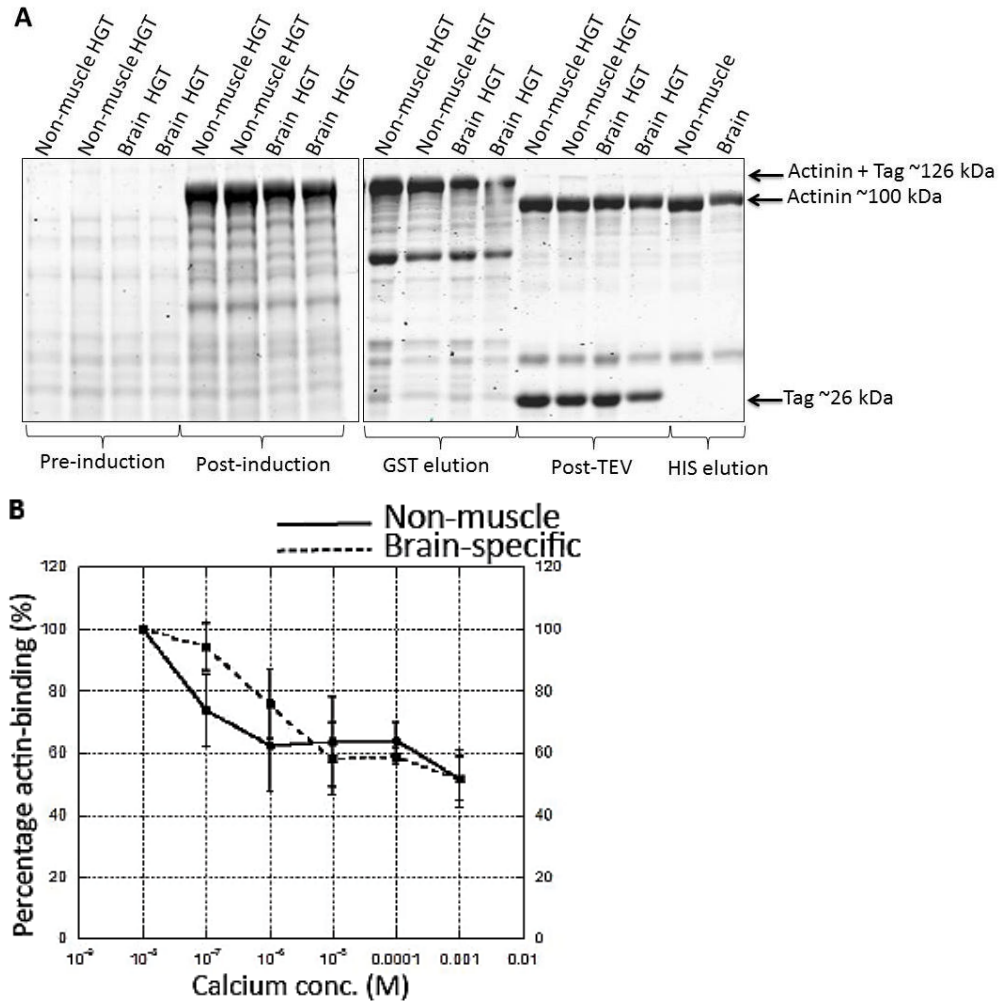

Figure 3.34 Calcium sensitivity assays comparing actinin-1 non-muscle (exon 19a) and brain-specific (exon 19a+19b) splice variants. Actin-binding assays were set up using fixed concentrations of actinin and actin under increasing calcium concrations (10 nM-1 mM). (A) The amount of bound actinin present in pellets post centrifugation was determined by densitometric analysis of Commassie stained SDS-PAGE gels. Molecular weight marker was used but is not shown. Bands are at expected sizes.Ultracentrifugation was performed at 112,000 g for 30 min to monitor actin-binding. Graphs plotting calcium concentration versus percentage of total pellet actinin are shown for actinin-1 non-muscle (exon 19a) and brain-specific (exon 19a+19b) splice variants. (n=3).

3.2.3.3 Determination of the calcium sensitivity of actin-binding for the alternatively spliced actinin-4 exon 8b variant

The calcium sensitivity of actin-binding was also compared for actinin-4 (exon 8a, 19a) and actinin-4 (exon 8b, 19a) containing splice variants (n=1). Like actinin-4 (exon 8a), the exon 8b expressing variant also proved to be Ca^{++}-sensitive and displayed decreases in actin-binding of approximately 60% at free calcium concentrations of 1 mM (Figure 3.35). Overall the intrinsic actin-binding properties of actinin-1 and -4 are very similar and seem unlikely to account for major functional differences between these proteins.

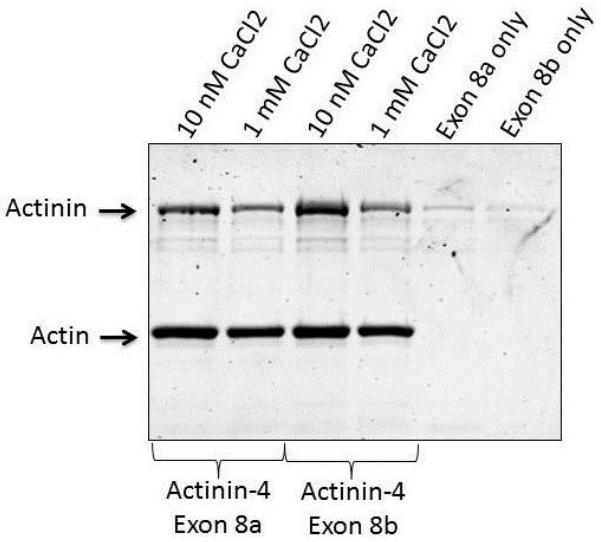

Actinin-4 Splice Variant	% Decease in actin-binding at 1 mM Ca^{++}
Exon 8a	47
Exon 8b	60

Figure 3.35 Calcium sensitivity assay comparing actinin-4 exon 8a and exon 8b splice variants. Actin-binding assays were set up using fixed concentrations of actinin and actin in the presence of either 10 nM or 1 mM calcium . Centrifugation was performed at 112,000 g for 30 min to monitor actin-binding. (Left) Bound actinin present in pellet samples with low and high calcium concentrations was analysed by Commassie stained SDS-PAGE gels. Molecular weight marker was used but is not shown. Bands are at expected sizes. (Right) Densitometric analysis of Commassie stained SDS-PAGE gels.

3.3 Analysis of heterodimer formation between the non-muscle actinins

Heterodimer formation has been reported to occur between the muscle isoforms (actinin-2 and -3). The non-muscle isoforms (actinin-1 and -4) are currently viewed as distinct homodimeric entities. However, studies of Ca^{++}-sensitive platelet actinins indicate that heterodimer formation may occur between the non-muscle isoforms. Non-muscle heterodimer formation could result in a protein with novel interaction partners and binding affinities.

In this part of the work my goals were to:

1) Determine if heterodimer formation is likely to occur between the non-muscle actinins based on structural analysis and *in vitro* binding assays.
2) Determine the propensity for non-muscle actinins to form heterodimers versus homodimers.
3) Determine if heterodimer formation occurs in cell lines.
4) Determine the relative amount of homodimers and heterodimers in cell lines.

3.3.1 Evolutionary conservation of the actinin dimer interface

It is unknown whether the non-muscle actinins have the ability to form heterodimers either with each other or with the muscle actinins. Dimerisation of actinin is largely mediated by the four spectrin-like repeats of the rod domain. To explore the potential for heterodimer formation I first examined the evolutionary conservation of amino acids present at the dimer interface, based on the known crystal structure of the human actinin-2 rod domain (Ylänne et al., 2001). Conservation scores based on an alignment of actinin-1 and actinin-4 sequences from divergent species were calculated and plotted onto the actinin-2 rod domain 3D structure using the ConSurf server (Ashkenazy et al., 2010; Landau et al., 2005). This analysis demonstrates that the dimer interface is highly conserved between actinin-1, -2 and -4 (Figure 3.36), with very few non-conservative amino acid substitutions. By contrast the exposed surface of the rod shows significantly less sequence conservation. This supports the idea that the dimer interface is almost completely conserved between actinins and that heterodimer formation could occur.

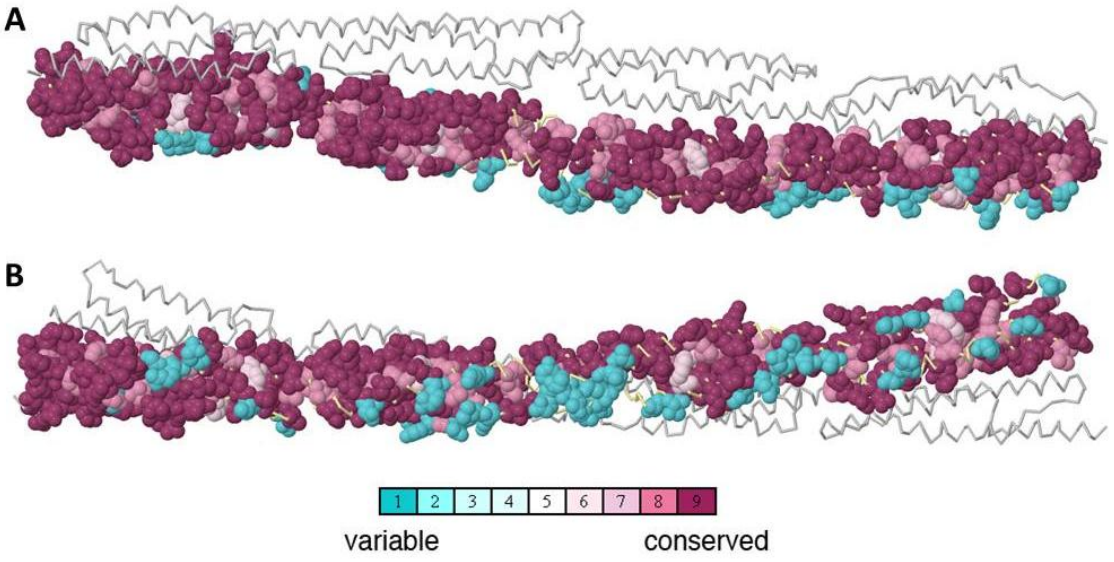

Figure 3.36 Evolutionary conservation of amino acids in the actinin-1, -2 and -4 rod domains. Conservation scores are plotted onto one subunit of the dimeric actinin-2 rod structure using the ConSurf server (backbone and side chains depicted as spheres). A backbone only trace of the other subunit is shown. Two views of the structure are shown to highlight the (A) conserved dimer interface and (B) less conserved, exposed surface of the rod. Conservation scores are visualised on a scale of nine grades with most variable positions coloured turquoise, and most conserved positions coloured maroon. The amino terminus (R1) of the coloured subunit is to the left.

3.3.2 Non-muscle actinins have the potential to form heterodimers

3.3.2.1 Yeast two-hybrid analysis of actinin heterodimer formation.

To investigate the possibility that actinin-1 and -4 can form heterodimers I tested the ability of actinin rod domains to interact with each other in yeast two-hybrid assays. Rod domains from actinin-1, -2 and -4 were cloned into both bait and prey vectors. Interactions between rod domains were monitored by activation of the *His3* and *LacZ* reporter genes (Table 3.2). Activation of the *His3* reporter was seen for every combination of rod domains indicating that they are able to form both homo- and heterodimers. In all cases the reporter gene expression for heterodimers was comparable to, or greater than, that for homodimers. Activation of the *LacZ* reporter was more variable, perhaps reflecting differences in expression levels between constructs, but again some homodimeric and heterodimer interactions were detected. Overall, these assays suggest that actinin-1, -2 and -4 rod domains can indeed form heterodimers as well as homodimers.

Bait \ Prey	Actinin-1		Actinin-2		Actinin-4		Empty vector	
	His3	β-gal	His3	β-gal	His3	β-gal	His3	β-gal
Actinin-1	++	-	+++	++	+++	-	-	-
Actinin-2	+++	+	+++	+	+++	+	-	-
Actinin-4	+++	-	+++	++	+	-	-	-
Empty vector	-	-	-	-	-	-	-	-

Table 3.2 Analysis of actinin homodimer and heterodimer formation by yeast two-hybrid assays. The ability of actinin-1/-2/-4 rod domains (baits) to interact with actinin-1/-2/-4 rod domains (preys) was tested using the yeast two-hybrid system. Empty bait and prey vectors were included as negative controls. Interactions between bait and prey were indicated by expression of two reporter genes – *His3* and *LacZ* coding for β-galactosidase (β-gal).

3.3.2.2 *In vitro* binding assay analysis of actinin-1 and -4 homodimeric versus heterodimeric interactions.

To obtain a more quantitative measure of the propensity for homo- versus heterodimer formation I performed *in vitro* binding assays using purified proteins. Initial attempts involved performing assays using GST-tagged R1-R2 domains in combination with R3-R4 domains of actinin-1 and -4. Since spectrin-like repeats R1 and R2 form an interaction surface with repeats R3 and R4 in the rod domain, splitting the rod in half in this manner should in theory allow comparison of the affinity of homodimer versus heterodimer formation for different actinins. However, degradation products of the GST R1-R2 protein appeared at the expected size of the R3-R4 domains (~28 kDa). This degradation band possibly represented the GST tag. Its presence would interfere with binding assay interpretation. Efforts to purify GST R1-R2 from its degradation products included GST-column purification, Fast Performance Liquid Chromatography (FPLC) and Size Exclusion Chromatography. However degradation protein bands remained visible post purification procedures. For this reason I switched to using a Maltose Binding Protein (MBP) tag. While I could successfully purify MBP R1-R2, no interaction was observed with R3-R4 domains. Efforts to optimise binding assay conditions included varying NaCl concentrations. However no interaction was observed. Based on this I concluded that the interaction surface between R1-R2 and R3-R4 may be insufficient to achieve an interaction. For this reason I extended the interaction surface to include the actin-binding domain (ABD) and the calmodulin-like domain (CaM). To do this I used constructs encoding the amino and carboxyl terminal halves of actinin-1 and -4 (ABD-R2 and R3-CaM). I expressed and purified GST-tagged ABD-R2 and His_6-tagged R3-CaM domains for both actinin-1 and -4. These fusion proteins were mixed in various combinations and the ability of R3-CaM to interact with ABD-R2 was assessed by purification of the complex using glutathione-sepharose beads (Figure 3.37A). Densitometric analysis was used to compare the levels of R3-CaM proteins bound to ABD-R2 proteins in each assay. The results show less than 5% differences in bound R3-CaM in heterodimeric versus homodimeric contexts indicating that non-muscle actinin homo- and heterodimers form with approximately equal affinity (Figure 3.37B).

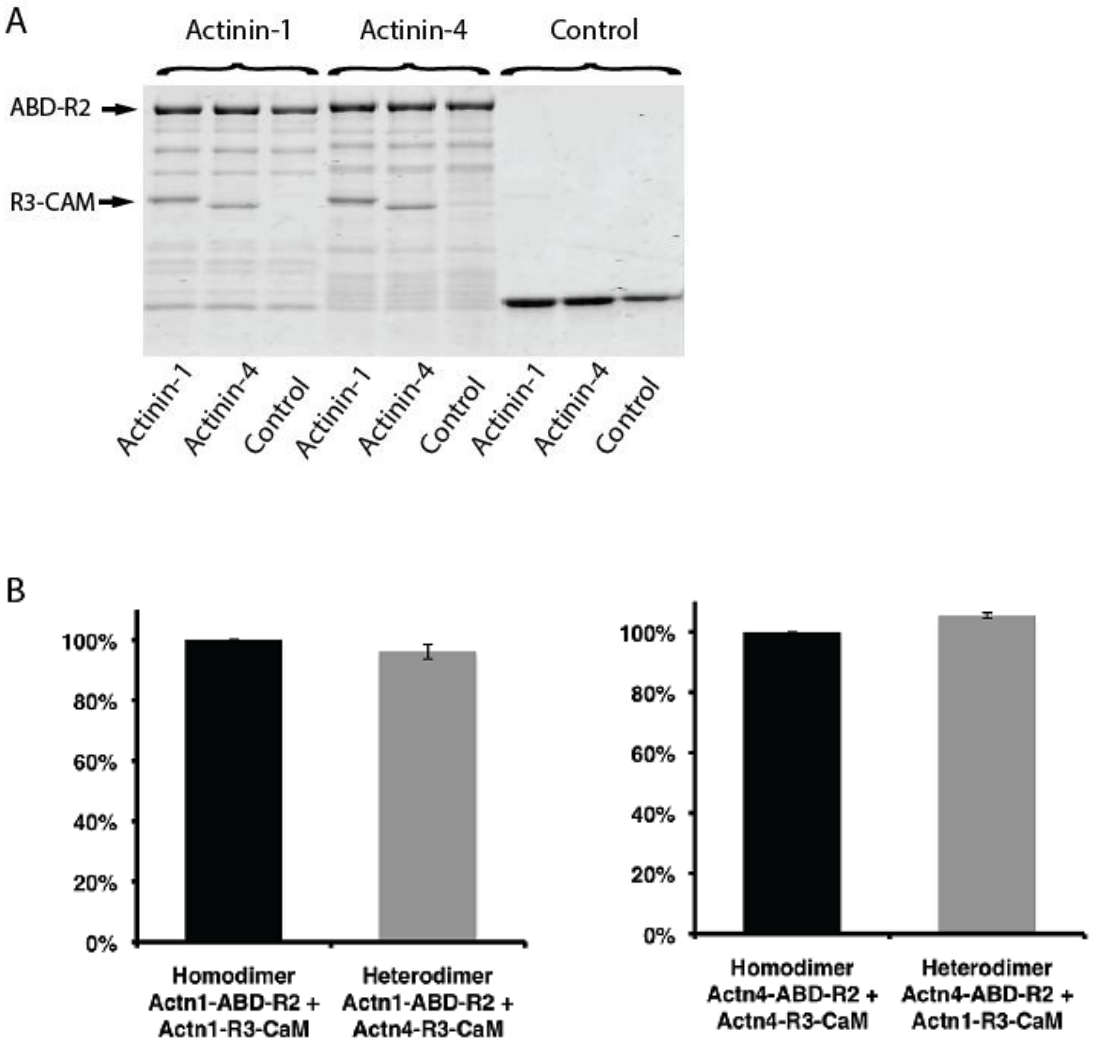

Figure 3.37 Analysis of the propensity for non-muscle actinins to form heterodimers. GST-tagged actinin-1/-4 ABD-R2 domains were incubated with His_6-tagged actinin-1/-4 R3-CaM domains and bound to glutathione sepharose. (A) After washing, eluted proteins were analysed on Coomassie-stained SDS-PAGE gels. Molecular weight marker was used but is not shown. Bands are at expected sizes. (B) Bound R3-Cam domains were quantified by densitometry and the amount of bound R3-CaM for heterodimeric interactions was expressed as a percentage of that observed for the equivalent homodimeric combination of proteins. Control=GST only or omission of R3-CaM domains of actinin-1 and -4.

3.3.3 Actinin-1 and -4 heterodimer formation in cultured cells.

3.3.3.1 Heterodimers are present in cells grown under a variety of conditions

The results so far demonstrate that actinin-1 and -4 rod domains can form heterodimers *in vitro* and in the yeast two-hybrid system. To assess whether the non-muscle actinins form heterodimers in cells in which they are co-expressed I used Native Polyacrylamide Gel Electrophoresis to maintain non-denaturing conditions in order to preserve and detect heterodimers. I first examined HeLa cells that have endogenous expression of actinin-1 and -4. Western blotting with isoform-specific antibodies revealed that each protein migrated as two bands on native gels. The upper band for actinin-4 co-migrates with the lower band for actinin-1 and this band is taken to represent actinin-1/4 heterodimers and the other bands to represent homodimers. A prominent heterodimer band was observed for confluent, proliferating and migrating HeLa cells as well as in cells that had been deprived of serum (Figure 3.38).

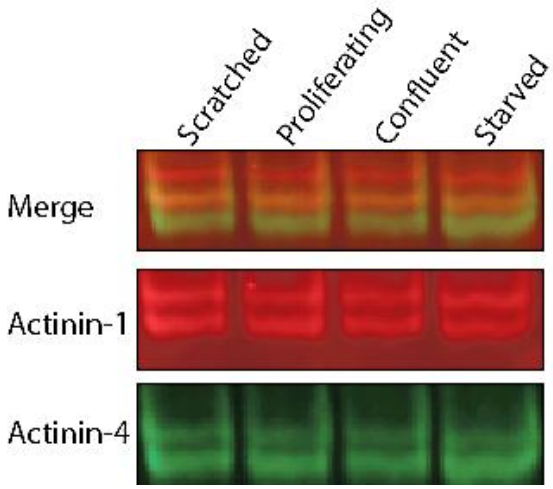

Figure 3.38 Actinin heterodimers in HeLa cells grown under a variety of conditions. Heterodimers were detected by Native PAGE and Western blotting using antibodies specific for actinin-1 (red) and actinin-4 (green). Upper red band represents actinin-1 present in homodimers, lower red band represents actinin-1 present in heterodimers, upper green band represents actinin-4 present in heterodimers and lower green band represents actinin-4 present in homodimers. Merged image shows heterodimers represented by an intermediate orange/yellow band. Antibodies: Actinin-1 [Santa Cruz (H2):sc-17829] and Actinin-4 [Immunoglobe (IG701)].

3.3.3.2 Non-muscle actinin heterodimers are prevalent in many cancer cell lines.

As discussed non-muscle actinin heterodimer formation occurs in HeLa cells grown under a variety of culture conditions. I also detected heterodimers in a number of other cancer cell lines indicating that this phenomenon was not specific to HeLa cells (Figure 3.39 top panel). Notably, MDA-MB-231 cells that express only actinin-4 do not show any heterodimer band verifying that the presence of this band is dependent on the presence of both actinin-1 and -4 (Figure 3.39 top panel). Non-tumourigenic MCF-10A breast cells exhibit higher levels of actinin and heterodimer formation relative to breast carcinoma MCF-7 cells (Figure 3.39 lower panel).

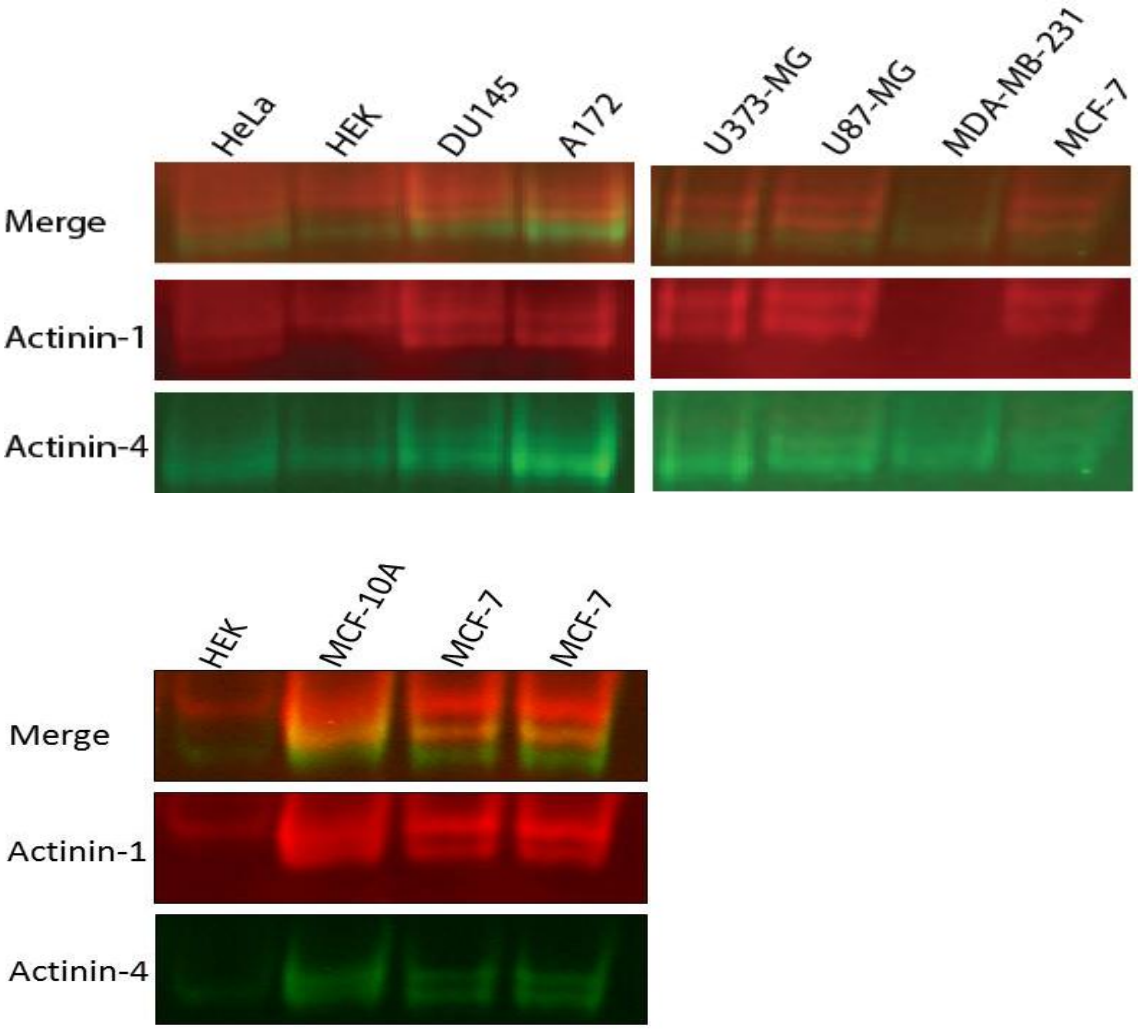

Figure 3.39 Native PAGE detection of actinin homodimers and heterodimers present in a panel of cell lines. Heterodimers were detected in a number of cells by Native PAGE and Western blotting using antibodies specific for actinin-1 (red) and actinin-4 (green). Upper red band represents actinin-1 present in homodimers, lower red band represents actinin-1 present in heterodimers, upper green band represents actinin-4 present in heterodimers and lower green band represents actinin-4 present in homodimers. Merged image shows heterodimers represented by an intermediate orange/yellow band. Antibodies: Actinin-1 [Santa Cruz (H2):sc-17829] and Actinin-4 [Immunoglobe (IG701)].

3.3.3.3 Knockdown of actinin-4 results in a shift from heterodimer to homodimer formation

As mentioned the presence of the heterodimeric band is dependent on the presence of both actinin-1 and -4. To further demonstrate this point and to examine the dynamics of heterodimer formation I performed siRNA-mediated knockdown of actinin-4 in MCF-7 cells. ~80% knockdown of actinin-4 protein levels was achieved in these cells, resulting in a large decrease in both actinin-4 homo- and heterodimers (Figure 3.40). This was mirrored by decreased actinin-1 in the heterodimeric state and a consequent increase in actinin-1 levels in the homodimeric state. Taken together these results verify that these non-muscle actinin heterodimers are dependent on the co-expression of both actinin-1 and -4, and that a reduction in the expression of either leads to a redistribution of the other towards the homodimeric state.

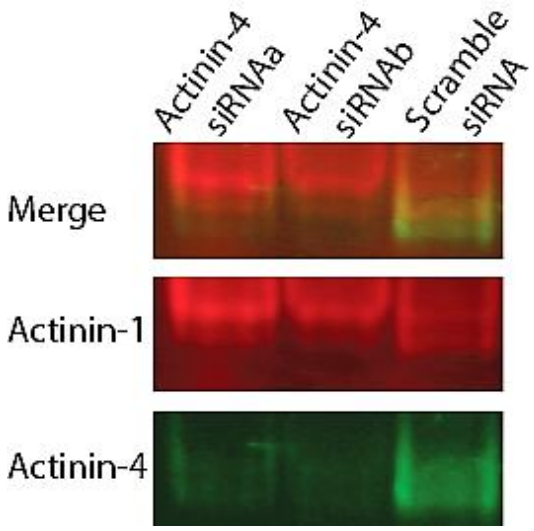

Figure 3.40 Native PAGE analyses of lysates from MCF-7 cells following siRNA-mediated knockdown of actinin-4. Western blot using antibodies specific for actinin-1 (red) and actinin-4 (green). Upper red band represents actinin-1 present in homodimers, lower red band represents actinin-1 present in heterodimers, upper green band represents actinin-4 present in heterodimers and lower green band represents actinin-4 present in homodimers. Merged image shows heterodimers represented by an intermediate orange/yellow band. ~80% actinin-4 knockdown was achieved. Antibodies: Actinin-1 [Santa Cruz (H2):sc-17829] and Actinin-4 [Immunoglobe (IG701)].

3.3.4 The relative abundance of actinin homodimers and heterodimers in cell lines.

I next sought to quantify the relative abundance of homo- and heterodimers in the cell lines examined. I first quantified the relative amounts of each actinin in the panel of cell lines and calculated the ratio of actinin-1: actinin-4 for each type of cell (Figure 3.41 see Section 2.7 for details). I then determined the proportion of each non-muscle actinin that was present as a heterodimer on native gels and used this to calculate the overall percentage of actinin1/4 heterodimers for each cell line (Figure 3.42). Surprisingly, where identified, heterodimers were more abundant than either homodimeric species and consumed close to 50% of the total non-muscle actinin in these cell lines. While heterodimers were observed in most cell lines that co-expressed actinin-1 and -4, they were undetectable in Human Embryonic Kidney (HEK) cells. While the total level of actinin detected in HEK cells is lower than the other cell lines, heterodimers should have been detectable if they represented a similar proportion of total actinin as in other cell lines. This suggests that the formation of actinin heterodimers either requires high levels of actinin expression or that heterodimer assembly is subject to cell line-specific regulatory mechanisms.

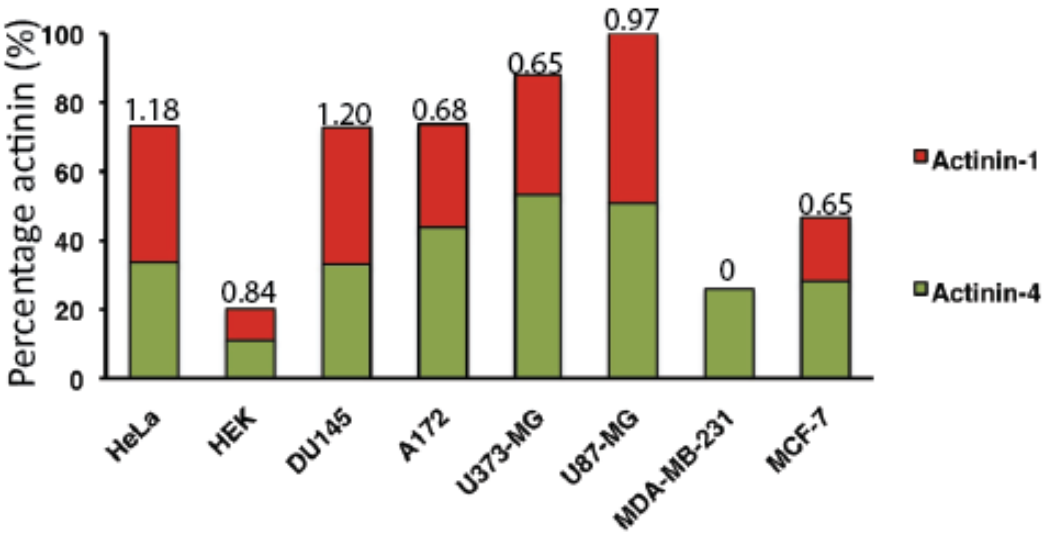

Figure 3.41 Relative amounts of actinin-1 and -4 present in a panel of cell lines. Full length actinin-1 and -4 constructs in the pEGFP-C2 vector (Clontech, Quintin, France) were transfected into HEK 293 cells. In order to determine their expression levels relative to each other Western blots of lysates were probed with a α-GFP antibody. Subsequently, lysates from cells transfected with these GFP-tagged actinin constructs were used to produce a standard curve to which specific actinin-1 and -4 antibody staining could be normalised. Using this standard curve in combination with lysates from various cell lines allowed comparison of the relative amount of actinin-1 and -4 within and between cells lines. Probing native gels with antibodies specific for actinin-1 and -4 followed by densitometic analysis allowed us to quantify the proportion of actinin-1 and -4 involved in heterodimer formation. Results are shown in bar chart format. The ratio of actinin-1: actinin-4 is indicated above the chart.

.

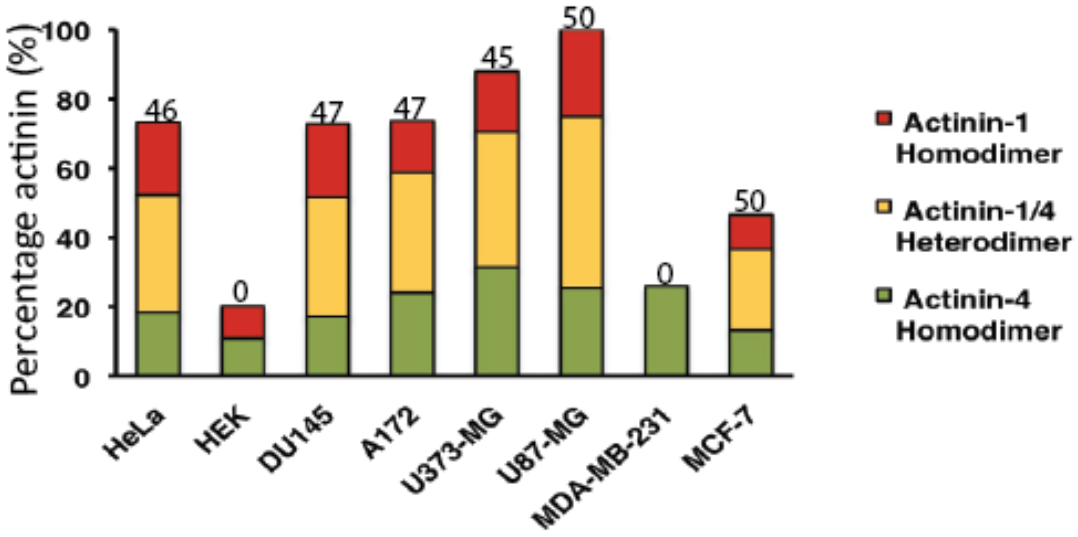

Figure 3.42 Actinin-1/actinin-4 heterodimers expressed as a proportion of total dimeric actinin. The proportion of each isoform present as heterodimers was quantified by Native PAGE and Western blotting and plotted onto the graph of relative actinin protein levels shown in Fig 3.41. The percentage (%) of heterodimer for each cell line is indicated above the graph.

3.3.5 Analysis of actinin isoforms present in platelets

Heterodimer formation was previously reported to occur between actinin isoforms present in human platelets (Landon et al., 1985). Through Western blot analysis using specific antibodies I detected expression of actinin-1, -2 and -4 in platelets. While this proves that multiple actinin isoforms are expressed in platelets, it raises the question of whether heterodimers can form between non-muscle and muscle actinin isoforms.

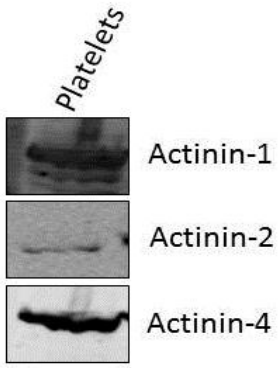

Figure 3.43 Western blot analysis of actinin isoforms present in human platelets. Using specific antibodies actinin-1, -2 and -4 isoforms were detected in lysates from human platelets. Antibodies: Actinin-1 [Santa Cruz (H2):sc-17829], Actinin-2 [Sigma (Clone EA-53)] and Actinin-4 [Immunoglobe (IG701)].

3.4 Identification of non-muscle actinin interacting partners

Given their similar actin-binding properties and propensity to form heterodimers, the isoform-specific functions of the non-muscle actinins are likely to be mediated by isoform-specific interactions with proteins other than actin filaments. Many actinin-interacting proteins are known and in most cases examined these interactions are common to multiple actinins. In other cases isoform-specificity has not been examined and thus very few validated isoform-specific interactions have been reported. I aimed to identify actinin-interacting proteins and to establish the isoform-specificity of novel or known actinin-interacting partners in a more systematic manner.

In this part of the work my goals were to identify actinin-interacting partners. To do so I used two approaches:

1) Yeast two-hybrid screening.
2) Tandem Affinity Purification (TAP)

3.4.1 Yeast two-hybrid screening

3.4.1.1 Identification of suitable actinin-1 and -4 bait proteins

I attempted to identify actinin-interacting partners though a yeast two-hybrid screen (Y2H). This firstly involved identifying suitable bait proteins for both actinin-1 and -4. Suitable bait proteins needed to fulfil three criteria: 1) interact with a positive control within the Y2H system, 2) do not auto-activate within the Y2H system, 3) both actinin-1 and -4 baits must represent the same protein domain of actinin so results can be comparable. I cloned a number of constructs encoding actinin-1 and -4 protein domains into Y2H bait vectors (Figure 3.44).

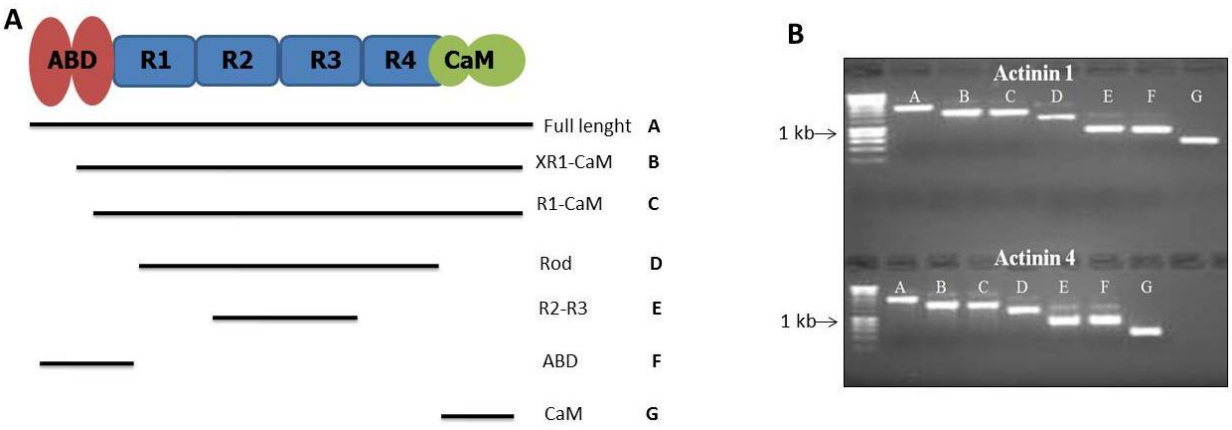

Figure 3.44 PCR amplification of DNA regions corresponding to actinin protein domains (A) Schematic representation of protein domains amplified (A-G). (B) DNA agarose gel showing corresponding actinin-1 (top) and -4 (bottom) PCR products (A-G).

I tested the suitability of a number of these bait constructs for use in the Y2H screen. The constructs encoding the rod domain of actinin-1 and -4 proved to be the most suitable pair of baits (Table 3.3). I would like to acknowledge Mr. Ronan McCarthy for his efforts in assisting me with the cloning of these constructs.

		Auto-activate		Interact with positive control	
Vector	**Domain**	**Actinin-1**	**Actinin-4**	**Actinin-1**	**Actinin-4**
pLEX	**Rod**	**No**	**No**	**Yes**	**Yes**
pLEX	CaM	Yes	Yes	U	U
pGBKT7	Full length	No	No	Yes	No
pGBKT7	XR1-C	Yes	No	U	No
pGBKT7	R1-C	Yes	No	U	No

Table 3.3 Suitability of actinin-1 and -4 constructs for use as baits in the Y2H screen. Bait constructs indicated were tested for their ability to interact with a positive control and for auto-activation within the Y2H system. The constructs encoding the actinin rod domain proved to be the most suitable (highlighted in green).Auto-activation of bait constructs meant their ability to interact with a positive control was uninterpretable (U).

3.4.1.2 Preliminary yeast two-hybrid screens

The constructs encoding the rod domains of actinin-1 and -4 were used as bait proteins in separate Y2H screens. Given the contrasting roles actinin-1 and -4 are reported to play in glioblastoma I screened a mouse brain cDNA library. 19 colonies resulted from transformation of the actinin-1 bait. Only 15 of these grew when restreaked onto selection plates. Only 1 colony resulted from transformation of the actinin-4 bait and this colony grew when restreaked on a selection plate. All colonies that grew when restreaked on selection plates were grown up and yeast plasmid purifications were performed in order to obtain prey plasmids. Restriction digests were performed on isolated prey plasmids in order to ensure that they each contained a DNA insert, identifying inserts in this manner would be indicative of an expressed prey protein (Figure 3.45).

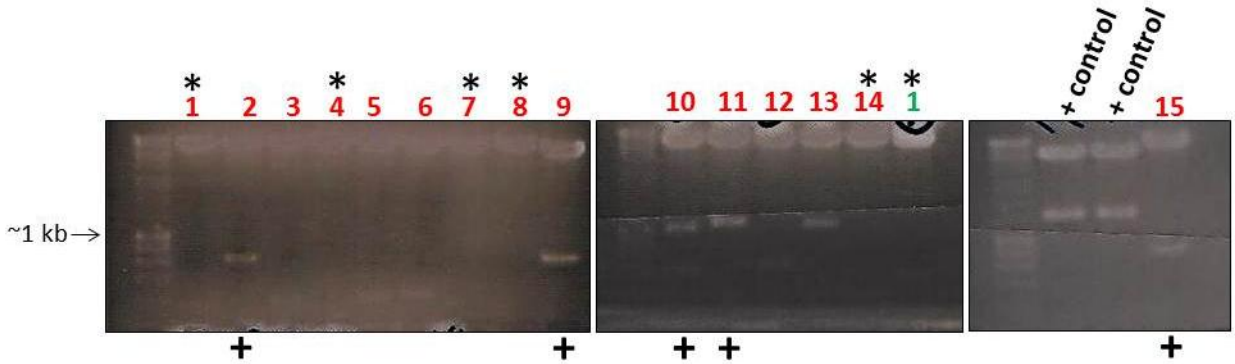

Figure 3.45 Restriction digests of prey plasmids. Digests of prey plasmids isolated from 15 yeast colonies that grew when restreaked on selection plates post transformation with actinin-1 bait (red). Digest of one yeast colony that grew when restreaked on a selection plate post transformation with actinin-4 bait (green). * indicates digests where no insert was observed. + indicates prey plasmids that interacted when retransformed with actinin-1 bait.

The absence of inserts post restriction digest could mean that the incorrect plasmid was isolated. For this reason I repeated plasmid purifications on yeast colonies where initial plasmid digests did not produce inserts. I ran both old and new plasmid digests in parallel on agarose gels to see if any discrepancies existed.

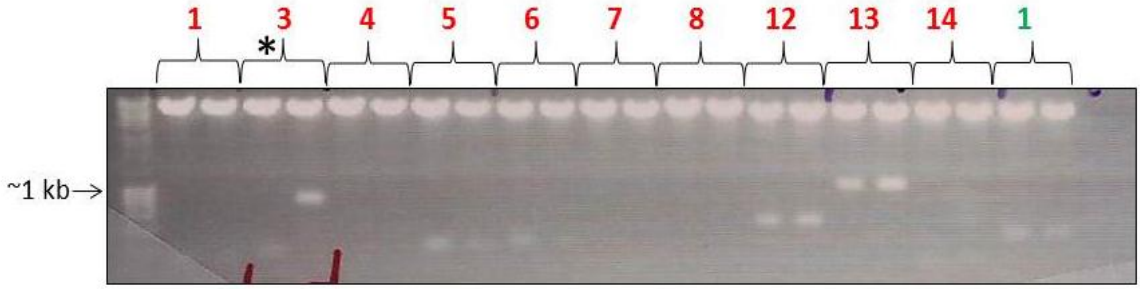

Figure 3.46 Restriction digests of repeat prey plasmid purifications. Prey plasmid purifications were repeated on colonies where initial plasmid digests did not produce inserts. Control prey plasmid purifications were also repeated on selected colonies where initial plasmid digests did produce inserts. Old (left) and new (right) plasmid digests are run side by side. Actinin-1 (red) and actinin-4 (green). * indicates digest pattern different from that observed on first round of preps.

Figure 3.46 shows that repeat prey plasmid purifications produced the same digest patterns previously observed in Figure 3.45, with the exception of colony #3 that showed a bigger insert than previously identified. However this new prey plasmid #3 did not interact with the actinin-1 bait when retransformed and for this reason it was excluded from the screen at this point. Actinin-1 interacting preys #2, 9, 10, 11 and 15 identified in Figure 3.45 did not interact with the control bait vector alone proving that they were genuine actinin-1 interacting proteins. They did however interact

when transformed with the actinin-4 rod proving that these preys are common interacting partners of both actinin-1 and -4. Sequencing of the prey plasmids identified three separate clones of Myozenin (Prey #2, #9 and #15). Myozenin is a known actinin-2 interacting protein also called FATZ and calsarcin-2 (Faulkner et al., 2000; Frey et al., 2000; Takada et al., 2001). Myozenin is regarded as a muscle-specific protein but by rtPCR analysis it was found to be expressed in the brain at all developmental stages (data not shown). I would like to acknowledge Ms. Anita Murphy for her efforts in analysing the developmental expression pattern of myozenin in the brain. Altogether these findings indicate that myozenin could interact with all three actinins that are expressed in the brain. Single clones for two other proteins Homeodomain-interacting protein kinase 1 (HIPK1) (Prey #10) and the polycomb protein Sex Comb on Midleg Homolog 1 (SCMH1) (Prey #11) were also identified.

3.4.1.3 Yeast two-hybrid screen of a brain cDNA library employing the actinin-1 rod as bait

Preliminary studies identified the actinin-1 rod domain as a more efficient bait protein than its actinin-4 counterpart. For this reason I chose to proceed with further screens of a mouse brain cDNA library employing solely this domain as bait. Any actinin-1 interactions identified could be confirmed or unconfirmed for actinin-4 post screen. Using the actinin-1 rod as a bait protein resulted in 71 colonies. Only 1 colony (#41) did not grow when restreaked on selection plates. Figure 3.47 shows restriction digests of plasmids (1-20) isolated from these colonies.

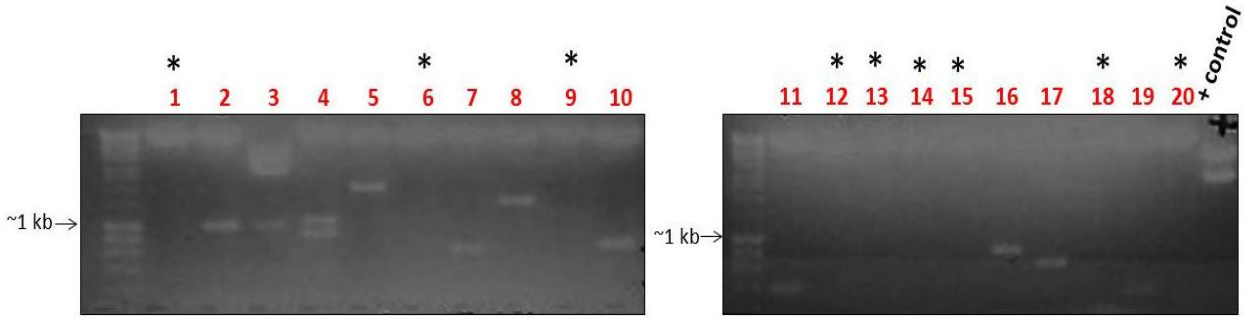

Figure 3.47 Restriction digests of prey plasmids. Digests of prey plasmids isolated from colonies 1-20 that grew when restreaked on selection plates post transformation with actinin-1 bait. Note none of these preys interacted when retransformed with actinin-1 bait (red). * indicates digests where no insert was observed.

The absence of inserts post restriction digest could mean that the incorrect prey plasmid was isolated. For this reason I repeated prey plasmid purifications on yeast colonies where initial plasmid digests did not produce inserts. I also isolated and performed digests on the remaining plasmids (21-71) (Figure 3.48).

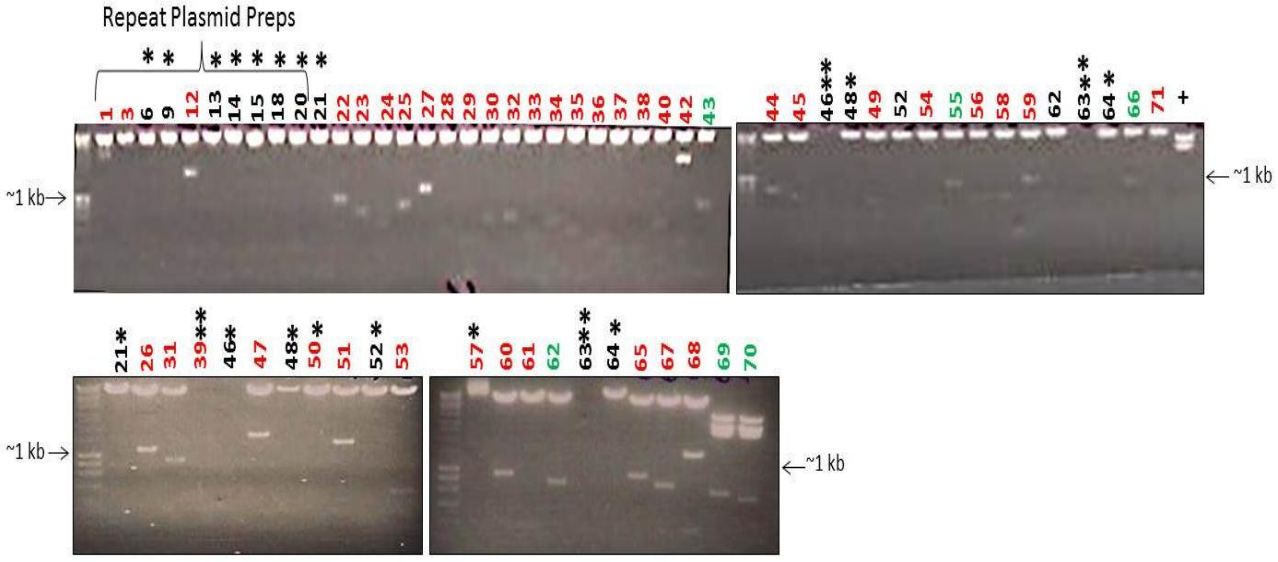

Figure 3.48 Restriction digests of prey plasmids. Digests of plasmids isolated from colonies that grew when restreaked on selection plates post transformation with actinin-1 bait. Bracket indicates repeat plasmid purifications of colonies where initial plasmid digests did produce inserts (Figure 3.47). Preys that interacted when retransformed with bait (green). Preys that did not interact when retransformed with bait (red). Prey plasmid purifications where no DNA was isolated (black). Plasmid purification digests were no insert was observed *

Prey plasmids that produced inserts on restriction digest were subsequently retransformed with the actinin-1 bait. Results of those retransformations are indicated in Figure 3.47 and Figure 3.48 (interaction = green, no interaction = red). Prey plasmids that did not produce DNA/inserts upon restriction digest were subject to a second round of plasmid purification (Figures 3.48 and 3.49).

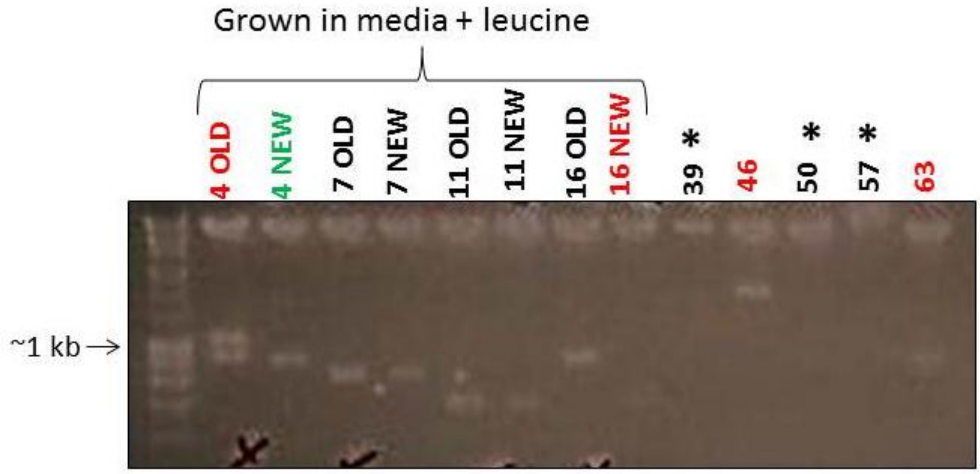

Figure 3.49 Restriction digests of prey plasmids. Digests of prey plasmids isolated from colonies that grew when restreaked on selection plates post transformation with actinin-1 bait. Bracket indicates repeat "new" plasmid purifications of colonies grown in the presence of leucine in an effort to deselect for non-specific prey plasmids. Preys that interacted when retransformed with bait (green). Preys that did not interact when retransformed with bait (red). Prey plasmid purification digests were no insert was observed *

At least two attempts were made to purify prey plasmids that did not produce inserts upon restriction digest. Three attempts were made in the case of preys #46 and #63 where no DNA was observed on the first two rounds of plasmid purification. While DNA and inserts were obtained in round three, no interaction was observed upon retransformation with the actinin-1 bait. Of the 71 colonies initially observed, 56 resulted in prey plasmids that produced inserts upon digest. Of these 56 plasmids, 7 positively interacted when retransformed with the actinin-1 bait. The remaining 49 did not interact upon retransformation with the actinin-1 bait proving that these were false positives. 14/71 prey plasmids did not produce inserts upon restriction digest. Even so, I still retransformed 10 of these plasmids with the actinin-1 bait to determine if any of these resulted from a genuine interaction, however no interaction was observed proving that these were also false positives. As mentioned colony #41 did not grow when restreaked on selection plates and therefore plasmid purifications/digests were not performed. It would appear from this screen that there was a high rate of false positives. One possible reason for this is that I was not purifying the correct prey plasmid from the yeast. It is possible that >1 prey plasmid may have been transformed per colony, however it is the prey plasmid that interacts with the actinin-1 bait that I needed to isolate. I grew a number of colonies in media

containing leucine in an effort to deselect for any additional non-specific prey plasmids that might be present. Figure 3.49 shows that under these conditions 2/4 preys isolated exhibit the same restriction digest pattern as previously observed. However, the remaining two prey plasmids (#4 and #16) exhibit different digest patterns suggesting that alternative prey plasmids had been isolated. Retransformation with the actinin-1 bait identified prey #4 as a genuine actinin-1 interacting partner. However prey #16 proved to be a false positive. At this point I had identified seven genuine actinin-1 interacting preys (4, 43, 55, 62, 66, 69 and 70). Based on the fact that preliminary screens (Section 3.4.1.2) identified three separate myozenin preys in this cDNA library as actinin-1 interacting partners, I subjected each of the seven prey plasmids to PCR analysis using primers specific for myozenin (Figure 3.50).

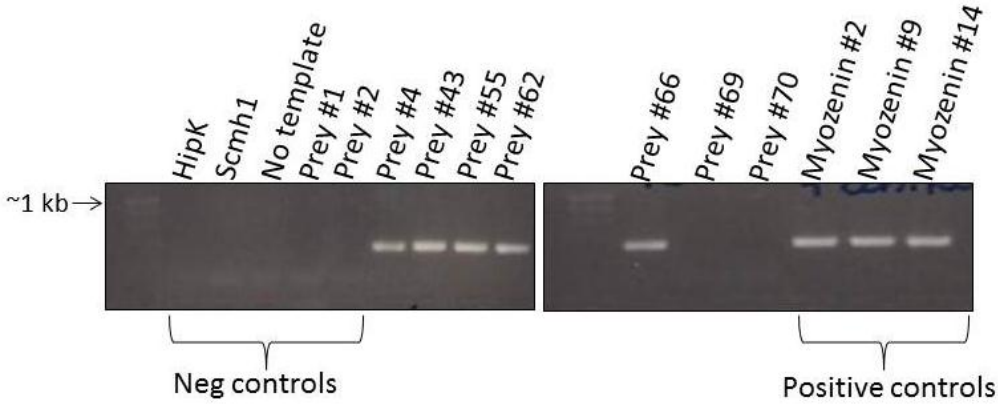

Figure 3.50 Screening for myozenin preys by PCR analysis. Actinin-1 interacting prey plasmids were subjected to PCR analysis using primers specific for myozenin. Preys plasmids (4, 43, 55, 62 and 66) were identified as myozenin. Negative controls included HIPK and SCMHI prey plasmids identified as actinin interacting proteins by preliminary studies. Negative controls also included prey plasmids #1 and #2 that did not interact with the actinin-1 bait. Positive controls included the three myozenin preys identified as actinin interacting proteins by preliminary studies.

PCR analysis identified 5/7 prey plasmids as myozenin (Figure 3.50). Transformation with the actinin-4 rod confirmed that myozenin interacts with both actinin-1 and -4. The remaining two prey plasmids (#69 and #70) that were not identified as myozenin also interacted with actinin-4. However, these two prey plasmids were found to auto-activate upon transformation with the empty bait vector proving that these were false positives. It is noteworthy to mention that I used β-galactosidase assays to confirm these results (data not shown). I carried out two sets of β-Gal assays. In Set #1 I tested a number of colonies that resulted from the initial

screen. In Set #2 I tested a number of colonies that resulted from retransformation of isolated prey plasmids (from initial colonies Set #1) with the actinin-1 bait. Interestingly I found a much higher number of positive β-Gal reactions in Set #1. 25 colonies that initially tested positive in Set #1 proved to be negative once their prey plasmids had been isolated and retransformed with actinin-1 bait (Set #2). This suggests that either the correct prey plasmid was not isolated or that there may have been some form of bacterial contamination of initial screens capable of producing β-Gal. It is important to mention at this point that all of the colonies that resulted in the identification of the myozenin-actinin interaction tested positive in both β-Gal assay sets and that the β-Gal negative controls were negative. This proves that technically I was successfully isolating prey plasmids and contamination was not a contribution of reagents employed for β-Gal assays. Only prey plasmids that contained inserts were considered possible interacting candidates. 22 out of the 25 prey plasmids that exhibited discrepancies between β-Gal assay sets contained inserts. Altogether this means that all prey plasmids studied in this screen were isolated in a technically competent manner and were deemed to genetically represent functional plasmids by restriction digest. However this does not rule out the fact that incorrect prey plasmids may have been isolated. Indeed efforts to deselect any non-specific prey plasmids by growing yeast in media containing leucine resulted in 2/4 alternative prey plasmids being isolated. However, only one of these plasmids (Prey #4) was identified as a genuine myozenin-interaction. Myozenin had already been identified 7 times (4 times in this screen and three times in the preliminary screen). Overall taking into account the fact that so few preys proved to be genuine interactions (~10%) along with the fact that most of the genuine preys represented the same protein (myozenin) and that all of the genuine preys interacted with both actinin-1 and -4, I did not feel that this screen warranted the time required for further investigations. Overall, given the number of known actinin rod interactions, the number of proteins identified in this screen was very low, suggesting that this yeast two-hybrid system was not an efficient screening method for identifying actinin-interacting partners.

3.4.2 Tandem Affinity Purification (TAP) of actinin-1 and -4.

3.4.2.1 Development and expression of TAP-tagged actinin-1 and -4 proteins

As an alternative approach to the Y2H system I used tandem affinity purification of actinin protein complexes coupled with mass spectrometry. Heterodimer formation between transfected and endogenous actinin could make it difficult to identify interacting partners unique to either actinin-1 or -4. For this reason I used HEK cells which do not exhibit significant heterodimer formation (see Figure 3.42). I established three stably transfected cell pools expressing TAP-tagged actinin-1 or actinin-4 as well as control cells expressing TAP-tagged YFP. At least 70% of cells in these pools expressed the TAP-tagged constructs and Western blotting indicated that expression levels were equivalent to endogenous actinin levels in HEK cells (data not shown). Figure 3.51 shows fluorescent images of the three cell pools employed.

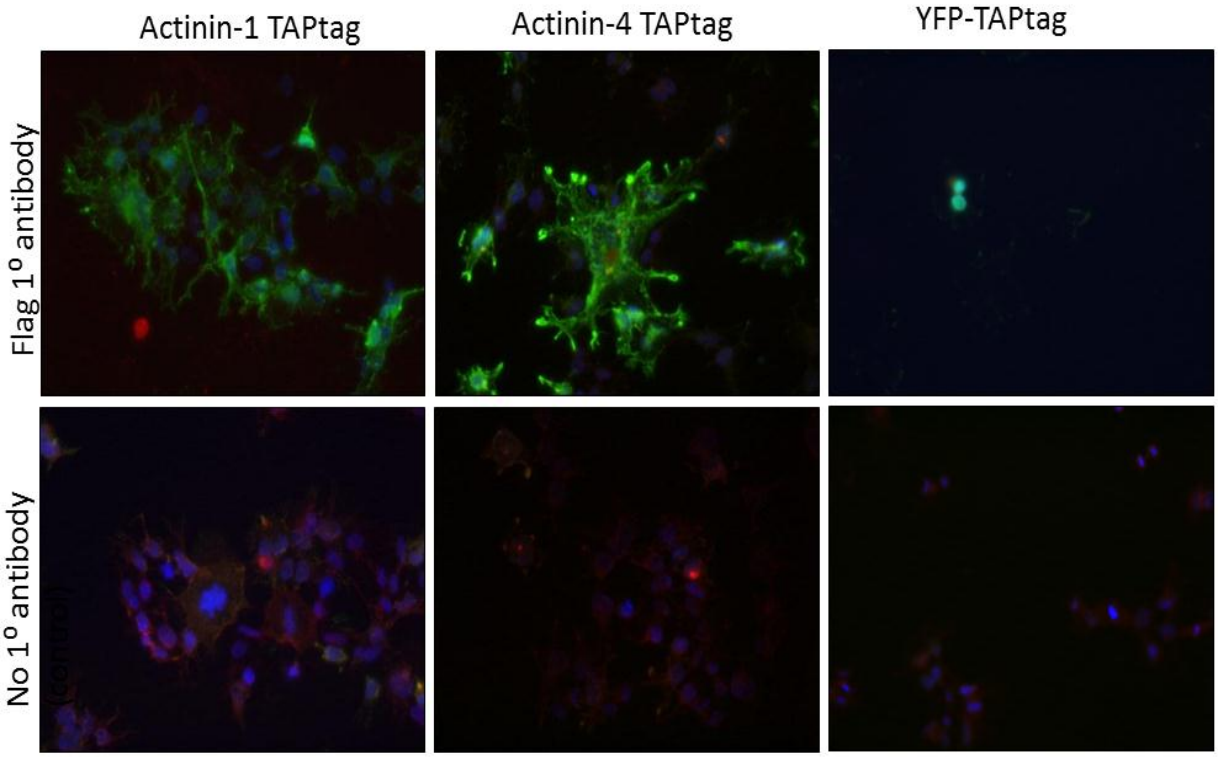

Figure 3.51 Fluorescent images of TAP-tagged actinin-1, -4 and YFP cell pools. HEK cells were transfected with TAP-tagged actinin-1, -4 and YFP expressing constructs. Over the course of ~10 passages, cells that stably expressed TAP-tagged proteins were selected. A Flag epitope was cloned in-frame with the TAP tag. This Flag tag allowed identification of TAP-tagged expressing cells though staining with an anti-Flag antibody (green). Cells were also stained with Phalloidin (red) to detect actin filaments. Dapi stained nuclei (blue).

Actinin-4 is reported to localise at sites of membrane ruffling and at the leading edge of cells (Araki et al., 2000; Honda et al., 1998). From Figure 3.51 it appears that while actinin-1 is diffusely expressed throughout the cytoplasm, actinin-4 tends to be localised to membraneous regions similar to patterns described in the literature. However to ensure that this pattern was representative of geniune actinin localisation within HEK cells and to rule out the possibility that the TAP tag is interfering with localisation, I examined endogenous actinin staining (Figure 3.52). Staining indicated that HEK cells express low levels of endogenous actinin-1 and -4. I observed diffuse staining of endogenous actinin-1 in the HEK cell cytoplasm. I also observed what initially appeared to be nuclear localisation of actinin-1. However upon further investigation I found that this was the result of secondary antibody cross-reactivity (data not shown). In contrast to endogenous actinin-1, actinin-4 appeared to be concentrated at membraneous regions, similar to the pattern observed for TAP-tagged actinin-4. Overall it appears that TAP tagged actinin-1 and -4 behave similarly to endogenous actinin isoforms, at least with respect to their localisation patterns. With this in mind I proceeded to individually purify TAP-tagged actinin-1, -4 and YFP from HEK cells through the sequential affinity purification steps of the Tandem Affinity Purification technique.

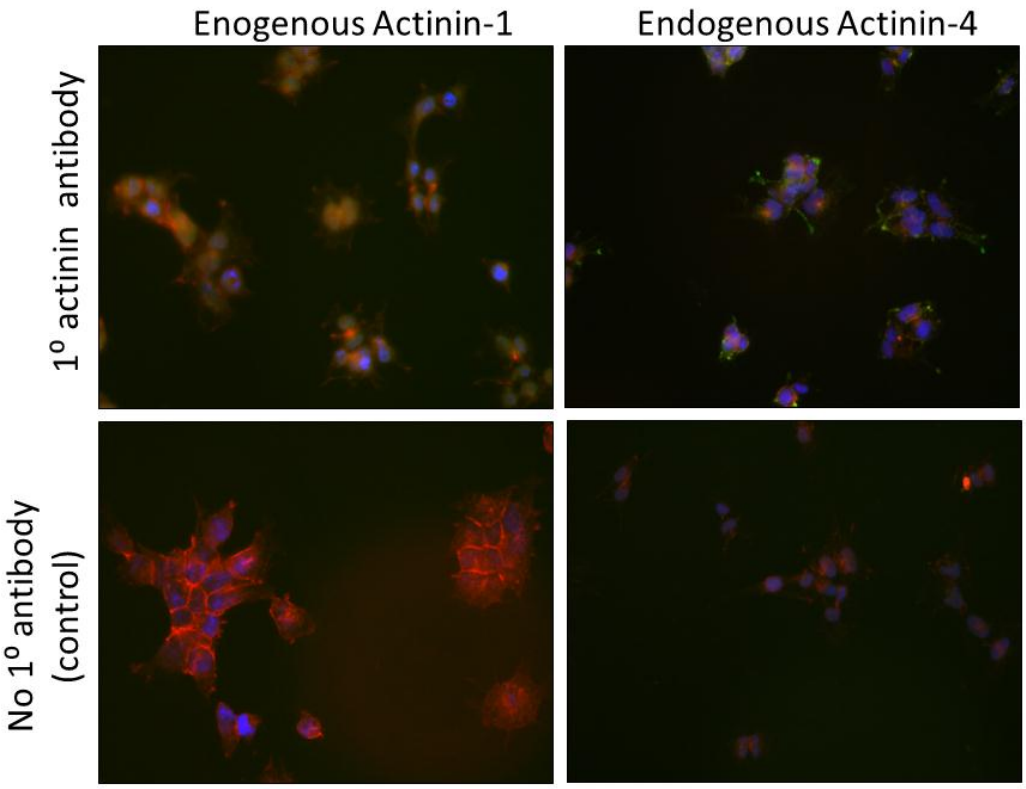

Figure 3.52 Fluorescent images of endogenous actinin-1 and -4 in HEK cells. HEK cells were probed for Actinin-1 [Santa Cruz (H2)sc:17829] and Actinin-4 (Honda). Cells were also stained with Phalloidin (red) to detect actin filaments. Dapi stained nuclei (blue).

Actinin-1, -4 and YFP were purified using IgG bead columns. IgG elutions were incubated with TEV protease and subsequently purified using calmodulin sepharose columns. Samples taken at various purification steps were analysed by denaturing gel electrophoresis (Figure 3.53). From Figure 3.53 it is clear that actinin-1 and -4 have been purified though the sequential purifications steps of the TAP technique. In contrast YFP was not successfully purified. Western blot analysis indicated that TAP-tagged YFP was expressed in cells (data not shown). It is possible that YFP interferes with the binding of the TAP tag to IgG beads and as a result may not be purified. However, the TAP-tagged YFP expressing cell line can still function as a negative control for non-specific binding of proteins to IgG/calmodulin beads. I would like to acknowledge Ms. Anjali Pai for her efforts in assisting me with these purifications.

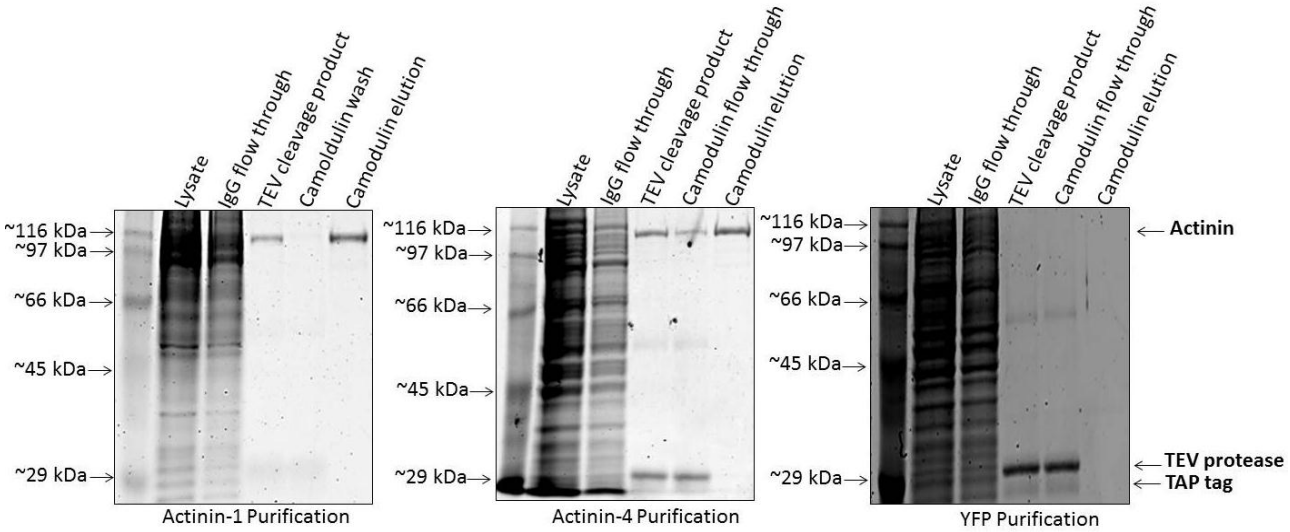

Figure 3.53 Tandem Affinity Purification (TAP) of actinin-1, -4 and YFP. IgG sepharose columns were used to purify TAP-tagged actinin-1, -4, and YFP from transfected HEK cell lysates. IgG elutions were incubated with TEV protease to remove the IgG binding domain of the TAP tag (TEV cleavage product). Samples were subsequently purified using calmodulin sepharose columns (calmodulin elution).

3.4.2.2 Analysis of actinin-interacting proteins identified by Tandem Affinity Purification

Calmodulin bead elutions of actinin-1, -4 and YFP were analysed by Coomassie stained SDS-PAGE gels. Each sample lane was cut into six bands (Figure 3.54). Actinin-1 and -4 appear in band #2. Proteins present in each band were analysed by nano-liquid chromatography and MS/MS mass spectrometry and identified by searching against the IPI protein database.

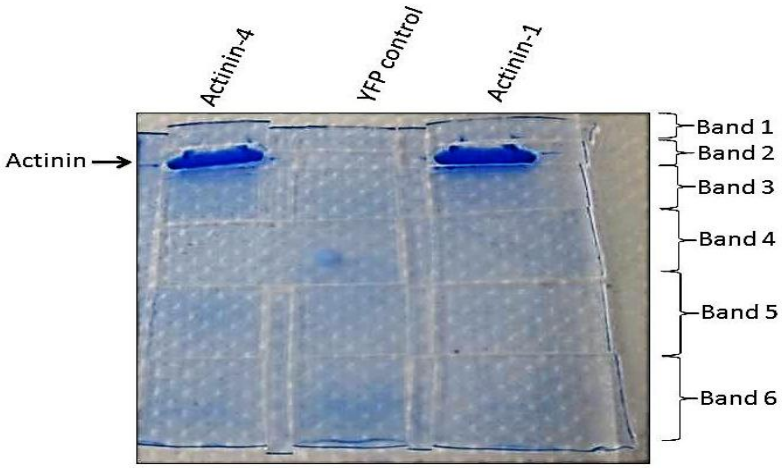

Figure 3.54 Calmodulin sepharose elutions of actinin-1, -4 and YFP samples were run on SDS-PAGE gels and stained with Coomassie blue. When loading samples there was a space left between each to avoid cross contamination of proteins. Each sample lane was cut into six bands. Actinin-1 and -4 appear in band #2. Each band was sent for mass spectrometric analysis to identify associated proteins.

Non-specific interactions present in the TAP-tagged YFP sample were likely false positives or environmental contaminants and were therefore eliminated (see Section 2.9) to generate lists of proteins specifically identified in affinity purified actinin-1 and actinin-4 complexes (Table 3.4). In order to ensure that proteins were identified as a result of their interaction with actinin and not simply due to their high expression level in a particular cell pool I quantified levels of mRNAs coding for selected proteins between TAP-tagged actinin-1, actinin-4 and YFP cell pools (Figure 3.55)

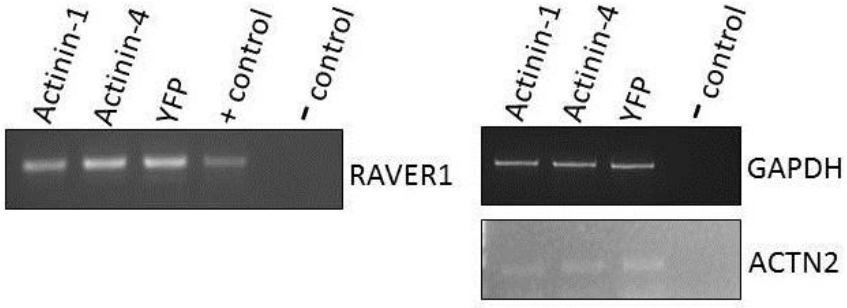

Figure 3.55 Analysis of RAVER1, ACTN2, and GAPDH cDNA levels between TAP-tagged actinin-1, -4 and YFP cell pools. cDNA levels of each protein remained relatively constant between cell pools. DNA ladders were used but are not shown. Bands are at expected sizes.

I found that cDNA levels of RAVER1 were similar between cell pools. This indicates that the identification of actinin-4 associated RAVER1 likely represents an isoform-specific interaction. Several well-characterised actinin-interacting proteins (underlined in the Table 3.4) including PALLD (Rönty et al., 2004), CAMK2B (Walikonis et al., 2001), PDLIM1 (Vallenius et al., 2000), PDLIM3 (Xia et al., 1997) and RAVER1 (Hüttelmaier et al., 2001) were identified validating the overall approach. Although I used HEK cells due to their low levels of endogenous heterodimers there appeared to be some degree of actinin-1/-4 heterodimer formation in the stably transfected cells used since actinin-1 was found in actinin-4 complexes and vice versa (Table 3.4C). Interestingly actinin-2 and -3 were also detected in both complexes providing further evidence that all combinations of heterodimers between muscle and non-muscle actinins are possible. The identification of similar ACTN2 cDNA levels between cells pools supports the notion that ACTN2 detected in actinin-1 and -4 cells pools was the result of genuine interactions. The fact that relatively few common proteins were detected in both actinin-1 and -4 complexes

suggests that despite the presence of some heterodimers, isoform-specific interactions could still be detected. More potential novel interacting proteins were identified for actinin-4 compared to actinin-1 and notably over half of these are proteins that are reported to localise partially or exclusively in the nucleus and have functions related to transcription, RNA binding and mRNA splicing. These observations fit with the reported localisation of actinin-4 to the nucleus (Honda et al., 1998; Chakraborty et al., 2006; Khurana et al., 2011; Kumeta et al., 2010; Bolshakova et al., 2007; Goffart et al., 2006). Overall this screen provides a list of putative actinin-1 and -4 specific interacting proteins that might mediate or contribute to some of the reported isoform-specific functions of actinin-4 in particular (see Table 3.4 A+B)

Table 3.4A Proteins identified only in actinin-1 complexes

Protein Symbol	Mascot Score	Name	Subcellular Location	Function
DDX17	210	Probable ATP-dependent RNA helicase DDX17 isoform 3	Nucleus	Transcriptional regulation
PALLD	175	Isoform 2 of Palladin	Cytosol	Actin cytoskeleton: organisation
CAMK2B	103	Calcium/calmodulin-dependent protein kinase type II subunit beta	Cytosol	Protein kinase
PDLIM3	103	PDZ and LIM domain protein 3	Cytosol	Actin cytoskeleton: organisation
PRDX2	100	Peroxiredoxin-2	Cytosol	Redox regulation in cells

Table 3.4B Proteins identified only in actinin-4 complexes

Gene Symbol	Mascot Score	Name	Subcellular Location	Function
LRPPRC	2257	Leucine-rich PPR motif-containing protein, mitochondrial	Mitochondria, Nucleus, Cytosol	RNA-binding
IQGAP2	1894	Isoform 1 of Ras GTPase-activating-like protein IQGAP2	Cytosol	Cytoskeletal regulation
DOCK7	588	Dedicator of cytokinesis protein 7	Cytosol	Cytoskeletal regulation
FLNC	544	Isoform 1 of Filamin-C	Cytosol	Actin cytoskeleton: cross-linker
RAVER1	457	ribonucleoprotein PTB-binding 1	Nucleus, Cytosol	mRNA splicing, cytoskeletal
SF3B2	432	Splicing factor 3B subunit 2	Nucleus	mRNA splicing
UBR5	399	E3 ubiquitin-protein ligase UBR5	Nucleus	Ubiquitination, Transcription
PRRC2A	353	Isoform 1 of Protein PRRC2A	Nucleus, Cytosol	mRNA Splicing
CDKN2AIP	203	CDKN2A-interacting protein	Nucleus	Activation of p53
PPFIA1	160	Isoform 1 of Liprin-alpha-1	Cytosol	Signalling / Scaffolding
TCEAL4	138	Isoform 2 of Transcription elongation factor A protein-like 4	Nucleus	Transcription
ELAVL1	126	Similar to ELAV-like protein 1	Nucleus, Cytosol	RNA-binding
SPRR2E	117	Small proline-rich protein 2E	Cytosol	Cytoskeletal component
SART1	113	U4/U6.U5 tri-snRNP-associated protein 1	Nucleus	mRNA splicing
TCERG1	108	Transcription elongation regulator 1	Nucleus	Transcription
MYH10	104	Isoform 1 of Myosin-10	Cytosol	Actin cytoskeleton: motor
SMARCC2	103	Isoform 2 of SWI/SNF complex subunit SMARCC2	Nucleus	Transcription
SF3B4	100	Splicing factor 3B subunit 4	Nucleus	mRNA splicing
MYL6	100	Non-muscle Myosin light chain 6	Cytosol	Actin cytoskeleton: motor

Table 3.4C Proteins identified both in actinin-1 and actinin-4 complexes

Gene Symbol	Mascot Scores	Name	Subcellular Location	Function
ACTN1	7522, 3925	Alpha actinin-1	Cytosol	Actin cytoskeleton: cross-linker
ACTN4	4814, 6909	Alpha actinin-4	Cytosol, Nucleus	Actin cytoskeleton: cross-linker
ACTN2	1961, 1114	Alpha actinin-2	Cytosol	Actin cytoskeleton: cross-linker
ACTN3	1366, 1071	Alpha-actinin-3	Cytosol	Actin cytoskeleton: cross-linker
MYH9	103, 391	Isoform 1 of Myosin-9	Cytosol	Actin cytoskeleton: motor
PDLIM1	208, 38	PDZ and LIM domain protein 1	Cytosol	Cytoskeletal, Stress fibres

4 Discussion

4.1 The effect of the non-muscle actinins on cell migration and localisation

4.1.1 Antibody characterisation

Through screening of a range of commercially available antibodies using GFP-tagged actinin isoforms I was able to identify actinin-1, -2 and -4 specific antibodies. These are α-actinin [Santa Cruz (H-2): sc-17829] (human), α-sarcomeric actinin [Sigma Clone (EA-53)] (human and mouse) and α-actinin-4 [Immunoglobe (IG701)] (human and mouse), respectively. Since α-actinin [Santa Cruz (H-2): sc-17829] did not detect mouse actinin-1, I tested α-actinin [Abnova (3F1)] that specifically detected both human and mouse transfected GFP-tagged actinin-1. While [Abnova (3F1)] and α-actinin-2 [Santa Cruz (A-25): 1030928] were specific in their detection of GFP-tagged actinin isoforms, they were not efficient at detecting endogenous actinin proteins. Therefore I currently do not possess a specific anti-mouse actinin-1 antibody. [Santa Cruz (H300): sc15335) is described by Santa Cruz as a "pan-actinin" antibody for both human and mouse actinins, however I found that this antibody did not detect mouse and only weakly detected human actinin-4. [Abnova (3F1)] and [Santa Cruz (H300): sc15335] recognised some lower molecular weight bands than the expected ~100 kDa band (data not shown). The detection of non-specific bands should be taken into account when employing these antibodies. I also identified α-actinin [Sigma (BM75.2)] as an antibody that detects both actinin-1 and -4. This is an important observation as previous studies have been carried out that employed α-actinin [Sigma (BM75.2)] as an "actinin-1 specific" antibody (Celli et al., 2006; Bolshakova et al., 2007). However, more recent studies have recognised this as a "pan-actinin antibody" (Quick & Skalli, 2010). Identifying these actinin antibodies would allow me to specifically study the expression and localisation of actinin-1, -2 or -4 as well as total non-muscle actinin (actinin-1 and -4).

4.1.2 The effect of actinin-1 and -4 knockdown on cell migration

Initially, I selected COS-7 and MCF-7 cells to optimise siRNA-mediated knockdown of actinin-1 and -4. Based on related studies in the literature I obtained satisfactory

knockdown levels of actinin-1 (77%) and -4 (>90%). Given that actinin-4 is the predominant isoform associated with the cancer phenotype I selected MCF-7 breast carcinoma cells that successfully facilitated siRNA-mediated knockdown of actinin-4 for initial migration studies. While migration levels decreased an average of 15% as a result of individual or combined actinin-1 and -4 knockdown these results were not statistically significant (n=3). This may be as a result of the fact that residual actinin protein levels are sufficient to contribute to migratory functions, at least in MCF-7 cells. It could also be due to the fact that MCF-7 cells may not be highly dependent on actinin-4 for migration. For this reason I selected two more aggressive cell lines that exhibit higher migration rates relative to MCF-7 cells, the breast carcinoma cell line MDA-MB-231 and the prostate carcinoma cell line DU145. While >90% actinin-1 knockdown levels were obtained in MDA-MB-231, only 50% actinin-4 knockdown was achieved. Increasing siRNA concentration and incubation time resulted in only 9% increase in actinin-4 knockdown. For this reason I focused on DU145 cells that close scratch wound assays in ~8 hours compared to 24 hours for MCF-7 cells. Greater than 80% actinin-4 and ~50% actinin-1 knockdown was achieved. However, no obvious effects on migration were observed. Based on the literature, knockdown of actinin-4 resulted in decreased migration of the glioblastoma cell lines A172 and U373-MG (Quick & Skalli, 2010). For this reason I studied the effect of siRNA-mediated knockdown of individual and combined actinin-1 and -4 on the migration of these cells. However, I observed no obvious effect on migration. The discrepancies observed may be explained by the fact that I obtained actinin-4 knockdown levels of <50% compared to 80% obtained by Quick and Skalli. The shortfall in the knockdown levels observed here is likely due to the fact that Quick and Skalli utilised the more robust knockdown approach of short hair-pin RNA as a means of RNA interference. Similar to MCF-7 cell results, the fact that actinin-1 and -4 knockdown did not cause any negative effects on DU145, A174 and U373-MG cell migration may be due to the fact that residual actinin levels are sufficient for normal cell migration. Limitations of siRNA to knockdown actinin may be due to a low turnover rate or the high stability of the protein. In future approaches such as shRNA may offer a more efficient means to study the effect of actinin knockdown. While 80% actinin-4 knockdown had an effect on the migration of glioblastoma cells (Quick & Skalli, 2010) this level of knockdown had no impact on MCF-7 cell migration indicating that actinin-4 dependence may be cell type

specific. The fact that the variety of cells studied exhibited normal migratory functions with as low as 20% of normal actinin-4 levels indicates that migration may not require high levels of actinin-4 relative to total levels present in some cells. This work proves that ≥50% of actinin-4 protein levels are not involved in the migratory functions of the cells studied, suggesting that migration may be a minor function of actinin-4 in some cell types. This brings into question what other functions are carried out by actinin-4. Indeed studies have revealed that actinin-4 knockdown affects cellular functions such as adhesion, proliferation and may even play a role as a transcription regulator (Quick & Skalli, 2010; Babakov et al., 2008). It is possible that some functions are more heavily dependent on actinin-4 than others. Determining heavily dependent actinin-4 functions may provide an insight into the differential effects of actinin-1 and -4.

4.1.3 Determination of the specific protein domain responsible for the distinct localisation patterns observed for actinin-1 and -4.

Discrepancies occur in the literature with regard to the role of actinin-1 and actinin-4 in cancer. Some reports describe these isoforms as having tumour suppressor activity whereas others report their involvement in tumourigenesis and metastases (Glück et al., 1993; Nikolopoulos et al., 2000; Craig et al., 2007; Honda et al., 1998). Conflicting reports also exist with regard to the localisation of these two non-muscle actinin isoforms. Actinin-1 is reported to be located at stress fibre dense regions while actinin-4 is proposed to accumulate in cellular ruffles, the cytoplasm of extended cells and the edges of cell clusters (Honda et al., 1998; Araki et al., 2000). Here, I tried to determine the localisation of these isoforms within MCF-7 cells. I conclude that actinin- 1 is dispersed within the cytoplasm of MCF-7 cells where it co-localises with actin. Reports in the literature suggest that actinin-1 localises at dense stress fibre regions. I found MCF-7 cells not to be representative of cells with many dense fibre regions. However, in some stress fibre regions I did observe the localisation of actinin-1. I observed that actinin-4 tends to accumulate at the edges of these cells in what could be described as cellular ruffles, reports of which exist in the literature (Araki et al., 2000). Previous reports also suggest that nuclear localisation of actinin-4 is related to a low infiltrative cancer whereas cytoplasmic localisation is

related to a higher propensity for tumour invasiveness and metastases. Here, I also describe the cytoplasmic localisation of actinin-4 within the MCF-7 metastatic cancer cell line. I further tried to gain an insight into the actinin protein domain that contributes to the patterns of localisation observed. Chimeric proteins with switched actin-binding domains showed localisation patterns similar to that of the original protein. Chimeric proteins with switched rod domains showed localisation patterns similar to that of the rod domain however, these patterns were not identical to the isoform from which the rod originated. Therefore, localisation cannot be entirely attributed to the rod domain. Finally, chimeric proteins with switched calmodulin-like domains appeared to resemble localisation patterns similar to that of the original protein. I conclude that while the rod domain might have a strong influence, the localisation of non-muscle actinin isoforms is likely to be a property of the entire protein where each domain contributes to the overall effect seen within the cell. The fact that the rod domain of actinin tended to influence localisation to some extent may not be surprising given the fact that this domain acts as a docking platform for protein interactions that are likely to influence actinin localisation (Djinovic-Carugo et al., 2002). While my observations tend to correlate with reported studies of endogenous actinin it is important to mention that monitoring protein localisation through use of a GFP tag has its limitations. Given that GFP is a 27 kDa protein it is important to be wary of deleterious effects of such a large protein tag on the function and localisation of the tagged protein (Tavaré et al., 2001). The GFP tag can interfere with a protein's native interactions. GFP-tagged proteins are often expressed at levels far greater than the endogenous native protein and thus alterations in protein localisation and function due to over-expression should always be carefully considered (Tavaré et al., 2001). On the other hand GFP allows the examination of a protein's localisation without the need for staining with specific antibodies, a method that can potentially result in high background and artefacts. It also allows the visualisation of proteins whose antibody epitopes may be blocked due to the nature of their endogenous interactions i.e. in dense structures like focal adhesions, and it eliminates the need for epitope retrieval techniques. Despite its limitations, the GFP tag has been used successfully for well over a hundred proteins indicating that it is a remarkably versatile tag (Tavaré et al., 2001). It is important to mention that the localisation studies carried out here employed MCF-7 cells that exhibit significant (~50%) heterodimer formation (Figure 3.39 and Figure 3.42). The ability of actinin-1

and -4 to form heterodimers raises the question of how they can exert distinct localisation patterns. It is possible that actinin-1 and -4 homodimers that make up ~50% of total non-muscle actinin levels in MCF-7 cells are responsible for the distinct localisation patterns observed, while heterodimer formation may account for overlapping localisation regions. Chan *et al.* identified that muscle heterodimer formation occurred when actinin-2 and -3 were co-expressed in the same cell line (Chan et al., 1998). This means that the transfected GFP-tagged isoforms employed here could form non-muscle heterodimers with endogenous actinin. This may explain some of the overlapping localisation patterns of actinin-1 and -4. However it is possible that transfected GFP-tagged actinin-1 and -4 may form homodimers with itself and endogenous actinin. Chan *et al.* suggested that homodimers were more likely to form when actinins where transfected separately due to rapid homodimerisation and the stability of the homodimer. Once translated, endogenous actinin enters either a homo- or hetero-dimeric state. Due to the stability of these dimers it is possible that transfected actinin may be more likely to dimerise with itself that with its endogenous counterpart. Since actinin-1 and -4 were transfected separately they may be likely form homodimers with themselves and thus display some of the distinct localisation patterns observed.

4.2 Alternative splicing and actin-binding properties of the non-muscle actinins

4.2.1 Actin-binding and calcium sensitivity properties of the non-muscle actinins

In this chapter I have systematically compared actin-binding affinities and Ca^{++}-sensitivities of actinin-1 and actinin-4 for the first time. Comparing the actin-binding properties of the most widely expressed Ca^{++}-sensitive forms of the two non-muscle actinins I found that the affinity of actinin-1 (exon 19a), and actinin-4 (exon 8a, 19a) for F-actin are quite similar with Kd values of 1.93 µM and 2.96 µM respectively. In addition their actin-bundling capacity and Ca^{++}-sensitivity of actin-binding and -bundling are nearly identical. Actinin-4 was first purified and cloned from chicken lung and was described as having low Ca^{++}-sensitivity (Imamuras et al., 1994). My results using recombinant human actinin do not agree with this

observation. This may reflect sequence differences in the EF- hand regions between human and chick actinin or post-translational modifications in the protein purified from tissue that are not present in the bacterial expressed actinin used in this work. It is possibly that the non-muscle actinins may differ in the extent by which they are regulated by other mechanisms. Indeed following epidermal growth factor (EGF) stimulation, actinin-4 is phosphorylated to a greater extent than actinin-1 (Shao et al., 2010). Phosphorylation in this manner decreases the affinity of actinin for actin. Phospholipid binding to smooth muscle actinin stimulates its interaction with actin (Fukami et al., 1992). Phospholid regulation of the non-muscle actinins has yet to be compared. The non-muscle actinins are widely co-expressed. Actinin-4 knockout mice display specific kidney defects but abnormalities in other tissues were not reported (Kos et al., 2003). The similar actin-binding properties that I observed for the two non-muscle actinins are in agreement with this apparent functional redundancy between them in most tissues.

4.2.2 Alternative splicing of non-muscle actinin exon 8 and exon 19

Alternative splicing of exon 19

While the actin-binding properties of the main Ca^{++}-sensitive non-muscle actinin isoforms are similar, this analysis of alternative splicing patterns reveals significant differences between actinin-1 and -4. In particular I found that the Ca^{++}–insensitive exon 19b variant of actinin-4 is only expressed in the nervous system. By contrast the exon 19b variant of actinin-1 is regarded as a smooth muscle isoform and is expressed in skeletal and smooth muscle as well as in the adult brain. The exon 19a and 19b variants of actinin-4 are co-expressed in the brain at all stages examined and thus actinin-4 does not exhibit the developmental switching from exon 19a to exon 19b-containing isoforms observed for actinin-1 as the brain matures. Neither was an 19a+19b variant of actinin-4 detected in the brain.

While splicing of actinin-1 and -4 exon 19 was conserved between human and mouse brain, I noticed differences in the splicing patterns of exon 19 that occurred in human heart and skeletal muscle tissues. Mouse heart and skeletal muscle tissues expressed both actinin-1 exon 19a and 19b isoforms, however human

tissues only expressed the 19b (Ca^{++}-insensitive) isoform. Actinin provides structure to muscle tissues by cross-linking actin. The muscle tissue microenvironment is subject to constant fluxes of calcium. From this point of view it may not be surprising that humans have evolved to solely express a Ca+-insensitive actinin-1 isoform in skeletal and cardiac tissues. Noteably mouse bladder solely expressed the actinin-1 exon 19b (Ca^{++}-insensitive) isoform, confirming that not all mouse muscle tissues express the 19a (Ca^{++}-sensitive) variant.

With regard to actinin-4, in addition to the exon 19a variant observed in mouse heart and skeletal muscle tissues, human skeletal muscle also expressed the combined exon 19a+19b variant. This is the first time detection of this actinin-4 variant has been reported.

Alternative splicing of exon 8

The alternative splicing of exon 8b, that is unique to actinin-4 occurs in the nervous system where it predominates over exon 8a, as well as in skeletal and smooth muscle-containing tissues where it is a minor species relative to the exon 8a variant. While I observed that the 8b variant predominants over the 8a variant in 7 independent PCRs of brain tissue (two human and five mouse), previous reports suggest that only trace amounts were detected in the brain relative to the 8a variant (Honda et al., 2004). This report was based on the fact that a nucleotide change in the variant transcript was predicted to produce a BanII restriction digest site. BanII digests were performed on exon 8 PCR products and the presence of an insert was taken as being indicative of the 8b variant. While this method may represent a qualitative means of exon 8b variant detection, it is not quantitatively sound as it is ultimately dependent on the efficiency of the restriction enzyme employed. Therefore, I report that the exon 8b variant predominates over the 8a variant in the human and mouse brain.

Alternative splicing mechanisms

Actinin-1 exon 19 has been used as a model to study the mechanisms underlying alternative splicing and clear roles for *trans*-acting splicing regulators

such as PTB (polypyrimididine tract binding protein) and CELF family members (CUG-BP and ETR3-like factors) have been delineated (Gromak et al., 2003; Suzuki et al., 2002). It will be interesting to examine how the differences in exon 19 splicing in actinin-4 compared to actinin-1 have arisen. Also, given that the pattern of expression of actinin-4 exon 8b in skeletal and smooth muscle is very similar to that of actinin-1 exon 19b in the same tissues, it is possible that some of the same splicing regulators and mechanisms are at play for both exon 8 and 19. This analyisis of splicing patterns can thus provide a starting point for more detailed mechanistic studies of the regulation of alternative splicing in actinins.

From an evolutionary perspective duplication and alternative splicing of exon 8 occurs in several invertebrate lineages and is thus more ancient than the alternative splicing of exon 19 which is restricted to chordates (Lek et al., 2010a). Gene duplication early in the vertebrate lineage produced four actinin genes. Alternative splicing of exon 19 was retained in actinin-1 and -4 but not in the muscle isoforms (actinin-2 and -3), in the mammalian lineage at least. Conservation of the alternatively spliced exon 8b is variable in actinin-1 and -2, absent from actinin-3 but has been retained in actinin-4 in mammals, birds, and fish (Lek et al., 2010a). This suggests that exon 8b in actinin-4 plays some essential, evolutionarily conserved function in the tissues in which it is expressed. Variations in the amino acid sequence encoded by exon 8 certainly have the potential to alter actin-binding properties and abnormal splicing of exon 8b is a feature of small cell lung cancer and neuroendocrine tumours (Honda et al., 2004; Miyanaga et al., 2012). However, the functional significance of alternative splicing of exon 8 is not clear. I found that the affinity of the exon 8b variant of actinin-4 for F-actin is not significantly different from that of the exon 8a variant and that both display similar Ca^{++} sensitivities. This contrasts with the enhanced actin-binding of the 8b variant previously reported (Honda et al., 2004). It should be noted however that Honda *et al.* measured the actin-binding affinity of the isolated ABD and the binding properties of this domain may be different in the context of the intact actinin dimer.

Overall these findings indicate that the actin-binding properties and Ca^{++}-sensitivities of actinin-1 (exon 19a), actinin-4 (exon 8a, 19a) and actinin-4 (exon 8b, 19a) are very similar and that expression of these isoforms may serve to fine tune the affinity of actinin for F-actin in particular contexts but would not alter actin-crosslinking properties very dramatically.

4.2.3 Muscle alternative splice variants

In muscle cells Ca^{++}-insensitive forms of actinin are thought to facilitate relatively stable crosslinking of actin filaments despite continuous fluxes in calcium associated with muscle contraction. These results show that while muscle cells express both exon 19a (Ca^{++}-sensitive) and 19b (Ca^{++}-insensitive) variants of actinin-1, they express only the exon 19a (Ca^{++}-sensitive) variant of actinin-4. This suggests that Ca^{++}-sensitive actinin-4 may have distinct functions in muscle compared to other actinin isoforms. Notably potential roles for actinin-4 as a transcriptional regulator during muscle differentiation have been described. Actinin-4 is found to be preferentally localised in the nucleus of myotubes during induction of myogenesis, suggesting a possible signalling role in muscle differentiation (Goffart et al., 2006). Actinin-4 is also reported to potentiate myocyte enhancer factor 2 (MEF2) transcription that leads to muscle differentiation (Chakraborty et al., 2006).

4.2.4 Brain alternative splice variants

In the brain actinins are components of the postsynaptic density at synapses (Walikonis et al., 2000). This data presents a complex picture of actinin splicing in the brain with Ca^{++}-sensitive and -insensitive variants of both actinin-1 (19a, 19b and 19a+19a) and actinin-4 (19a and 19b) being co-expressed. The muscle actinin-2 isoform is also expressed in particular brain regions (Walikonis et al., 2000). Since synapses are sites of calcium influx, Ca^{++}-insensitive actinin isoforms may be required to maintain the integrity of the postsynaptic actin-based cytoskeleton in neurons. The expression of multiple actinins and complexity of actinin splicing in the brain points to the potential importance of fine tuning the crosslinking of actin filaments at neuronal synapses where actinin interacts with several key proteins involved in synaptic plasticity (Wyszynski et al., 1997; Walikonis et al., 2001). In addition to synaptic functions in neurons actinin-1 and -4 are also expressed in glial cells (Cahoy et al., 2008) and upregulation of actinin-4 has been reported in glioblastoma and is proposed to promote cell migration and metastasis (Quick & Skalli, 2010; Sen et al., 2009). In the four glioblastoma cell lines examined, I found

a reversion of actinin-1 splicing to the exon 19a (Ca^{++}-sensitive) isoform observed in the immature brain. These cell lines also predominantly express the exon 8a and 19a (Ca^{++}-sensitive) –expressing actinin-4 isoforms. Neuroblastoma and cervical carcinoma HeLa cells also express the exon 19a (Ca^{++}-sensitive) actinin-4 isoform. Cancer cells are known to exhibit characteristics of immature cells. This is reflected by the fact that the actinin-1 exon 19a expressing variant observed in the immature brain was also dected in numerous cancer cell lines including glioblastoma, neuroblastoma and HeLa cells. Thus for both actinin-1 and -4 brain-specific splicing patterns are absent from glioblastoma cell lines and only Ca^{++}-sensitive actinin isoforms are expressed. This shift from Ca^{++}-insensitve to Ca^{++}-sensitive actinins may be of significance given the role intracellular calcium plays in the process of cancer cell migration and proliferation (Prevarskaya et al., 2011).

4.3 The non-muscle actinin heterodimer

The non-muscle actinins are generally regarded as distinct homodimeric entities. For example actinin-1 and -4 have been reported to have differential localisation patterns in cells (Honda et al., 1998; Bolshakova et al., 2007; Goffart et al., 2006; Araki et al., 2000). In addition these non-muscle isoforms have been reported to play differential and sometimes opposing roles in cellular processes such as cell migration, proliferation and adhesion (Celli et al., 2006; Quick & Skalli, 2010; Sen et al., 2009). Heterodimer formation is known to occur between the muscle actinins -2 and -3 both *in vitro* and *in vivo* (Chan et al., 1998). Heterodimer formation in platelets has also been reported and probably involves actinin-1 but the second actinin isoform involved was not identified (Gache et al., 1984; Landon et al., 1985). To date, the ability of the non-muscle actinins to form heterodimers has not been directly investigated. This work presents evidence that actinin-1 and -4 can form heterodimers with each other as well as with actinin-2. The observed conservation between the dimer interface of actinin-1 and -4 provided the first indication that heterodimer formation between these non-muscle actinin isoforms may occur. Yeast two-hybrid studies supported this theory while also suggesting that heterodimer formation may occur between the rod domains of non-muscle actinins (Ca^{++}-sensitive) and muscle actinin-2 (Ca^{++}-insensitive).

Using truncated actinins (ABD-R2/R3-CaM), this work shows that actinin-1 and -4 heterodimeric interactions appear to be equally as strong as those between homodimers *in vitro*. It has been suggested that the entire rod domain contributes to actinin dimerisation and that the ABD and CaM domain may not make a significant contibution to this process relative to the rod domain. I found that the inclusion of the ABD and CaM domains was neccessary for homo-/hetero-dimer formation as the R1-R2 and R3-R4 domains alone were insufficient for dimerisation. This is supported by observations that the CaM domain alone can interact strongly with the opposite subunit in the dimer independent of the spectrin-like repeats (Young & Gautel, 2000). It is noteworthy that the R1-R2 and R3-R4 domains of actinin were previously shown to interact in a yeast two-hybid assay (Young & Gautel, 2000). However, this study focused on the muscle isoform actinin-2. Due to sequence differences between muscle and non-muscle actinin isoforms one cannot assume that the R1-R2 and R3-R4 domains of these proteins behave in a similar manner. However, it is possible that the maltose-binding protein (MBP) tag attached to the R1-R2 domain may have interfered with dimerisation with R2-R3 and that the inclusion of the ABD domain prevented this interference. While the *in vitro* binding assays proved that the non-muscle actinins have the ability to form heterodimers, it was not clear whether this would occur in cells co-expressing full length actinins, since homodimer formation between proteins being translated from the same mRNA may be favoured. Additionally, since actinin-1 and -4 are separate gene products their transcripts may be under different control. Spatial and temporal differences in their gene expression may play a critical role in the final composition of actinin dimers. This was previously hypothesised for the muscle actinin isoforms (Gache et al., 1984). It was important therefore to examine the extent of heterodimer formation between endogenously expressed actinins in cells. The results presented here indicate that significant non-muscle heterodimer formation occurs in a number of cell lines examined. Most surprising was the observation that heterodimers appear to be more abundant than either homodimer species in many cell lines.

How can one reconcile these observations with the reported distinct localisations and functions of actinin-1 and -4 in some of these same cell lines (Quick & Skalli, 2010; Honda et al. 1998; Sen et al., 2009; Goffart et al., 2006; Araki et al., 2000; Celli et al., 2006) ?. Based on similarities in amino acid sequence and actin-binding properties it seems likely that actinin-1 and -4 homodimers as well

as heterodimers will share many functions in cells. Homodimers of either actinin-1 or -4 may then mediate the isoform-specific functions that have been reported. Heterodimers may have unique actin-binding properties particularly if Ca^{++}-sensitive (non-muscle) and -insensitive (muscle) monomers were involved. Also, since some actinin binding proteins may bind across the dimer interface of the rod domain, heterodimers may have unique interacting partners that don't bind to either homodimer (Chi et al., 2008). The degree of heterodimer formation varied between cell lines and heterodimers were not observed in HEK cells despite the fact that they express both actinin-1 and -4. Actinin expression in HEK cells is somewhat lower than the other cell lines but if the homodimer:heterodimer ratio was similar to other cells then heterodimers would still be detectable in HEK cells. This suggests that heterodimer formation may either require high cellular concentrations of actinins or may be regulated in a cell line specific manner. Notably HEK cells are a non-cancerous cell line. For this reason I extended my investigation of heterodimer formation to the non-tumourigenic breast cell line MCF-10A. Surprisingly relative to breast carcinoma MCF-7 cells and HEK cells, MCF-10A cells showed the highest levels of heterodimer formation. This correlated with the fact that MCF-10A cells expressed the highest levels of actinin-1 and -4, supporting the theory that heterodimer formation may be a consequence of high actinin levels present in cells. It is noteworthy that the MCF-10A cell line was initially derived from adherent cells in a population. HEK cells exhibit weak adherence. This suggests that high actinin levels and as a possible consequence heterodimer formation may be linked with cell adherence. While the MCF-10A cells are non-tumourigenic they are an immortalised cell line that do not exhibit signs of differentiation or senescence (Tait et al., 1990). Lack of differentiation and evasion of senescence are both hallmarks of cancer. Therefore these cells may not provide the best model of a non-cancerous state. For this reason one cannot rule out the possibility that heterodimer formation may be characteristic of the cancer phenotype. Over-expression of actinin-4 has been reported in many types of tumours and is associated with high grade malignancies and poor outcomes (Yamamoto et al., 2007; Barbolina et al., 2010; Honda et al., 2005; Kikuchi et al., 2008; Quick & Skalli, 2010). These actinin-4 knockdown experiments combined with Native-PAGE analysis indicates that when over-expressed, actinin-4 may be capable of forcing actinin-1 into the heterodimer state. This suggests that the cancer phenotype associated with actinin-4 over expression

may not only be a consequence of acquisition or enhancement of an actinin-4 specific function but may reflect the disruption of actinin-1 specific functions due to the sequestration of actinin-1 into heterodimers (see Figure 1.6). Alternatively these heterodimers may also have unique tumourigenic or metastasis promoting properties not possessed by homodimers. Thus the functional consequence of actinin-4 overexpression in a particular tumour may depend on the level of actinin-1 expression and the degree to which actinin-1 is sequestered into heterodimers.

While this current work focuses on cell lines, further evalutation of the role of heterodimers will require analysis of tissues. Of particular interest will be comparative analysis of heterodimer formation in healthy versus cancerous tissues. While Native-PAGE has faciliated the study of actinin homo-/hetero-dimers, it is important to mention that visualisation of actinin homo-/hetero-dimers can be obscured by the native nature of polyacrylamide gels. By definition native gels preserve a proteins natural confirmation and interactions. The migration pattern of a protein on a native polyacrylamide gel is affected by its endogenous interactions, thus the uniformity of migration and the clarity of visualisation that can be achieved by SDS-PAGE is not maintained by Native-PAGE. As a consequence many of my attempts to detect homo-/hetero-dimers by Native-PAGE resulted in smeared uninterpretable images. Efforts to optimise the native gel protocol included the addition of NaCl, NP40, sodium deoxycholate and SDS to cell lysis buffers. However, these measures either had no effect or disrupted homo-/hetero-dimer formation. The best images that I have obtained to date were obtained from freshly lysed cells that underwent Native-PAGE as described in Section 2.2.3. The complex architecture of tissue relative to cell lines compounds the challenge of homo-/hetero-dimer visualisation. For this reason this current work is restricted to cell lines.

Supporting the hypothesis of *in vivo* heterodimer formation are reports of heterodimer formation between muscle actinin isoforms purified from skeletal muscle (Chan et al., 1998). Previous studies of platelet actinin reported heterodimer formation between two Ca^{++}-sensitive actinin isoforms (Landon et al., 1985). I used specific antibodies that detected both actinin-1 and -4 in isolated human platelets. Together this suggests that the heterodimers detected by Landon *et al.* may represent those that formed between actinin-1 and -4. Landon *et al.* reported that one of these actinins represented a low Ca^{++}-sensitive isoform. The results presented here suggest that both non-muscle actinins exhibit similar Ca^{++} sensitivities. Landon *et al.*

performed Ca^{++} sensitivity assays using endogenous actinin isolated by fractionation of platelet lysates. However, I used recombinant bacterially expressed actinin isoforms. The discrepancy with regard to Ca^{++}-sensitivity of one of these isoforms may be due to the effects of protein modification absent from the recombinant isoforms used here, but present in those isolated from platelets. It could also be due to the fact that the low Ca^{++} sensitive isoform may represent a muscle actinin isoform. Using an actinin-2 specific antibody I detected actinin-2 in platelets. Altogether this supports the hypothesis that actinin heterodimers can form *in vivo* and raises the possibility that heterodimers can form between muscle and non-muscle actinin isoforms. The yeast two-hybrid studies carried out as part of this work support this hypothesis. In theory, at certain calcium concentrations heterodimers between non-muscle and muscle actinin isoforms would be able to bind but not cross-link actin filaments thereby providing a cell with another tool for fine-tuning the stability of actin and actinin-containing structures (see Figure 4.1B).

4.4 Actinin-interacting partners

The observation that the non-muscle actinins have similar affinities for actin filaments and similar calcium sensitivities indicates that differences in actin-binding properties are unlikely to explain the isoform-specific functions, such as those that have been attributed to actinin-4. One possible explanation for such functions could be that actinin-4 has unique interacting partners thereby allowing it to carry out functions unmatched by actinin-1. Here I used a yeast two-hybid (Y2H) approach in an effort to identify actinin-interacting partners. While Y2H screening is a well characterised method used for the identification of protein interactions, it can fail to detect protein interactions that are dependent certain cellular conditions not present in a yeast cell i.e. phosphorylation. Therefore I also used Tandem Affinity Purification (TAP) of transfected full length actinin-1 and -4 from Human Embryonic Kidney (HEK) cells in a further effort to identify non-muscle actinin interacting partners.

Actinin links to the MDM2-p53 pathway

The MDM2-p53 tumour suppressor pathway is highly implicated in cancer development. Around half of all cancers carry p53 mutations (Ryan et al., 2001). In this pathway MDM2 negatively regulates p53 function. Yeast two-hybrid screens previously identified the MDM2-binding protein MTBP that can induce cell cycle arrest independent of p53 status (Boyd et al., 2000). This cell cycle arrest could be blocked by MDM2. MTBP can also suppress cell migration and filopodia formation independent of p53 status (Agarwal et al., 2012). Together, this suggests the existence of an alternative growth control pathway that may be in part regulated by MDM2. The suppressive effects of MTBP on migration have been attributed, at least in part, to its ability to inhibit the actin-binding function of actinin-4. This highlights actinin-4 as a key player in mediating cancer progression independent of p53 status. Interestingly two actinin-interacting proteins identified by this work are linked directly to the MDM2-p53 tumour suppressor pathway namely, HIPK and CDKN2AIP which will be discussed in Section 4.4.1 and 4.4.2 respectively.

4.4.1 Yeast two-hybrid screens

Many reported yeast two-hybrid (Y2H) screens that describe actinin interactions result from the detection of actinin as a prey protein when using a different protein of interest as bait. Here the rod domain of actinin-1 was employed as a bait protein in the Y2H screen in an effort to identify differential interacting partners of the non-muscle actinins. The rod domain of actinin has been described as a docking platform for various protein interactions. This yeast two-hybid (Y2H) screen identified one known (Myozenin) and two novel Homeodomain-Interacting Protein Kinase 1 (HIPK) and Sex Comb on Midleg Homolog 1 (SCMHI) actinin-interacting partners.

Through Y2H screening of a skeletal muscle cDNA library, actinin-2 was previously found to interact with myozenin (Takada et al., 2001). Further investigations confirmed that both muscle isoforms (actinin-2 and -3) could interact with myozenin (Takada et al., 2001). This work provides the first report of myozenin interacting with the non-muscle actinin isoforms (1 and 4). Myozenin is regarded as a muscle-specific protein, however through rtPCR analysis it was found to be expressed at all developmental stages in the brain (data not shown). These findings

indicate that myozenin could interact with all three actinins that are expressed in the brain. It has been speculated that myozenin may modulate actinin dimerisation as the myozenin binding sites of actinin occur at regions involved in dimerisation (Takada et al., 2001), however this has not been confirmed. It is noteworthy to mention that the ability to bind both Ca^{++}-insensitive and -sensitive isoforms of actinin could allow a protein to regulate a more diverse range of functions. For instance at high calcium concentrations complexes of myozenin-actinin-actin would be more stable if the actinin isoform involved was muscle (Ca^{++}-insensitive) as opposed to non-muscle (Ca^{++}-sensitive). With that said the involvement of Ca^{++}-sensitive non-muscle actinin isoforms may allow for fine tuning of such interactions though calcium regulation. Through Y2H screening I also identified the Sex Comb on Midleg Homolog 1 (SCMHI) protein as an actinin-1 and -4 interacting partner. SCMHI is a polycomb protein originally identified in *Drosophila* (Berger et al., 1999). The *Drosophila* gene Sex Comb on Midleg shares motifs with a *Drosophila* tumour suppressor called lethal malignant brain tumour (Tomotsune et al., 1999). Recessive mutations of the lethal malignant brain tumour gene are associated with malignant transformation of the neuroblasts in the larval brain (Wismar et al., 1995). Murine studies suggest that SCMHI may play a role in regulation of homoeotic genes during embryogenesis (Tomotsune et al., 1999). The interaction of SCMHI and actinin supports the notion that actinin can associate with components involved in the regulation of gene transcription.

The Y2H screen employed here identified Homeodomain Interacting Protein Kinase 1 (HIPK) as an actinin-1 and -4 interacting partner. HIPKs are nuclear serine/threonine kinases. Studies indicate HIPKs, especially HIPK2 act as versatile switchboards that contribute to the regulation of remarkably diverse nuclear pathways involved in gene transcription, cell survival, proliferation, response to DNA damage, differentiation, and development (Rinaldo et al., 2008). HIPK1 expression has been identified in invasive breast cancer tissue but not in non-cancerous tissue (Park et al., 2012). HIPK1 is highly expressed in human breast cancer cell lines (Kondo et al., 2003). HIPK1 was previously found to interact with p53 though a Y2H screen employing p53 as bait (Kondo et al., 2003). HIPK2 is also known to interact with p53 (Rinaldo et al., 2008). *Hipk1* −/− mouse embryonic fibroblasts exhibit reduced transcription of *Mdm2* and are more susceptible than transformed *Hipk1* +/+ cells to apoptosis induced by DNA damage (Kondo et al.,

2003). Carcinogen-treated *Hipk1* −/− mice develop fewer and smaller skin tumours than *Hipk1* +/+ mice (Kondo et al., 2003). This suggests that HIPK1 may play a role in tumourigenesis, perhaps through regulation of p53 and/or Mdm2. Indeed in 2011, the NORE protein that is frequently silenced in primary adenocarcinoma was found to induce polyubiquitation and proteasomal degradation of HIPK1 by facilitating it's interaction with mdm2 E3 ligase (Lee et al., 2012).

4.4.2 Identification of putative actinin-4 interactions by TAPTAG Purification

The Tandem Affinity Purification (TAP) approach identified CDKN2AIP as a specific actinin-4 interacting partner. CDKN2AIP is known to directly interact with and enhance p53 function (Hasan et al., 2004; Hasan et al., 2008). CDKN2AIP acts as a transcriptional repressor of *HDM2* (human homolog of mouse *Mdm2*). It also interacts with HDM2 and undergoes degradation by a HDM2-dependent proteasome pathway. This supports the notion that non-muscle actinins can interact with proteins that directly associate with the MDM2-p53 tumour suppressor pathway. The notion that actinin can associate with nuclear components critical in regulating gene transcription, cell survival and proliferation is supported by the fact that actinin-4 is found in nuclear complexes and can directly interact with the transcription factor NFκB (Babakov et al., 2008; Khotin et al., 2009). Functional interactions of actinin-4 with several transcriptional regulators have been described (Chakraborty et al., 2006; Khurana et al., 2011; Goffart et al., 2006).

The TAP proteomics screen revealed a number of other putative actinin-4 specific interacting proteins that might be linked to the described functions of actinin-4 in cancer and as a nucleo-cytoplasmic shuttling protein (Table 3.4). This approach identified cytoskeletal components such as Myosin-10 and Filamin-C as well as two proteins – IQGAP2 and DOCK7, that have the potential to modulate actin dynamics through their regulation of Rho family GTPases. DOCK7 has been shown to act as a guanine nucleotide exchange factor for Rac1 and Rac3 (Watabe-Uchida et al., 2006), while IQGAP2 can regulate Rac1 and Cdc42, though not by acting as a classical GTPase activating protein (Brill et al., 1996). These cytoskeletal proteins/regulators could potentially mediate some of the effects on cell migration and metastasis that have been ascribed to actinin-4 in the context of cancer.

Apart from these cytoskeletal proteins most of the remaining proteins identified in TAP-tagged actinin-4 complexes are nuclear proteins including CDKN2AIP as previously discussed. This supports the idea that actinin-4 can shuttle in and out of the nucleus (Kumeta et al., 2010). The remaining nuclear proteins identified are involved in either transcription or RNA binding/splicing. Functional interactions of actinin-4 with several transcriptional regulators have been described (Chakraborty et al., 2006; Khurana et al., 2011; Babakov et al., 2008; Goffart et al., 2006) and the proteins identified here may expand this list. No clear role for actinin-4 in RNA splicing has ever been described but two previous studies have identified components of the splicing machinery (heterogeneous nuclear ribonucleoproteins) in actinin-4 immunoprecipitates (Hara et al., 2007), (Khotin et al., 2010).

Interacting partners may support actinin-4 nuclear localisation

The surprising ability of actinin-4 to translocate to the nucleus and regulate transcription is now well established (Honda et al., 1998; Chakraborty et al., 2006; Kumeta et al., 2010; Babakov et al. 2008; Bolshakova et al. 2007; Goffart et al., 2006) . No such role has been reported for actinin-1. Indeed actinin-1 maintains its cytoplasmic localisation under conditions for which nuclear translocation of actinin-4 has been observed (Honda et al., 1998; Bolshakova et al., 2007; Goffart et al., 2006). Nuclear translocation of actinin-4 is importin-independent and is mediated by the spectrin-like repeats of the rod domain (Kumeta et al., 2010). It may be that due to sequence differences in the rod domain actinin-1 lacks the ability to enter the nucleus and therefore cannot interact with nuclear proteins. Alternatively, both actinins may be able to shuttle in and out of the nucleus but that actinin-4 specific interactions with transcriptional regulators or other nuclear proteins retain actinin-4 in the nucleus and allow it to play a role in transcriptional regulation. In agreement with this the nuclear export signals that have been identified in actinin-4 (Kumeta et al., 2010) are conserved in actinin-1 (unpublished observations). The identification of actinin-4 specific interactions with nuclear proteins would lend further support to this idea.

4.5 Summary

While many actinin-interacting partners are likely to be common to multiple actinin isoforms, others may be isoform-specific. However, in many actinin studies the issue of isoform-specificity of actinin ligands has not been tested. In some studies that did address the issue of isoform specificity, the actinin antibodies employed appear to have been incorrectly characterised. This work identified isoform-specific actinin antibodies that facilitated a comprehension comparative study of the non-muscle actinins. Actinins are primarily known for their actin-binding function. The non-muscle actinins are reported to exert distinct effects from each other. The possibility that these distinct effects may be related to differential actin-binding properties had not been previously addressed. This work finds that while the non-muscle actinins have similar actin-binding properties, alternative splice variants of these isoforms are differentially expressed. In particular, expression of the actinin-4 exon 8b variant is restricted to neuronal tissues. While both exon 19a and exon 19b expressing variants of actinin-1 are present in muscle tissues, the actinin-4 exon 19a (Ca^{++}-sensitive) variant is the only variant of actinin-4 observed. This suggests a possible non-redundant role for this variant in muscle. Alterative splicing has been reported as an evolutionary mechanism though which proteins can diverge. Indeed it is hypothesised that the restricted expression of the muscle isoform actinin-3 compared to that of actinin-2 is thought to be an evolutionary mechanism of divergence. This suggests that the differential expression of actinin-4 splice variants may be a means of diverging from actinin-1. Actinins, in particular actinin-4 have been implicated in cancer progression. These splicing studies show that there is a shift in expression from Ca^{++}-insensitive to Ca^{++}-sensitive variants of both actinin-1 and -4. This may provide an insight into altered splicing mechanisms observed in cancer. Overall this work shows that a variety of actinin splice variants are expressed simultaneously in numerous tissues, in particular, the brain. Adding to this complexity is the observation that heterodimers have the potential to form between non-muscle, muscle and non-muscle/muscle actinin isoforms. The fact that non-muscle heterodimers are more abundant than homodimers in many cancer cells raises the questions of heterodimer function and regulation.

The observation of numerous actinin splice variants and heterodimer formation provides a potential mechanism for divergence of non-muscle actinin functions and interactions. Individually it appears that the non-muscle actinins are diverging from each other though differential expression of their splice variants. Together it appears the non-muscle actinins are potentially increasing their interaction networks though heterodimerising with each other. Indeed this work has identified a number of putative isoform-specific interacting partners of actinin-1 and -4. The non-muscle actinin heterodimer could potentially interact with isoform-specific proteins and potentially novel interacting partners, not common to either actinin-1 or -4 alone. Figure 4.1A presents a model that highlights the potential implications of heterodimer formation on the non-muscle actinin protein interaction network. The ability to interact with different proteins or with the same proteins with different affinities has been suggested as a means though which the muscle actinin isoforms are diverging form each other (Lek et al., 2010b). This work suggests that the non-muscle actinins may be following a similar evolutionary path. This work identifies a number of actinin-4 specific interacting partners that may help to explain the unique functions of actinin-4. This work also highlights actinin-4 splice variants with restricted expression. This suggests that actinin-4 may be evolving specialised functions. This idea is reflected by the muscle isoform actinin-3. Together this suggests that the non-muscle/muscle actinin isoforms may be following a neo-functional evolutionary path where one isoform (actinin-1/actinin-2) retains the ancestral properties while the other (actinin-4/actinin-3) is free to evolve. However further studies are required to define the specialised functions of actinin-4 (and actinin-3) if this hypothesis is to be proved. This work indicates the potential for heterodimers to form between non-muscle and non-muscle/muscle actinin isoforms. The formation of heterodimers between actinin monomers with different Ca^{++} sensitivities could result in a heterodimer with novel actin-binding properties. Fig 4.1B highlights the potential novel properties of actinin heterodimers between variants that exhibit different Ca^{++}-sensitivities.

Regardless of how the actinins have emerged they can no longer be viewed as distinct entities from each other but rather as proteins with numerous splice variants that have the potential to form heterodimers with potential novel protein characteristics. This work provides evidence for such a model and represents a shift from how the non-muscle actinins are currently viewed.

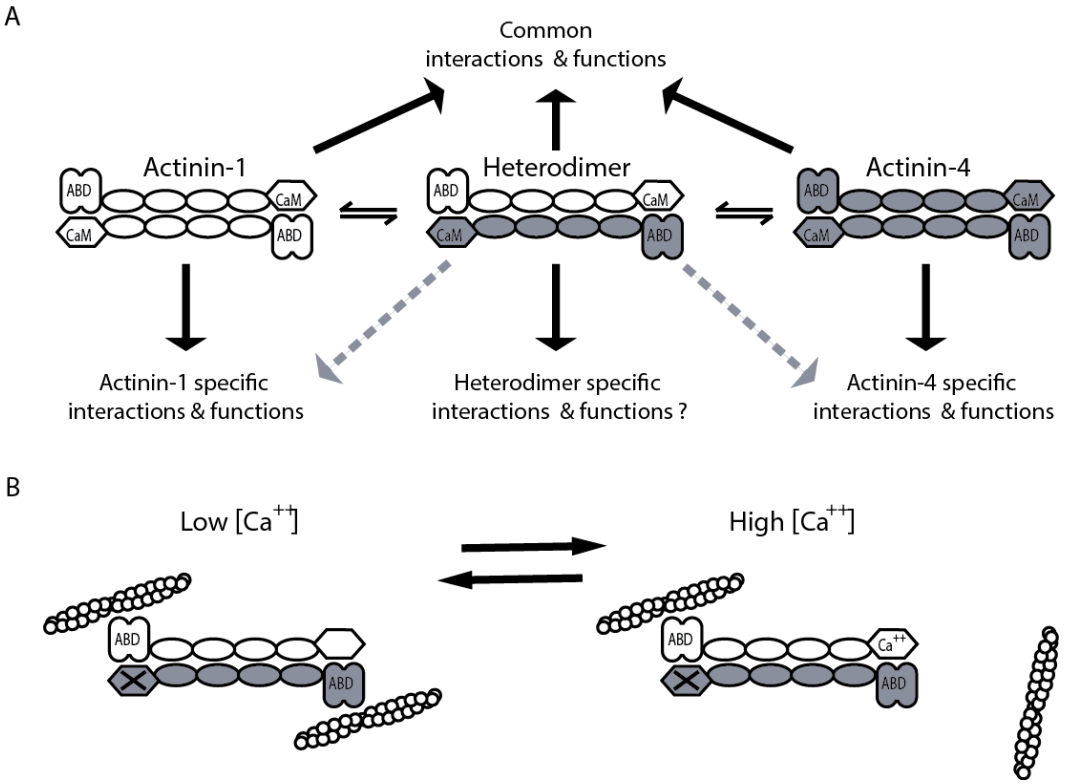

Fig 4.1 (A) A model of how actinin-1 and -4-specific functions may arise from isoform-specific interactions with other proteins. The majority of interacting proteins are likely to be shared by both non-muscle actinins and would mediate common actinin functions. These proteins would be expected to also bind actinin-1/4 heterodimers. Actinin-1 or -4-specific interactions would mediate isoform-specific functions. Such proteins might also interact with heterodimers (dashed arrows) but some could be homodimer-specific. On the other hand there could be heterodimer-specific interactions or functions. In this scenario increased expression of one isoform, actinin-4 for example, would not only enhance actinin- 4-specific functions but could sequester actinin-1 into heterodimers and thus inhibit actinin-1 functions and potentially increase heterodimer-specific functions. (**B**) **Potential novel properties of actinin heterodimers**. Tissues such as the brain and muscle, co-express Ca^{++}-sensitive (white) and Ca^{++}-insensitive (grey) actinin isoforms. The formation of heterodimers between these would be predicted to generate an actinin dimer with one Ca^{++}- sensitive and one Ca^{++}-insensitive ABD. These heterodimers would cross-link actin filaments at low but not at high calcium concentrations. They would however be predicted to remain bound to actin filaments at one end rather than dissociating away from the cytoskeleton. This would have implications for Ca^{++}-dependent remodelling of actin networks containing these heterodimers. Actin-bundling by such heterodimers would be Ca^{++}-sensitive but actin-binding would not be Ca^{++}-sensitive.

5 Conclusion

.

The non-muscle actinins are predominantly known for their ability to bind and cross-link actin in a Ca^{++}-sensitive manner. While this work did not show statistically significant differences between the actin-binding affinities or Ca^{++}-sensitivities of the non-muscle actinins it cannot be ruled out that the small differences observed could have functional implications on the effects of these proteins. It is noteworthy that some of the distinct effects of the muscle actinins are suggested to be due to these isoforms having distinct affinities for the same protein (Lek et al., 2010b). Indeed the need for more sensitive binding assays has been highlighted in the case of the muscle actinin isoforms (Lek et al., 2010b). While the actin-binding properties of the non-muscle actinins are similar, the slight differences observed may act to fine tune the affinity of actinin for F-actin in particular contexts. However the observed differences would not alter actin cross-linking properties very dramatically and are therefore unlikely to explain the reported isoform-specific functions of the non-muscle actinins. It is important to note that comparative studies of actin-binding affinity tend to be effected by temperature with larger differences being observed at lower temperatures (Landon et al., 1985). However the biological relevance of interactions observed at low temperatures is questionable.

This work suggests that isoform-specific functions may be attributed to the ability of actinin-1 and -4 to differentially interact with other proteins. Indeed divergence in protein interaction networks has been described as a mechanism through which the muscle actinin isoforms may have diverged (Lek et al., 2010b). Many studies that have identified actinin interacting-partners have focused solely on one actinin isoform. The interaction studies described here compare both actinin-1 and -4 and identify a number of putative actinin-4-specific interactions that might be linked to the reported unique functions of actinin-4 in cancer and as a nucleo-cytoplasmic shuttling protein. They also identified a number of interacting partners common to actinin-1 and -4, the binding affinity of which may warrent further investigation based on the aforementioned reports of muscle actinin interactions.

Alternative splicing and tissue-specific expression are other examples of how the muscle actinins have diverged from each other (Lek et al., 2010b). This work describes the tissue-specific alternative splicing of actinin-4 for the first time and shows that expression of the exon 8b and exon 19b variants occurs primarily in the nervous system. This work identifies the exon 19a (Ca^{++}-sensitive) -expressing variant as the only actinin-4 variant present in skeletal and smooth muscle samples

suggesting that this variant may have novel functions in muscle. This work also shows that there is a switch from Ca^{++}-insensitive to Ca^{++}-sensitive variants of actinin-1 and -4 in glioblastoma and neuroblastoma cells compared to healthy brain, highlighting a possible alternative splicing mechanism in cancer cells. This work shows that Ca^{++}-sensitive and -insensitive isoforms of both actinin-1 and actinin-4 are co-expressed in the brain. Studies of the brain NMDA receptor support the notion that both Ca^{++}-insensitive and -sensitive actinin isoforms are required for receptor function (Wyszynski et al., 1998; Krupp et al., 1999). This work provides evidence for non-muscle heterodimer formation *in vivo*.

Given the observed propensity of the actinins to form heterodimers, this presents a complicated picture in which actinin dimers may be composed of several different combinations of monomers particularly in the nervous system where I identified Ca^{++}-sensitive and -insensitive isoforms of both actinin-1 and actinin-4 and where the Ca^{++}-insensitive actinin-2 isoform is also expressed . Overall these findings indicate that actinin-1 and actinin-4 don't exist solely as distinct homodimeric entities but that they can readily form heterodimers composed of monomers that may have different properties and interacting partners. This significantly alters the context in which one views the isoform-specific functions of the non-muscle actinins.

6 Bibliography

Abramoff, M. D., Magalhães, P. J., & Ram, S. J. (2004). Image Processing with ImageJ. *Biophotonics International*, **11**(7), 36–42.

Agarwal, N., Adhikari, A. S., Iyer, S. V, Hekmatdoost, K., Welch, D. R., & Iwakuma, T. (2012). MTBP suppresses cell migration and filopodia formation by inhibiting ACTN4. *Oncogene*, (**February**), 1–9.

Araki, N., Hatae, T., Yamada, T., & Hirohashi, S. (2000). Actinin-4 is preferentially involved in circular ruffling and macropinocytosis in mouse macrophages: analysis by fluorescence ratio imaging. *Journal of Cell Science*, **113**, 3329–3340.

Ashkenazy, H., Erez, E., Martz, E., Pupko, T., & Ben-Tal, N. (2010). ConSurf 2010: calculating evolutionary conservation in sequence and structure of proteins and nucleic acids. *Nucleic acids research*, **38**(Web Server issue), 529–533.

Babakov, V. N., Petukhova, O. A., Turoverova, L. V., Kropacheva, I. V., Tentler, D. G., Bolshakova, A. V., Podolskaya, E. P., Magunussen, K.E., & Pinaer, G.P. (2008). RelA/NF-kappaB transcription factor associates with alpha-actinin-4. *Experimental Cell Research*, **314**(5), 1030–1038.

Babu, Y. S., Bugg, C. E., & Cook, W. J. (1988). Structure of calmodulin refined at 2.2 Å resolution. *Journal of Molecular Biology*, **204**(1), 191–204.

Bang, M. L., Mudry, R. E., McElhinny, A. S., Trombitás, K., Geach, A. J., Yamasaki, R., Sorimachi, H., Granzier, H., Gregoric, C. C. & Labeit, S. (2001). Myopalladin, a novel 145-kilodalton sarcomeric protein with multiple roles in Z-disc and I-band protein assemblies. *The Journal of Cell Biology*, **153**(2), 413–427.

Barbolina, M. V., Adley, B. P., Kelly, D. L., Fought, A. J., Scholters, P., Shea, L. D., & Stack, M. S. (2008). Motility-related actinin alpha-4 is associated with advanced and metastatic ovarian carcinoma. Lab Investigations, **88**(6), 602–614.

Bauer, K., Kratzer, M., Otte, M., Luber de Quintana, K., Hagmann, J., Arnold, G. J., Eckerskorn, C., Lottspeich, F. & Siess, W. (2000). Human CLP36 , a PDZ-domain and LIM-domain protein , binds to α-actinin-1 and associates with actin filaments and stress fibers in activated platelets and endothelial cells. *Blood*, **96**(13), 4236–4245.

Bañuelos, S., Saraste, M., & Djinović Carugo, K. (1998). Structural comparisons of calponin homology domains: implications for actin binding. *Structure*, **6**(11), 1419–1431.

Beck, M. R., Otey, C. A., & Campbell, S. L. (2011). Structural characterisation of the interactions between palladin and α-actinin. *Journal of Molecular Biology*, **413**(3), 712–725.

Bennett, J. P., Zaner, K. S., & Stossel, T. P. (1984). Isolation and some properties of macrophage α -actinin: evidence that it is not an actin gelling protein. *Biochemistry*, **23**(21), 5081–5086.

Berger, J., Kurahashi, H., Takihara, Y., Shimada, K., Brock, H. W., & Randazzo, F. (1999). The human homolog of Sex comb on midleg (SCMH1) maps to chromosome 1p34. *Gene*, **237**(1), 185–191.

Berman, Y., & North, K. N. (2010). A gene for speed: the emerging role of α -actinin-3 in muscle metabolism. *Physiology*, **25**, 250–259.

Bhatt, A., Kaverina, I., Otey, C., & Huttenlocher, A. (2002). Regulation of focal complex composition and disassembly by the calcium-dependent protease calpain. *Journal of Cell Science*, **115**(17), 3415–25.

Bolshakova, A., Petukhova, O., Turoverova, L., Tentler, D., Babakov, V., Magnusson, K. E., & Pinaev, G. (2007). Extra-cellular matrix proteins induce re-distribution of α-actinin-1 and α-actinin-4 in A431 cells. *Cell Biology International*, **31**, 360–365.

Boyd, M. T., Vlatkovic, N., & Haines, D. S. (2000). A novel cellular protein (MTBP) binds to MDM2 and induces a G_1 arrest that is suppressed by MDM2. *The Journal of Biological Chemistry*, **275**;41(13), 31883–31890.

Brill, S., Li, S., Lyman, C. W., Church, D. M., Wasmuth, J. J., Weissbach, L., Bernards, A. & Snijders, A., J. (1996). The Ras GTPase-activating-protein-related human protein IQGAP2 harbors a potential actin binding domain and interacts with calmodulin and Rho family GTPases. *Molecular and Cellular Biology*, **16**(9), 4869–4878.

Burridge, K., & Fermisco, J., R. (1981). Non-muscle α-actinins are calcium-sensitive actin-binding proteins. *Nature*, **294**, 565–567.

Cabello, N., Remelli, R., Canela, L., Soriguera, A., Mallol, J., Canela, E. I., Robbins, M. J., Lluis, C., Franco, R., McIlhinney, R. A. J. & Ciruela, F. (2007). Actin-binding protein alpha-actinin-1 interacts with the metabotropic glutamate receptor type 5b and modulates the cell surface expression and function of the receptor. *The Journal of Biological Chemistry*, **282**(16), 12143–12153.

Cahoy, J. D., Emery, B., Kaushal, A., Foo, L. C., Zamanian, J. L., Christopherson, K. S., Xing, Y., Lubischer, J. L., Kreig, P. A., Krupenko, S. A., Thompson, W. J. & Barres, B. A. (2008). A transcriptome database for astrocytes, neurons, and oligodendrocytes: a new resource for understanding brain development and function. *The Journal of Neuroscience*, **28**(1), 264–278.

Carpén, O., Pallai, P., Staunton, D. E., & Springer, T. A. (1992). Association of intercellular adhesion molecule-1 (ICAM-1) with actin-containing cytoskeleton and α -actinin. *The Journal of Cell Biology*, **118**(5), 1223–1234.

Celli, L., Ryckewaert, J.-J., Delachanal, E., & Duperray, A. (2006). Evidence of a functional role for interaction between ICAM-1 and nonmuscle alpha-actinins in leukocyte diapedesis. *Journal of Immunology*, **177**, 4113–4121.

Chakraborty, S., Reineke, E. L., Lam, M., Li, X., Liu, Y., Gao, C., Khurana, S. & Kao, H.-Y. (2006). α -actinin 4 potentiates myocyte enhancer factor-2 transcription activity by antagonizing histone deacetylase 7. *The Journal of Biological Chemistry*, **281**(46), 35070–35080.

Chan, Y., Tong, H. Q., Beggs, A. H., & Kunkel, L. M. (1998). Human skeletal muscle-specific α -actinin-2 and -3 isoforms form homodimers and heterodimers *in vitro* and *in vivo*. *Biochemical and Biophysical Research Communications*, **248**(1), 134–139.

Chi, R. J., Simon, A. R., Bienkiewicz, E. A., Felix, A., & Keller, T. C. S. (2008). Smooth muscle titin Zq domain interaction with the smooth muscle α -actinin central rod. *The Journal of Biological Chemistry*, **283**(30), 20959–20967.

Chiu, C., Bagnall, R. D., Ingles, J., Yeates, L., Kennerson, M., Donald, J. A., Jormakka, M., Lind, J. M. & Semarian, C. (2010). Mutations in alpha-actinin-2 cause hypertrophic cardiomyopathy: a genome-wide analysis. *Journal of the American College of Cardiology*, **55**(11), 1127–1135.

Choi, C. K., Vicente-Manzanares, M., Zareno, J., Whitmore, L. A., Mogilner, A. & Horwitz, A. R. (2008) Actin and α-actinin orchestrate the assembly and maturation of nascent adhesions in a myosin II motor-independent manner. *Nature Cell Biology*, **10**(9), 1039-1050.

Craig, D. H., Haimovich, B., & Basson, M. D. (2007). α -actinin-1 phosphorylation modulates pressure-induced colon cancer cell adhesion through regulation of focal adhesion kinase-Src interaction. *American Journal of Physiology. Cell Physiology,* **293**, 1862–1874.

Crawford, A. W., Michelsen, J. W., & Beckerle, M. C. (1992). An interaction between zyxin and alpha-actinin. *The Journal of Cell Biology*, **116**(6), 1381–1393.

Cuevas, B. D., Abell, A. N., Witowsky, J. A., Yujiri, T., Johnson, N. L., Kesavan, K., Ware, M., Jones, P. L., Weed, S. A., DeBiasi, R. L., Yashitomo, O., Tyler, K. L. & Johnson, G. L. (2003). MEKK1 regulates calpain-dependent proteolysis of focal adhesion proteins for rear-end detachment of migrating fibroblasts. *The EMBO journal*, **22**(13), 3346–3355.

Cybulsky, A. V., & Kennedy, C. R. J. (2011). Podocyte injury associated with mutant α-actinin-4. *Journal of Signal Transduction*, 1–11.

Delmonico, M. J., Zmuda, J. M., Taylor, B. C., Cauley, J. A., Harris, T. B., Manini, T. M., Schwartz, A., Li, R., Roth, S. M., Hurley, B. F., Bava, D. C., Ferrell, R. E. & Newman, A. B. (2008). Association of the ACTN3 Genotype and Physical Functioning With Age in Older Adults. *The Journal of Gerontology. Series A, Biological Science and Medical Science*, **63**(11), 1227–1234.

Des Marais, D. L., & Rausher, M. D. (2008). Escape from adaptive conflict after duplication in an anthocyanin pathway gene. *Nature*, **454**, 762–765.

Dixson, J. D., Forstner, M. R. J., & Garcia, D. M. (2003). The alpha-actinin gene family: a revised classification. *Journal of Molecular Evolution*, **56**(1), 1–10.

Djinovic-Carugo, K., Gautel, M., Ylänne, J., & Young, P. (2002). The spectrin repeat: a structural platform for cytoskeletal protein assemblies. *FEBS letters*, **513**, 119–123.

Djinović-Carugo, K., Young, P., Gautel, M., & Saraste, M. (1999). Structure of the alpha-actinin rod: molecular basis for cross-linking of actin filaments. *Cell*, **98**, 537–546.

Dourdin, N., Bhatt, A. K., Dutt, P., Greer, P. A., Arthur, J. S. C., Elce, J. S., & Huttenlocher, A. (2001). Reduced cell migration and disruption of the actin cytoskeleton in calpain-deficient embryonic fibroblasts. *The Journal of Biological Chemistry*, **276**(51), 48382–48388.

Drees, B. E., Andrews, K. M., & Beckerle, M. C. (1999). Molecular dissection of zyxin function reveals its involvement in cell motility. *The Journal of Cell Biology*, **147**(7), 1549–1559.

Dubreuil, R. R. (1991). Structure and evolution of the actin crosslinking proteins. *BioEssays*, **13**(5), 219–226.

Duhaiman, A. S., & Bamburg, J. R. (1984). Isolation of brain α -actinin. Its characterization and a comparison of its properties with those of muscle α -actinins. *Biochemistry*, **23**(8), 1600–1608.

Durand, D. (2003). Vertebrate evolution: doubling and shuffling with a full deck. *TRENDS in Genetics*, **19**(1), 2–5.

Dwir, O., Kansas, G. S., & Alon, R. (2001). Cytoplasmic anchorage of L-selectin controls leukocyte capture and rolling by increasing the mechanical stability of the selectin tether. *The Journal of Cell Biology*, **155**(1), 145–156.

Faulkner, G., Pallavicini, A., Comelli, A., Salamon, M., Bortoletto, G., Ievolella, C., Trevisan, S. et al. (2000). FATZ, a filamin-, actinin-, and telethonin-binding protein of the Z-disc of skeletal muscle. *The Journal of Biological Chemistry*, **275**(52), 41234–41242.

Force, A., Lynch, M., Pickett, F. B., Amores, A., Yan, Y. L., & Postlethwait, J. (1999). Preservation of duplicate genes by complementary, degenerative mutations. *Genetics*, **151**, 1531–1545.

Foster, P. G., & Hickey, D. A. (1999). Compositional bias may affect both DNA-based and protein-based phylogenetic reconstructions. *Journal of Molecular Evolution*, **48**, 284–290.

Fraley, S. I., Feng, Y., Krishnamurthy, R., Kim, D.-H., Celedon, A., Longmore, G. D. & Wirtz, D. (2010) A distinctive role for focal adhesion proteins in three dimensional cell motility. Nature Cell Biology, **12**(6), 598-604.

Franzot, G., Sjöblom, B., Gautel, M., & Djinović Carugo, K. (2005). The crystal structure of the actin binding domain from α -actinin in its closed conformation: structural insight into phospholipid regulation of α -actinin. *Journal of Molecular Biology*, **348**, 151–165.

Frey, N., Richardson, J. A., & Olson, E. N. (2000). Calsarcins, a novel family of sarcomeric calcineurin-binding proteins. *Proceedings of the National Academy of Sciences of the United States of America*, **97**(26), 14632–14637.

Fukami, K., Endo, T., Imamura, M., & Takenawa, T. (1994). α -Actinin and vinculin are PIP2-binding proteins involved in signaling by tyrosine kinase. *The Journal of Biological Chemistry*, **269**(2), 1518–22.

Fukami, K., Furuhashi, K., Inagaki, M., Endo, T., Hatano, S., & Takenawa, T. (1992). Requirement of phosphatidylinositol 4,5-bisphosphate for α-actinin function. *Nature*, **359**, 150–152.

Fyrberg, C., Ketchum, A., Ball, E., & Fyrberg, E. (1998). Characterization of lethal Drosophila melanogaster alpha-actinin mutants. *Biochemical Genetics*, **36**(9-10), 299–310.

Gache, Y., Landon, F., & Olomucki, A. (1984). Polymorphism of α-actinin from human blood platelets. Homodimeric and heterodimeric forms. *European Journal of Biochemistry*, **141**, 57–61.

Giannone, G., Rondé, P., Gaire, M., Beaudouin, J., Haiech, J., Ellenberg, J., & Takeda, K. (2004). Calcium rises locally trigger focal adhesion disassembly and enhance residency of focal adhesion kinase at focal adhesions. *The Journal of Biological Chemistry*, **279**(27), 28715–28723.

Gimona, M., Djinovic-Carugo, K., Kranewitter, W. J., & Winder, S. J. (2002). Functional plasticity of CH domains. *FEBS letters*, **513**, 98–106.

Glück, U., & Ben-Ze'ev, A. (1994). Modulation of alpha-actinin levels affects cell motility and confers tumorigenicity on 3T3 cells. *Journal of Cell Science*, **107**, 1773–1782.

Glück, U., Kwiatkowski, D. J., & Ben-Ze'ev, A. (1993). Suppression of tumorigenicity in simian virus 40-transformed 3T3 cells transfected with α -actinin cDNA. *Proceedings of the National Academy of Sciences of the United States of America*, **90**, 383–387.

Goffart, S., Franko, A., Clemen, C. S., & Wiesner, R. J. (2006). Alpha-actinin 4 and BAT1 interaction with the *cytochrome c* promoter upon skeletal muscle differentiation. *Current Genetics*, **49**, 125–135.

Goicoechea, S. M., Bednarski, B., García-Mata, R., Prentice-Dunn, H., Kim, H. J., & Otey, C. A. (2009). Palladin contributes to invasive motility in human breast cancer cells. *Oncogene*, **28**(4), 587–598.

Gonzalez, A. M., Otey, C., Edlund, M., & Jones, J. C. R. (2001). Interactions of a hemidesmosome component and actinin family members. *Journal of Cell Science*, **114**, 4197–4206.

Grabarek, Z. (2006). Structural basis for diversity of the EF-hand calcium-binding proteins. *Journal of Molecular Biology*, **359**, 509–525.

Greenwood, J. A., Theibert, A. B., Prestwich, G. D., & Murphy-Ullrich, J. E. (2000). Restructuring of focal adhesion plaques by PI 3-kinase. Regulation by PtdIns (3,4,5)-P_3 binding to α -actinin. *The Journal of Cell Biology*, **150**(3), 627–642.

Gromak, N., Matlin, A. J., Cooper, T. A., & Smith, C. W. J. (2003). Antagonistic regulation of α -actinin alternative splicing by CELF proteins and polypyrimidine tract binding protein. RNA, **9**, 443–456.

Gupta, V., Discenza, M., Guyon, J. R., Kunkel, L. M., & Beggs, A. H. (2012). α-Actinin-2 deficiency results in sarcomeric defects in zebrafish that cannot be rescued by α-actinin-3 revealing functional differences between sarcomeric isoforms. *FASEB*, **26***(5)*, 1892–1908.

Guvakova, M. A., Adams, J. C., & Boettiger, D. (2002). Functional role of α -actinin, PI 3-kinase and MEK1/2 in insulin-like growth factor I receptor kinase regulated motility of human breast carcinoma cells. *Journal of Cell Science*, **115**(21), 4149–4165.

Hara, T., Honda, K., Shitashige, M., Ono, M., Matsuyama, H., Naito, K., Hirohashi, S. & Yamada, T. (2007). Mass spectrometry analysis of the native protein complex containing actinin-4 in prostate cancer cells. *Molecular & Cellular Proteomics*, **6**(3), 479–491.

Hasan, M. K., Yaguchi, T., Harada, J. I., Hirano, T., Wadhwa, R., & Kaul, S. C. (2008). CARF (collaborator of ARF) interacts with HDM2: evidence for a novel regulatory feedback regulation of CARF-p53-HDM2-p21WAF1 pathway. *International Journal of Oncology*, **32**, 663–671.

Hasan, M. K., Yaguchi, T., Minoda, Y., Hirano, T., Taira, K., Wadhwa, R., & Kaul, S. C. (2004). Alternative reading frame protein (ARF)-independent function of CARF (collaborator of ARF) involves its interactions with p53: evidence for a novel p53-activation pathway and its negative feedback control. *The Biochemical Journal*, **380**, 605–610.

Heiska, L., Kantor, C., Parr, T., Critchley, D. R., Vilja, P., Gahmberg, C. G., & Carpén, O. (1996). Binding of the cytoplasmic domain of intercellular adhesion molecule-2 (ICAM-2) to alpha-actinin. *The Journal of Biological Chemistry*, **271**(42), 26214–26219.

Henderson, J. M., Alexander, M. P., & Pollak, M. R. (2009). Patients with ACTN4 mutations demonstrate distinctive features of glomerular injury. *Journal of the American Society of Nephrology,* **20**, 961–968.

Honda, K, Yamada, T., Endo, R., Ino, Y., Gotoh, M., Tsuda, H., Yamada, Y., Chiba, H. & Hirohashi, S. (1998). Actinin-4, a novel actin-bundling protein associated with cell motility and cancer invasion. *The Journal of Cell Biology*, **140**(6), 1383–1393.

Honda, K., Yamada, T., Hayashida, Y., Idogawa, M., Sato, S., Hasegawa, F., Ino, Y., Ono, M. & Hirohashi, S.(2005). Actinin-4 increases cell motility and promotes lymph node metastasis of colorectal cancer. *Gastroenterology*, **128**, 51–62.

Honda, K., Yamada, T., Seike, M., Hayashida, Y., Idogawa, M., Kondo, T., Ino, Y., & Hirohashi, S.(2004). Alternative splice variant of actinin-4 in small cell lung cancer. *Oncogene*, **23**, 5257–5262.

Hughes, A. L. (1999). Phylogenies of developmentally important proteins do not support the hypothesis of two rounds of genome duplication early in vertebrate history. *Journal of Molecular Evolution*, **48**, 565–576.

Hüttelmaier, S., Illenberger, S., Grosheva, I., Rüdiger, M., Singer, R. H., & Jockusch, B. M. (2001). Raver1, a dual compartment protein, is a ligand for PTB/hnRNPI and microfilament attachment proteins. *The Journal of Cell Biology*, **155**(5), 775–785.

Imamuras, M., & Masakis, T. (1992). A novel nonmuscle alpha-actinin: Purification and characterization of chicken lung alpha-actinin. *The Journal of Biological Chemistry*, **267**(36), 25927–25933.

Imamuras, M., Sakurai, T., Ogawa, Y., Ishikawa, T., Goto, K., & Masaki, T. (1994). Molecular cloning of low-Ca2 + -sensitive-type non-muscle α-actinin. *European Journal of Biochemistry,* **223**, 395–401.

Ispolatov, I., Yuryev, A., Mazo, I., & Maslov, S. (2005). Binding properties and evolution of homodimers in protein–protein interaction networks. *Nucleic Acids Research*, **33**(11), 3629–3635.

Izaguirre, G., Aguirre, L., Hu, Y. P., Lee, H. Y., Schlaepfer, D. D., Aneskievich, B. J., & Haimovich, B. (2001). The cytoskeletal/non-muscle isoform of α -actinin is phosphorylated on its actin-binding domain by the focal adhesion kinase. *The Journal of Biological Chemistry*, **276**(31), 28676–28685.

Jayadev, R., Kuk, C. Y., Low, S. H., & Murata-Hori, M. (2012). Calcium sensitivity of α-actinin is required for equatorial actin assembly during cytokinesis. *Cell Cycle*, **11**(10), 1929 – 1937.

Jiang, W. G. (1995). Membrane ruffling of cancer cells: a parameter of tumour cell motility and invasion. *European Journal of Surgical Oncology*, **21**, 307–309.

Jin, L. (2011). The actin associated protein palladin in smooth muscle and in the development of diseases of the cardiovasculature and in cancer. *Journal of Muscle Research and Cell Motility*, **32**(1), 7–17.

Kaplan, J.M., Kim, S.H., North, K. N., Rennke, H., Correia, A., Tong, H.-Q., Mathis, B. J., Rodríguez-Peréz, J.-C., Allen, P.G., Beggs, A. H. & Pollak, M.R. (2000) Mutations in ACTN4, encoding α-actinin-4, cause familial focal segmental glomerulosclerosis. *Nature Genetics,* **24**, 251-250.

Kasahara, M. (2007). The 2R hypothesis: an update. *Current Opinion in Immunology*, ***19***, 547–552.

Khotin, M. G., Turoverova, L. V., Podolskaya, E. P., Krasnov, I. A., Solovyeva, A. V., Aksenova, V. Y., Magnusson, K.-E., Pineau, G. P. & Tentler, D. G. (2009). Analysis of nuclear protein complexes comprising α-actinin-4 by 2D-electrophoresis and mass spectrometry. *Cell and Tissue Biology*, **3**(5), 431–437.

Khotin, M., Turoverova, L., Aksenova, V., Barlev, N., Borutinskaite, V. V., Vener, A., Bajenova, O., Magnusson, K. E., Pinaeu, G. P. & Tentler, D. (2010). Proteomic analysis of ACTN4-interacting proteins reveals it's a putative involvement in mRNA metabolism. *Biochemical and Biophysical Research Communications*, **397**(2), 192–196.

Khurana, S., Chakraborty, S., Cheng, X., Su, Y.-T., & Kao, H.-Y. (2011). The actin-binding protein, actinin alpha 4 (ACTN4), is a nuclear receptor coactivator that promotes proliferation of MCF-7 breast cancer cells. *The Journal of Biological Chemistry*, **286**(3), 1850–1859.

Kikuchi, S., Honda, K., Tsuda, H., Hiraoka, N., Imoto, I., Kosuge, T., Umaki, T., Onozato, K., Shitashige, M., Yamaguchi, U., Ono, M., Tsuchida, A., Aoki, T., Inazawa, J., Hirohashi, S. & Yamada, T. (2008). Expression and gene amplification of actinin-4 in invasive ductal carcinoma of the pancreas. *Clinical Cancer Research,* **14**(17), 5348–5356.

Klaavuniemi, T., Kelloniemi, A., & Ylänne, J. (2004). The ZASP-like motif in actinin-associated LIM protein is required for interaction with the α -actinin rod and for targeting to the muscle Z-line. *The Journal of Biological Chemistry*, **279**(25), 26402–26410.

Klaavuniemi, T., & Ylänne, J. (2006). Zasp/Cypher internal ZM-motif containing fragments are sufficient to co-localize with α -actinin--analysis of patient mutations. *Experimental Cell Research*, **312**, 1299–1311.

Knudsen, K. A., Soler, A. P., Johnson, K. R., & Wheelock, M. J. (1995). Interaction of α -actinin with the cadherin/catenin cell-cell adhesion complex via alpha-catenin. *The Journal of Cell Biology*, **130**(1), 67–77.

Kobayashi, R., & Tashima, Y. (1983). Purification and characterization of an alpha-actinin-like protein from porcine kidney. *Biochemica et Biophysica Acta*, **745**(2), 209-216.

Koizumi, T., Nakatsuji, H., Fukawa, T., Avirmed, S., Fukumori, T., Takahashi, M., & Kanayama, H. (2010). The role of actinin-4 in bladder cancer invasion. *Urology*, **75**(2), 357–364.

Kondo, S., Lu, Y., Debbas, M., Lin, A. W., Sarosi, I., Itie, A., Wakeham, A., Tuan, J., Elliott, G., Ma, W., Bechimal, S., Lowe, S. W., Mak, T. W. & Thukral, S. K. (2003). Characterization of cells and gene-targeted mice deficient for the p53-binding kinase homeodomain-interacting protein kinase 1 (HIPK1). *Proceedings of the National Academy of Sciences of the United States of America*, **100**(9), 5431–5436.

Kos, C. H., Le, T. C., Sinha, S., Henderson, J. M., Kim, S. H., Sugimoto, H., Kalluri, R., Gerszten, R.E. & Pollak, M. R. (2003). Mice deficient in α-actinin-4 have severe glomerular disease. *Journal of Clinical Investigations*, **111**, 1683–1690.

Kremerskothen, J., Teber, I., Wendholt, D., Liedtke, T., Böckers, T.M. & Barnekow, A. (2002). Brain-specific splicing of α-actinin 1 mRNA, **295**, 678–681.

Krupp, J. J., Vissel, B., Thomas, C. G., Heinemann, S. F., & Westbrook, G. L. (1999). Interactions of calmodulin and α-actinin with the NR1 subunit modulate Ca2+-dependent inactivation of NMDA receptors. *The Journal of Neuroscience*, **19**(4), 1165-1178.

Kumeta, M., Yoshimura, S. H., Harata, M., & Takeyasu, K. (2010). Molecular mechanisms underlying nucleocytoplasmic shuttling of actinin-4. *Journal of Cell Science*, **123**, 1020–1030.

Landau, M., Mayrose, I., Rosenberg, Y., Glaser, F., Martz, E., Pupko, T., & Ben-Tal, N. (2005). ConSurf 2005: the projection of evolutionary conservation scores of residues on protein structures. *Nucleic Acids Research*, **33**(Web Server issue), 299–302.

Landon, F., Gache, Y., Touitou, H., & Olomucki, A. (1985). Properties of two isoforms of human blood platelet α-actinin. *European Journal of Biochemistry*, **153**, 231–237.

Larkin, M. A., Blackshields, G., Brown, N. P., Chenna, R., McGettigan, P. A., McWilliam, H., Valentin, F., Wallace, I. M., Wilm, A., Lopez, R., Thompson, J. D., Gibson, T J. & Higgins, D. G. (2007). Clustal W and Clustal X version 2.0. *Bioinformatics*, **23**(21), 2947–2948.

Laukaitis, C. M., Webb, K. D., & Horwitz, A. F. (2001) Differential dynamics of 5 integrin, paxillin and actinin during formation and disassembly of adhesions in migrating cells. The Journal of Cell Biology, **153**(7), 1427-1440

Lee, D., Park, S. J., Sung, K. S., Park, J., Lee, S. B., Park, S. Y., Lee, H. J., Ahn, J. W., Choi, S. J., Lee, S. G., Kim, S. H., Kim, D. G., Kim, J., Kim, J. and Choi, C. Y. (2012). Mdm2 associates with Ras effector NORE1 to induce the degradation of oncoprotein HIPK1. *EMBO Reports*, **13**(2), 163–169.

Lee, S. H., Weins, A., Hayes, D. B., Pollak, M. R., & Dominguez, R. (2008). Crystal structure of the actin-binding domain of α-actinin-4 Lys255Glu mutant implicated in focal segmental glomerulosclerosis. *Journal of Molecular Biology*, **376**(2), 317–324.

Lek, M., MacArthur, D. G., Yang, N., & North, K. N. (2010a). Phylogenetic analysis of gene structure and alternative splicing in α-actinins. *Molecular Biology and Evolution*, **27**(4), 773–780.

Lek, M., Quinlan, K. G. R., & North, K. N. (2010b). The evolution of skeletal muscle performance: gene duplication and divergence of human sarcomeric α-actinins. *BioEssays,* **32**, 17–25.

Lewit-Bentley, A., & Réty, S. (2000). EF-hand calcium-binding proteins. *Current Opinion in Structural Biology*, **10**, 637–643.

Louis, E. J. (2007). Making the most of redundancy. *Nature*, **449**, 673–674.

Low, S. H., Mukhina, S., Srinivas, V., Ng, C.-Z. & Murata-Hori, M. (2010). Domain analysis of α-actinin reveals new aspects of its association with F-actin during cytokinesis. *Experimental Cell Research*, **316**, 1925-1934.

MacArthur, D. G., Seto, J. T., Raftery, J. M., Quinlan, K. G., Huttley, G. A., Hook, J. W., Lemckert, F. A., Kee, A. J., Edwards, M. R., Berman, Y., Hardeman, E., Gunning, P. W., Easteal, S., Yang, N. & North, K.N. (2007). Loss of ACTN3 gene function alters mouse muscle metabolism and shows evidence of positive selection in humans. *Nature Genetics*, **39**(10), 1261–1165.

Maunes, J. F., Kleeq, C. B., & Beckinghams, K. (1992). Ca^{2+} binding and conformational change in two series of point mutations to the individual Ca^{2+} binding sites of calmodulin. *The Journal of Biological Chemistry*, **267**(8), 5286–5295.

Michailidis, I. E., Helton, T. D., Petrou, V. I., Mirshahi, T., Ehlers, M. D., & Logothetis, D. E. (2007). Phosphatidylinositol-4,5-bisphosphate regulates NMDA receptor activity through α-actinin. *The Journal of Neuroscience,* **27**(20), 5523–5332.

Michaud, J.-L. (2003). Focal and segmental glomerulosclerosis in mice with podocyte-specific expression of mutant α-actinin-4. *Journal of the American Society of Nephrology*, **14**, 1200–1211.

Millake, D. B., Blanchard, A. D., Patel, B., & Critchley, D. R. (1989). The cDNA sequence of a human placental α-actinin. *Nucleic Acids Research*, **17**(16), 6725.

Mills, M. A., Yang, N., Weinberger, R. P., Vander Woude, D. L., Beggs, A. H., Easteal, S., & North, K. N. (2001). Differential expression of the actin-binding proteins, α-actinin-2 and -3, in different species: implications for the evolution of functional redundancy. *Human Molecular Genetics*, **10**(13), 1335–1346.

Mimura, N., & Asano, A. (1986). Isolation and characterization of a conserved actin-binding domain from rat hepatic actinogelin, rat skeletal muscle, and chicken gizzard alpha-actinins. *The Journal of Biological Chemistry*, **261**(23), 10680–10687.

Miyanaga, A., Honda, K., Tsuta, K., Masuda, M., Yamaguchi, U., Fujii, G., Miyamoto, A., Shinagawa, S., Miura, N., Tsuda, H., Sakuma, T., Gemma, A. & Yamada, T. (2012). Diagnostic and prognostic significance of the alternatively spliced ACTN4 variant in high-grade neuroendocrine pulmonary tumours. *Annals of Oncology,* 1–7.

Mohapatra, B., Jimenez, S., Lin, J. H., Bowles, K. R., Coveler, K. J., Marx, J. G., Chrisco, M. A., Murphy, R. T., Lurie, P. R., Schwarty, R. J., Elliott, P. M., Vatta, M., McKenna, W., Towbin, J. A. and Bowles, N. E. (2003). Mutations in the muscle LIM protein and α-actinin-2 genes in dilated cardiomyopathy and endocardial fibroelastosis. *Molecular Genetics and Metabolism*, **80**, 207–215.

Moulder, G. L., Cremona, G. H., Duerr, J., Stirman, J. N., Fields, S. D., Martin, W., Qadota, H., Benian, G. M., Lu, H. & Barstead, R. J. (2010). α-actinin is required for proper assembly of Z-disk / focal adhesion-like structures and for efficient locomotion in Caenorhabditis elegans. *Journal of Molecular Biology*, **403**(4), 516–528.

Mukai, H, Toshimori, M., Shibata, H., Kitagawa, M., Shimakawa, M., Miyahara, M., Sunakawa, H. & Ono, Y. (1996). PKN associates and phosphorylates the head-rod domain of neurofilament protein. *The Journal of Biological Chemistry*, **271**(16), 9816–9822.

Mukai, H., Toshimori, M., Shibata, H., Takanaga, H., Kitagawa, M., Miyahara, M., Shimakawa, M. & Ono. Y. (1997). Interaction of PKN with α-Actinin . *Journal of Biological Chemistry*, **272**(8), 4740–4746.

Mukhina, S., Wang, Y. L., & Murata-Hori, M. (2007). Alpha-actinin is required for tightly regulated remodeling of the actin cortical network during cytokinesis. *Developmental Cell*, **13**(4), 554–565.

Mykkänen, O.-M., Grönholm, M., Rönty, M., Lalowski, M., Salmikangas, P., Suila, H., & Carpén, O. (2001). Characterization of human palladin, a microfilament associated protein. *Molecular Biology of the Cell*, **12**, 3060–3073.

Nakagawa, N., Hoshijima, M., Oyasu, M., Saito, N., Tanizawa, K., & Kuroda, S. (2000). ENH, containing PDZ and LIM domains, heart/skeletal muscle-specific protein, associates with cytoskeletal proteins through the PDZ domain. *Biochemical and Biophysical Research Communications*, **272**, 505–512.

Niemi, A.-K., & Majamaa, K. (2005). Mitochondrial DNA and ACTN3 genotypes in Finnish elite endurance and sprint athletes. *European Journal of Human Genetics,* **13**, 965–969.

Nieset, J. E., Redfield, A. R., Jin, F., Knudsen, K. A., Johnson, K. R., & Wheelock, M. J. (1997). Characterization of the interactions of α-catenin with α-actinin and β-catenin/plakoglobin. *Journal of Cell Science*, **110**, 1013–1022.

Nikolopoulos, S. N., Spengler, B. A., Kisselbach, K., Evans, A. E., Biedler, J. L., & Ross, R. A. (2000). The human non-muscle α-actinin protein encoded by the ACTN4 gene suppresses tumorigenicity of human neuroblastoma cells. *Oncogene*, **19**, 380–386.

Noegel, A., Witke, W., & Schleicher, M. (1987). Calcium-sensitive non-muscle α-actinin contains EF-hand structures and highly conserved regions. *FEB*, **221**(2), 391–396.

Norman, B., Esbjörnsson, M., Rundqvist, H., Österlund, T., Von Walden, F., & Tesch, P. A. (2009). Strength, power, fiber types, and mRNA expression in trained men and women with different ACTN3 R577X genotypes. *Journal of Applied Physiology*, **106**, 959–965.

Ooshio, T., Irie, K., Morimoto, K., Fukuhara, A., Imai, T., & Takai, Y. (2004). Involvement of LMO7 in the association of two cell-cell adhesion molecules, nectin and E-cadherin, through afadin and α-actinin in epithelial cells. *The Journal of Biological Chemistry*, **279**(30), 31365–31373.

Otey, C. A., Pavalko, F. M., & Burridge, K. (1990). An interaction between α-actinin and the β_1 integrin subunit *in vitro*. *The Journal of Cell Biology*, **111**, 721–729.

Otey, C. A. & Carpen, O. (2004). α-actinin revisited: a fresh look at an old player. *Cell Motility and the Cytoskeleton*, **58**, 104–111.

Parast, M. M., & Otey, C. A. (2000). Characterization of palladin, a novel protein localized to stress fibers and cell adhesions. *The Journal of Cell Biology*, **150**(3), 643–656.

Park, B. W., Park, S., Koo, J. S., Kim, S. I., Park, J. M., Cho, J. H., & Park, H. S. (2012). Homeodomain-interacting protein kinase 1 (HIPK1) expression in breast cancer tissues. *Japanese Journal of Clinical Oncology*, **42**(12), 1138-1145.

Pavenstädt, H., Kriz, W., & Kretzler, M. (2003). Cell biology of the glomerular podocyte. *Physiological Reviews*, **83**, 253–307.

Pogue-Geile, K. L., Chen, R., Bronner, M. P., Crnogorac-Jurcevic, T., Moyes, K. W., Dowen, S., Otey, C. A., Crispin, P. A., George, R. P., Whitcomb, D. C. & Brentnall, T.A. (2006). Palladin mutation causes familial pancreatic cancer and suggests a new cancer mechanism. *PLoS Medicine*, **3**(12), e516.

Pomiès, P., Louis, H. A, & Beckerle, M. C. (1997). CRP1, a LIM domain protein implicated in muscle differentiation, interacts with α-actinin. *The Journal of Cell Biology*, **139**(1), 157–168.

Prevarskaya, N., Skryma, R., & Shuba, Y. (2011). Calcium in tumour metastasis: new roles for known actors. *Nature Reviews. Cancer*, **11**(8), 609–618.

Quick, Q., & Skalli, O. (2010). Alpha-actinin 1 and alpha-actinin 4: contrasting roles in the survival, motility, and RhoA signaling of astrocytoma cells. *Experimental Cell Research*, **316**, 1137–1147.

Raae, A. J., Bañuelos, S., Ylänne, J., Olausson, T., Goldie, K. N., Wendt, T., Hoenger, A. & Saraste, M. (2003). Actin binding of a minispectrin. *Biochimica et Biophysica Acta*, **1646**(1-2), 67–76.

Rajfur, Z., Roy, P., Otey, C., Romer, L., & Jacobson, K. (2002). Dissecting the link between stress fibres and focal adhesions by CALI with EGFP fusion proteins. *Nature Cell Biology*, **4**(4), 286–293.

Reichl, E. M., & Robinson, D. N. (2007). Putting the brakes on cytokinesis with α-actinin. *Developmental Cell*, **13**, 460–462.

Reinhard, M., Zumbrunn, J., Jaquemar, D., Kuhn, M., Walter, U., & Trueb, B. (1999). An α-actinin binding site of zyxin is essential for subcellular zyxin localization and α-actinin recruitment. *Journal of Biological Chemistry*, **274**(19), 13410–13418.

Rikova, K., Guo, A., Zeng, Q., Possemato, A., Yu, J., Haack, H., Nardone, J., Lee, K., Reeves, C., Li, Y., Hu, Y., Tan, Z., Stokes, M., Sullivan, L., Mitchell, J., Wetzel, R., MacNeill, J., Ran, J. M., Yuan, J., Bakalarshi, C. E., Kornhausser, J. M., Smith, B., Li, D., Zhou, X., Gygi, S. P., Gu, T.-T., Polakiewicz, R.D., Rush, J. & Comb, M.J. (2007). Global survey of phosphotyrosine signaling identifies oncogenic kinases in lung cancer. *Cell*, **131**, 1190–1203.

Rinaldo, C., Siepi, F., Prodosmo, A., & Soddu, S. (2008). HIPKs: Jack of all trades in basic nuclear activities. *Biochimica et Biophysica Acta*, **1783**, 2124–2129.

Robison, A. J., Bass, M. A., Jiao, Y., MacMillan, L. B., Carmody, L. C., Bartlett, R. K., & Colbran, R. J. (2005). Multivalent interactions of calcium/calmodulin-dependent protein kinase II with the postsynaptic density proteins NR2B, densin-180, and alpha-actinin-2. *The Journal of Biological Chemistry*, **280**(42), 35329–35336.

Roland, C. L., Harken, A. H., Sarr, M. G., & Barnett, C. C. (2007). ICAM-1 expression determines malignant potential of cancer. *Surgery*, **141**, 705–707.

Rosenberg, S., Stracher, A., & Burridge, K. (1981). Isolation and characterization of a calcium-sensitive α-actinin-like protein from human platelet cytoskeletons. *The Journal of Biological Chemistry*, **256**(24), 12986–12991.

Rosenmund, C., & Westbrook, G. (1993). Calcium-induced actin depolymerization reduces NMDA channel activity. *Neuron*, **10**(5), 805–814.

Roulier, E. M., Fyrberg, C., & Fyrberg, E. (1992). Perturbations of Drosophila α-actinin cause muscle paralysis, weakness, and atrophy but do not confer obvious nonmuscle phenotypes. *The Journal of Biological Chemistry*, **116**(4), 911–922.

Rush, J., Moritz, A., Lee, K. A., Guo, A., Goss, V. L., Spek, E. J., Zhang, H., Zha, X.-M., Polakiewicz, R. D. & comb, M. J. (2005). Immunoaffinity profiling of tyrosine phosphorylation in cancer cells. *Nature Biotechnology*, **23**(1), 94–101.

Ryan, K. M., Phillips, A. C., & Vousden, K. H. (2001). Regulation and function of the p53 tumor suppressor protein. *Current Opinion in Cell Biology*, **13**, 332–337.

Rönty, M., Taivainen, A., Moza, M., Otey, C. A., & Carpén, O. (2004). Molecular analysis of the interaction between palladin and alpha-actinin. *FEBS letters*, **566**, 30–34.

Saleh, M., Vaillancourt, J. P., Graham, R. K., Huyck, M., Srinivasula, S. M., Alnemri, E. S., Steinberg, M. H., Nolan, V., Baldwin, C. T., Hotchkiss, R. S., Buchman, T. G., Zehnbauer, B. A., Hayden, M. R., Ferrer, L. A., Ray, S. & Nicholson, D. W. (2004). Differential modulation of endotoxin responsiveness by human caspase-12 polymorphisms. *Letters to Nature*, **429**, 75–79.

Salmikangas, P., Mykkänen, O. M., Grönholm, M., Heiska, L., Kere, J., & Carpén, O. (1999). Myotilin, a novel sarcomeric protein with two Ig-like domains, is encoded by a candidate gene for limb-girdle muscular dystrophy. *Human molecular genetics*, **8**(7), 1329–1336.

Schultheiss, T., Choi, J., Lin, Z. X., DiLullo, C., Cohen-Gould, L., Fischman, D., & Holtzer, H. (1992). A sarcomeric α-actinin truncated at the carboxyl end induces the breakdown of stress fibers in PtK2 cells and the formation of nemaline-like bodies and breakdown of myofibrils in myotubes. *Proceedings of the National Academy of Sciences of the United States of America*, **89**, 9282–9286.

Sen, S., Dong, M., & Kumar, S. (2009). Isoform-specific contributions of α-actinin to glioma cell mechanobiology. *PloS one*, **4**(12), e8427.

Seto, J. T., Lek, M., Quinlan, K. G. R., Houweling, P. J., Zheng, X. F., Garton, F., MacArthur, D. G., Raftery, J. M., Garvey, S. M., Hauser, M. A., Yang, N., Head, S. I. & North, K. N. (2011). Deficiency of α-actinin-3 is associated with increased susceptibility to contraction-induced damage and skeletal muscle remodeling. *Human Molecular Genetics*, **20**(15), 2914–2927.

Shao, H., Wu, C., & Wells, A. (2010). Phosphorylation of alpha-actinin 4 upon epidermal growth factor exposure regulates its interaction with actin. *The Journal of Biological Chemistry*, ***2*85**(4), 2591–2600.

Shibasaki, F., Fukami, K., Fukui, Y., & Takenawa, T. (1994). Phosphatidylinositol 3-kinase binds to α-actinin through the p85 subunit. *The Biochemical Journal*, **302**, 551–557.

Sistani, L., Dunér, F., Udumala, S., Hultenby, K., Uhlen, M., Betsholtz, C., Tryggvason, Wernessan, A. & Patrakka, J. (2011). Pdlim2 is a novel actin-regulating protein of podocyte foot processes. *Kidney International*, **80,** 1045–1054.

Sjoblom, B., Salmazo, A., & Djinovic-Carugo, K. (2008). Alpha-actinin structure and regulation. *Cell and Molecular Life Sciences*, **65**, 2688–2701.

Stenmark, H., Vitale, G., Ullrich, O., & Zerial, M. (1995). Rabaptin-5 is a direct effector of the small GTPase Rab5 in endocytic membrane fusion. *Cell*, **83**, 423–432.

Suzuki, H., Jin, Y., Otani, H., Yasuda, K., & Inoue, K. (2002). Regulation of alternative splicing of α-actinin transcript by Bruno-like proteins. *Genes To Cells*, **7**, 133–141.

Tait, L., Soule, H. D., & Russo, J. (1990). Ultrastructural and Immunocytochemical Characterization of an immortalized human breast epithelial cell line, MCF-10. *Cancer Research*, **50**, 6087–6094.

Takada, F., Vander Woude, D. L., Tong, H. Q., Thompson, T. G., Watkins, S. C., Kunkel, L. M., & Beggs, A. H. (2001). Myozenin: an α-actinin- and gamma-filamin-binding protein of skeletal muscle Z lines. *Proceedings of the National Academy of Sciences of the United States of America*, **98**(4), 1595–1600.

Tavaré, J. M., Fletcher, L. M., & Welsh, G. I. (2001). Using green fluorescent protein to study intracellular signalling. *The Journal of Endocrinology*, ***170***, 297–306.

Taylor, K. A., & Taylor, D. W. (1993). Projection image of smooth muscle alpha-actinin from two-dimensional crystals formed on positively charged lipid layers. *Journal of Molecular Biology*, **230**(1), 196–205.

te Velthuis, A. J. & Bagowski, C. P. (2007). PDZ and LIM domain-encoding genes: molecular interactions and their role in development. *The Scientific World Journal*, **7**, 1470–1492.

Thomas, G. H., Newbern, E. C., Korte, C. C., Bales, M. A., Muse, S. V, Clark, A. G., & Kiehart, D. P. (1997). Intragenic duplication and divergence in the spectrin superfamily of proteins. *Molecular Biology and Evolution*, **14**(12), 1285–1295.

Tomotsune, D., Takihara, Y., Berger, J., Duhl, D., Joo, S., Kyba, M., Shirai, M., Ohta, H., Matsuala, Y., Honda, B. M., Simon, J., Shimada, K., Brock, H. W. & Randazzo, F. (1999). A novel member of murine Polycomb-group proteins, Sex comb on midleg homolog protein, is highly conserved, and interacts with RAE28/mph1 in vitro. *Differentiation*, **65**(4), 229–239.

Torrado, M., Senatorov, V. V, Trivedi, R., Fariss, R. N., & Tomarev, S. I. (2004). Pdlim2, a novel PDZ-LIM domain protein, interacts with α-actinins and filamin A. *Investigative Ophthalmology & Visual Science*, **45**(11), 3955–3963.

Triplett, J. W., & Pavalko, F. M. (2006). Disruption of α-actinin-integrin interactions at focal adhesions renders osteoblasts susceptible to apoptosis. *American Journal of Physiology. Cell Physiology*, **29**1, 909–921.

Vallenius, T., Scharm, B., Vesikansa, A., Luukko, K., Schäfer, R., & Mäkelä, T. P. (2004). The PDZ-LIM protein RIL modulates actin stress fiber turnover and enhances the association of α-actinin with F-actin. *Experimental Cell Research*, **293**, 117–128.

Vallenius, T., Luukko, K., & Mäkelä, T. P. (2000). CLP-36 PDZ-LIM protein associates with nonmuscle α-actinin-1 and α-actinin-4. *Journal of Biological Chemistry*, **275**(15), 11100–11105.

Vallenius, Tea, & Mäkelä, T. P. (2002). Clik1: a novel kinase targeted to actin stress fibers by the CLP-36 PDZ-LIM protein. *Journal of Cell Science*, **115**, 2067–2073.

Viel, A. (1999). α-actinin and spectrin structures: an unfolding family story. *FEBS Letters*, **460**, 391–394.

Virel, A., Addario, B., & Backman, L. (2007). Characterization of Entamoeba histolytica α-actinin2. *Molecular and Biochemical Parasitology*, **154**, 82–89.

Virel, A., & Backman, L. (2004). Molecular evolution and structure of alpha-actinin. *Molecular Biology and Evolution*, **21**(6), 1024–1031.

Virel, A., & Backman, L. (2006). Characterization of Entamoeba histolytica alpha-actinin. *Molecular and Biochemical Parasitology*, **145,** 11–17.

Virel, A., & Backman, L. (2007). A comparative and phylogenetic analysis of the α-actinin rod domain. *Molecular Biology and Evolution*, **24**(10), 2254–2265.

Wachsstock, D. H., Wilkins, J. A., & Lin, S. (1987). Specific interaction of vinculin with α-actinin. *Biochemical and Biophysical Research Communications*, **146**(2), 554–560.

Waites, G. T., Graham, I. R., Jackson, P., Millake, D. B., Patel, B., Blanchard, A. D., Weller, P. A., Eperon, I.C. & Critchley, D. R. (1992). Mutually exclusive splicing of calcium-binding domain exons in chick α-actinin. *The Journal of Biological Chemistry*, **267**(9), 6263–6271.

Walikonis, R. S., Jensen, O. N., Mann, M., Provance, D. W., Mercer, J. A, & Kennedy, M. B. (2000). Identification of proteins in the postsynaptic density fraction by mass spectrometry. *The Journal of Neuroscience,* **20**(11), 4069–4080.

Walikonis, R. S., Oguni, A., Khorosheva, E. M., Jeng, C.-J., Asuncion, F. J., & Kennedy, M. B. (2001). Densin-180 forms a ternary complex with the α-subunit of Ca2+/calmodulin-dependent protein kinase II and α-actinin. *The Journal of Neuroscience*, **21**(2), 423–433.

Wallraff, E., Schleicher, M., Modersitzki, M., Rieger, D., Isenberg, G., & Gerisch, G. (1986). Selection of *Dictyostelium* mutants defective in cytoskeletal proteins: use of an antibody that binds to the ends of α-actinin rods. *The EMBO journal*, **5**(1), 61–67.

Walsh, S., Liu, D., Metter, E. J., Ferrucci, L., & Roth, S. M. (2008). ACTN3 genotype is associated with muscle phenotypes in women across the adult age span. *Journal of Applied Physiology*, **105**, 1486–1491.

Watabe-Uchida, M., John, K. A., Janas, J. A., Newey, S. E., & Van Aelst, L. (2006). The Rac activator DOCK7 regulates neuronal polarity through local phosphorylation of stathmin/Op18. *Neuron*, **51**, 727–739.

Webb, D. J., Parsons, J. T., & Horwitz, A. F. (2002). Adhesion assembly, disassembly and turnover in migrating cells - over and over and over again. *Nature Cell Biology*, **4**, 97–100.

Weins, Astrid, Schlondorff, J. S., Nakamura, F., Denker, B. M., Hartwig, J. H., Stossel, T. P., & Pollak, M. R. (2007). Disease-associated mutant alpha-actinin-4 reveals a mechanism for regulating its F-actin-binding affinity. *Proceedings of the National Academy of Sciences of the United States of America*, **104**(41), 16080–16085.

Welsch, T., Keleg, S., Bergmann, F., Bauer, S., Hinz, U., & Schmidt, J. (2009). Actinin-4 expression in primary and metastasized pancreatic ductal adenocarcinoma. *Pancreas*, **38**(8), 968–976.

Winkler, J., Lünsdorf, H., & Jockusch, B. M. (1997). Flexibility and fine structure of smooth-muscle α-actinin. *European Journal of Biochemistry*, **248**, 193–199.

Wismar, J., Löffler, T., Habtemichael, N., Vef, O., Geissen, M., Zirwes, R., Altmeyerj, W., Sass, H. & Gateff, E.(1995). The *Drosophila melanogaster* tumor suppressor gene *lethal(3)malignant brain tumor* encodes a proline-rich protein with a novel zinc finger. *Mechanisms of Development*, **53**, 141–154.

Witke, W, Hofmann, A., Köppel, B., Schleicher, M., & Noegel, A. A. (1993). The Ca(2+)-binding domains in non-muscle type α-actinin: biochemical and genetic analysis. *The Journal of Cell Biology*, **121**(3), 599–606.

Witke, W., Schleicher, M., Lottspeich, F. & Noegel, A. (1986). Studies on the transcription , translation, and structure of α-actinin in *Dictyostelium discoideum* and protein sequence analysis. *The Journal of Cell Biology*, **103**, 969–975.

Wyszynski, M., Kharazia, V., Shanghvi, R., Rao, A., Beggs, A. H., Craig, A. M., Weinberg, R. & Sheng, M. (1998). Differential regional expression and ultrastructural localization of alpha-actinin-2, a putative NMDA receptor-anchoring protein, in rat brain. *The Journal of Neuroscience,* **18**(4), 1383–1392.

Wyszynski, M., Lin, J., Rao, A., Nigh, E., Beggs, A. H., Craig, A. M., & Sheng, M. (1997). Competitive binding of α-actinin and calmodulin to the NMDA receptor. *Nature*, **385**, 439–442.

Xia, H., Winokur, S. T., Kuo, W.-L., Altherr, M. R., & Bredt, D. S. (1997). Actinin-associated LIM protein: identification of a domain interaction between PDZ and spectrin-like repeat motifs. *The Journal of Cell Biology*, **139**(2), 507–515.

Xu, X., Song, Y., Li, Y., Chang, J., Zhang, H., & An, L. (2010). The tandem affinity purification method: an efficient system for protein complex purification and protein interaction identification. *Protein Expression and Purification*, **72**, 149–156.

Yamada, S., Yanamoto, S., Yoshida, H., Yoshitomi, I., Kawasaki, G., Mizuno, A., & Nemoto, T. K. (2010). RNAi-mediated down-regulation of α-actinin-4 decreases invasion potential in oral squamous cell carcinoma. *International Journal of Oral & Maxillofacial Surgery*, **39**(1), 61–67.

Yamamoto, S., Tsuda, H., Honda, K., Kita, T., Takano, M., Tamai, S., Inazawa, J., Yamada, T. & Matsubara, O. (2007). Actinin-4 expression in ovarian cancer: a novel prognostic indicator independent of clinical stage and histological type. *Modern Pathology*, **20**(12), 1278–1285.

Yamamoto, S., Tsuda, H., Honda, K., Takano, M., Tamai, S., Imoto, I., Inazawa, J., Yamada, T. & Matsubara, O. (2012). ACTN4 gene amplification and actinin-4 protein overexpression drive tumour development and histological progression in a high-grade subset of ovarian clear-cell adenocarcinomas. *Histopathology*, **60**(7), 1073–1083.

Yan, Q., Sun, W., Kujala, P., Lofti, Y., Vida, T. A. & Bean, A. J. (2005) CART: An HRS/actinin-4/BERP/myosin V protein complex required for efficient receptor recycling, *Molecular Biology of the Cell*, **16**, 2470-2482.

Yang, N., MacArthur, D. G., Gulbin, J. P., Hahn, A. G., Beggs, A. H., Easteal, S., & North, K. (2003). ACTN3 genotype is associated with human elite athletic performance. *American Journal of Human Genetics*, **73**, 627–631.

Ylänne, J., Scheffzek, K., Young, P., & Saraste, M. (2001). Crystal structure of the α-actinin rod reveals an extensive torsional twist. *Structure*, **9**, 597–604.

Yngvadottir, B., Xue, Y., Searle, S., Hunt, S., Delgado, M., Morrison, J., Whittaker, P., Deloukos, P. & Tyler-Smith, C. (2009). A genome-wide survey of the prevalence and evolutionary forces acting on human nonsense SNPs. *American Journal of Human Genetics*, **84**, 224–234.

Young, P., Ferguson, C., Bañuelos, S., & Gautel, M. (1998). Molecular structure of the sarcomeric Z-disk: two types of titin interactions lead to an asymmetrical sorting of α-actinin. *The EMBO journal*, **17**(6), 1614–1624.

Young, P., & Gautel, M. (2000). The interaction of titin and α-actinin is controlled by a phospholipid-regulated intramolecular pseudoligand mechanism. *The EMBO journal*, **19**(23), 6331–6340.

Zhou, J., Olcese, R., Qin, N., Noceti, F., Birnbaumer, L., & Stefani, E. (1997). Feedback inhibition of Ca^{2+} channels by Ca^{2+} depends on a short sequence of the C terminus that does not include the Ca^{2+} -binding function of a motif with similarity to Ca^{2+} -binding domains. *Proceedings of the National Academy of Sciences of the United States of America*, **94**, 2301–2305.

Zhou, X., Perez, F., Han, K., & Jurivich, D. A. (2006). Clonal senescence alters endothelial ICAM-1 function. *Mechanisms of Ageing and Development*, **127**, 779–785.

Zühlke, R. D., & Reuter, H. (1998). Ca^{2+}-sensitive inactivation of L-type Ca^{2+} channels depends on multiple cytoplasmic amino acid sequences of the α_{1C} subunit. *Proceedings of the National Academy of Sciences of the United States of America*, **95**, 3287–3294.

7 Appendix

Biochemical Journal Immediate Publication. Published on 04 Apr 2013 as manuscript BJ20121824

An analysis of splicing, actin-binding properties, heterodimerisation and molecular interactions of the non-muscle α-actinins.

Kate Foley[*] and Paul Young[*,†]

[*] Department of Biochemistry,
University College Cork,
Cork,
Ireland

[†] Corresponding author
Email: p.young@ucc.ie
Telephone: +353 21 420 5994
FAX: +353 21 420 5462

THIS IS NOT THE VERSION OF RECORD - see doi:10.1042/BJ20121824

Accepted Manuscript

Licenced copy. Copying is not permitted, except with prior permission and as allowed by law.
© 2013 The Authors Journal compilation © 2013 Biochemical Society

Biochemical Journal Immediate Publication. Published on 04 Apr 2013 as manuscript BJ20121824

Abstract

The non-muscle α-actinin isoforms (actinin-1 and -4) are closely related, dimeric actin filament-crosslinking proteins. Despite high sequence similarity, unique properties have been ascribed to actinin-4 in particular. For example, actinin-4, but not actinin-1, is essential for normal glomerular function in the kidney, is overexpressed in several cancers and can translocate to the nucleus to regulate transcription. To understand the molecular basis for such isoform-specific functions we have comprehensively compared these proteins in terms of alternative splicing, actin-binding properties, heterodimer formation and molecular interactions for the first time. We find that the calcium-insensitive variant of actinin-4 is expressed only in the nervous system and thus cannot be regarded as a smooth muscle isoform, as is the case for the calcium-insensitive variant of actinin-1. Actin-binding properties of actinin-1 and -4 are similar and are unlikely to explain isoform-specific functions. Surprisingly, we reveal that actinin-1/-4 heterodimers, rather than homodimers, are the most abundant form of actinin in many cell lines. Finally, we use a proteomics approach to identify potential isoform-specific interactions. Our findings indicate that actinin-1 and -4 can readily form heterodimers composed of monomers that may have different properties and interacting proteins. This significantly alters our view of non-muscle actinin function.

Short Title:
Analysis of splicing and molecular interactions of non-muscle actinins.

Key words:
actinin, non-muscle actinin, actinin heterodimer, actinin-1, actinin-4, spectrin repeats

THIS IS NOT THE VERSION OF RECORD - see doi:10.1042/BJ20121824

Accepted Manuscript

Licenced copy. Copying is not permitted, except with prior permission and as allowed by law.
© 2013 The Authors Journal compilation © 2013 Biochemical Society

Biochemical Journal Immediate Publication. Published on 04 Apr 2013 as manuscript BJ20121824

THIS IS NOT THE VERSION OF RECORD - see doi:10.1042/BJ20121824

Introduction

The α-actinins are a major family of actin filament cross-linking proteins. Actinins are dimeric proteins with each monomer consisting of an N-terminal actin-binding domain (ABD), a rod domain composed of four spectrin-like repeats (R1-R4) and a C-terminal calmodulin-like domain (CaM). Actinin-1 and -4 are regarded as non-muscle isoforms[1]. They are distinguished from muscle actinins by alternative splicing of exon 19, encoding part of the first EF-hand motif of the CaM domain. For actinin-1, splicing of exon 19a and 19b generates isoforms that bind actin in either a Ca^{++}-sensitive or -insensitive manner respectively (Figure 1a)[2]. This splicing is usually mutually exclusive and the resulting isoforms are commonly refered to as the "non-muscle" and "smooth muscle" actinins respectively. Additionally, a brain-specific actinin-1 variant containing both exons 19a and 19b has been described in the rat brain[3]. For clarity we refer to actinin splice variants according to the exons they contain (19a, 19b or 19a+b) rather than their expression patterns. Actinin-4 also has alternate versions of exon 19 that are predicted to confer Ca^{++} sensitivity and -insensitivity[4], but the expression patterns of actinin-4 exon 19 splice variants has not been examined. In addition, actinin-4 exhibits alternative splicing of exon 8 (Figure 1b). Based on structural studies, alternative splicing of exon 8 may alter actin-binding properties but this has not been thoroughly investigated[5]. Different splicing patterns or actin-binding characteristics may explain functional differences between actinin-1 and -4 but these properties of the non-muscle actinins have not been comprehensively compared.

The actinin rod domain is responsible for dimerisation and forms a spacer of fixed length between the ABDs in the resulting antiparallel dimer [6-8]. Heterodimer formation has been reported to occur between the muscle actinins (actinin-2 and -3)[9] however, this has not been examined for the non-muscle isoforms. Thus, actinin-1 and -4 are generally regarded as being distinct homodimeric entities, despite the fact that they are co-expressed in many tissues and cell types. A secondary function of the rod domain is to act as a binding site for other proteins. A multitude of interacting proteins have been described for actinins and these bind to the rod as well as the ABD and CaM domains [1, 10, 11]. While many actinin binding partners are likely to be common to multiple actinin isoforms, others may be isoform-specific. However, in many studies the issue of isoform-specificity of actinin ligands has not been tested. Such isoform-specific interactions are likely to confer unique functional properties to different actinins and thus merit a more systematic examination.

Actinin-1 and -4 are very closely related, sharing 87% amino acid identity[12]. Despite this high degree of sequence similarity, numerous differences in cellular localisation and function of the non-muscle actinins have been reported and a number of unique properties have been ascribed to actinin-4 in particular. For example, actinin-4 is the predominant actinin isoform reported to be associated with cancer. Elevated levels of actinin-4 protein are found in a number of cancers including ovarian[13, 14], colorectal[15], pancreatic[16] and astrocytoma[17], and are associated with high grade tumours and poor patient outcomes[14, 16, 17]. Furthermore actinin-4 expression promotes cell motility[12, 13, 17, 18] and enhances the metastatic potential of colorectal cancer cells[15]. The functions of actinin-4 in cancer cells are likely to be caused by some unique characteristics of actinin-4 that are not shared by actinin-1. Another actinin-4-specific function is its role in the formation and function of glomeruli in the kidney. Genetic studies identified point mutations in the actinin-4 gene that cause focal segmental glomerulosclerosis[19]. In agreement with this, mice deficient in actinin-4 exhibit podocyte foot-process enfacement and glomerular disease, even though these mice express normal levels of actinin-1[20]. This suggests that, in the kidney at least, actinin-1 and -4 are not functionally redundant. An additional unique function of actinin-4 is its ability to translocate to the nucleus where it can act as a transcriptional regulator[21-24]. The molecular basis for most of these isoform-specific functions of actinin-4 is unclear.

In an effort to understand the molecular mechanisms underlying these unique functions of actinin-4 we compared the alternative splicing, actin-binding affinities,

Accepted Manuscript

Licenced copy. Copying is not permitted, except with prior permission and as allowed by law.
© 2013 The Authors Journal compilation © 2013 Biochemical Society

Biochemical Journal Immediate Publication. Published on 04 Apr 2013 as manuscript BJ20121824

dimerisation properties and interacting partners of the non-muscle actinins. We find that the affinity and Ca^{++}-sensitivity of actin filament binding of exon 19a variants of actinin-1 and -4 are very similar but that the expression pattern of the Ca^{++}-insensitive exon 19b variants differs significantly for actinin-1 and -4. We also describe the actin-binding properties of the brain-specific actinin-1 and actinin-4 splice variants for the first time. Our examination of actinin dimerisation reveals very surprisingly that actinin-1/-4 heterodimers, rather than homodimers, are the most abundant actinin species in many cell lines. To examine actinin molecular interactions in a more systematic manner we have performed yeast two-hybrid screens and analysed affinity purified actinin-1 and -4 protein complexes to identify putative isoform-specific interacting proteins. This thorough analysis of actinin-1 and -4 provides the basis for further investigation and comparison of the diverse functions of the non-muscle actinins.

THIS IS NOT THE VERSION OF RECORD - see doi:10.1042/BJ20121824

Accepted Manuscript

Licenced copy. Copying is not permitted, except with prior permission and as allowed by law.
© 2013 The Authors Journal compilation © 2013 Biochemical Society

Biochemical Journal Immediate Publication. Published on 04 Apr 2013 as manuscript BJ20121824

THIS IS NOT THE VERSION OF RECORD - see doi:10.1042/BJ20121824

Materials and Methods

Antibodies, cell lines and reagents

The following antibodies were used: α-Actinin-1 (Santa Cruz, California Cat# (H-2):sc17829), α-actinin-4 (Immunoglobe, Himmelstadt, Germany Cat# IG701), α-Actinin-2/3 (Sigma, Arklow, Ireland Cat# A7811 clone EA-53), α-GFP (Millipore, Cork, Ireland Cat# MAB3580), α-GFP (Abcam, Cambridge, UK Cat# ab290) and α-FLAG (Sigma, Arklow, Ireland Cat# F3165). Chemicals were obtained from Sigma (Arklow, Ireland) unless otherwise stated and restriction enzymes were purchased from New England Biolabs (Hitchin, UK). Cell lines used included A172, U-87MG and U-373MG that were purchased from Cell Line Services (Eppelheim, Germany). Human embryonic kidney 293 cells (HEK 293), MDA-MB-231, DU145, HeLa and MCF-7 cells were a kind gift from Prof. Rosemary O' Connor (University College Cork, Ireland).

Reverse transcription PCR (rtPCR)

Tissues were dissected from C57 BL6J mice and embryos. Animal experiments at University College Cork were approved by the University Ethics Committee and conducted under a license from the Irish Department of Health and Children. RNA was extracted using TriPure Isolation Reagent (Roche Applied Science, Burgess Hill, UK) according to the manufacturer's instructions. 1ug of RNA was used per cDNA reaction using the Protoscript AMV First Stand cDNA synthesis kit (New England Biolabs, Hitchin, UK). 1ul of cDNA was used per rtPCR reaction. For rtPCR analysis of actinin-4 exon 8, forward primers that flank exon 8 were used in conjunction with reverse primers specific for exon 8b and reverse primers that flank exon 8 were used in conjunction with forward primers specific for exon 8a. For analysis of actinin-1 and -4 exon 19, primers that flank this exon were used and bands corresponding to exon 19a (128bp) and 19b (113bp) were separated on 4% agarose gels. Sequences of primers used for rtPCR are provided in the Supplementary Methods available online.

cDNA constructs, protein expression and purification

Details of all cDNA constructs and the methods used for recombinant protein expression and purification are provided in the Supplementary Methods available online.

Actin-cosedimentation assays

Human platelet actin (Cytoskeleton Inc., Denver, USA) was mixed in G-actin buffer (5 mM Tris pH 8.0, 0.2 mM $MgCl_2$, 0.2 mM ATP, 0.5 mM dithiothreitol (DTT)). Actin and actinin proteins were cleared by ultra-centrifugation at 112,000 g for 30 min at 4 ^{0}C. Actin was polymerised by addition of 1/100 volume of 100X polymerisation buffer (2 M NaCl, 0.1 M $MgCl_2$) and incubated for 30 min at 4 ^{0}C. Actin and actinin proteins were mixed in 10 mM Tris-HCl pH 7.5, 100 mM NaCl, 1 mM NaN_3, 1 mM $MgCl_2$, 0.1 mM ATP, 0.1 mM DTT and incubated for 30 min at 30 ^{0}C. To determine the Kd for actin-binding 2 µM actin was used per assay along with a range of actinin concentrations (0.25-30 µM) in the presence of 0.2 mM EGTA. For Ca^{++}-sensitivity analysis 2 µM actin and 2.5 µM actinin were mixed in a variety of free Ca^{++} concentrations (100 nM-1 mM) that were obtained using a Ca^{++}:EGTA buffer system. Polymerised actin was separated by ultracentrifugation at 112,000 g for 30 min at 30 ^{0}C. Pellets and supernatants were brought to the same total volume of SDS sample buffer, boiled, and equal volumes loaded on 12% SDS-polyacrylamide gels. Assays that omitted actin were used as controls for non-specific trapping of actinin. For actin-bundling assays centrifugation was performed at 10,000 g.

Analysis of evolutionary conservation of the actinin rod dimerisation interface

This analysis was based on the human actinin-2 rod domain for which a crystallographic structure is known [7]. A multiple sequence alignment of this sequence with actinin-1 and -4 sequences from divergent species (human, mouse, frog, zebrafish and chicken) was generated. With this alignment set as the input, the ConSurf server was used to calculate and plot

Licenced copy. Copying is not permitted, except with prior permission and as allowed by law.
© 2013 The Authors Journal compilation © 2013 Biochemical Society

Accepted Manuscript

Biochemical Journal Immediate Publication. Published on 04 Apr 2013 as manuscript BJ20121824

conservation scores onto the actinin-2 rod domain 3D structure[25, 26]. Conservation scores that are considered unreliable by ConSurf are colored yellow and shown in stick rather than space filling representation.

Yeast Two-Hybrid analysis

Rod domains from actinin-1, -2 and -4 were cloned into both bait and prey vectors as described. To assess actinin rod domain heterodimerisation bait and prey constructs were co-transformed into the *Saccharomyces cerevisiae* L40 strain and activation of the *lacZ* and *HIS3* reporter genes assayed as previously described[8]. Yeast two-hybrid screens using either actinin-1 or -4 rod domain pLEX-K bait constructs were performed using a P3 mouse brain cDNA library in the pAD-GAL4 vector as described previously[27]. The transformation efficiency for the actinin-1 and actinin-4 screens was $2.4x10^6$ and $6x10^5$ colony forming units respectively. Prey clones identified from the actinin-1 screen were tested for interaction with the actinin-4 bait by co-transforming both plasmids into L40 cells.

***In vitro* heterodimer binding assays**

GST-tagged ABD-R2 and His_6-tagged R3-CaM regions from both actinin-1 and -4 were expressed, purified and dialyzed into binding assay buffer (20 mM Tris pH 7.5, 50 mM NaCl, 5 mM β-mercaptoethanol). Experiments were designed to assay for homodimer and heterodimer formation. Briefly, 0.1 mg of GST-tagged ABD-R2 domains of actinin-1 or -4 were incubated with 50 µl GST beads which were subsequently mixed with 0.1 mg of R3-CaM domains of actinin-1 or -4. Beads were incubated for 30 min at 4 ^{0}C and washed 3 times in binding assay buffer for 5 min at 4 ^{0}C. Proteins were eluted in 50 µl 2X SDS-PAGE loading dye. Eluted proteins were run on 12% SDS-PAGE gels and stained with Coomassie blue. Densitometric analysis was used to compare the levels of R3-CaM proteins bound to ABD-R2 proteins for heterodimer and homodimer formation.

Cell culture and transfections

A172, HeLa, HEK293, MCF-7, MDA-MB-231 and U-87MG cells were cultured in Dulbecco's Modified Eagle Media (Sigma D6429), 10% fetal bovine serum (FBS), 1% penicillin/streptomycin and 1% L-glutamine. DU145 cells were cultured in RPMI (Sigma R8758), 10% FBS, 1% L-glutamine and 1% penicillin/streptomycin. U-118MG and U-373MG cells were cultured in Minimum Essential Medium Eagle (Sigma M5650), 10% FBS, 1% L-glutamine, 1% penicillin/streptomycin, 0.1 mM non-essential amino acids and 1 mM sodium pyruvate. Serum starvation was carried out by growing a confluent cell monolayer in media containing 10% FBS. Cells were washed twice in PBS and grown for a further 48 hr in the absence of FBS. Cell migration was induced by applying multiple scratches to a confluent cell monolayer using a sterile tip ~16 hr pre-harvest. Confluent cell layers were obtained by seeding 800,000 cells in a 10cm diameter plate 48hr pre-harvest. Proliferating cells were obtained by seeding 200,000 cells ~16 hr pre-harvest.

siRNA knockdown of actinin-4

MCF-7 cells were seeded in 6-well dishes so as to be 50% confluent for transfection. Two Silencer Select® Pre-designed siRNAs targeting actinin-4 (ID: s959 and s960 Cat# 4427037) together with a non-targeting negative control (Cat# 4390843) were purchased from Ambion (Life technologies, Carlsbad, California, USA). Cells were transfected in serum-free media with 10 nM siRNA using 3 µl lipofectamine purchased from Invitrogen (Life Technologies, Carlsbad, California, USA). Transfections were conducted in 1 ml DMEM. 5 hr post transfection media was adjusted to 10% FBS. Cells were harvested 72 hr post transfection.

Native Polyacrylamide Gel Electrophoresis (Native PAGE)

Standard polyacrylamide gel electrophoresis protocol was followed with the exception that SDS, β-mercaptoethanol and boiling steps were omitted. The PROTEAN II xi cell electrophoresis instrument was employed (Bio-Rad, Hercules, California). Cells were washed twice in PBS and lysed in 150 mM NaCl, 50 mM Tris-Cl pH 7.5, 1% NP40, 10% glycerol, 2

THIS IS NOT THE VERSION OF RECORD - see doi:10.1042/BJ20121824

Accepted Manuscript

Licenced copy. Copying is not permitted, except with prior permission and as allowed by law.
© 2013 The Authors Journal compilation © 2013 Biochemical Society

Biochemical Journal Immediate Publication. Published on 04 Apr 2013 as manuscript BJ20121824

mM NaF, 1 mM Na_3VO_4 and 1 protease inhibitor cocktail tablet/10 ml (Roche, Clare, Ireland). Cells were incubated in lysis buffer for 30 min and centrifuged at 16,100 g for 15 min at 4^0C. 3X PAGE loading buffer (without SDS and β-mercaptoethanol) was added to lysates on ice. Samples were then loaded on 6% native polyacrylamide gels (without SDS). Lysates were run for 5 hours in PAGE running buffer (without SDS) at a current of 24 mA. Running buffer was refreshed after 2.5 hr. Western blot detection was performed on an Odyssey Classic infrared scanner (LI-COR Biosciences, Cambridge, UK).

Determination of the relative amount of actinin-1 and -4 within and between cell lines

Full length actinin-1/-4 constructs in the pEGFP-C2 vector (Clontech, Quintin, France) were transfected into HEK 293 cells as described. In order to determine their expression levels relative to each other Western blots of lysates were probed with α-GFP antibody. Subsequently lysates from cells transfected with these GFP-tagged actinin constructs were used to produce a standard curve to which specific actinin-1 and -4 antibody staining could be normalised. Using this standard curve in combination with lysates from various cell lines allowed comparison of the relative amount of actinin-1 and -4 within and between cells lines. Probing native gels with antibodies specific for actinin-1 and -4 followed by densitometric analysis allowed us to quantify the proportion of actinin-1 and -4 involved in heterodimer formation.

Tandem Affinity Purifications

Constructs encoding TAP-tagged actinin-1, -4 and YFP were transfected in HEK 293 cells and grown for 4 cell passages. Using a fluorescent microscope, YFP/GFP-expressing cells were selected over the course of ~10 passages. In this manner stable cell pools in which >70% of cells were YFP/GFP positive were obtained. Five 15 cm diameter cell culture dishes were grown to confluence for each round of purification. Cells were washed twice in PBS and lysed in 5 ml lysis buffer (150 mM NaCl, 50 mM Tris-Cl pH 7.5, 1% NP40, 10% glycerol, 2 mM NaF, 1 mM Na_3VO_4 and 1 protease inhibitor cocktail tablet/10 ml (Roche, Clare, Ireland) for 30 min and centrifuged at 16,100 g for 15 min at 4^0C. Lysates were run 5 times through columns containing 1ml IgG beads. Beads were washed 3 times in 10 ml of lysis buffer. 2 ml of TEV cleavage buffer (lysis buffer plus 0.5 mM EDTA, 1 mM DTT) and TEV protease (0.1 mg/ml) was added to the columns. Columns were incubated for 1.5 hr at room temperature, mixing occasionally. The eluate was adjusted to 2 mM $CaCl_2$ and added to 300 µl calmodulin sepharose beads. Beads were incubated for 1 hr at 4^0C. Beads were washed 3 times in 1 ml of wash buffer (lysis buffer plus 2 mM $CaCl_2$). Bound proteins were eluted in 300 µl 2X SDS-loading dye that was subsequently concentrated down to 50 µl. Eluted proteins were loaded on 12% SDS-PAGE gels and run for 2 hr at 100V. Each sample lane was divided into 6 gel segments for mass spectrometric analysis.

Protein Identification by Mass Spectrometry

Mass spectrometric analysis was performed at the FingerPrints Proteomics facility at University of Dundee, Scotland. Peptides were obtained using an in-gel digestion protocol and extracted prior to analysis by 1D nLC-MS/MS using an LTQ Orbitrap Velos Pro mass spectrometer (Thermo Scientific, Hemel Hempstead, United Kingdom). MS/MS data were searched against the IPI-human database (91464 sequences; 36355611 residues; European Bioinformatics Institute www.ebi.ac.uk) using in-house Mascot software (Matrix Science, London, UK). Identified proteins were ranked according to Mascot protein scores and listed using protein symbols as identifiers in Excel software (Microsoft Corporation, Redmond, USA). The COUNTIF function of Excel was used to identify proteins present in one or both purified actinin complexes but not in the control sample. A Mascot protein score of 100 was then applied as a cut off value to limit results to proteins that have been very reliably identified. This roughly corresponds to proteins with two distinct peptide matches. In the case of proteins present in both actinin complexes, at least one of the protein scores had to be greater than 100. Probable environmental contaminants such as keratins were then removed. Information about the subcellular localisation and functions of the remaining proteins was obtained from the Uniprot database (www.uniprot.org). Proteins that were likely to be false positives based on clear

THIS IS NOT THE VERSION OF RECORD - see doi:10.1042/BJ20121824

Accepted Manuscript

Licenced copy. Copying is not permitted, except with prior permission and as allowed by law.
© 2013 The Authors Journal compilation © 2013 Biochemical Society

Biochemical Journal Immediate Publication. Published on 04 Apr 2013 as manuscript BJ20121824

subcellular localisations that differ from the cytoplasmic and nuclear localisations that have been reported for actinins were then eliminated (secreted, mitochondrial matrix and ER/Golgi lumenal proteins) to obtain the final filtered list of identified proteins.

Results

Actinin-1 and -4 show tissue-specific differences in alternative spicing patterns

While the splicing of exon 19 in actinin-1 has been well characterised, the expression patterns of alternatively spliced actinin-4 isoforms have not been described in detail. Since splicing could confer unique properties to actinin-4, we employed reverse transcriptase PCR (rtPCR) to address this deficit in our knowledge. We first compared the tissue specificity of exon 19 splicing between actinin-1 and -4 by examining a panel of murine tissues. As previously reported for rat [3], the Ca^{++}-insensitive, exon 19b variant of actinin-1 was expressed in the maturing brain, cardiac and skeletal muscle, and in smooth muscle containing tissues such as stomach, intestine and bladder, while the brain-specific exon 19a+b variant was expressed postnatally in the brain and in adult spinal cord (Figure 1c). Actinin-1 exon 19a predominated in other tissues and in the immature brain (Figure 1c). For actinin-4 expression of the exon 19a variant was even more widespread and this was the only isoform detected in non-neuronal tissues (Figure 1c). In the brain actinin-4 exon 19a and 19b variants were equally abundant at all developmental stages examined and no 19a+b isoform was detected (Figure 1c). Thus in contrast to actinin-1, it is the Ca^{++}-sensitive, exon 19a version of actinin-4 that is expressed in skeletal muscle and smooth muscle, while the Ca^{++}-insensitive, exon 19b variant is restricted to neural tissues.

Actinin-4, unlike actinin-1, also exhibits alternative splicing of exon 8. The expression of actinin-4 exon 8 variants was examined by rtPCR using primers specific for exon 8a and 8b. The 8a variant was detected in all tissues examined (Figure 1c). By contrast the 8b variant was restricted to the brain, spinal cord, skeletal and cardiac muscle, and smooth muscle rich tissues. We next wanted to assess the relative expression of the 8a and 8b exons in some of these tissues. Since the PCR products obtained with different exon-specific primers cannot be directly compared, we instead used common flanking primers to amplify the exon 8 region of actinin-4 from P28 brain, kidney, lung, intestine, heart, and skeletal muscle and directly sequenced several independent PCR products for each tissue. Examination of sequencing chromatographs revealed that while exon 8b was by far the predominant variant expressed in the brain it was a very minor or undetectable component compared to exon 8a in the other tissues (data not shown).

Since our analysis in mice revealed that both non-muscle actinins are expressed as multiple splice variants in the neuronal tissues we wanted to establish if these splicing patterns were conserved in humans and whether alterations in splicing might occur in glioblastoma cells, given that actinin-4 is upregulated in glioblastomas and other cancers. rt-PCR from normal adult human brain tissue showed that alternative splicing patterns for actinin-1 and -4 exon 19 and actinin-4 exon 8 are conserved between murine and human brain (Figure 1d). Thus actinin-1 exon 19a+b and 19b variants and actinin-4 exon 19a, 19b, 8a and 8b variants were detected, with exon 8b being the predominant actinin-4 exon 8 variant present as assessed by direct sequencing of PCR products generated with flanking primers. In four glioblastoma cell lines examined, we found that there is a switch from exon 19b (Ca^{++}-insensitive) containing splice variants seen in normal brain to exclusively exon 19a (Ca^{++} -sensitive) variants of both actinin-1 and -4 (Figure 1d). These cell lines appeared to express exclusively the actinin-4 exon 8a variant compared to exon 8b that predominates in normal tissue (Figure 1d).

THIS IS NOT THE VERSION OF RECORD - see doi:10.1042/BJ20121824

Accepted Manuscript

Licenced copy. Copying is not permitted, except with prior permission and as allowed by law.
© 2013 The Authors Journal compilation © 2013 Biochemical Society

Biochemical Journal Immediate Publication. Published on 04 Apr 2013 as manuscript BJ20121824

THIS IS NOT THE VERSION OF RECORD - see doi:10.1042/BJ20121824

Actinin-1 and -4 have similar actin-binding properties

The actin-binding properties of actinin-1 and -4 have not been directly compared. Since differences between the proteins in this regard might underlie distinct functions, we employed actin cosedimentation assays to examine these properties. We first compared the affinity of actin-binding for the most widely expressed Ca^{++}-sensitive, actinin-1 (exon 19a) and actinin-4 (exon 8a, 19a) splice variants. In addition, actinin-4 (exon 8b, 19a) was also examined to determine whether inclusion of the variant exon 8b modulated actin-binding properties. Full-length actinins were recombinantly-expressed in *E. coli* to ensure pure homodimeric proteins were obtained, and the affinity tag used for purification was removed to prevent interference with actin-binding. Supernatants and pellets from cosedimentation assays were analysed on Coomassie-stained polyacrylamide gels and the proportion of actinin in each fraction quantified (Figure 2a). A single, ligand-binding site was assumed, and rectangular hyperbolic curves were fitted to plots of bound versus free actinin in order to calculate dissociation constants (Kd). Kd values calculated for actinin-1 (exon 19a), actinin-4 (exon 8a, 19a) and actinin-4 (exon 8b, 19a) were 1.93±0.56 μM, 2.96±0.38 μM and 3.96±1.19 μM respectively (Figure 2b). The differences in calculated Kd values between these isoforms did not reach statistical significance (Student's T-test). It appears therefore that the non-muscle actinins differ only very slightly in their binding affinity for actin filaments.

The Ca^{++}-sensitivity of actin-binding was also evaluated. Comparison of the actinin-1 (exon 19a) and actinin-4 (exon 8a, 19a) splice variants revealed very similar Ca^{++}-sensitivities with actin- binding decreasing by 50-60% at free Ca^{++} concentrations above 10 μM (Figure 2c and 2d). There was also a dramatic decrease in actin-bundling at these free Ca^{++} concentrations, that again was similar for both actinins (Figure 2e). By comparision actin-bundling by exon 19b-containing isoforms of both actinins was relatively insensitive to Ca^{++} at concentrations likely to occur in the cytosol (Figure 2e). The Ca^{++}-sensitivity of actin-binding was also examined for actinin-4 containing exon 8b and the brain-specific actinin-1 splice variant containing both exons 19a and 19b. Both of these isoforms were Ca^{++}-sensitive and displayed decreases in actin-binding of approximately 60% and 40% respectively at high free Ca^{++} concentrations (data not shown). Overall the intrinsic actin-binding properties of actinin-1 and -4 are very similar and seem unlikely to account for major functional differences between these proteins.

Non-muscle actinins have the potential to form heterodimers

It is unknown whether the non-muscle actinins have the ability to form heterodimers either with each other or with the muscle actinins. Dimerisation of actinins is largely mediated by the four spectrin-like repeats of the rod domain. To explore the potential for heterodimer formation we first examined the evolutionary conservation of amino acids present at the dimer interface, based on the known crystal structure of the human actinin-2 rod domain[7]. Conservation scores based on an alignment of actinin-1 and -4 sequences from divergent species were calculated and plotted onto the actinin-2 rod domain 3D structure using the ConSurf server [25, 26]. This analysis demonstrates that the dimer interface is highly conserved between actinin-1, -2 and -4 (Figure 3a), with very few non-conservative amino acid substitutions. By contrast the exposed surface of the rod shows significantly less sequence conservation. This supports the idea that the dimer interface is almost completely conserved between actinins and that heterodimer formation could occur.

To investigate this possibility directly we tested the ability of actinin rod domains to interact with each other in yeast two-hybrid assays. Rod domains from actinin-1,-2 and -4 were cloned into both bait and prey vectors. Interactions between rod domains were monitored by activation of the *HIS3* and *LacZ* reporter genes (Table 1). Activation of the *HIS3* reporter was seen for every combination of rod domains indicating that they are all capable of forming both homo- and heterodimers. In all cases the reporter gene expression for heterodimers was comparable to, or greater than, that for homodimers. Activation of the *LacZ* reporter was more variable, perhaps reflecting differences in expression levels between constructs, but again some homodimeric and heterodimer interactions were detected. Overall,

Accepted Manuscript

Licenced copy. Copying is not permitted, except with prior permission and as allowed by law.
© 2013 The Authors Journal compilation © 2013 Biochemical Society

Biochemical Journal Immediate Publication. Published on 04 Apr 2013 as manuscript BJ20121824

these assays suggest that actinin-1, -2 and -4 rod domains can indeed form heterodimers as well as homodimers.

To obtain a more quantitative measure of the propensity for homo- versus heterodimer formation we performed *in vitro* binding assays using purified proteins. To do this we used constructs encoding the amino and carboxyl terminal halves of actinin-1 and -4 (ABD-R2 and R3-CaM). Since spectrin-like repeats R1 and R2 form an interaction surface with spectrin-like repeats R3 and R4 in the rod domain, splitting the rod in half in this manner allows us to compare the affinity of homo- versus heterodimer formation for different actinins. We expressed and purified GST-tagged ABD-R2 and His_6-tagged R3-CaM domains for both actinin-1 and -4. These fusion proteins were mixed in various combinations and the ability of R3-CaM to interact with ABD-R2 was assessed by purification of the complex using glutathione sepharose beads (Figure 3b). Densitometric analysis was used to compare the levels of R3-CaM proteins bound to ABD-R2 proteins in each assay. The results show less than 5% differences in bound R3-CaM in homo- versus heterodimeric contexts indicating that non-muscle actinin homo- and heterodimers should form with approximately equal affinity (Figure 3c).

Non-muscle actinin heterodimers are prevalent in many cancer cell lines.

Our results to date demonstrate that actinin-1 and -4 rod domains can form heterodimers in the yeast two-hybrid system and *in vitro*. To assess whether the non-muscle actinins form heterodimers in cells in which they are co-expressed, we used native polyacrylamide gel electrophoresis to maintain non-denaturing conditions in order to preserve and detect heterodimers. We first examined HeLa cells that have endogenous expression of actinin-1 and 4. Western blotting with isoform-specific antibodies revealed that each protein migrated as two bands on native gels. The upper band for actinin-4 co-migrates with the lower band for actinin-1 and we take this band to represent actinin-1/-4 heterodimers and the other bands to represent homodimers. A prominent heterodimer band was observed for confluent, proliferating and migrating HeLa cells as well as in cells that had been deprived of serum (Figure 4a). Thus non-muscle actinin heterodimer formation occurs in HeLa cells grown under a variety of culture conditions. We also detected heterodimers in a number of other cancer cell lines, indicating that this phenomenon was not specific to HeLa cells (Figure 4b). Notably, MDA-MB-231 cells that express only actinin-4 do not show any heterodimer band verifying that the presence of this band is dependent on the presence of both actinin-1 and -4. To further demonstrate this point and to examine the dynamics of heterodimer formation we performed siRNA-mediated knockdown of actinin-4 in MCF-7 cells (Figure 4c). An ~80% knockdown of actinin-4 levels was achieved in these cells, resulting in a large decrease in both actinin-4 homo- and heterodimers. This was mirrored by decreased actinin-1 in the heterodimeric state and a consequent increase in actinin-1 levels in the homodimeric state. Taken together these results verify that these non-muscle actinin heterodimers are dependent on the co-expression of both actinins and that a reduction in the expression of either leads to a redistribution of the other towards the homodimeric state.

We next sought to quantify the relative abundance of homo- and heterodimers in the cell lines examined. We first quantified the relative amounts of each actinin in our panel of cell lines and calculated the ratio of actinin-1:actinin-4 for each type of cells (Figure 4d, see methods for details). We then determined the proportion of each actinin that was present as a heterodimer on native gels and used this to calculate the overall percentage of actinin-1/-4 heterodimers for each cell line (Figure 4e). Surprisingly, in those cell lines in which heterodimers were identified, they were more abundant than either homodimeric species and consumed close to 50% of the total non-muscle actinin.

Screening approaches to identify interacting partners of actinin-1 and actinin-4

Given their similar actin-binding properties and propensity to form heterodimers, isoform-specific functions of the non-muscle actinins are likely to be mediated by isoform-specific interactions with proteins other than actin filaments. Many actinin interacting proteins are known and in most cases for which it has been examined, these interactions are

THIS IS NOT THE VERSION OF RECORD - see doi:10.1042/BJ20121824

Accepted Manuscript

Licenced copy. Copying is not permitted, except with prior permission and as allowed by law.
© 2013 The Authors Journal compilation © 2013 Biochemical Society

Biochemical Journal Immediate Publication. Published on 04 Apr 2013 as manuscript BJ20121824

common to multiple actinins. In other cases isoform specificity has not been examined and thus very few validated isoform-specific interactions have been reported. We wanted to identify actinin interacting proteins and establish the isoform specificity of novel or known actinin interaction partners in a more systematic manner. We first employed the yeast two-hybrid system. While full-length proteins could not be used as baits for screening due to auto-activation of the reporter genes, the rod domains of both actinin-1 and -4 were suitable. Screening a mouse brain cDNA library with the actinin-1 rod yielded 10 positive clones; whereas a screen with the actinin-4 rod did not generate any positive clones. Among the actinin-1 positives were multiple clones for myozenin – a known actinin-2 interacting protein [28]. When directly co-transformed, the myozenin preys were also able to interact with the actinin-4 bait indicating that this is not an isoform-specific interaction. Single clones for two other proteins Homeodomain-interacting protein kinase 1 (HIPK1) and Polycomb protein SCMH1 were identified in our actinin-1 rod domain screen and were found to also interact with actinin-4, but were not investigated further. Overall, given the number of known actinin rod interactions, the number of proteins identified in our screen was very low and suggest that the yeast two-hybrid system was not an efficient screening method for our purpose.

As an alternative approach we used tandem affinity purification of actinin protein complexes coupled with mass spectrometry. Heterodimer formation between transfected and endogenous actinin could make it difficult to identify interacting-partners unique to either actinin-1 or -4. For this reason we used HEK cells which do not exhibit significant heterodimer formation (Figure 4b). We established stably transfected cell pools expressing TAP-tagged actinin-1 or -4 as well as control cells expressing TAP-tagged YFP. At least 70% of cells in these pools expressed the TAP-tagged constructs and western blotting indicated that expression levels were equivalent to endogenous actinin levels in HEK cells (data not shown). TAP-tagged actinin-1, -4 and YFP protein complexes were purified, and subjected to denaturing gel electrophoresis. Proteins present in each sample were analyzed by nano-liquid chromatography and MS/MS mass spectrometry and identified by searching against the IPI protein database. Non-specific interactions present in TAP-tagged YFP complexes and likely false positives or environmental contaminants were eliminated (see methods) to generate lists of proteins specifically identified in affinity purified actinin-1 and -4 complexes (Table 2). Several well-characterised actinin-interacting proteins were identified – validating the overall approach (underlined in the Table 2). Although we used HEK cells due to their low levels of endogenous heterodimers there appeared to be some degree of actinin-1/-4 heterodimer formation in our stably transfected cells since actinin-1 was found in actinin-4 complexes and visa versa (Table 2). Interestingly actinin-2 and -3 were also detected in both complexes providing further evidence that all combinations of heterodimers between muscle and non-muscle actinins are possible. The fact that relatively few common proteins were detected in both actinin-1 and -4 complexes suggested that despite the presence of some heterodimers, isoform-specific interactions could still be detected. More novel putative actinin-4 interacting partners were identified compared to actinin-1. Notably over half of these are proteins that are reported to localise partially or exclusively in the nucleus and have functions related to transcription, RNA-binding and mRNA splicing. These observations fit with the reported localisation of actinin-4 to the nucleus[12, 21-23, 29, 30]. Overall this screen provides a list of putative actinin-1 and -4 -specific interacting-proteins that might mediate or contribute to some of the reported isoform-specific functions of actinin-4 in particular.

Discussion

Alternative splicing and actin-binding properties of the non-muscle actinins

In this study we have systematically compared the alternative splicing patterns and actin-binding properties of actinin-1 and -4 for the first time. Having compared the actin-binding properties of the most widely expressed Ca^{++}-sensitive forms of the two non-muscle

THIS IS NOT THE VERSION OF RECORD - see doi:10.1042/BJ20121824

Accepted Manuscript

Licenced copy. Copying is not permitted, except with prior permission and as allowed by law.
© 2013 The Authors Journal compilation © 2013 Biochemical Society

Biochemical Journal Immediate Publication. Published on 04 Apr 2013 as manuscript BJ20121824

THIS IS NOT THE VERSION OF RECORD - see doi:10.1042/BJ20121824

actinins, we find that the affinity of actinin-1 (exon 19a), and actinin-4 (exon 8a, 19a) for F-actin are quite similar with Kd values of 1.93 μM and 2.96 μM respectively. In addition, their actin-bundling capacity and Ca^{++}-sensitivity of actin-binding and -bundling are nearly identical. Actinin-4 was first purified and cloned from chicken lung and was described as having low Ca^{++}-sensitivity[31, 32]. Our results using recombinant human actinin do not agree with this observation. This may reflect sequence differences in the EF-hand motifs between human and chick actinin or post-translational modifications in the protein purified from tissue that are not present in our bacterially expressed actinin. The non-muscle actinins are widely co-expressed. Yet actinin-4 knockout mice display specific kidney defects, while abnormalities in other tissues were not reported [20]. The similar actin-binding properties that we observe for the two non-muscle actinins are in agreement with this apparent functional redundancy between them in most tissues.

While actin-binding properties of the main Ca^{++}-sensitive non-muscle actinin isoforms are similar, our analysis of alternative splicing patterns reveals significant differences between actinin-1 and -4. In particular we find that the Ca^{++}-insensitive exon 19b variant of actinin-4 is only expressed in the nervous system. By contrast the exon 19b variant of actinin-1 is regarded as a smooth muscle isoform and is expressed in muscle and smooth muscle as well as in the adult brain. The exon 19a and 19b variants of actinin-4 are co-expressed in the brain at all stages examined; thus actinin-4 does not exhibit the developmental switching from the exon 19a to exon 19b-containing isoforms as observed for actinin-1 as the brain matures. Neither was an exon 19a+b variant of actinin-4 detected in the brain.

In muscle and smooth muscle cells Ca^{++}-insensitive forms of actinin are thought to facilitate relatively stable cross-linking of actin filaments despite continuous fluxes in Ca^{++} associated with muscle contraction [33]. Our results show that while muscle cells express both the Ca^{++}-sensitive and -insensitive variants of actinin-1, they express only the Ca^{++}-sensitive (exon 19a) variant of actinin-4. This Ca^{++}-sensitive actinin-4 may have distinct functions in muscle compared to other muscle actinin isoforms. Notably, potential roles for actinin-4 as a transcriptional regulator during muscle differentiation have been described [21, 30]. In the brain, actinins are components of the postsynaptic density at synapses [34]. Our data presents a complex picture of actinin splicing in the brain with Ca^{++}-sensitive and -insensitive variants of both actinin-1 (19a, 19a+b and 19b) and actinin-4 (19a and 19b) being co-expressed. Alternative splicing of actinins in neurons may serve to fine-tune the cross-linking of actin filaments at neuronal synapses where actinins interact with several key proteins involved in synaptic plasticity[35, 36]. In addition to synaptic functions in neurons, actinin-1 and -4 are also expressed in glial cells, and upregulation of actinin-4 has been reported in glioblastoma and proposed to promote cell migration and metastasis [17, 18]. In four glioblastoma cell lines we find a reversion of actinin-1 splicing to the exon 19a isoform observed in the immature brain. These cell lines also predominantly express the 19a–containing actinin-4 isoform. Thus for both actinin-1 and -4 only Ca^{++}-sensitive actinin isoforms are expressed in glioblastoma cells which may be of significance given the role intracellular Ca^{++} plays in the process of cancer cell migration and proliferation [37].

Alternative splicing of exon 8 occurs in several invertebrate lineages[4] and has been conserved in mammals, birds, amphibians and fish for actinin-4 but not the other actinins [4]. This suggests that exon 8b of actinin-4 plays some essential, evolutionarily conserved function. We find that alternative splicing of exon 8b occurs in the nervous system where it predominates over exon 8a, as well as in muscle and smooth muscle-containing tissues where it is a minor species relative to the exon 8a variant. Variations in the amino acid sequence encoded by exon 8 certainly have the potential to alter actin-binding properties and abnormal splicing of exon 8b is a feature of small cell lung cancer [38, 39]. However, the functional significance of alternative splicing of exon 8 has remained unclear. We find that the affinity of the exon 8b variant of actinin-4 for F-actin is not significantly different from that of the exon 8a variant and that both display similar Ca^{++}-sensitivities. This contrasts with the enhanced actin-binding of the 8b variant previously reported by Honda *et al* (2004)[38]. It

Accepted Manuscript

Licenced copy. Copying is not permitted, except with prior permission and as allowed by law.
© 2013 The Authors Journal compilation © 2013 Biochemical Society

Biochemical Journal Immediate Publication. Published on 04 Apr 2013 as manuscript BJ20121824

should be noted however that Honda *et al*. measured actin-binding of the isolated ABD and that the binding properties of this isoform may be different in the context of the intact actinin dimer. Overall our findings indicate that the actin- binding properties of actinin-1, and the exon 8a and 8b variants of actinin-4 are very similar. Expression of these isoforms may thus serve to fine tune the affinity of actinin for F-actin in particular contexts but would not alter actin cross-linking properties very dramatically.

Implications of non-muscle actinin heterodimerisation

The non-muscle actinins are generally regarded as distinct homodimeric entities. For example actinin-1 and -4 have been reported to have differential localisation in cells[12, 29, 30, 40] and to play differential, and sometimes opposing roles in cellular processes such as cell migration, proliferation and adhesion [17, 41]. Heterodimer formation is known to occur between the muscle actinins -2 and -3[9]. To our knowledge the ability of the non-muscle actinins to form heterodimers had not been directly investigated prior to this study. We present evidence from yeast two hybrid and *in vitro* binding assays that actinin-1 and -4 can form heterodimers with each other, as well as with actinin-2, in agreement with the conservation of the dimer interface between these isoforms. Furthermore, we examined the extent of heterodimer formation between endogenously expressed actinins in cells. Significant non-muscle heterodimer formation was observed in six of eight cell lines examined. Most surprisingly we found that heterodimers are more abundant than either homodimer species in these cell lines. In fact, these proportions of homo- and heterodimers are close to what would be expected if the probability of a newly-translated actinin monomer forming either a homo or heterodimer is simply proportional to the relative abundance of actinin-1 and -4 in the cell. Thus in a cell line in which actinin-1 and -4 are expressed equally, such as U87-MG (Figure 4d, 4e), there is 25% of each homodimer and 50% actinin-1/actinin-4 heterodimer. This would indicate that preferential homodimer formation between proteins being translated from the same mRNA does not occur. Alternatively homodimer formation may be favoured initially but monomeric subunits may subsequenntly be exchanged between until an equilibrium is reached between homo and heterodimers.

In our experiments, the degree of heterodimer formation varied between cell lines, and heterodimers were not observed in HEK cells despite that fact that they express both actinin-1 and -4. Actinin expression in HEK cells is somewhat lower than the other cell lines, but if the homodimer:heterodimer ratio was similar to other cells then heterodimers would still be detectable. This suggests that heterodimer formation may either require high cellular concentrations of actinins or may be regulated in a cell line-specific manner. Notably HEK cells were the only non-cancer cell line examined. Over-expression of actinin-4 has been reported in many types of tumours and is associated with high grade malignancies and poor outcomes[12, 15-17]. Our data indicates that when overexpressed, actinin-4 may be capable of forcing actinin-1 into the heterodimer state. This suggests that the cancer phenotype associated with actinin-4 over expression may not only be a consequence of acquisition or enhancement of an actinin-4-specific function but may reflect the disruption of actinin-1-specific functions due to the sequestration of actinin-1 into heterodimers. Alternatively these heterodimers may also have unique tumourigenic or metastatic promoting properties not possessed by homodimers. Thus the functional consequence of actinin-4 overexpression in a particular tumour may depend on the level of actinin-1 expression and the degree to which actinin-1 is sequestered into heterodimers.

The question of whether actinin-1/actinin-4 heterodimers exist in normal tissues *in vivo* also arrises. While we have not examined this directly in the present study, the presence of actinin heterodimers in platelets was well characterised by Olomucki and co-workers almost 30 years ago [42, 43]. These heterodimers probably contain actinin-1, but at that time actinin-4 had not been cloned, so the exact identity of these heterodimers remained unclear. Using isoform specific antibodies we find that, in addition to actinin-1, human platelets have high levels of actinin-4 as well as some sarcomeric actinin (actinin-2/3) (Supplementary

THIS IS NOT THE VERSION OF RECORD - see doi:10.1042/BJ20121824

Accepted Manuscript

Licenced copy. Copying is not permitted, except with prior permission and as allowed by law.
© 2013 The Authors Journal compilation © 2013 Biochemical Society

Biochemical Journal Immediate Publication. Published on 04 Apr 2013 as manuscript BJ20121824

Figure 1). Taken together this strongly indicates that platelets contain actinin-1/actinin-4 heterodimers and potentially heterodimers formed between muscle and non-muscle isoforms. The co-expression of multiple actinins in many tissues suggests that a variety of heterodimeric actinin species are likely to occur *in vivo*.

Actinin protein:protein interactions

Our observation that the non-muscle actinins have similar affinities for actin filaments and similar Ca^{++}- sensitivities indicates that differences in actin-binding properties are unlikely to explain isoform-specific functions, such as those that have been attributed to actinin-4. One possible explanation for such characteristics could be that actinin-4 has unique interacting partners thereby allowing it to carry out functions unmatched by actinin-1. Our proteomics screen revealed a number of putative actinin-4-specific binding proteins that might be linked to the described functions of actinin-4 in cancer and as a nucleo-cytoplasmic shuttling protein (Table 2). We identified cytoskeletal components like Myosin-10 and Filamin-C as well as two proteins – IQGAP2 and DOCK7, that have the potential to modulate actin dynamics through their regulation of Rho family GTPases. DOCK7 has been shown to act as a guanine nucleotide exchange factor for Rac1 and Rac3 [44], while IQGAP2 can regulate Rac1 and Cdc42, though not by acting as a classical GTPase activating protein [45]. These cytoskeletal proteins/regulators could potentially mediate some of the effects on cell migration and metastasis that have been ascribed to actinin-4 in the context of cancer. Apart from these cytoskeletal proteins, most of the remaining proteins identified in TAP-tagged actinin-4 complexes are nuclear proteins. This supports the idea that actinin-4 can shuttle in and out of the nucleus[23]. One of these nuclear proteins, CDKN2AIP is known to activate p53 and thus might connect actinin-4 to cancer phenotypes[46]. The remaining nuclear proteins identified are involved in either transcription or RNA binding / splicing. While there is no known role for actinin-4 in RNA splicing, several functional interactions of actinin-4 with transcriptional regulators have been described[21, 22, 24, 30]. The proteins identified here may expand this list.

Conclusions

Our data describes the tissue-specific alternative splicing of actinin-4 in detail for the first time. We also report that actin-binding properties of the non-muscle actinins are virtually identical. Additionally, we find that actinin-1 and -4 do not exist solely as distinct homodimeric entities but that they can readily form heterodimers composed of monomers that may have different properties and interacting proteins. Overall these findings significantly alter the context in which one views the isoform-specific functions of the non-muscle actinins.

Acknowledgements

This work was funded primarily through the Health Research Board, PhD Scholars Programme in Cancer Biology (PhD/2007/4). We thank Martha Phelan for help in preparing washed platelets. We are grateful to Anita Murphy, Anjali Pai and Gary Williamson for their contributions to the project while working in the laboratory, and to thank Kellie Dean for reading the manuscript.

THIS IS NOT THE VERSION OF RECORD - see doi:10.1042/BJ20121824

Accepted Manuscript

Licenced copy. Copying is not permitted, except with prior permission and as allowed by law.
© 2013 The Authors Journal compilation © 2013 Biochemical Society

Biochemical Journal Immediate Publication. Published on 04 Apr 2013 as manuscript BJ20121824

Bibliography

1 Otey, C. A. and Carpen, O. (2004) Alpha-actinin revisited: a fresh look at an old player. Cell Motil Cytoskeleton. **58**, 104-111

2 Waites, G. T., Graham, I. R., Jackson, P., Millake, D. B., Patel, B., Blanchard, A. D., Weller, P. A., Eperon, I. C. and Critchley, D. R. (1992) Mutually exclusive splicing of calcium-binding domain exons in chick alpha-actinin. J Biol Chem. **267**, 6263-6271

3 Kremerskothen, J., Teber, I., Wendholt, D., Liedtke, T., Bockers, T. M. and Barnekow, A. (2002) Brain-specific splicing of alpha-actinin 1 (ACTN1) mRNA. Biochem Biophys Res Commun. **295**, 678-681

4 Lek, M., MacArthur, D. G., Yang, N. and North, K. N. (2010) Phylogenetic analysis of gene structure and alternative splicing in alpha-actinins. Mol Biol Evol. **27**, 773-780

5 Franzot, G., Sjoblom, B., Gautel, M. and Djinovic Carugo, K. (2005) The crystal structure of the actin binding domain from alpha-actinin in its closed conformation: structural insight into phospholipid regulation of alpha-actinin. J Mol Biol. **348**, 151-165

6 Djinovic Carugo, K., Young, P., Gautel, M. and Saraste, M. (1999) Structure of the alpha-actinin rod: molecular basis for cross-linking of actin filaments. Cell. **98**, 537-546

7 Ylanne, J., Scheffzek, K., Young, P. and Saraste, M. (2001) Crystal Structure of the alpha-Actinin Rod Reveals an Extensive Torsional Twist. Structure (Camb). **9**, 597-604.

8 Young, P. and Gautel, M. (2000) The interaction of titin and alpha-actinin is controlled by a phospholipid-regulated intramolecular pseudoligand mechanism. Embo J. **19**, 6331-6340

9 Chan, Y., Tong, H. Q., Beggs, A. H. and Kunkel, L. M. (1998) Human skeletal muscle-specific alpha-actinin-2 and -3 isoforms form homodimers and heterodimers in vitro and in vivo. Biochem Biophys Res Commun. **248**, 134-139

10 Djinovic-Carugo, K., Gautel, M., Ylanne, J. and Young, P. (2002) The spectrin repeat: a structural platform for cytoskeletal protein assemblies. FEBS letters. **513**, 119-123

11 Sjoblom, B., Salmazo, A. and Djinovic-Carugo, K. (2008) Alpha-actinin structure and regulation. Cell Mol Life Sci. **65**, 2688-2701

12 Honda, K., Yamada, T., Endo, R., Ino, Y., Gotoh, M., Tsuda, H., Yamada, Y., Chiba, H. and Hirohashi, S. (1998) Actinin-4, a novel actin-bundling protein associated with cell motility and cancer invasion. J Cell Biol. **140**, 1383-1393

13 Barbolina, M. V., Adley, B. P., Kelly, D. L., Fought, A. J., Scholtens, D. M., Shea, L. D. and Stack, M. S. (2008) Motility-related actinin alpha-4 is associated with advanced and metastatic ovarian carcinoma. Lab Invest. **88**, 602-614

14 Yamamoto, S., Tsuda, H., Honda, K., Takano, M., Tamai, S., Imoto, I., Inazawa, J., Yamada, T. and Matsubara, O. (2012) ACTN4 gene amplification and actinin-4 protein overexpression drive tumour development and histological progression in a high-grade subset of ovarian clear-cell adenocarcinomas. Histopathology. **60**, 1073-1083

15 Honda, K., Yamada, T., Hayashida, Y., Idogawa, M., Sato, S., Hasegawa, F., Ino, Y., Ono, M. and Hirohashi, S. (2005) Actinin-4 increases cell motility and promotes lymph node metastasis of colorectal cancer. Gastroenterology. **128**, 51-62

Licenced copy. Copying is not permitted, except with prior permission and as allowed by law.
© 2013 The Authors Journal compilation © 2013 Biochemical Society

THIS IS NOT THE VERSION OF RECORD - see doi:10.1042/BJ20121824

Accepted Manuscript

Biochemical Journal Immediate Publication. Published on 04 Apr 2013 as manuscript BJ20121824

16 Kikuchi, S., Honda, K., Tsuda, H., Hiraoka, N., Imoto, I., Kosuge, T., Umaki, T., Onozato, K., Shitashige, M., Yamaguchi, U., Ono, M., Tsuchida, A., Aoki, T., Inazawa, J., Hirohashi, S. and Yamada, T. (2008) Expression and gene amplification of actinin-4 in invasive ductal carcinoma of the pancreas. Clin Cancer Res. **14**, 5348-5356

17 Quick, Q. and Skalli, O. (2010) Alpha-actinin 1 and alpha-actinin 4: contrasting roles in the survival, motility, and RhoA signaling of astrocytoma cells. Exp Cell Res. **316**, 1137-1147

18 Sen, S., Dong, M. and Kumar, S. (2009) Isoform-specific contributions of alpha-actinin to glioma cell mechanobiology. PLoS One. **4**, e8427

19 Kaplan, J. M., Kim, S. H., North, K. N., Rennke, H., Correia, L. A., Tong, H. Q., Mathis, B. J., Rodriguez-Perez, J. C., Allen, P. G., Beggs, A. H. and Pollak, M. R. (2000) Mutations in ACTN4, encoding alpha-actinin-4, cause familial focal segmental glomerulosclerosis. Nat Genet. **24**, 251-256

20 Kos, C. H., Le, T. C., Sinha, S., Henderson, J. M., Kim, S. H., Sugimoto, H., Kalluri, R., Gerszten, R. E. and Pollak, M. R. (2003) Mice deficient in alpha-actinin-4 have severe glomerular disease. J Clin Invest. **111**, 1683-1690

21 Chakraborty, S., Reineke, E. L., Lam, M., Li, X., Liu, Y., Gao, C., Khurana, S. and Kao, H. Y. (2006) Alpha-actinin 4 potentiates myocyte enhancer factor-2 transcription activity by antagonizing histone deacetylase 7. J Biol Chem. **281**, 35070-35080

22 Khurana, S., Chakraborty, S., Cheng, X., Su, Y. T. and Kao, H. Y. (2011) The actin-binding protein, actinin alpha 4 (ACTN4), is a nuclear receptor coactivator that promotes proliferation of MCF-7 breast cancer cells. J Biol Chem. **286**, 1850-1859

23 Kumeta, M., Yoshimura, S. H., Harata, M. and Takeyasu, K. (2010) Molecular mechanisms underlying nucleocytoplasmic shuttling of actinin-4. J Cell Sci. **123**, 1020-1030

24 Babakov, V. N., Petukhova, O. A., Turoverova, L. V., Kropacheva, I. V., Tentler, D. G., Bolshakova, A. V., Podolskaya, E. P., Magnusson, K. E. and Pinaev, G. P. (2008) RelA/NF-kappaB transcription factor associates with alpha-actinin-4. Exp Cell Res. **314**, 1030-1038

25 Ashkenazy, H., Erez, E., Martz, E., Pupko, T. and Ben-Tal, N. (2010) ConSurf 2010: calculating evolutionary conservation in sequence and structure of proteins and nucleic acids. Nucleic Acids Res. **38**, W529-533

26 Landau, M., Mayrose, I., Rosenberg, Y., Glaser, F., Martz, E., Pupko, T. and Ben-Tal, N. (2005) ConSurf 2005: the projection of evolutionary conservation scores of residues on protein structures. Nucleic Acids Res. **33**, W299-302

27 Young, P., Ferguson, C., Banuelos, S. and Gautel, M. (1998) Molecular structure of the sarcomeric Z-disk: two types of titin interactions lead to an asymmetrical sorting of alpha-actinin. EMBO J. **17**, 1614-1624

28 Takada, F., Vander Woude, D. L., Tong, H. Q., Thompson, T. G., Watkins, S. C., Kunkel, L. M. and Beggs, A. H. (2001) Myozenin: an alpha-actinin- and gamma-filamin-binding protein of skeletal muscle Z lines. Proc Natl Acad Sci U S A. **98**, 1595-1600

29 Bolshakova, A., Petukhova, O., Turoverova, L., Tentler, D., Babakov, V., Magnusson, K. E. and Pinaev, G. (2007) Extra-cellular matrix proteins induce re-distribution of alpha-actinin-1 and alpha-actinin-4 in A431 cells. Cell Biol Int. **31**, 360-365

THIS IS NOT THE VERSION OF RECORD - see doi:10.1042/BJ20121824

Accepted Manuscript

Licenced copy. Copying is not permitted, except with prior permission and as allowed by law.
© 2013 The Authors Journal compilation © 2013 Biochemical Society

Biochemical Journal Immediate Publication. Published on 04 Apr 2013 as manuscript BJ20121824

30 Goffart, S., Franko, A., Clemen, C. S. and Wiesner, R. J. (2006) Alpha-actinin 4 and BAT1 interaction with the cytochrome c promoter upon skeletal muscle differentiation. Curr Genet. **49**, 125-135

31 Imamura, M. and Masaki, T. (1992) A novel nonmuscle alpha-actinin. Purification and characterization of chicken lung alpha-actinin. J Biol Chem. **267**, 25927-25933

32 Imamura, M., Sakurai, T., Ogawa, Y., Ishikawa, T., Goto, K. and Masaki, T. (1994) Molecular cloning of low-Ca(2+)-sensitive-type non-muscle alpha-actinin. Eur J Biochem. **223**, 395-401

33 Blanchard, A., Ohanian, V. and Critchley, D. (1989) The structure and function of alpha-actinin. J Muscle Res Cell Motil. **10**, 280-289.

34 Walikonis, R. S., Jensen, O. N., Mann, M., Provance, D. W., Jr., Mercer, J. A. and Kennedy, M. B. (2000) Identification of proteins in the postsynaptic density fraction by mass spectrometry. J Neurosci. **20**, 4069-4080.

35 Walikonis, R. S., Oguni, A., Khorosheva, E. M., Jeng, C. J., Asuncion, F. J. and Kennedy, M. B. (2001) Densin-180 forms a ternary complex with the (alpha)-subunit of Ca2+/calmodulin-dependent protein kinase II and (alpha)-actinin. J Neurosci. **21**, 423-433.

36 Wyszynski, M., Lin, J., Rao, A., Nigh, E., Beggs, A. H., Craig, A. M. and Sheng, M. (1997) Competitive binding of alpha-actinin and calmodulin to the NMDA receptor. Nature. **385**, 439-442

37 Prevarskaya, N., Skryma, R. and Shuba, Y. (2011) Calcium in tumour metastasis: new roles for known actors. Nat Rev Cancer. **11**, 609-618

38 Honda, K., Yamada, T., Seike, M., Hayashida, Y., Idogawa, M., Kondo, T., Ino, Y. and Hirohashi, S. (2004) Alternative splice variant of actinin-4 in small cell lung cancer. Oncogene. **23**, 5257-5262

39 Weins, A., Schlondorff, J. S., Nakamura, F., Denker, B. M., Hartwig, J. H., Stossel, T. P. and Pollak, M. R. (2007) Disease-associated mutant alpha-actinin-4 reveals a mechanism for regulating its F-actin-binding affinity. Proc Natl Acad Sci U S A. **104**, 16080-16085

40 Araki, N., Hatae, T., Yamada, T. and Hirohashi, S. (2000) Actinin-4 is preferentially involved in circular ruffling and macropinocytosis in mouse macrophages: analysis by fluorescence ratio imaging. J Cell Sci. **113 (Pt 18)**, 3329-3340

41 Celli, L., Ryckewaert, J. J., Delachanal, E. and Duperray, A. (2006) Evidence of a functional role for interaction between ICAM-1 and nonmuscle alpha-actinins in leukocyte diapedesis. J Immunol. **177**, 4113-4121

42 Gache, Y., Landon, F. and Olomucki, A. (1984) Polymorphism of alpha-actinin from human blood platelets. Homodimeric and heterodimeric forms. Eur J Biochem. **141**, 57-61

43 Landon, F., Gache, Y., Touitou, H. and Olomucki, A. (1985) Properties of two isoforms of human blood platelet alpha-actinin. Eur J Biochem. **153**, 231-237

44 Watabe-Uchida, M., John, K. A., Janas, J. A., Newey, S. E. and Van Aelst, L. (2006) The Rac activator DOCK7 regulates neuronal polarity through local phosphorylation of stathmin/Op18. Neuron. **51**, 727-739

45 Brill, S., Li, S., Lyman, C. W., Church, D. M., Wasmuth, J. J., Weissbach, L., Bernards, A. and Snijders, A. J. (1996) The Ras GTPase-activating-protein-related human protein IQGAP2 harbors a potential actin binding domain and interacts with calmodulin and Rho family GTPases. Mol Cell Biol. **16**, 4869-4878

THIS IS NOT THE VERSION OF RECORD - see doi:10.1042/BJ20121824

Accepted Manuscript

Licenced copy. Copying is not permitted, except with prior permission and as allowed by law.
© 2013 The Authors Journal compilation © 2013 Biochemical Society

Biochemical Journal Immediate Publication. Published on 04 Apr 2013 as manuscript BJ20121824

46 Hasan, M. K., Yaguchi, T., Minoda, Y., Hirano, T., Taira, K., Wadhwa, R. and Kaul, S. C. (2004) Alternative reading frame protein (ARF)-independent function of CARF (collaborator of ARF) involves its interactions with p53: evidence for a novel p53-activation pathway and its negative feedback control. Biochem J. **380**, 605-610

47 Ronty, M., Taivainen, A., Moza, M., Otey, C. A. and Carpen, O. (2004) Molecular analysis of the interaction between palladin and alpha-actinin. FEBS letters. **566**, 30-34

48 Xia, H., Winokur, S. T., Kuo, W. L., Altherr, M. R. and Bredt, D. S. (1997) Actinin-associated LIM protein: identification of a domain interaction between PDZ and spectrin-like repeat motifs. J Cell Biol. **139**, 507-515

49 Huttelmaier, S., Illenberger, S., Grosheva, I., Rudiger, M., Singer, R. H. and Jockusch, B. M. (2001) Raver1, a dual compartment protein, is a ligand for PTB/hnRNPI and microfilament attachment proteins. J Cell Biol. **155**, 775-786

50 Vallenius, T., Luukko, K. and Makela, T. P. (2000) CLP-36 PDZ-LIM protein associates with nonmuscle alpha-actinin-1 and alpha-actinin-4. J Biol Chem. **275**, 11100-11105

THIS IS NOT THE VERSION OF RECORD - see doi:10.1042/BJ20121824

Accepted Manuscript

Licenced copy. Copying is not permitted, except with prior permission and as allowed by law.
© 2013 The Authors Journal compilation © 2013 Biochemical Society

Biochemical Journal Immediate Publication. Published on 04 Apr 2013 as manuscript BJ20121824

Table 1. Analysis of actinin homodimer and heterodimer formation by yeast two-hybrid assay.

The ability of actinin-1/-2/-4 rod domains (baits) to interact with actinin-1/-2/-4 rod domains (preys) was tested using the yeast two-hybrid system. Empty bait and prey vectors were included as negative controls. Interactions between bait and prey were indicated by expression of two reporter genes – *His3* and *LacZ* coding for β-galactosidase (β-gal).

Bait \ Prey	Actinin-1		Actinin-2		Actinin-4		Empty vector	
	His3	β-gal	His3	β-gal	His3	β-gal	His3	β-gal
Actinin-1	++	+	+++	-	+++	-	-	-
Actinin-2	+++	++	+++	++	+++	++	-	-
Actinin-4	+++	-	+++	-	+	-	-	-
Empty vector	-	-	-	-	-	-	-	-

THIS IS NOT THE VERSION OF RECORD - see doi:10.1042/BJ20121824

Accepted Manuscript

Licenced copy. Copying is not permitted, except with prior permission and as allowed by law.
© 2013 The Authors Journal compilation © 2013 Biochemical Society

Biochemical Journal Immediate Publication. Published on 04 Apr 2013 as manuscript BJ20121824

Table 2. Proteomic analysis of actinin-1 and -4 interacting proteins

Proteins previously reported to interact with actinin are underlined

Proteins identified only in actinin-1 complexes

Protein Symbol	Mascot Score	Name	Subcellular Location	Function
DDX17	210	Probable ATP-dependent RNA helicase DDX17 isoform 3	Nucleus	Transcriptional regulation
PALLD[47]	175	Isoform 2 of Palladin	Cytosol	Actin cytoskeleton: organisation
CAMK2B[35]	103	Calcium/calmodulin-dependent protein kinase type II subunit beta	Cytosol	Protein kinase
PDLIM3[48]	103	PDZ and LIM domain protein 3	Cytosol	Actin cytoskeleton: organisation
PRDX2	100	Peroxiredoxin-2	Cytosol	Redox regulation in cells

Proteins identified only in actinin-4 complexes

Gene Symbol	Mascot Score	Name	Subcellular Location	Function
LRPPRC	2257	Leucine-rich PPR motif-containing protein, mitochondrial	Mitochondria, Nucleus, Cytosol	RNA-binding
IQGAP2	1894	Isoform 1 of Ras GTPase-activating-like protein IQGAP2	Cytosol	Cytoskeletal regulation
DOCK7	588	Dedicator of cytokinesis protein 7	Cytosol	Cytoskeletal regulation
FLNC	544	Isoform 1 of Filamin-C	Cytosol	Actin cytoskeleton: cross-linker
RAVER1[49]	457	ribonucleoprotein PTB-binding 1	Nucleus, Cytosol	mRNA splicing, cytoskeletal
SF3B2	432	Splicing factor 3B subunit 2	Nucleus	mRNA splicing
UBR5	399	E3 ubiquitin-protein ligase UBR5	Nucleus	Ubiquitination, Transcription
PRRC2A	353	Isoform 1 of Protein PRRC2A	Nucleus, Cytosol	mRNA Splicing
CDKN2AIP	203	CDKN2A-interacting protein	Nucleus	Activation of p53
PPFIA1	160	Isoform 1 of Liprin-alpha-1	Cytosol	Signaling / Scaffolding
TCEAL4	138	Isoform 2 of Transcription elongation factor A protein-like 4	Nucleus	Transcription
ELAVL1	126	Similar to ELAV-like protein 1	Nucleus, Cytosol	RNA-binding
SPRR2E	117	Small proline-rich protein 2E	Cytosol	Cytoskeletal component
SART1	113	U4/U6.U5 tri-snRNP-associated protein 1	Nucleus	mRNA splicing
TCERG1	108	Transcription elongation regulator 1	Nucleus	Transcription
MYH10	104	Isoform 1 of Myosin-10	Cytosol	Actin cytoskeleton: motor
SMARCC2	103	Isoform 2 of SWI/SNF complex subunit SMARCC2	Nucleus	Transcription
SF3B4	100	Splicing factor 3B subunit 4	Nucleus	mRNA splicing
MYL6	100	Non-muscle Myosin light chain 6	Cytosol	Actin cytoskeleton: motor

Proteins identified both in actinin-1 and -4 complexes

Gene Symbol	Mascot Scores	Name	Subcellular Location	Function
ACTN1	7522, 3925	Alpha actinin 1	Cytosol	Actin cytoskeleton: cross-linker
ACTN4	4814, 6909	Alpha actinin 4	Cytosol, Nucleus	Actin cytoskeleton: cross-linker
ACTN2	1961, 1114	Alpha actinin 2	Cytosol	Actin cytoskeleton: cross-linker
ACTN3	1366, 1071	Alpha actinin-3	Cytosol	Actin cytoskeleton: cross-linker
MYH9	103, 391	Isoform 1 of Myosin-9	Cytosol	Actin cytoskeleton: motor
PDLIM1[50]	208, 38	PDZ and LIM domain protein 1	Cytosol	Cytoskeletal, Stress Fibers

THIS IS NOT THE VERSION OF RECORD - see doi:10.1042/BJ20121824

Accepted Manuscript

Licenced copy. Copying is not permitted, except with prior permission and as allowed by law.
© 2013 The Authors Journal compilation © 2013 Biochemical Society

Biochemical Journal Immediate Publication. Published on 04 Apr 2013 as manuscript BJ20121824

Figure Legends

Figure 1

Analysis of the alternative splicing patterns of actinin-1 and -4 exons 8 and 19

(**A**) Schematic depiction of the alternative splicing of exon 19 that encodes part of the first EF-hand of the non-muscle actinins. Mutually exclusive splicing results in the inclusion of either exon 19a or exon 19b to generate Ca^{++}-sensitive and -insensitive isoforms respectively (black lines). Inclusion of both exons in the mature mRNA transcript can also occur for actinin-1[3] (grey lines). Primers flanking exon 19 were used for rtPCR and are indicated by arrows (**B**) Schematic depiction of mutually exclusive alternative splicing of exon 8 in actinin-4. Primer pairs in which one primer was specific for either exon 8a or 8b were used for rtPCR and are indicated by arrows. (**C**) rtPCR analysis of the alternative splicing patterns of actinin-1 and -4 exon 19 and actinin-4 exon 8 that occur in various murine tissues as indicated. The 15bp size difference between exon 19a and 19b allows these two splice variants to be distinguished. (**D**) rtPCR analysis of the alternative splicing patterns of actinin-1 and -4 exon 19 and actinin-4 exon 8 that occur in normal human brain versus a panel of human glioblastoma cell lines.

Figure 2

Comparison of the actin-binding affinities and Ca^{++}-sensitivities of actinin-1 and -4

(**A**) Representative actin-binding assay for actinin-1 (exon 19a). Increasing concentrations of actinin as indicated were incubated with F-actin, and subjected to centrifugation at 112,000 g. Bound and free actinin were quantified from Coomassie blue-stained SDS PAGE gels of the pellet and supernatant samples. (**B**) Calculation of the actin-binding affinity of actinin-1 (exon 19a), actinin-4 (exon 8a, 19a) and actinin-4 (exon 8b, 19a). Representative plots of bound versus free actinin are shown. The indicated Kd values for the interaction of each isoform with actin were calculated from data from ≥ 3 independent assays. (**C**) Comparison of the Ca^{++}-sensitivity of actin-binding between actinin-1 (exon 19a) and actinin-4 (exon 8a, 19a). Fixed concentrations of F-actin and actinin were incubated in the presence of the indicated free Ca^{++} concentrations. Pellet samples were analysed by Coomassie-stained SDS-PAGE gels. **(D)** Graph of bound actinin versus Ca^{++} concentration was plotted to analyse the Ca^{++}-sensitivity of actin-binding for actinin-1 (exon 19a) and actinin-4 (exon 19b). **(E)** Graph of bound actin versus Ca^{++} concentration was plotted to analyse the Ca^{++}-sensitivity of actin-bundling for several non-muscle actinin isoforms. Bundling assays were performed in a similar manner to actin-binding assays but with centrifugation at 10,000 g. Actinin-1 (exon 19a) = solid line square black data points; actinin-1 (exon 19b) = solid line square white data points, actinin-4 (exon 8a, 19a) = dashed line circular black data points and actinin-4 (exon 8b, 19b) = dashed line circular white data points.

THIS IS NOT THE VERSION OF RECORD - see doi:10.1042/BJ20121824

Accepted Manuscript

Licenced copy. Copying is not permitted, except with prior permission and as allowed by law.
© 2013 The Authors Journal compilation © 2013 Biochemical Society

Biochemical Journal Immediate Publication. Published on 04 Apr 2013 as manuscript BJ20121824

Figure 3

Analysis of the propensity for non-muscle actinins to form heterodimers

(**A**) Evolutionary conservation of amino acids in the actinin-1, -2 and -4 rod domains. Conservation scores are plotted onto one subunit of the dimeric actinin-2 rod structure using the ConSurf server [25, 26] (backbone and side chains depicted as spheres). A backbone only trace of the other subunit is shown. Two views of the structure are shown to highlight the conserved dimer interface (left) and less conserved, exposed surface of the rod (right). Conservation scores are visualised on a scale of nine grades with most variable positions colored turquoise, and most conserved positions colored maroon. The amino terminus (R1) of the colored subunit is to the left. (**B**) *In vitro* analysis of actinin-1 and -4 homodimeric versus heterodimeric interactions. GST-tagged actinin-1/-4 ABD-R2 domains were incubated with His_6-tagged actinin-1/-4 R3-CaM domains and bound to glutathione sepharose. After washing, eluted proteins were analysed on Coomassie-stained SDS-PAGE gels. (**C**) Bound R3-CaM domains were quantified by densitometry and the amount of bound R3-CaM for heterodimeric interactions was expressed as a percentage of that observed for the equivalent homodimeric combination of proteins.

Figure 4

Actinin-1 / -4 heterodimer formation in cultured cells.

(**A**) Actinin heterodimers in HeLa cells grown under a variety of conditions. Heterodimers were detected by native PAGE and western blotting using antibodies specific for actinin-1 (red) and actinin-4 (green). Upper red band represents actinin-1 present in homodimers, lower red band represents actinin-1 present in heterodimers, upper green band represents actinin-4 present in heterodimers and lower green band represents actinin-4 present homodimers. Merged image shows heterodimer represented by an intermediate orange/yellow band. (**B**) Native PAGE detection of actinin homodimers and heterodimers present in a panel of cell lines. (**C**) Native PAGE analysis of lysates from MCF-7 cells following siRNA-mediated knockdown of actinin-4. (**D**) Relative amounts of actinin-1 and -4 present in the indicated cell lines as determined by SDS PAGE and quantitative western blotting. The ratio of actinin-1:actinin-4 is indicated above the chart. (**E**) Actinin-1/actinin-4 heterodimers expressed as a proportion of total dimeric actinin for the indicated cell lines. The proportion of each isoform present as heterodimers was quantified by native PAGE and western blotting and plotted onto the graph of relative actinin levels shown in (D). The percentage of heterodimer for each cell line is indicated above the graph.

THIS IS NOT THE VERSION OF RECORD - see doi:10.1042/BJ20121824

Accepted Manuscript

Licenced copy. Copying is not permitted, except with prior permission and as allowed by law.
© 2013 The Authors Journal compilation © 2013 Biochemical Society

Biochemical Journal Immediate Publication. Published on 04 Apr 2013 as manuscript BJ20121824

Figure 1
Analysis of the alternative splicing patterns of actinin-1 and -4 exons 8 and 19

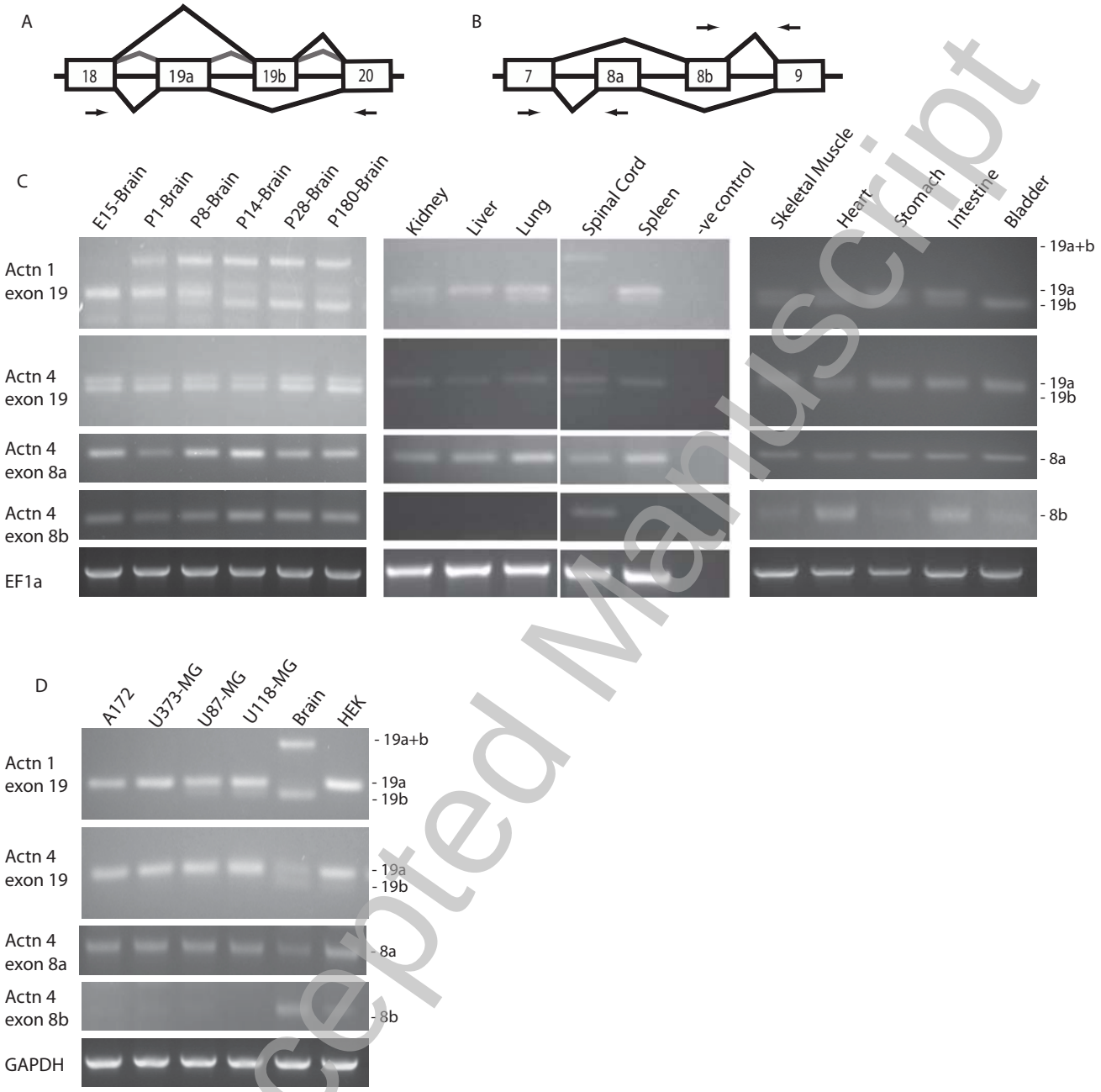

THIS IS NOT THE VERSION OF RECORD - see doi:10.1042/BJ20121824

Accepted Manuscript

Licenced copy. Copying is not permitted, except with prior permission and as allowed by law.
© 2013 The Authors Journal compilation © 2013 Biochemical Society

Biochemical Journal Immediate Publication. Published on 04 Apr 2013 as manuscript BJ20121824

Figure 2. Analysis of the actin-binding affinities and calcium-sensitivities of the non-muscle actinins

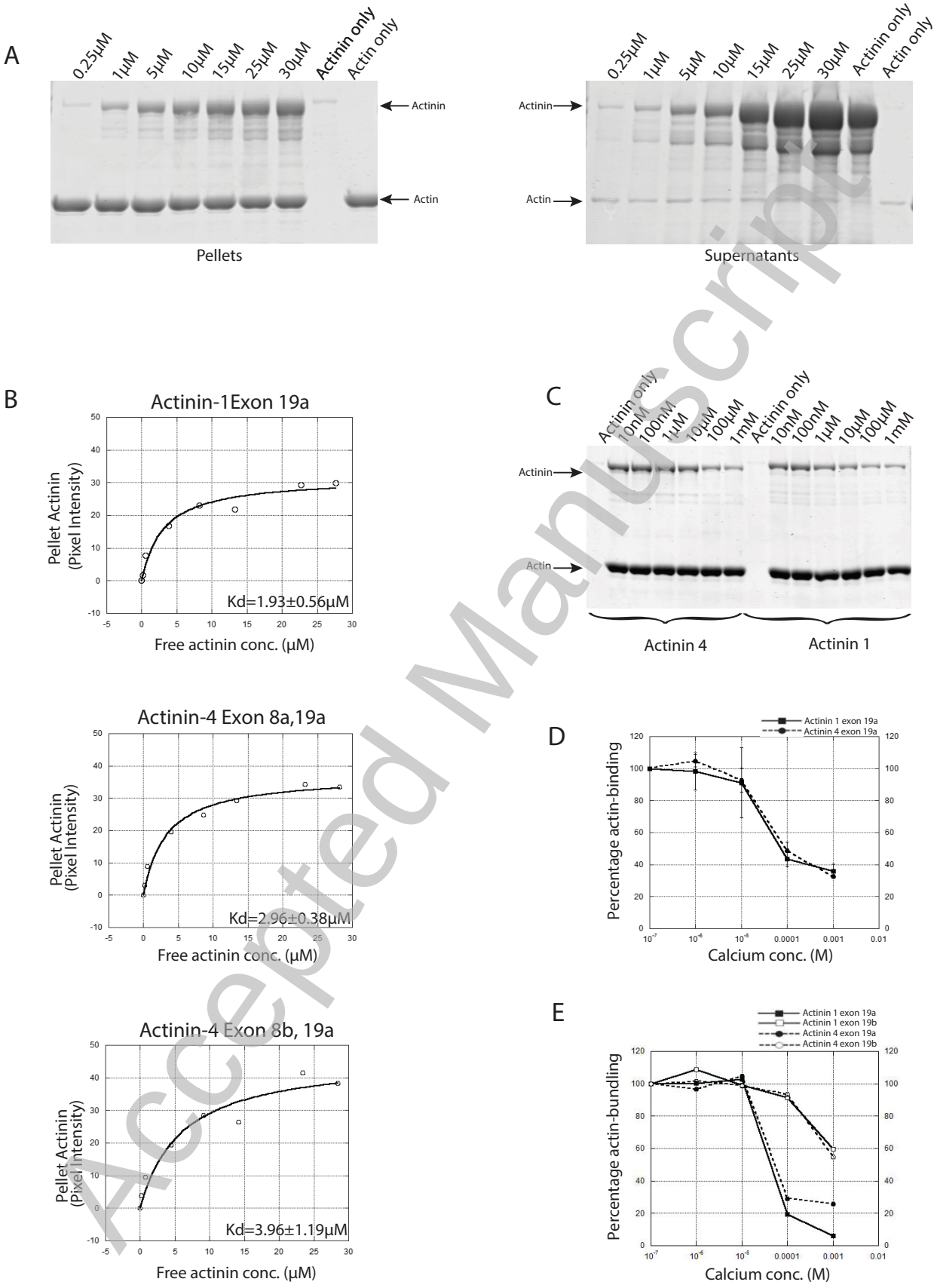

THIS IS NOT THE VERSION OF RECORD - see doi:10.1042/BJ20121824

Accepted Manuscript

Licenced copy. Copying is not permitted, except with prior permission and as allowed by law.
© 2013 The Authors Journal compilation © 2013 Biochemical Society

Biochemical Journal Immediate Publication. Published on 04 Apr 2013 as manuscript BJ20121824

Figure 3
Analysis of the propensity for non-muscle actinins to form heterodimers

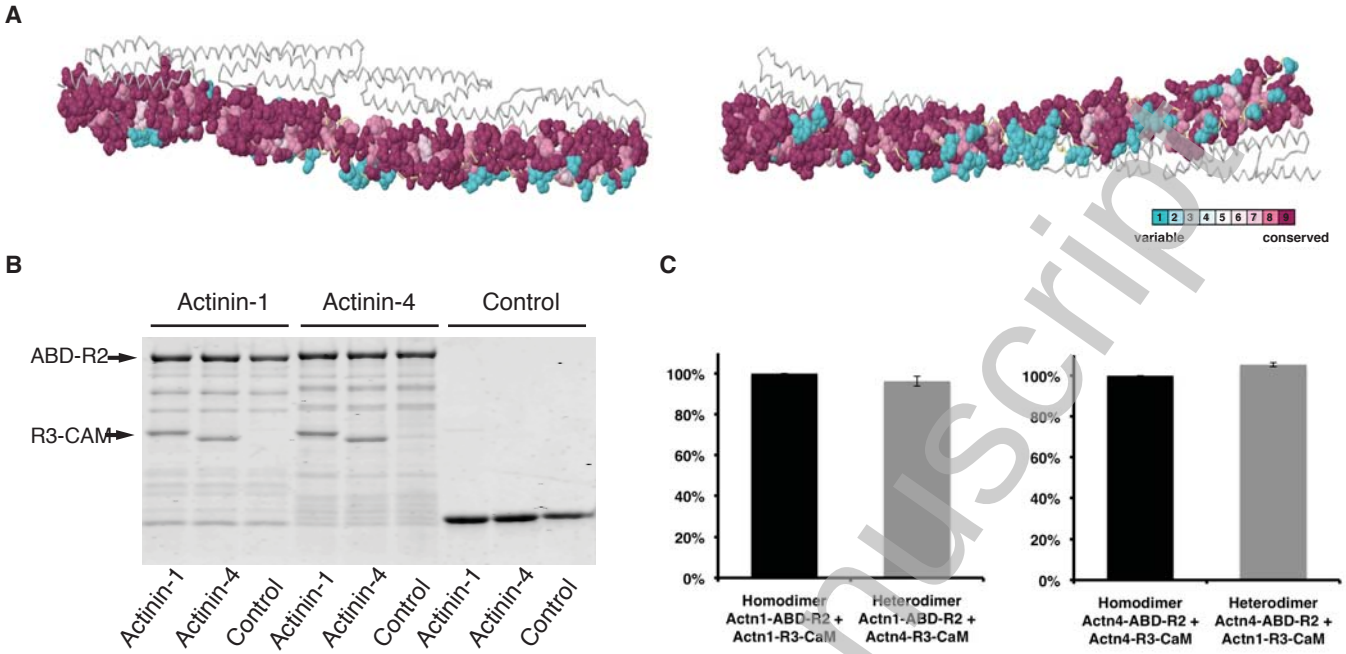

THIS IS NOT THE VERSION OF RECORD - see doi:10.1042/BJ20121824

Accepted Manuscript

Licenced copy. Copying is not permitted, except with prior permission and as allowed by law.
© 2013 The Authors Journal compilation © 2013 Biochemical Society

Biochemical Journal Immediate Publication. Published on 04 Apr 2013 as manuscript BJ20121824

Figure 4
Actinin-1 / -4 heterodimer formation in cultured cells.

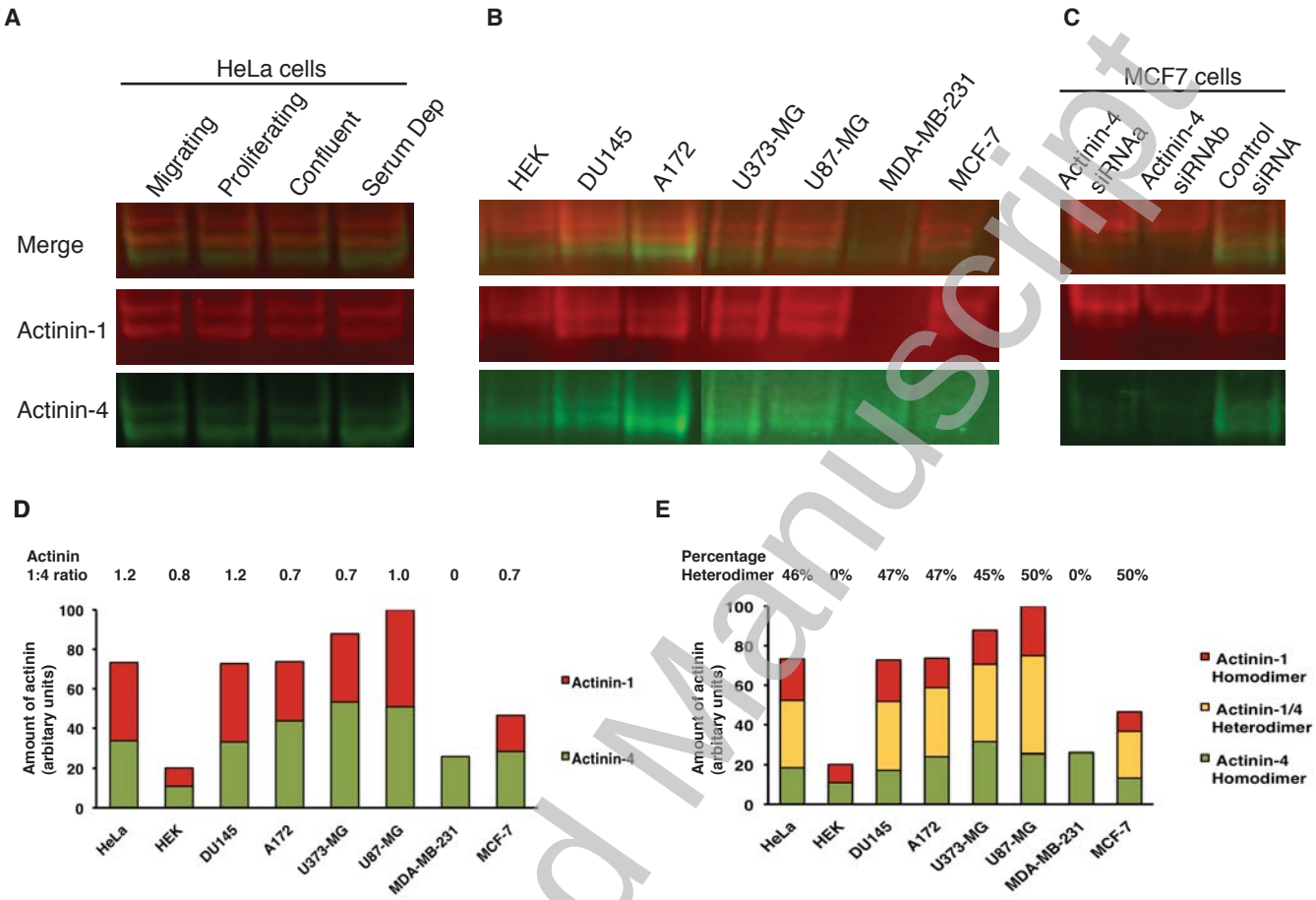

THIS IS NOT THE VERSION OF RECORD - see doi:10.1042/BJ20121824

Accepted Manuscript

Licenced copy. Copying is not permitted, except with prior permission and as allowed by law.
© 2013 The Authors Journal compilation © 2013 Biochemical Society